Lead-induced toxicity and tolerance in *Talinum triangulare* (Jacq.) Willd.

Thesis submitted to the University of Hyderabad

for the degree of

DOCTOR OF PHILOSOPHY

By

ABHAY KUMAR

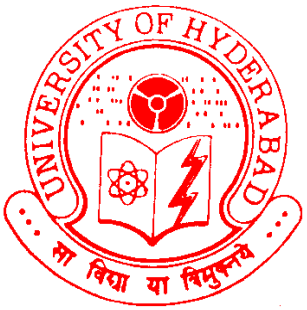

Department of Plant Sciences
School of Life Sciences
University of Hyderabad
Hyderabad 500046

February, 2013

Regd No. 08LPPH14

Department of Plant Sciences
School of Life Sciences
University of Hyderabad
Hyderabad 500046

DECLARATION

I, Abhay Kumar, hereby declare that this thesis entitled **"Lead-induced toxicity and tolerance in *Talinum triangulare* (Jacq.) Willd"** submitted by me under the guidance and supervision of **Professor M.N.V. Prasad, Department of Plant Sciences, School of Life Sciences, University of Hyderabad, Hyderabad-500046**, is an original and independent research work. I also declare that it has not been submitted previously in part or in full to this University or any other University or Institution for the award of any degree or diploma.

Date: **Signature:**

Name: **Abhay Kumar**

Regd. No.: **08LPPH14**

Department of Plant Sciences
School of Life Sciences
University of Hyderabad
Hyderabad 500046

CERTIFICATE

This is to certify that this thesis entitled "**Lead-induced toxicity and tolerance in *Talinum triangulare* (Jacq.) Willd**" is a bonafide work done by **Mr. Abhay Kumar**, a research scholar for Ph.D. programme in Plant Sciences, Department of Plant Sciences, School of Life Sciences, University of Hyderabad under my guidance and supervision. This thesis has not been submitted previously in part or in full to this or any other University or Institution for the award of any degree or diploma.

Professor M.N.V. Prasad
Supervisor

Head
Department of Plant Sciences

Incharge Dean
School of Life Sciences

"In memory of my Grandfather"

This thesis is dedicated to my beloved Parents and family members

Acknowledgments

It is with great pleasure that I express my deep sense of gratitude to my supervisor Prof. M.N.V. Prasad for his constant guidance, encouragement and support given to me during the course of this work which helped me to complete it successfully.

My sincere thanks to Prof. R.P. Sharma, Incharge Dean, School of Life Sciences, Prof. M. Ramanadham and Prof. A. S. Raghavendra, former Deans, School of Life Sciences for allowing me to use the school facilities for my research work.

Thanks are due to Prof. Attipalli R. Reddy, Head, Department of Plant Sciences; Prof. Appa Rao Podile, former Head, Department of Plant Sciences for all administrative support for my research work.

I am highly grateful to Prof. Attipalli R. Reddy and Prof. Ch. Venkat Ramana, my doctoral committee members for their valuable suggestions and kind help.

I would like to thank Prof. V.S. Raju, Department of Botany, Kakatiya University for helping me in identification and taxonomic categorization of experimental plant material Talinum triangulare used in the study.

My sincere thanks to Prof. Bramha B. Panda and Dr. V. Mohan Murli Achari, Department of Botany, University of Berhampur, Berhampur, Orisa for permitting me to investigate the DNA damage through comet assay in University of Behrampur.

I also thank all the faculty members of School of Life Sciences for providing the necessary help in several respects throughout my Ph. D. tenure.

I thank, Ms. Monica and Ms. Kalpana, Proteomics facility for their help in my proteomics work, Mr. Prashanth, Metabolomics facility for his help during metobolomics work, Ms. Nalini and Mr S. Pavan Kumar, Central Instrumentation Laboratory (CIL) and for their help with confocal and Scanning electron microscopic studies.

My sincere thanks to Prof. M.V. Rajasekharan, Dean School of Chemistry and Prof. D. Basavaiah, former Dean, School of Chemistry for allowing me to use the FTIR facility of School of Chemistry for my research work.

I also thank Mr. M. Laxminarayan, FESEM/EDS facility, School of Physics for his help with my EDS analysis.

I express my heartfelt thanks to my previous and present labmates Oksana Sytar, Jayaram, Lalhruaitluanga, Rima, Narsimhamurthi, Muhammad Saif, Abin, Dhanraj, Annapurna, Bhadru and Jeremy for maintaining a cheerful environment in the lab.

I am grateful to the University of Hyderabad, for providing financial assistance in the form of University Fellowship (BBL).

I thank Mr. Satish and Mr. E. Anand for their help in the field and lab work.

I also thank all the non-teaching staff members of Department of Plant Sciences and School of Life Sciences for their help in the official works during my research period.

I thank UGC, DBT and DST for funding in the lab and DST-FIST, UGC-SAP and DBT-CREBB for funding to the department and school.

I also thank DST, New Delhi and 11th-ICOBTE-2011 for providing travel grant and Young Scientist award, respectively, for attending the 11th-ICOBTE-2011 Conference in Florence Italy was held on 3-7, July 2011.

I am highly grateful to my friends Debashree, Bimo, Ahan, Abhay, Suresh, Subha Narayan, Shyam , Satpal, Anirudh, Naveen, Dilip, Pawan, Deepankar, Sumit, Rakesh, Anirban, Sachidanand, Kapil, Prateek, Soorat, Israr, Srinivas, Kamal and many more for their affection and support throughout my research tenure and also for making my stay in the University a wonderful memory.

My special thanks to my parents, family members and my nice Nayan, Nandika and Samridhi for their love, patience, support and confidence in me.

Last but not the least, I thank the Almighty for his blessings which helped me to successfully achieve this goal

Abhay Kumar

TABLE OF CONTENTS

LIST OF FIGURES

LIST OF TABLES

SYMBOLS AND ABBREVIATIONS

ALAD	δ-Aminolevulinic acid dehydratase
ANOVA	Analysis of variance
APX	Ascorbate peroxidase
AsA	Ascorbate
ATP	Adenosine triphosphate
ATSDR	Agencies for Toxic Substances and Dieses Registry
CAT	Catalase
Chl	Chlorophylls
2-DE	Two-D electrophoresis
2D-PAGE	Two-dimensional polyacrylamide gel electrophoresis
DHA	Dehydroascorbate
DHAR	Dehydroascorbate reductase
DMRT	Duncan's multiple range test
DMSO	Dimethylsulfoxide
DTNB	5, 5'-Dithio-bis-2-nitrobenzoic acid
DTT	1,4-Dithiothreitol
dw	Dry weight
γ-ECS	γ-Glutamylcysteine synthetase
EDS	Energy dispersive X-rays spectroscopy
EDTA	Ethylenediaminetetraacetic acid
EPA	(United State) Environmental Protection Agencies
ESEM	Environmental scanning electron microscope
ETR	Electron transport rate
FESEM	Field emmision scanning electron microscope
F_m	Maximal fluorescence yield
F_o	Dark or minimum fluorescence yield
FTIR	Fourier transform infrared spectroscopy
F_v/F_m	Maximal PSII quantum yield
fw	Fresh weight
GR	Glutathione reductase
GSH	Glutathione (reduced)
GSSG	Glutathione (Oxidised)
GST	Glutathione-S-transferase
HMs	Heavy metals
HSDB	Hazardous Substances Data Bank
IARC	International Agency for Research on Cancer
IEF	Isoelectric focusing
LHC II	Light harvesting complex II
LMP agarose	Low melting point agarose
LOX	Lipoxygenase
MALDI-TOF	Matrix-assisted laser desorption/ionization time of flight
MDA	Malondialdehyde

MDHA	Monodehydroascorbate
MDHAR	Monodehydroascorbate reductase
MoM-GOI	Ministry of Mines- Government of India
MoCM-GOI	Ministry of Coal and Mines- Government of India
MS	Mass spectrometry
$NAD(P)^+$	Nicotinamide adenine dinucleotide phosphate
NADPH	Reduced $NAD(P)^+$
NBT	Nitro blue tetrazolium chloride
NMP agarose	Normal melting point agarose
NPSH	Non-protein thiols
$O_2^{\bullet-}$	Superoxide radical
OEC	Oxygen evolving complex
OH•	hydroxyl radical
Pb	Lead
$Pb(NO_3)_2$	Lead nitrate
P_m	Maximal P700 change
PMSF	Phenylmethylsulfonylfluoride
POD	Peroxidase
PSI	Photosystem I
PSII	Photosystem II
PVP	Polyvinylpyrrolidone
PVPP	Polyvinylpolypyrrolidone
*q*N	Coefficient of nonphotochemical quenching
*q*P	Coefficient of photochemical quenching
RC	Reaction center
ROC	Report on Carcinogens
ROS	Reactive oxygen speices
RT	Room temparature
RWC	Relative water content
SDS-PAGE	Sodium dodecyl sulfate polyacrylamide gel electrophoresis
–SH	Thiol group
SOD	Superoxide dismutase
SQDG	sulphoquinovosyldiacyl-glycerol
TBA	Thiobarbituric acid
TEM	Transmission electron microscope
TCA	Trichloroacetic acid
TEMED	N,N,N',N'- Tetramethylethylenediamine
WHO	World Health Organization
w/v	Weight/volume
Y(I)	Photochemical quantum yield of PSI
[Y(NO)]	Quantum yields of non-regulated energy dissipation of PSII
[Y(NPQ)]	Quantum yields of regulated energy dissipation of PSII.
Φ_{PSII}	Effective PSII quantum yield

General Introduction

Introduction

Environment has offered itself as a surrounding substance of infinite mysteries for observers, especially with regard to its components and their functions against toxic contamination. Researchers have always looked up to environment as an inexhaustible source of inspiration that allows them to understand its components like plant, a perspective that has afforded them various models through which one can seek to solve many complex problems of the environment. Heavy metals (HMs) such as cadmium (Cd), lead (Pb), nickel (Ni), mercury (Hg), copper (Cu), zinc (Zn), calcium (Ca), magnesium (Mg), manganese (Mn), cobalt (Co) and metalloids i.e. arsenic (As) contamination to the environment and their potential to lead threats for human health and the environment, through their accumulation in soil, water and in the food chain.

Lead ($_{82}Pb^{207.2}$, Latin "plumbum") is a heavy, bluish-grey metal that naturally occurring metallic element, one of the components of the Earth's crust and present everywhere in our environment. Pb is noncombustible metal, having low melting point of 327.46 °C and density is 11.34 g cm^{-3}, mainly produced as a by-product of Zn and Pb mining and refining. However, Pb is usually found in Pb-compounds with two or more elements rather than metallic form. Its potential risks to human health have been well studied and documented. Lead (Pb) is a naturally occurring element, is a member of Group 14 (IVA) of the periodic table. According to Agency for Toxic Substances and Disese Registry, Pb ranks second among the hazardous metals known to be toxic to human and non-human biota (Anonymous-ATSDR 2011a). Pb is easily modulated and shaped and form alloys after combination with other metals. In the environment, Pb exists in three oxidation states: the metallic Pb(0) form, rarely exist in nature; Pb(II), primarily exists and Pb(IV), is only formed under extremely oxidizing conditions and inorganic Pb(IV) compounds are not found under ordinary environmental conditions (Anonymous-ATSDR

2007). Pb is amphoteric, forming plumbous and plumbic salts in acid and plumbites and plumbates in alkali. In the electromotive series, Pb positioned slightly above hydrogen and therefore should theoretically replace hydrogen in acids (King and Ramachandran 1995; Sutherland and Milner 1990).

Natural Sources of Pb

Lead is extremely persistent in the soil, air, water and foodstuffs and has no biological significance. It is present in the Earth's crust at an average concentration of 15–20 $mgKg^{-1}$. The natural occurrence of Pb in the environment results mainly from ongoing phenomena, such as weathering of rocks and abrasion, volcanic eruptions, sea and salt lake aerosols, forest fires and end products of radioactive decay of radioactive elements. Naturally, Pb is a mixture of four stable isotopes such as ^{208}Pb (51–53%), ^{206}Pb (23.5–27%), ^{207}Pb (20.5–23%), and ^{204}Pb (1.35–1.5%), where these isotopes are the stable decay product of three naturally radioactive elements: ^{208}Pb from thorium, ^{206}Pb from uranium and ^{207}Pb from actinium (Anonymous-HSDB 2007; Anonymous-ATSDR 2007). In the atmosphere, Pb compounds are present in form of particle, and hence the average half-life and lifetime for particles in the atmosphere is estimated to be about 4 to 15 days (Anonymous-ATSDR 2007).

Primary Pb is obtained from mined ore. Pb is not a particularly abundant element, but its deposits ore are readily accessible and widely distributed worldwide. Pb, primarily in the form of lead-sulfide (PbS) in galena ore, constitutes approximately 10 to 17 milligrams per kilogram ($mg\ Kg^{-1}$) or 0.001% to 0.002% of the Earth's crust (Anonymous-MoM-GOI 2011). Pb ores are usually found associated with Zn ores and out of 59 identified ore minerals of Pb most common are galena (PbS, 86.6%), cerussite ($PbCO_3$, 77.5%), anglesite ($PbSO_4$, 70%) and minium (Pb_3O_4). Weathering of galena formed the cerussite and anglesite minerals. Pb can be recovered from ore deposits of Pb, Zn, Pb-Zn, Ag and Cu. Pb

and Zn are the most widely used non-ferrous metal, after Al and Cu (Anonymous-EPA 2004, 2005, 2007). The global reserve base of Pb is estimated around 170 million tonnes. Out of that Australia leads with 35% world reserve base of Pb, followed by China, USA and Kazakhstan and others (**Fig. 1A**). Further, India is known to have rich deposits of many ores and minerals. Indian reserve base of Pb showed that Rajasthan is endowed with the largest resources of Pb-Zn ore that accounted for 468.51 million tonnes (90%) followed by Bihar (11.43 mt), Maharashtra (9.272 mt), Madhya Pradesh (6.920 mt) and Andhra Pradesh (6.620 mt) (Latha and Pavanaguru 2010) (**Fig. 1B**). Resources are also established in Gujarat, Meghalaya, Orissa, Sikkim, Tamil Nadu, Urrarakhand and West Bengal (Anonymous-MoM- GOI, 2011). Government of India report showed that the total amounts of Pb-Zn ores are estimated at 522.580 million tones as on April, 2005 (Anonymous-MoM-GOI, 2011).

Resources from technogenic activities

Lead is a traditional metal with contemporary applications, which responsible for increased Pb production and consumption worldwide. The greatest increase of environmental Pb has been observed during the past six decades as a result of human activity (Anonymous-ATSDR 2007). Pb ranks after only Fe, Cu, Al and Zn in worldwide metal use (Howe 1981; Anonymous-ROC 2011). The extensive use of Pb is largely due to its ease of casting, high density, low melting point, ease of fabrication, acid resistance, electrochemical reaction with sulfuric acid, and chemical stability in air, water, and soil (King and Ramachandran 1995; Anonymous-ATSDR 2007). Pb is mainly used in battery, paint and gasoline industries. Being the top Pb resource countries, the Pb production in Australia, China and USA were accounted for more than half of primary Pb production. Other Pb producing countries are Peru, Canada, Mexico, Sweden, Morocco, South Africa and North Korea. Globally total annual Pb production is about 8.8 mt; about half is

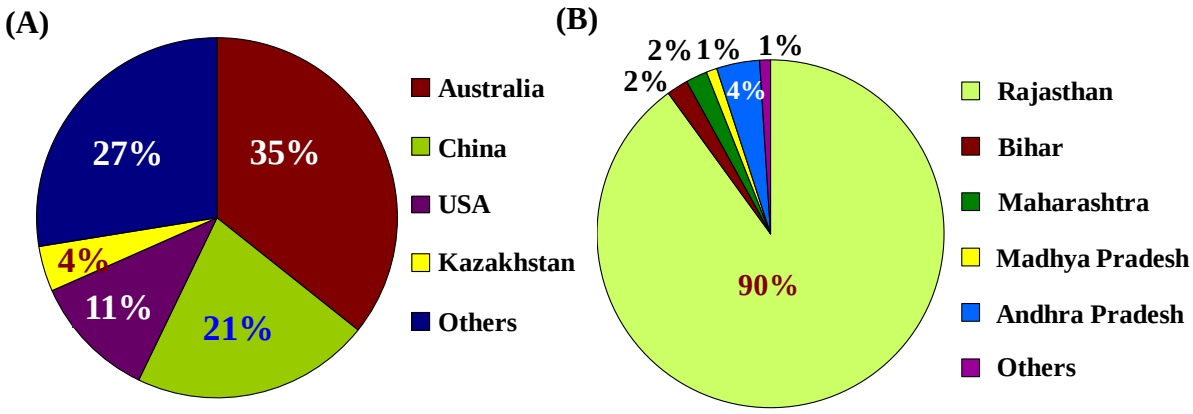

Fig. 1 Lead reserve; **(A)** Global; **(B)** India

produced from recycled scrap and residues. In the year of 2003–2004, the world's total Pb production was 6.663 mt, of which the contribution of India was 0.082 mt (Anonymous-MoCM-GOI 2003; Anonymous-MoM-GOI 2011).

Anthropogenic Pb releases either from the manufacture, use and disposal of intentionally utilizing Pb products. Various anthropogenic sources of Pb to the environment are shown in **Fig. 2**. Pb and its alloys are commonly found in pipes, storage batteries, weights, shot and ammunition, cable covers, and sheets used to shield us from radiation. Pb compounds are used as a pigment in paints, glasses, dyes, and ceramic glazes, pigmented plastics, enamels, Pb stabilized polyvinylchloride (PVC) products, Pb electronic and in caulk. Pb compounds are used in construction materials for tank linings, piping and corrosive gases and in petroleum refining, halogenation, sulfonation, extraction, condensation and metallurgy (Anonymous-ATSDR 2007). It is also used in ceramics, plastics, electronic devices, as a component of Pb batteries, and in the production of ammunition, solder, cable covering, and sheet Pb (**Fig. 2**; Anonymous-HSDB, 1995). Pb pigments produce intense colorings such as yellow, orange and red, and are well known pigments in artists' colors, plastics, glasses, ceramics and enamels. All the major soluble, insoluble and organic Pb compounds have many industrial and domestic uses (**Table1**).

Organic form of Pb such tetraethyl and tetramethyl-Pb were widely used as an anti-knock additive in motor-vehicle fuels, which was the major causative agent for atmospheric Pb contamination (Dutta and Mookerjee 1981; Sharma et al 2008). Later, United State Environmental Protection Agency (EPA) initiated a phase-out of leaded gasoline in the early 1970s and by 1996; the use of Pb in fuel for on-road motor vehicles was totally banned, resulted in to major decrease the Pb percent in the ambient air (Anonymous-ATSDR 2007). However, even the use of Pb in bullets and shot as well as in fishing sinkers is being reduced because of its harm to the environment.

Environmental fate and metabolism of Pb

Lead emissions occur to the three major compartments of the environment such as air, water and soil (Anonymous-EPA 2004, 2005, 2007). But there may be possibility of inter exchange of Pb between these three compartments after initial deposition. Air contamination due to Pb gasoline and pigment dust. In the air it inters from the burning of coal and household waste, and metal mining and refining processes (Anonymous-EPA 2007). Water bodies are contaminating though the domestic sewage and industrial waste (Anonymous-EPA 2005). Landfills or other sites may contain waste from Pb ore mining, ammunition manufacturing, or other industrial activities such as battery production (Anonymous-EPA 2004). Disposal of Pb-containing products, leaks from hazardous waste sites, and Pb-pesticides contribute to Pb in soil. Air contaminants are considerable more mobile than those to water which in turn are considered more mobile than those to soils (Anonymous-EPA 2004). Pb sources to surface water sediment include deposits of Pb-containing dust from the atmosphere, waste water from industries, urban runoff, and mining piles (Anonymous-EPA 2005, 2007). The fate of Pb in soil is affected by adsorption at mineral interfaces. Once Pb falls onto soil, it strongly sticks to soil particles and remains in the upper layer of soil particles or sediment in water for many years.

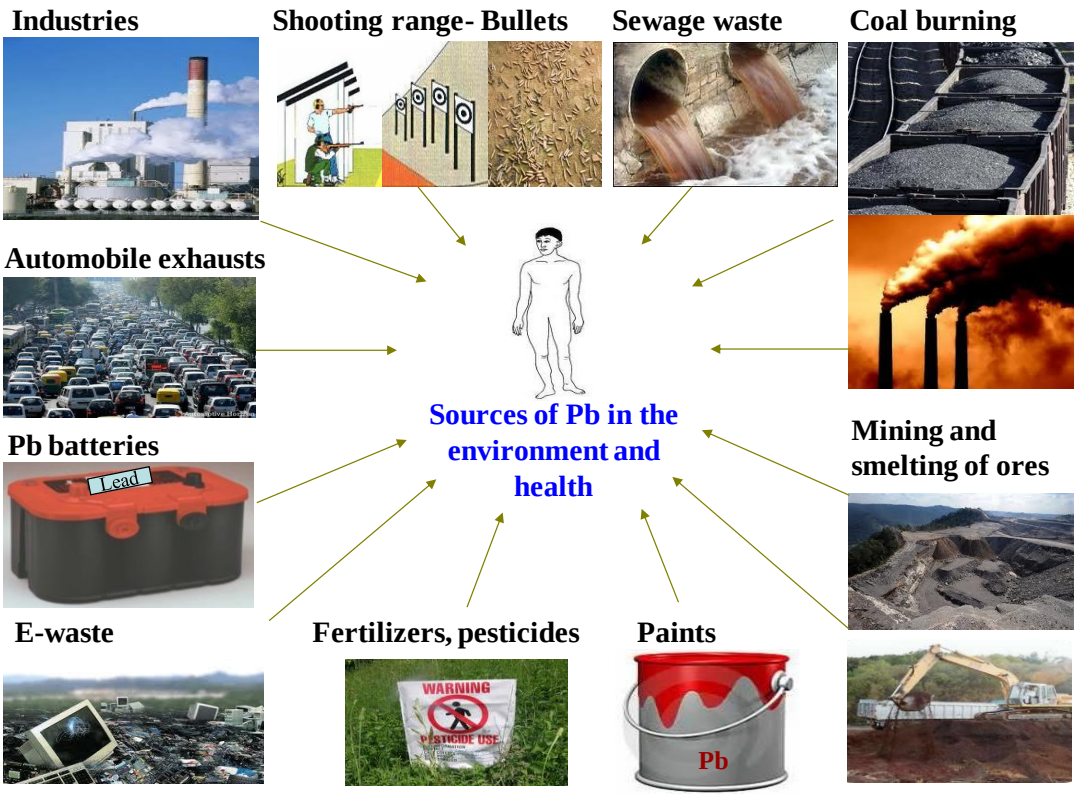

Fig. 2 Common sources of Pb in the environment and health (geogenic and technogenic).

Small amounts of Pb may enter rivers, lakes, and streams when soil particles are moved by rainwater. The major source to environmental Pb is secondary Pb, which is obtained from scrap or recycled Pb. Approximately 97% of secondry Pb produced from recycled Pb-acid batteries. Pb emissions to soils environment must be considered in three different classes; 1) The use of Pb containing fertilizers may thus cause deposition of Pb in the soil, which may be transferred to agricultural products, 2) emissions to non-agricultural soils, arises mainly from the industry, metals production and fossil fuel combustion, and 3) depositions in controlled landfills due to from disposal of spent Pb-containing products, products which may contain Pb impurities, and naturally-occurring wastes which inherently contain trace levels of Pb. Increasing incineration of Pb-contamination will eventually due to increased Pb emissions to the environment and transfer through food chain, it increased risk to human health and other biota (Murti 1987).

Table 1 Lead compounds and their uses in industrial, domestic products. (Anonymous-ATSDR 2007; Anonymous-ROC 2011).

Pb Compounds	**Uses**
Pb-acetate	Water repellent, and mordant for cotton dyes
Pb-acetate trihydrate	Varnishes, chrome pigments and as an analytical reagent
Pb-chloride	Asbestos clutch, catalyst and flame retardant
Pb-nitrate	Matches, explosives, heat stabilizer in nylon and coating on paper for photothermography
Pb-subacetate	Sugar analysis and clarifying organic solutions
Pb-azide; Pb-styphnate	Munitions manufacture
Pb-carbonate	Catalysts and in coatings for thermographic copying
Pb-fluoride	Catalysts and in the electronic and optical industries
Pb-naphthenate	Catalysts and varnish drier
Pb-phosphate;	Stabilizers in the plastics industry
Pb-iodide	Photography and in thermoelectric materials
Pb-sulfate	Galvanic batteries (with zinc)
Pb-oxide	Ceramics and as a vulcanizing agent in rubber and plastics
Pb-sulfide	Ceramics and as a humidity sensor in rockets.
Pb-chromate	Pigment in paints, rubber, and plastics
Pb-tetraoxide	Plasters, ointments, glazes, and varnishes
Pb-thiocyanate	safety matches and cartridges
Pb-arsenate	Formerly was used as an insecticide and herbicide
Tetraethyl-Pb; tetramethyl-Pb	anti-knock additive in motor-vehicle fuels

Lead effects to human health

Lead is a potentially toxic metal (Anonymous-WHO, 1992) which was classified as a human carcinogen by the International Agency for Research on Cancer (Anonymous-IARC, 2011). EPA considered that national ambient air quality standard for Pb is 1.5 μg m^{-3} and the greater concentration of Pb in is not suitable for human survival. According to them blood Pb level more than 10 μg dL^{-1} is tolerant, increased Pb level than this limit need medical cure and Pb removal from blood. Under the lead-copper rule (LCR), EPA requires testing of public water systems, and if more than 10% of the samples at residences

contain 0.015 mg L^{-1} Pb levels, actions must be taken to lower these levels. In the smelting and refining of Pb, mean concentrations of Pb in air can reach 4,470 μg m^{-3}; in the manufacture of storage batteries, mean airborne concentrations of Pb from 50 to 5,400 μg m^{-3} have been recorded; and in the breathing zone of welders of structural steel, an average Pb concentration of 1,200 μg m^{-3} has been found. Jathar et al. (1981) conducted a field study in Ahmedabad with limited samples of air, food and water. The study showed that ambient air Pb concentration varied from 0.35 to 1.77 μg m^{-3}, food grains contained 0.7 μg g^{-1} where as cooked food showed a mean of 0.8 μ gm^{-1}, drinking water samples registered a level around 0.013 μg g^{-1}. It is supposed that food and air seemed to be a major source for Pb intake in human body, which accounted for about 0.4 mg of daily intake and about 7.2% Pb of the total daily intake from air is only (Murti 1987). Pandey et al. (2010) investigated the mid stream water quality of Ganga river at Varanasi, India as influenced by aerially-driven HMs. Data showed that Ganga river receives substantially high atmospheric inputs of Cd, Cr, Cu, Pb and Zn. Non-permissible limit of Cd, Ni and Pb along with Zn, Cr and Cu were identified at various sampling sites (Pandey et al. 2010).

The available data on Pb contamination in air, water, soil and food represent the higher possibility for general population to expose to Pb. The greatest potential for human exposure to Pb arises from its previous use as an additive in gasoline and as a pigment in both interior and exterior paints, which resulted in its widespread dispersal throughout the environment, (Murti 1987; Anonymous-ATSDR 2007; Kumar and Gottesfeld 2008). Occupational, Pb exposure occurs for workers in the Pb smelting and refining industries, battery manufacturing plants, steel welding or cutting operations, rubber, plastics industries and printing industries, firing ranges, radiator repair shops and Pb soldering industries. A huge amount of information is available on the Pb effects on human health. The highest risk of health effects from Pb exposure are preschool-age children and pregnant women and their fetuses (Kaul et al. 2003). According to Health Effect Institute (HEI) more than

fifteen million children in developing countries in Asia are suffering from severe neurological damage due to Pb poising (Anonymous-EPA 2004; Anonymous-ATSDR 2007). Studies of Pb workers suggest that long-term exposure to Pb may be associated with increased mortality due to cerebrovascular disease. Pb has long been known to alter the hematological system by inhibiting δ-aminolevulinic acid dehydratase (ALAD) enzyme involved in heme biosynthesis. Pb-induces skeletal maturation, which might predispose to osteoporosis in later life, dental caries in children and periodontal bone loss. Prolonged Pb-induced toxic symptoms include dullness, irritability, poor attention span, epigastric pain, constipation, vomiting, convulsions, coma, and death (Ahmad et al. 2004). Blood Pb concentration of 40–80 μg/dL Pb in workers induces neurobehavioral effects such as malaise, irritability, forgetfulness, fatigue, lethargy, headache, weakness, impotence, dizziness, decrease intelligence quotient (IQ) and paresthesia. It is also reported that occupationally or environmentally exposure to Pb causes abortion and preterm delivery in women and alterations in sperm and decreased fertility in men. Pb exposure caused DNA damage and EPA and IARC have determined that Pb is a probable human carcinogen based on sufficient evidence from studies in animals and inadequate evidence in humans (Anonymous-ATSDR 2011b).

Lead availability to plant

Similar to other non-essential elements (As, Hg and Cd) and excess essential elements (Cu, Ni, Zn, Fe and Ca), Pb is a highly toxic element for plant and other organisms at all concentrations, and have no metabolic significance (Sharma and Dubey 2005; Sengar et al. 2008). Pb, like other HMs, is non-biodegradable and non-thermodegradable and thus readily accumulates to toxic levels in the soil due to the long-term application of wastewater. One important pathway for dietary uptake of Pb could be through crops or food irrigated with contaminated wastewater (Uwah et al. 2009). Sharma et al. (2007)

reported about the HMs contamination of soil and a highly nutritious leafy vegetable, *Beta vulgaris* (Shakarkand), resulting from wastewater in sub-urban area of Varanasi, India. However, the study confirmed that in the edible portion of *B. vulgaris*, the Pb, Cd and Ni concentration were higher than the permissible limits of the Indian standard during the growing season (Sharma et al. 2007).

An investigation was made for possible hyperaccumulator of HMs from contaminated soil by using seventeen wild-growing plants and nine cultivated plants. Wild-growing plants are *Dactylis glomerata, Cynodon dactylon, Anthoxanthum odoratum, Lollium perenne, Agrostis giganthea, Vicia sativa, Trifolium pratense, Medicago falcate, Lotus corniculatus, Ranunculus arvenis, Helleborus odorus, Equisetum arvense, Amaranthus retroflexus, Taraxacum officinale, Prunus avium, Euphorbia cyparissias, Gallium aparine* and cultivated plants are *D. glomerata, Phleum pratense, Lolium multiflorum, L. perenne, Arrhenatherum elatius, Festuca pratensis, Festuca arundinaceae, L. corniculatus, T. pratense* (Maric et al. 2012). Maric et al. (2012) reported that all wild-growing and cultivated species are accumulating considerable amount of Pb which are ranged between 5.3–10.3 and 16.4–28.7 mg Kg^{-1}, respectively. Pb accumulation in plants is mainly through root uptake from soil, expect in special cases where aerial accumulation in leaf possible. *Zea mays* L. grown in a typical zinc smelting impacted area of southwestern China, accumulated Pb and Cd to a toxic level via their roots and/or leaves. Data represented that the elevated concentrations of Pb and Cd in the surrounding soils (69–2300 mg g^{-1} and 7.4–55 mg g^{-1}, respectively) and maize plants was possibly due to smelting activities. Isotope analysis of Pb revealed that the Pb in the stalk (1.8–2.9 μg g^{-1} dry weight (dw) and root (8.1–220 μg g^{-1} dw) tissues was mainly derived from root uptake, while foliar uptake of atmospheric Pb was the dominant pathway for Pb to the leaf (25–130 μg g^{-1} dw) and grain (0.85–1.4 μg g^{-1} dw) tissues of maize (Bi et al. 2009). Root considered as a main accumulation site for Pb in many plants grown in contaminated soil

and water (Probst et al. 2009; Tang et al. 2009). Since the diet is the main source of exposure to Pb for the general population, intensive research has been done on the accumulation of Pb in edible plant tissues (Sharma et al. 2007; Brunet et al. 2008; Nautiyal and Sinha 2012). A field survey of Pb content in edibles showed that majority of the Pb accumulated in roots (root: soil ranging from 0.02 to 0.51) with some translocation to shoots (shoot:soil as high as 0.10) and below detectable level in fruits grown in contaminated soil (Finster et al. 2004). Wang et al. (2006a) were conducted an experiment to analyze the uptake and transfer potential of Cd and Pb to edible part of six vegetable from contaminated soils. Analysis showed that leafy vegetable accumulate higher amount of Pb [mg Kg^{-1} fresh weight (fw)] than non-leafy vegetables such as Chinese cabbage (0.052), pakchoi (0.061), water spinach (0.097), towel gourd (0.028), eggplant (0.029) and cowpea (0.052). Pb contamination and accumulation not only affect the food but also beverage plant such as tea, a widely consumed beverage. Tea plant are growing in acidic soil garden, which provide a better translocation factor and medium for Pb uptake by roots (17.3 mg Kg^{-1} dw) and transfer to the mature leaf (3.5 mg Kg^{-1} dw) part (Han et al. 2007).

Lead accumulation in plants: laboratory experiments

Once plants interact with HMs such Pb, they followed two mechanisms (i) metal avoidance and (ii) metal uptake (**Fig. 3**). Metal avoidance includes active efflux, redox barrier, and metal precipitation in the soil-rizhosphere and shaded the leaf to avoid the metal accumulation (Siedlecka et al. 2001; Nagajyoti et al. 2010). On the other hand, plants take up Pb from soils or water in response to concentration gradients induced by selective uptake of ions by roots. Pb is captured by root cells of the plants after its mobilization in the soil, which mainly depends upon: (i) diffusion of Pb along the concentration gradient which is formed due to Pb uptake and thereby depletion of the element in the root vicinity; (ii) interception by roots, where soil volume is displaced by

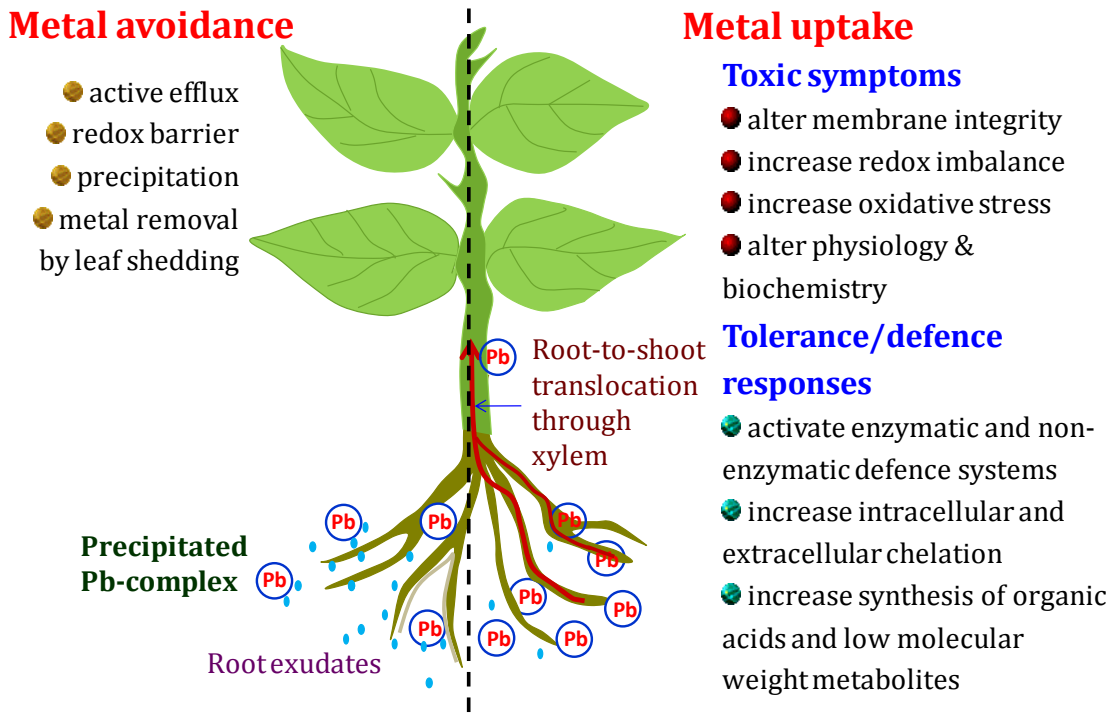

Fig. 3 Mechanisms of metal avoidance, uptake and tolerance in plant (Siedlecka et al. 2001).

root volume after growing, and (iii) flow of metal elements from bulk soil solution down the water potential gradient (Marschner 1995). The uptake of Pb, both by roots and leaves, increases with increasing external Pb concentration. Nevertheless, the uptake has no linear relation with increasing concentration. Pb compartmentalization in plants tissues involves Pb mobilization from roots to aerial parts of the plant (translocation). The level of accumulation of elements differs between and within species. Like other few HMs, there are no clear reports about the plasma membrane channels for Pb uptake, but it is still unidentified how Pb goes into the root tissue.

On the other hand, Arazi et al. (1999) reported that transgenic tobacco plants expressing *NtCBP4* (*Nicotiana tabacum* calmodulin-binding protein) tolerate higher levels of Ni^{2+} but are hypersensitive to Pb^{2+}, reflecting the exclusion of Ni^{2+} but the accumulation of more Pb^{2+} than wild type plants. After accumulation in to the roots tissues, for most of

the plant species, the majority of absorbed Pb (approximate 90%) is accumulated in the roots and only a small percentage of Pb may be transported to the aerial part of the plants and as has been reported in *Vicia faba* (Piechalak et al. 2002), *Pisum sativum*, and *Phaseolus vulgaris* (Małecka et al. 2009; Shahid et al. 2011), *Vigna unguiculata* (Kopittke et al. 2007a), *Nicotiana tabacum*, (Gichner et al. 2008), *Lathyrus sativus* (Brunet et al. 2008), *Zea mays* (Gupta et al. 2009), *Avicennia marina* (Yan et al. 2010), *Allium sativum* (Jiang and Liu 2010) and in *Sedum alfredii* (Huang et al. 2012).

Although, similar to some other HMs, Pb display the translocation restriction phenomenon, this phenomenon is not common to all HMs. The degree of Pb translocation can be well explained by the translocation factor (Pb in aerial parts/Pb in roots) (Arshad et al. 2008; Uzu et al. 2009). Usually the numeric values is rather low for Pb, which suggests that maximum amount of Pb has been sequestered in the roots tissues (Uzu et al. 2009; Rossato et al. 2012). Several studies revealed the basic reason of limited transport of Pb from roots to aerial plant parts, which includes immobilization by negatively charged pectins and lignin or binding to carboxylic group of mucilage uronic acids within the cell wall (Marmiroli et al. 2005; Islam et al. 2007; Kopittke et al. 2007a; Sengar et al. 2008; Arias et al. 2010), precipitation of insoluble Pb salts in intercellular spaces (Kopittke et al. 2007a; Islam et al. 2007; Meyers et al. 2008; Małecka et al. 2009) or sequestration in the vacuoles of cortical and rhizodermal cells (Seregin et al. 2004; Kopittke et al. 2007; Pourrut et al. 2011a). However, these explanations are not well sufficient to demonstrate the low translocation rate of Pb from root to shoot. Although, the endoderm acts as a physical barrier and plays an important role in this phenomenon. Following apoplastic transport, accumulated Pb is blocked in the endodermis by the Casparian strip and must follow symplastic transport, where the major part of Pb is sequestered by plant detoxification systems (Jarvis and Leung 2002; Chaudhury and Panda 2005; Kaur et al. 2013). Verbruggen et al. (2009) suggested that transportation of metals from roots to aerial

parts requires movement through the xylem vessels of vascular bundle or vascular flow. X-ray mapping demonstrated high amount of Pb deposition in xylem and phloem cells (Marmiroli et al. 2005; Arias et al. 2010; Zheng et al. 2012). While passing through the xylem, Pb can form complexes with amino or organic acids (Marmiroli et al. 2005; Vadas and Ahner 2009; Maestri et al. 2010). Organic acids such as carboxylic acid and amino acids such histidine and methionine are potential metal chelators (Sharma and Dietz 2006). Amino acids, and several transporter proteins are involved in the root-to-shoot translocation of Pb (Manara 2012). Metal ions are also translocated from source to sink tissue via phloem (Rascio and Navari-Izzo 2011). Various studies reported about the Pb binding to carboxylic group of mucilage uronic acids on plant root surface (Wierzbicka 1998; Marmiroli et al. 2005). Other plants tolerate and detoxify Pb by inactivation excretion and complexation by ligands and compartmentalization in to tissues (Sharma and Dubey, 2005; Anjuman et al. 2012). Moreover, accumulated Pb in the plants showed various toxicity symptoms; tolerance responses and detoxification mechanisms (Sharma nd Dybey 2005; Sengar et al. 2008).

Lead-induced toxicity in plants

Once plants are exposed with Pb, even at low (μM) concentrations they showed various degrees of toxic symptoms (Vadas and Ahner 2009; Wang et al. 2012a,b). Despite the toxicity of HMs including Pb, several plants growing in metals polluted media, are able to exclude, accumulate or hyperaccumulate HMs and acquire a wide range of adaptive strategies (**Fig. 3**). Hyperaccumulator plants are accumulating generally high level of Pb in their tissues with showing much toxic symptoms or without incurring damage to their basic metabolic functions (Hu et al. 2012; Huang et al. 2012; Liu et al 2012; Kaur et al. 2013). Accumulated Pb in the cells is bound to ion exchangeable locations in the cell walls and was get precipitated extracellularly by phosphate and carbonate (Sengar et al. 2008).

Table 2 Summary of the Pb accumulation/uptake level in roots, stems and leaves of various plants exposed to various concentrations of Pb through hydroponic or liquid nutrient media for different treatment durations. AE- accumulating ecotypes; NAE- non-accumulating ecotypes; [a]- whole plant Pb accumulation; [*]- shoot Pb accumulation)

Plant name	Treatment concentrations	Durations (days)	Pb Accumulation level in plant tissues (mg Kg^{-1} dw)			Reference
			Roots	Stem	Leaves	
Triticum aestivum	15.00 mM	5	1.22[a]	—	—	Lamhamdi et al. 2013
Spinacia oleracea			0.99[a]			
Pisum sativum	2000 mg L^{-1}	28	3600	—	55	Rodriguez et al. 2013
Brassica juncea *Sesuvium portulacastrum*	0.40 mM	21	1400 µ L^{-1} 700 µ L^{-1}	—	—	Ghnaya et al. 2013
Sedum alfredii	0.20 mM	1	~6250	~460	~77	Huang et al. 2012
Vallisneria natans	0.075 mM	6	—	—	0.0095	Wang et al. 2012
Pluchea sagittalis	1.00 mM	30	8031	1650	~1400	Rossato et al. 2012
Ficus microcarpa	0.20 mM	1	~700	—	—	Liu et al. 2012
Cajanus cajan	1.00 mM	27	~4000	~70	~70	Nautiyal and Sinha 2012

Spirodela polyrhiza	0.40 mM	7	19,223.8	—	—	Qiao et al. 2012
Triticum aestivum	0.25−0.5 mM	4	2.256−2.807 (mg g^{-1} dw)	0.220−0.271* (mg g^{-1} dw)	—	Kaur et al. 2012
Pistia stratiotes	2.00 mM	8	203 (fw)	—	18.2 (fw)	Vesely et al. 2012
Elsholtzia splendens	0.20 mM	30	45,183.6	1657.6	380.9	Zhang et al. 2011
Sesbania drummondii	1.25 mM	10	58590	1268	—	Israr et al. 2011
Vicia faba	0.005 mM	1/4	61	—	—	Shahid et al. 2011
Jatropha curcas	1.00 mM Kg^{-1} 4.00 mM Kg^{-1}	60	1600 3900	—	200 580	Shu et al. 2011
Helianthus annuus	20 mgL^{-1}	7	67130	783*	—	Strubinska and Hanaka 2011
Brassica rapa	0.5−5 mM	6	8049.70−13829.60	—	—	Cenkci et al. 2010
Arabis paniculata	0.386 mM	18	33,900	12,800	—	Tang et al. 2009
Zea mays	0.001 mM	1/12	65	—	—	Vadas and Ahner 2009
Wolffia arrhiza	0.1 mM	14 days	0.82[a] (mg g^{-1} fw)	—	—	Piotrowska et al. 2009
Brassica napus	1.00 mM	1/12	200	—	—	Vadas and Ahner 2009
Zea mays	0.20 mM	7	70.425	0.995*	—	Gupta et al. 2009

Lathyrus sativus	0.50 mM	4	0.150	—	—	Brunet et al. 2008
Sedum alfredii	0.20 mM	21	7781	2746*	—	Huang et al. 2008
Vicia faba	0.01 mM	21	~32	—	—	Pourrut et al. 2008
Sedum alfredii (AE)	0.20 mM	12	7600	1198*	—	Liu et al. 2008
Sedum alfredii (NAE)	0.2 mM	12	9238	603*	—	Liu et al. 2008
Raphanus sativus	0.1− 0.5 mM	35	300−450	55−153*	—	Gopal and Rizvi 2008
Vigna unguiculata	0.00033 mM	13	1300	54	—	Kopittke et al. 2007a
Tamarix smyrnensis	4.00 mM	70	95 (ppm)	—	—	Kadukova and Kalogerakis 2007
Ceratophyllum demersum	0.1 mM	7	1.75 mg g^{-1} dw	—	—	Mishra et al. 2006
Brassica oleracea	1.0 mM	43	~1100	~145	~560	Sinha et al. 2006
Sedum alfredii	1.5 mM	7	18449 (fw)	58 (fw)	2.0 (fw)	Sun et al. 2005
Medicago sativa	0.2 mM	10	~52000	~10000	~2500	López et al. 2005
Lupinus luteus	350 mg L^{-1}	2	70	—	—	Rucinska et al. 2004
Zea mays	1.0 mM	2	0.0081	0.00051	—	Seregin et al. 2004
Oryza sativa	1.0 mM	20	1.3065 (mmol g^{-1} dw)	—	0.8008 (mmol g^{-1} dw)	Verma and Dubey 2003

The unprecipitated or unbound Pb is moved possibly through Ca channels to the other part of the cells (Manara et al. 2012) showed the various toxic symptoms (Sengar et al. 2008; Sing et al. 2011). The most evident symptoms of its toxicity are chlorosis and stunting. Chlorosis as results of Pb uptake, transport and replacement of essential elements like Ca, Mg, Fe, Mn, Cu, Zn, P and K, resulted in to alteration in other metabolic pathways and physiological processes (Pourrut et al. 2011a; Lamhamdi et al. 2013). One of the primary responses evoked by Pb is the production of toxic reactive oxygen species (ROS) through various mechanisms involving electron transfer (Shu et al. 2012), which further leads to oxidative stress (Israr et al. 2011; Qiao et al. 2012). Oxidative stress is a state where the balance between oxidants production exceeds the ability of various antioxidant systems to remove the destructive oxy free radicals leading to significant physiological and biochemical impairment (Shaw et al. 2004; Kaur et al. 2012; Shahid et al. 2012). The ROS molecules include superoxide anion ($O_2^{\bullet-}$) perhydroxyl radical ($HO_2^{\bullet-}$), hydrogen peroxide (H_2O_2), hydroxyl radical ($OH^{\cdot}$), alkoxyl radical ($RO^{\bullet}$), peroxyl radical ($ROO^{\bullet}$), organic hydroperoxide (ROOH), singlet oxygen ($^1O_2$), excited carbonyl (RO*) (Møller and Sweetlove 2010). Superoxide ions act as oxidants where it can oxidize the sulphur, ascorbate, metal and dismutated in to H_2O_2 enzymatically with the help of superoxide dismutase (SOD). The H_2O_2 is not a real free radical because all of its electrons are paired positions, but is capable of initiating reduction and highly reactive $OH^{\bullet}$ formation in the presence of a metal reductant, specifically Fe (Shaw et al., 2004). The process is known as Haber-Weiss Fenton reaction and can be explained as:

$$O_2^{\bullet} + H_2O_2 \xrightarrow{Fe^{2+}/\,Fe^{3+}} {}^{\bullet}OH + OH^- + O_2$$

Pb affects the structure and function of macromolecules directly or indirectly through production of free-radical reactions by oxidative reactions, demonstrated as disruption of membrane integrity and oxidative modifications of proteins and DNA (Sengar et al. 2008;

Pourrut et al. 2011a,b). Presence of Pb in the plant cell caused an increase in activities of peroxidase and hydrolytic enzyme. ROS damage the membrane lipid and caused lipid peroxidation, a process initiated by abstraction of hydrogen atom from the methylene group (-CH2-) of the polyunsaturated fatty acids of the membrane lipid by hydroxyl radical. Lipid peroxidation can also be induced enzymatically by enxymes phospholipases and lipoxygenases (LOX) (Hu et al. 2007; Liu et al. 2008; Huang et al. 2012). Pb like other toxic HMs, directly affects the plant physiology by inhibiting the enzymes involved in the biosynthesis of photosynthetic pigments such as δ-aminolevulinic acid dehydratase (ALAD) (Myśliwa-Kurdziel and Strzałka 2002; Mishra et. al. 2006; Cenkci et al. 2010; Shu et al. 2012) and protochlorophyllide reductase (Burzynski and Kolbus 2004).

Proteins and DNA would be the major targets for Pb or Pb-induced ROS directly or indirectly. ROS attacks on proteins results in site-specific amino acid modifications (Sharma and Dietz 2006), fragmentation of the peptide chain, and aggregation of cross-linked reaction products increased susceptibility to proteolysis (Braconi et al. 2011). Pb is considered as an effective mitotic poison (turbagens) due to their known affinity for –SH groups and induces various types of spindle disturbances (Patra et al. 2004). It is possible that Pb may involve in the interaction with DNA either directly or indirectly (Gichner et al. 2004). enzymatic antioxidants are superoxide dismutase (SOD, E.C. 1.15.1.1), catalase (CAT, E.C. 1.11.1.6), glutathione reductase (GR, E.C. 1.6.4.2), peroxidase (POD, E.C. 1.11.1.7), ascorbate peroxidase (APX, E.C. 1.11.1.11) and guaiacol peroxidases (GPX, E.C. 1.11.1.7) and non-enzymatic antioxidants such as, carotenoids, anthocyanins, ascorbic acid (AsA), glutathione and tocopherol (Kanoun-Boule et al, 2009; Maleva et al, 2009; Munne-Bosch, 2005) which are able to suppress the reactive oxygen species in the chloroplasts as well as the cytosol. The details about the enzymatic and non-enzymatic antioxidants are described in subsequent objectives.

Table 3 Summary of the responses of various plants to different Pb concentrations for different durations: ICP-MS, Inductive coupled plasma mass spectroscopy; HPLC, high performance liquid chromatography; NMR, nuclear matrix resonance; PSII, photosystems II; DHA, dehydroascorbate; MDA, monodehydroascorbate reductase; AsA, ascorbic acid; GPX, guaicol peroxidase; GR, glutathione reductase; SEM, scanning electron microscope; TEM, transmission electron microscope; APX, ascorbate peroxidase; CAT, catalsae; SOD, superoxide dismutase; POD, peroxidase; GSH, glutathione; ROS, reactive oxygen species; GST, glutathione-S-transferase; EDS, energy dispersive X- rays spectroscopy.

Plants	Concentration	Duration (days)	Parameter	Plant specific responses	Reference
Sesuvium portulacastrum *Brassica juncea*	0.20–0.40 mM		Pb translocation, HPLC, ICP-MS	Pb contents in xylem sap of the *S. portulacastrum* were significantly greater than in that of *B. juncea*. Malic and citric acids contents were modified in the presence of Pb, where citric acid could be highly implicated in Pb translocation	Ghnaya et al. 2013
Triticum aestivum *Spinacia oleracea*	0.15–3.00 mM	5	Nutrient uptake, metabolites, proline	Reduced uptake of all mineral ions and results in profound metabolic changes. spinach appears far more resistant	Lamhamdi et al. 2013
Pisum sativum	2000 mg L^{-1}	28	Microsatellites (Simple Sequence Repeats, SSR), mutagenicity	Pb caused dose dependent induction in microsatellite instability, where roots are more sensitive organ. SSR technique is sensitive to detect Pb-induced mutagenicity in plants	Rodriguez et al. 2013

Lupinus luteus	150 mg L^{-1}	2	Proline metabolisms, NMR diffusometry	Proline metabolism is sensitive to Pb. Fluorescence staining showed that deposition of callose in cell walls seems to be responsible for the reduction in the rate of water movement through the vacuolar continuum. NMR spectroscopy showed that Pb caused a deceleration in water transport in the roots	Rucińska-Sobkowiak et al. 2013
Vigna mungo	0.125–0.625 mM	1/4	Cytogentic and genotoxic analysis	Pb caused chromosomal aberrations in root tip cells, which suggested that Pb may exhibit genotoxic effect on plant	Siddiqui 2012
Zea mays	0.005 mM	1	PSII fluorescence measurements, protein blotting and mass spectrometry	Pb had less affect on PSII activity in mesophyll cells than bundle sheath. Pb-induces phosphorylation of the PSII core proteins (D1, D2 and CP43), which can affect stability of the PSII complexes and the rate of D1 protein degradation	Romanowska et al. 2012
Jatropha curcas	0.50–4.00 mM	6	Toxicity index, photoynthetic function, antioxidants	Pb induces oxidative stress in seedlings and stem cuttings and that elevated activity of antioxidative enzymes and decrease net photosynthesis, stomatal conductance and transpiration rate	Shu et al. 2012
Pluchea sagittalis	0.20–1.00 mM	30	Pb uptake, distribution and antioxidants	Pb content in roots, stems, and leaves increased with external Pb level. Pb alters the activities of δ-aminolevulinic acid dehydratase (ALAD), APX, SOD, CAT enzymes and thiols, ascorbate contents	Rossato et al. 2012

Cajanus cajan	0.05–1.00 mM	13	Antioxidants	Pb caused oxidative damage, which declined chlorophyll and induced carotenoids, proline, and non-protein thiol contents and SOD and peroxidase activities	Nautiyal and Sinha 2012
Salsola passerine Chenopodium album	0.50–1000.00 mgL^{-1}	10	Tolerance mechanisms	*S. passerina* exhibited higher Pb tolerance than *C. album* in terms of the, bio-activities of SOD and POD, and lower MDA production through cell wall precipitation and state transfer of free Pb into anchorage	Hu et al. 2012
Vallisneria natans	0.010–0.10 mM	2–6	Histochemical staining, oxidative stress, antioxidants	Pb caused oxidative damage and clearly increased the activities of SOD, CAT, POD, GR and APX enzymes and contents of MDA, non-protein thiols and DHA, while the contents of chlorophyll, carotenoids, AsA and GSH decreased	Wang et al. 2012
Spirodela polyrhiza	0.025–0.40 mM	7	Biochemical and physiological strategies	Pb caused phytotoxicity with alteration in various antioxidants and nutrient elements polyamines, total spermidine along with polyamine oxydase and ornithine decarboxylase activities	Qiao et al. 2012
Lespedeza chinensis Lespedeza davidii	0.50 mM	7	Ultrastructural, subcellular localization by TEM	Pb transported to apoplastic and symplastic pathways and detoxified by cell wall sequestration, autophagy, vacuolar compartmentalization as Pb-phosphate	Zheng et al. 2012

Triticum aestivum	0.05–0.50 mM	4	Oxidative damage, root ultrastructural changes	Pb enhanced SOD and CAT activities, while APX and GPX activities declined. Pb caused thinning of cell wall, Pb deposition along the cell wall, formation of amoeboid protrusion, lesions and nicks, increased the number of mitochondria, and reduction in nucleoli size and induced puff formation	Kaur et al. 2012
Sesbania drummondii	250 mg L^{-1}	10	Oxidative stress, antioxidants	Hyperaccumulator of Pb, and significantly induced the SOD, APX, GR activities and GSH and GSSG concentrations	Israr et al. 2011
Vicia faba	0.001–0.020 mM		Comet assay, genotoxicity	Pb caused the DNA strand-breakage and chromosome aberrations in a dose-dependent manner (up to 0.010 mM). Comet assay showed direct interaction of Pb with DNA. The results highlight, for the first time in vivo and in whole-plant roots, the relationship between ROS, DNA strand-breaks and chromosome aberrations induced by Pb.	Pourrut et al. 2011b
Elsholtzia splendens	0.10–0.20 mM	7	Micro-X-ray fluorescence imaging and Chlorophyll fluorescence	Pb mostly accumulated in to the roots. Fluorescence analysis showed plant can tolerate up to 0.10 mM Pb and was mostly restricted in the vascular bundles and epidermis tissues of both stem and leaf	Zhang et al. 2011
Najas indica	0.001–0.10 mM	1, 2, 4, 7	Toxicity, tolerance, detoxification	Plant tolerate the Pb stress by inducing the thiol synthesis and enzymatic and non-enzymatic antioxidants	Singh et al. 2010

Brassica rapa	0.50–5.00 mM	6	chlorophyll biosynthesis, RAPD- DNA profiles	Pb in the leaves of fodder turnip seedlings resulted in the reduction of ALAD activity, chlorophyll synthesis and genomic template stability and caused DNA damage	Cenkci et al. 2010
Zea mays	0.025–0.20 mM	1, 4, 7	Antioxidant defense mech-anisms	Pb, but only small percentage translocated to upper part. Pb resulted in oxidative stress but it effectly controlled due to significant increases in antioxidants	Gupta et al. 2009
Wolffia arrhiza	0.001–1.0 mM	7, 14	Pb- jasmonic acid interactions	Jasmonic acid increased the resistance against Pb stress at (0.0001−0.010 mM) and at further concentration act as stress inducer by increasing the Pb accumulation	Piotrowska et. al. 2009
Arabis paniculata	0.024–0.386 mM	18	Field survey, hydroponiccs experiments	*A. paniculata* is Hyperaccumulator of Pb in both conditions and certain levels of Pb induced a stimulatory effect on the biomass production and chlorophyll concentrations	Tang et. al. 2009
Lathyrus sativus	0.50 mM	4	Toxicity and tolerance at the transcription level	ROS scavenging and sequestration of Pb ions were stimulated through transcript-ional mechanisms regulating the activities of GR, GST and APX to a lesser extent	Brunet et al. 2009
Sedum alfredii	0.20–0.40 mM	14	Phytotoxicity responses of two ecotypes and ultrastruct-ural changes	Accumulating ecotype is much tolerant than non-accumulating ecotype to Pb, which was confirmed by the changes in the growth parameters, MDA and activities of SOD and CAT enzymes and ultrastructural analysis of the spongy mesophyll cells	Liu et. al. 2008

Sedum alfredii	0.20 and 0.40 mM	21	Pb-EDTA interaction	Pb treatment increased oxidative stress, Cu and Fe contents and declined Mg, Ca and K concentration, which were reversed in the presence of external EDTA	Huang et al. 2008
Brassica juncea	3.2–217 μM	3	Uptake and localization of Pb	Pb uptake was restricted largely to root tissue. SEM/EDS showed that intracellular deposition and endocytosis of Pb into a subset of vacuoles was observed suggested that identification of the membrane transport mechanism(s) responsible for intracellular Pb uptake	Meyers et al. 2008
Potamogeton crispus	5.0–20.0 mgL^{-1}	3	Oxidative system, ultrastructural changes	Pb induces antioxidative enzymes activities along with structural alteration, includes disruption of chloroplast, mitocondria and nuclear membrane, condensation of chromatin and dispersion of nucleoli	Hu et al. 2007
Lupinus luteus	350 mgL^{-1}	1 (21 h)	Oxidative stress	Pb-induced ROS productions were involved in signal transduction, resulted in to activation of tolerance mechanisms	Przymusiński et al. 2007
Ceratophyllum demersum	1.00–100.00 mM	1, 2, 4, 7	Oxidaive stress and glutathione metabolisms	Inhibition of ALAD, Impaired uptake of Mn and Fe; Chl degradation by increased chlorophyllase activity; EC increased upto 142%	Mishra et. al. 2006

Experimental plant: *Talinum triangulare*

Talinum triangulare (Jacq.) Willd. (Ceylon spinach) is a terrestrial herbaceous plant with erect, simple or branching stems (**Fig. 4A-D**). Formerly this genus belongs to the family Portulacaceae, which are known to bear ornamental and attractive flowers (Hickey and King 1981; Foxcroft et al. 2008). But recently, family Portulacaceae disintegrated into six new families based on molecular and morphological analysis (Nyffeler and Eggli 2010; Ocampo and Columbus 2010). According to Nyffeler and Eggli (2010) and Ocampo and Columbus (2012) now genus *Talinum* comes under family Talinaceae. *Talinum* is a small genus with 50 species mostly found in the tropics, subtropics and warmer parts of the world (Hickey and King 1981). *T. triangulare* flowers and fruits throughout the year and flowers are small and showy, open in the morning and close in the late afternoon (**Fig. 4D**). Apart from its ornamental value, *Talinum* are widely used as leafy vegetable plants in the tropics including India, Arabia, Africa and America. In south-eastern States of Nigeria, *Talinum* is being cultivated and considered as a highly desirable vegetable plant (Ukpong and Moses 2001). Almost all its parts are useful and used as traditional medicine and are good source of antioxidant micronutrients (xanthophyll carotenoids) such as lutin (89.79 mg/100 g dw) and zeaxanthin (1.22 mg/100 g dw), in the leaves (Khoda et al. 1992; Lakshminarayana et al. 2007). *Talinum* are serving as the important source of flavonoids, mineral constituents, saponins, tocopherol, vitamin C and proteins in diet of major human population (Andarwulan et al. 2010; Panyaphu et al. 2011). Moreover, these properties make this plant as a promising candidate for rich source of the antioxidants as well as other medicinal values (Panyaphu et al. 2011). Additionally, the extract of *T. triangulare* showed antioxidative and hepatoprotective properties in mice against different cell toxicants (Liang et al. 2012). Large Human population used this plant extract in hypertension (Gbolade 2012), use for treating measles (Ajibesin et al. 2008) and in fever (Allabi et al. 2011).

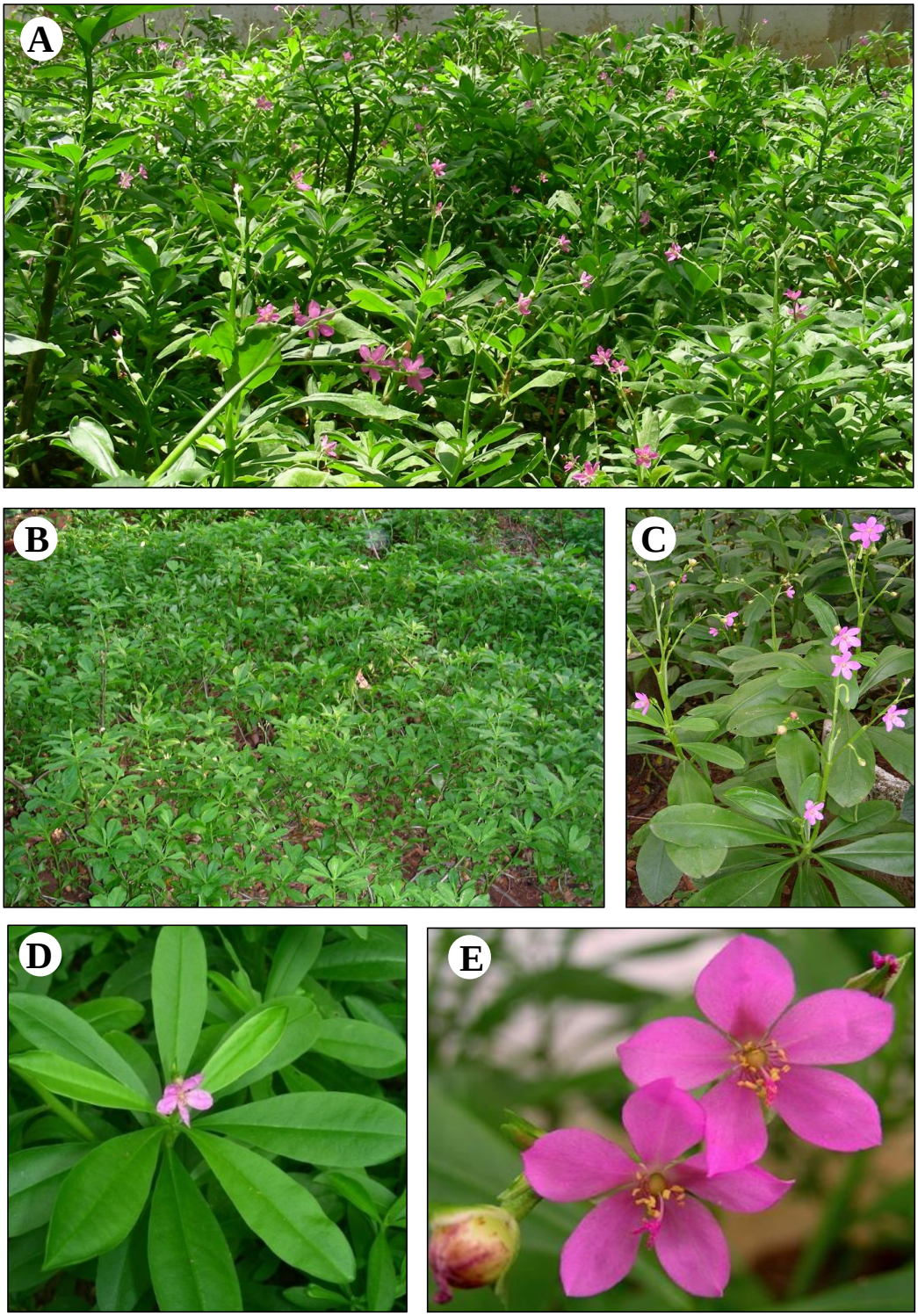

Fig. 4 ***T. triangulare*** **in field conditions maintained in Botanical garden, University of Hyderabad: (A)**, **(B)** and **(C)** Plants with widespread flowers and seeds in field; (**D**) plantlets grown in the pots and (**E**) flowers of *T. triangulare*.

T. triangulare shows close resemblance with *T. cuneifolium* in habit, gross morphological characters and base chromosome numbers but differ in only pollen morphology (Nyananyo and Olowokudejo 1986). The distinguished characters between these two species are briefly described on the basis of pollen features, seed surface morphology, and stomatal epidermal surfaces (Nyananyo and Olowokudejo 1986). The former belonging to pantoporate with 24–32 apertures (pollen type III) and later to pantocolpate with 15 aperture (pollen type II) (Nyananyo and Olowokudejo 1986; Nyanayo 1992). It is observed that plants (e.g., spinach, turnip leaves) that tend to accumulate HMs are appearing to be the most effective for the toxicity bioassay studies.

T. triangulare: A metallophyte

Since, *T. triangulare* is a common leafy vegetable among the other classes of vegetable that are grown in different parts of Nigeria, India and other parts of the world. The use of polluted water, contaminate soils and over use of pesticides knowingly or unknowingly for better cultivating of *Talinum* is a common practice for local farmers. Moreover, the unavailability of healthy agricultural inputs and high consumption of vegetables, many of the industrial, residential area, contaminate site, dump sites and polluted area have been converted as vegetable cultivating field (Adeniyi 1995; Yusuf et al 2003; Sekhar et al. 2007; Uwah et al. 2009). To analyze the HMs in edible part of the vegetable plant is always a desirable effort for many researchers in the past few decades (Uwah et al. 2009). The analysis of HMs in *T. triangulare* grown in Maiduguri, Nigeria showed that plant leaves were accumulated some HMs (Cr > Fe > Mn > Zn > Ni > Co > As > Pb > Cu > Cd due to use of waste water as well as excessive usage of manure, fertilizers, pesticides and herbicides in the study area (Uwah et al. 2009). However, the accumulated HMs were below toxic level as suggested by EPA and WHO (Uwah et al. 2009). In Nigeria, the information on the toxic elements in foods marketed in the country is very limited. Ukhun

et al. (1990) reported about the fresh vegetable available at various traditional markets in Nigeria have been analyzed for HMs contamination, Out of all vegetable, *T. triangulare* was contaminate with Cu (0.04), Zn (0.11), Mn (0.19), Pb (0.25), Cd (0.01), As (0.31) μg g^{-1} (Ukhun et al. 1990). The levels of Cd, Cu and Ni have been analyzed in *T. triangulare* grown at three industrial and three residential sites in Nigeria (Yusuf et al. 2003). Results obtained from the study showed that the HMs levels were higher in plant grown at industrial area than residential area. The Cd, Cu and Ni accumulation in the edible part of the plant ranged grown at industrial area were between μg g^{-1} dw 1.50 ± 0.09, 51.53 ± 7.18 and 1.33 ± 0.31 μg g^{-1} dw, respectively. While the level HMs grown at residential area were 0.81 ± 0.50, 24.41 ± 3.09 and 0.83 ± 0.27 μg g^{-1} dw for Cd, Cu and Ni, respectively. The average of Cd, Cu and Ni concentration in soils of industrial area were 13.41, 106.14 and 24.73 μg g^{-1} dw and in the soil of residential area were 7.98, 63.28 and 12.78 μg g^{-1} dw, respectively (Yusuf et al. 2003).

In India, Tiagi and Aery (1986) have reported first time about the Cu accumulation in leaf of *Talinum portulacifolium* from Khetri Copper Deposite of Rajasthan (India). It is reported to accumulate 394 μg g^{-1} dw Cu in its leaves (Tiagi and Aery 1986). Furthermore, Sekhar et al (2007) have suggested that *Talinum cuneifolium* as a suitable candidate for phytoremediation of As, as it accumulated higher concentration of As in its tissues grown at many sites in the industrial region of Patancheru, Hyderabad, India (Sekhar et al. 2007). Moreover, a laboratory experiments conducted with stem cuttings of *T. triangulare* in hydroponic media showed that the accumulation capacities of stem cuttings for Cu, Pb, Ni and Cd are much higher than other good accumulators of HMs (Rajkumar et al. 2009). The treatment concentrations and durations were affecting the number of leaves and initiation of root primordia. The stem cuttings were treated with Cu, Pb, Ni and Cd at concentration range of 0.50–20 mg L^{-1} for a treatment period of 49 days. Results obtained from these experiments showed that accumulation of Cu and Pb in stem tissues were ranged between

81.0–1,475.0 and 0.8–14.0, respectively, whereas the concentration above 2.0 mg L^{-1} Ni and 4.0 mg L^{-1} were reported to toxic concentrations and decay of the stem cuttings were observed at those concentrations points (Rajkumar et al. 2009).

Problems and Prospects

Literature surveys have confirmed that few reports are available on accumulation of HMs, particularly Pb, in *T. triangulare*. To the best of my knowledge, there is no literature available on Pb accumulation for *T. triangulare* under controlled conditions. There is also lack of information about the mechanisms involved in high accumulation capacities for toxic HMs, particularly Pb, and toxic symptoms and tolerance responses against those accumulated HMs in *T. triangulare*. Hence there is an urge for detailed investigations of toxicity and tolerance mechanisms in *T. triangulare* during Pb stress conditions.

Objectives

1. Establishment of field stock, hydroponics and study of Pb dose-responses.
2. Pb uptake and changes in morpho-physiological and biochemical parameters.
3. Pb-induced oxidative damage, genotoxicity and function of enzymatic and non-enzymatic antioxidants.
4. Pb-induced responses of ascorbate-glutathione, related metabolites and enzymes.
5. Proteomic approach for root proteins identifications exposed to Pb.

Objective 1

Establishment of field stock, hydroponics and study of Pb dose-responses

Introduction

The commercial production of ornamental plants is of a great economic importance in worldwide agriculture. The ornamental industry has widely applied *in vitro* propagation for large-scale plant multiplication of elite superior varieties. The propagation through shoot cutting of herbaceous plants has wide applications in ornamental plant production and the interest in ornamental or foliage plant production is increasing rapidly as result of their economic importance and their diversity. In soil, propagation through seed germination is a way to develop terrestrial plants. But, the soil system may affect seedlings growth due to different soil texture and the availability of nutrients. Similarly, in *Talinum*, soil nutrients like phosphorus, potassium and nitrogen in different combinations and pH cause variations in stem weight, leaf width or leaf area (Ukpong and Moses 2001). Besides this, *in vitro* propagation, by means of stem cuttings, is a key tool in plant biotechnology that exploits the totipotency of plant cells for rapid expansion and multiplication of plants. The main advantage of *in vitro* (vegetative) propagation is to produce a large number of vegetative propagules, adventitious roots and leaves. It is a reliable way of multiplying plants in a short period of time (Jain and Ochatt 2010). The regeneration of adventitious roots in excised leafy plant shoots is a crucial phenomenon and rooting ability depends on the many endogenous and exogenous factors such as species, type of cuttings, composition of nutrient medium, season of propagation, environment and propagation system (Németh 1986; Hartmann et al. 2002). *T. triangulare* is relatively easy to grow and has attractive foliage under an ideal environment. The importance of various species of genus *Talinum* was studied by various authors. **Table 4** is representing the geographic distribution and economic importance of genus *Talinum*.

Table 4 Geographical distribution and economic importance of different species of *Talinum*.

Species	Geographical Distribution	Economic importance	References
T. triangulare	Edo State, Nigeria	Herbal recipes for treating hypertension	Gbolade et al. 2012
T. triangulare	China	Antioxidant, hepatoprotective activities	Liang et al. 2011
T. triangulare	Benin	Useful in fever (leaf)	Allabi et al. 2011
T. triangulare	Nigeria	Measles (external use)	Ajibesin et al. 2008
T. paniculatum	Trinidad,	Ornamental, medicinal	Foxcroft et al. 2008
T. cuneifolium	Africa, America, Arabia, India	Ornamental, medicinal, vegetable	Lakshminarayana et al. 2007; Raju et al. 2007
T. triangulare	Africa, America, Arabia, India, Japan	Ornamental, saponins, vegetable	Fasuyi 2007; Khoda et al. 1992
T. calcaricum	America, Columbia, Georgia	Ornamental	Harris and Martin 1991
T. calycinum	America	Ornamental	Harris and Martin 1991
T. parviflorum	America	Ornamental	Harris and Martin 1991
T. mengesii	America, Georgia	Ornamental	Black and Murdy 1972
T. teretifolium	America, Georgia	Ornamental	Black and Murdy 1972

Stem cuttings of *T. triangulare* can propagate in hydroponic media and have potential to accumulate heavy metals (HMs) from contaminated media (Rajkumar et al. 2009). The aim of this study to established the *T. triangulare* in field, pot and hydroponic media. The propagation of plants was performed through stem cuttings. Further, we studied the dose and duration symmetric responses of Pb treatment at different concentrations and durations in hydroponic conditions. The study was performed to explore the stem cutting method in order to promote additional experimental applications.

Materials and methods

Plant material

T. trianulare is a succulent perennial plant that inhabits soil communities along the perimeter of rock outcrops. Materials required for experiments were collected from a field bank maintained as stock plant at the University of Hyderabad, India (**Fig. 5A**). Stem cuttings were excised from the branching portion by hand with a sharp razor blade. The average cutting diameter of each plant shoot was 5.0–7.0 mm and shoot height ranged from about 17–22 cm. The rooting test of each plant species involved three replication each consisting of 8 cuttings. Immediately after excision from the stock plants, the cuttings were propagated in soil and hydroponic media without any wetting agent treatment.

Propagation in soil

Stem cuttings of *T. triangulare* plants were potted in 5-L pots filled with a mixture of red soil and sand (pH-6.8) under greenhouse condition. Inside the greenhouse the photosynthetic photon flux density (PPFD) ranged from 900–1200 μmol m^{-2} s^{-1} with an average sunlight of 9–13 h day^{-1}. Potted *T. triangulare* plants were watered daily and examined for the formation of flowers and vegetative propagules (**Fig. 5B,C**).

Propagation in hydroponic medium

Excised stem cuttings of *T. triangulare* were placed in conical flask containing 100 mL of 10% modified Hoagland's media (**Table 5**) in plant growth chamber at 16/8 h day/night and at 28 ± 2 ºC (**Fig.6A,B**; Hoagland and Arnon, 1950). Phosphate and sulphate were replaced by chloride and nitrate and the pH of the modified solution was maintained at pH 4.8 to avoid the precipitation of nutrient media. Plants were kept for 3-weeks for

regeneration and acclimatization of adventitious roots (**Fig. 6C**). The nutrient media was replaced every 3 days to provide a fresh dose of nutrient elements and to avoid algal growth. Algal culture binds to the root outer surface and reduces the absorption of nutrient elements and inhibits root growth.

Table 5 Salt composition of modified Hoagland's nutrient solution.

Salts/Compounds	**Concentrations**
Macronutrients	
KCl	5.0 mM
$Ca(NO_3)_2$. $4H_2O$	2.0 mM
$MgCl_2$. $6H_2O$	2.0 mM
Micronutrients	
H_3BO_3	4.5 µM
$MnCl_2$. $4H_2O$	1.0 µM
$ZnCl_2$	0.8 µM
$Cu(NO_3)_2$. $3H_2O$	0.03 µM
$(NH_4)_6Mo_7O_{24}$	0.01 µM
Fe-EDTA	
$FeCl_3$	4.4 µM
EDTA	3.0 µM

Evaluation of propagules and rooting in hydroponic medium

Adventitious root formation in *T. triangulare* stem cuttings was calculated after a rooting period of 7, 14 and 21 days. Rooting of cuttings was not always successful and the percentage of surviving cuttings was calculated at 7 days. Cuttings that survived were used to analyze the mean number of vegetative propagules, mean root length and fresh weight (fw) at three different sampling periods (7, 14 and 21 days) to evaluate the commercial quality of stem cuttings.

Pb treatment: dose-duration analysis

The rational for selecting the various Pb concentration and treatment duration for the experimentation was based on preliminary bioassay with respect to toxicity. After three weeks of acclimatization, stem cuttings with uniform adventitious roots and leaves were selected and treated with $Pb(NO_3)_2$ at different Pb concentrations (0.05–5.00 mM Pb) in 10% modified Hoagland's solution for maximum 13 days to select the treatment concentration and treatment durations.

Statistical analysis

The experiments were repeated at least three times and the data presented corresponds to the mean values ± S.E. (standard errors) of three replicates (Microsoft Office 2003). One-way analysis of variance (ANOVA) were done with all the data to confirm the variability of data, and performed Duncan's multiple range test (DMRT) by using SIGMASTAT software (version 11.0) to determine the significant difference between treatment group. *P* values ≤ 0.05 were considered significantly different with each other and denoted by different letters.

Results

Propagation in soil

In the soil system survival rate of the plant cuttings was 87% at 7 days. Potted cuttings were healthy and flowered within a week of culture. In the soil system, stem cuttings of 21 and 14 days showed a 3.2 and 2.3 fold increases in the number of flowers than 7 days stem cuttings, respectively (**Fig. 7A**). Similarly, stem cuttings propagated for 21 days showed a 1.4 fold more increases in the number of flowers than stem cuttings propagated for 14 days (**Fig. 7A**). *Talinum* is predominantly self-pollinated or vegetatively propagated. Thus, for 21 days the vegetative propagules showed a 4.2 and 1.6 fold increase more than 7 and 14 days, respectively. Furthermore, 14 days cuttings showed a 2.6 fold increase in the number of propagules more than 7 days cuttings (**Fig. 7B**).

Propagation in hydroponic medium

Results of our study showed that the propagation of stem cuttings in hydroponic media and laboratory conditions generally produced a high survival rate of 94% at 7 days. In terms of vegetative propagules, 21 days stem cutting showed a 3.8 and 1.8 fold increases more than 7 and 14 days stem cuttings, respectively (**Fig. 7B**). In hydroponic media, stem cuttings of 21 and 14 days showed a 6.2 and 3.0 fold increases; respectively in the root length more than 7 days stem cuttings (**Fig. 6D, 7C**). Similarly, stem cuttings propagated for 21 days showed a 1.6 fold increase in the root length more than stem cuttings propagated for 14 days (**Fig. 7C**). Furthermore, 21 days root fw showed a 1.6 and 6.2 fold increases more than 14 and 7 days stem cuttings, respectively (**Fig. 7D**). Similarly, stem cuttings of 14 days showed a 3.7 fold increased in the root fw more than stem cuttings of 7 days (**Fig. 7D**).

Selection of Pb concentration for treatment

Pb treatment at different concentrations caused different level of phytotoxicity, which includes chlorosis, visible damage of leaf, stem and root. Based on visible observation Pb concentrations of 0.25, 0.50, 0.75, 1.00 and 1.25 mM were selected for treatment concentrations (**Table 6**). Most of selected Pb concentrations were showing less, moderate and high toxic symptoms at maximum seven days of treatments (**Fig. 8**).

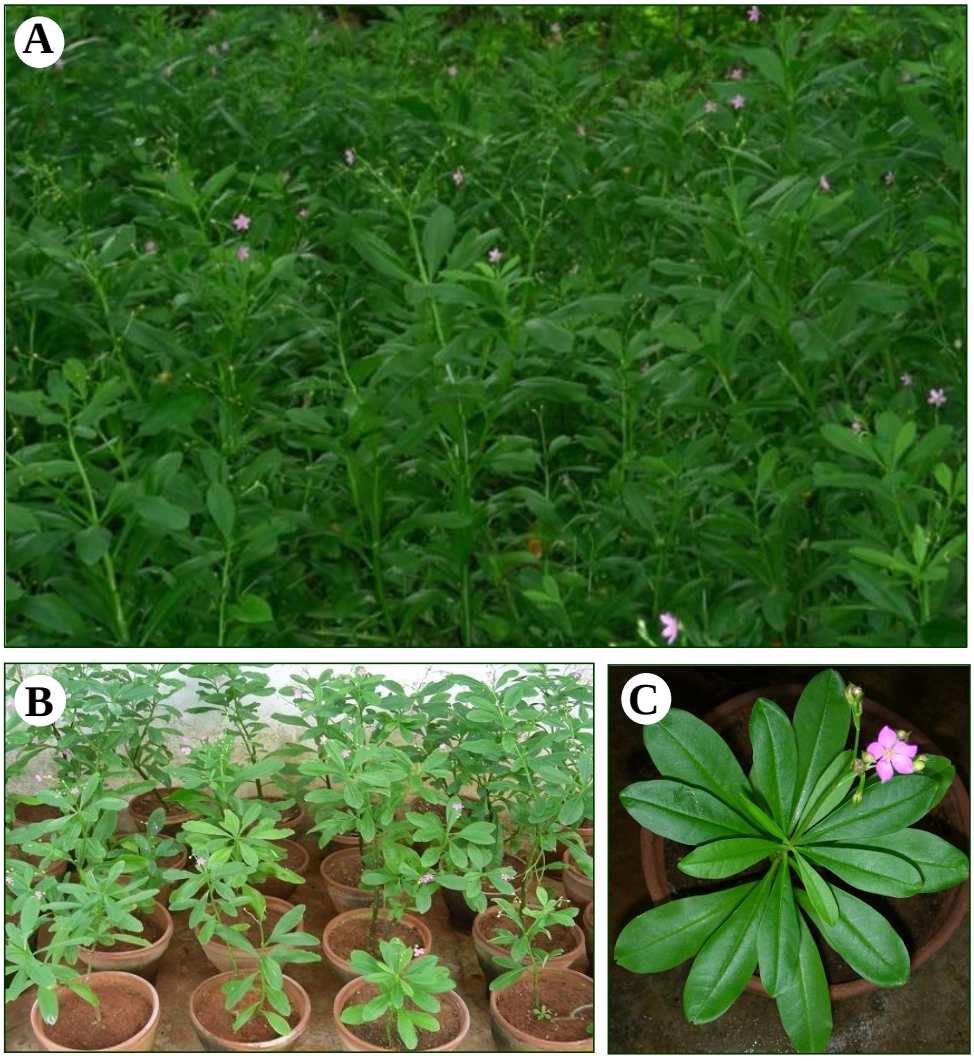

Fig. 5 Propagation of *T. triangulare* in field and greenhouse conditions: Widespread plants with flowers and seeds in field **(A)**, plantlets grown in the pots under greenhouse condition **(B)** and plant in soil culture at 21 days **(C)**.

Thus, maximum 7 days was selected as treatment durations. The flasks without $Pb(NO_3)_2$ were kept with each set of experiments to serve as control. After treatments, roots, stem leaves were excised after maximum 7 days and were processed for analysis of various endpoints described in subsequent objectives.

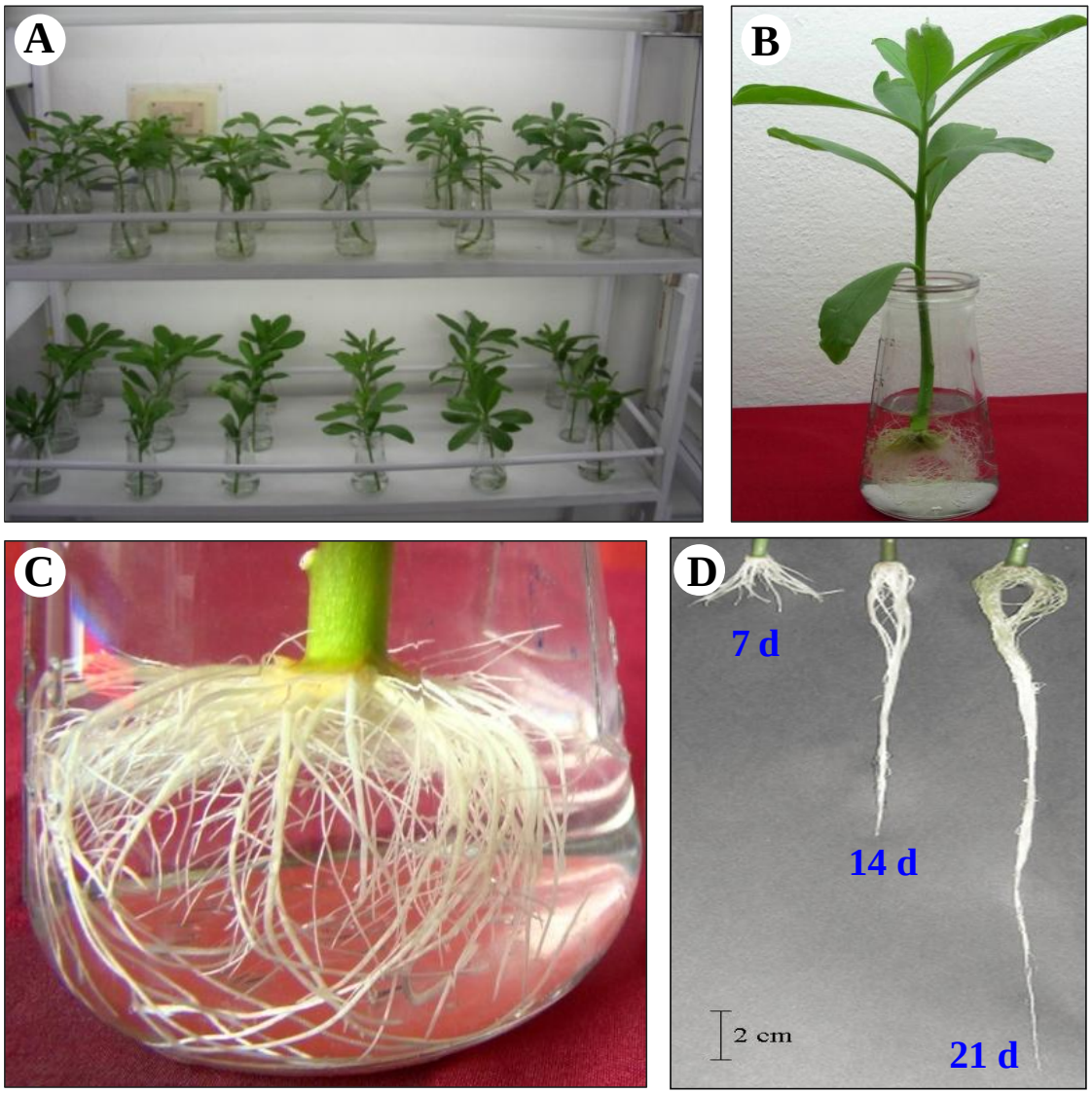

Fig. 6 Propagation of *T. triangulare* in hydroponic conditions. (A) Hydroponic set-up for stem cuttings in modified Hoagland's nutrient solutions in laboratory conditions, **(B)** plantlets grown in the hydroponics media with adventitious roots, **(C)** adventitious roots of *T. triangulare* in hydroponic media in laboratory conditions after two weeks and **(D)** adventitious roots developed under hydroponic conditions at 7, 14 and 21 days.

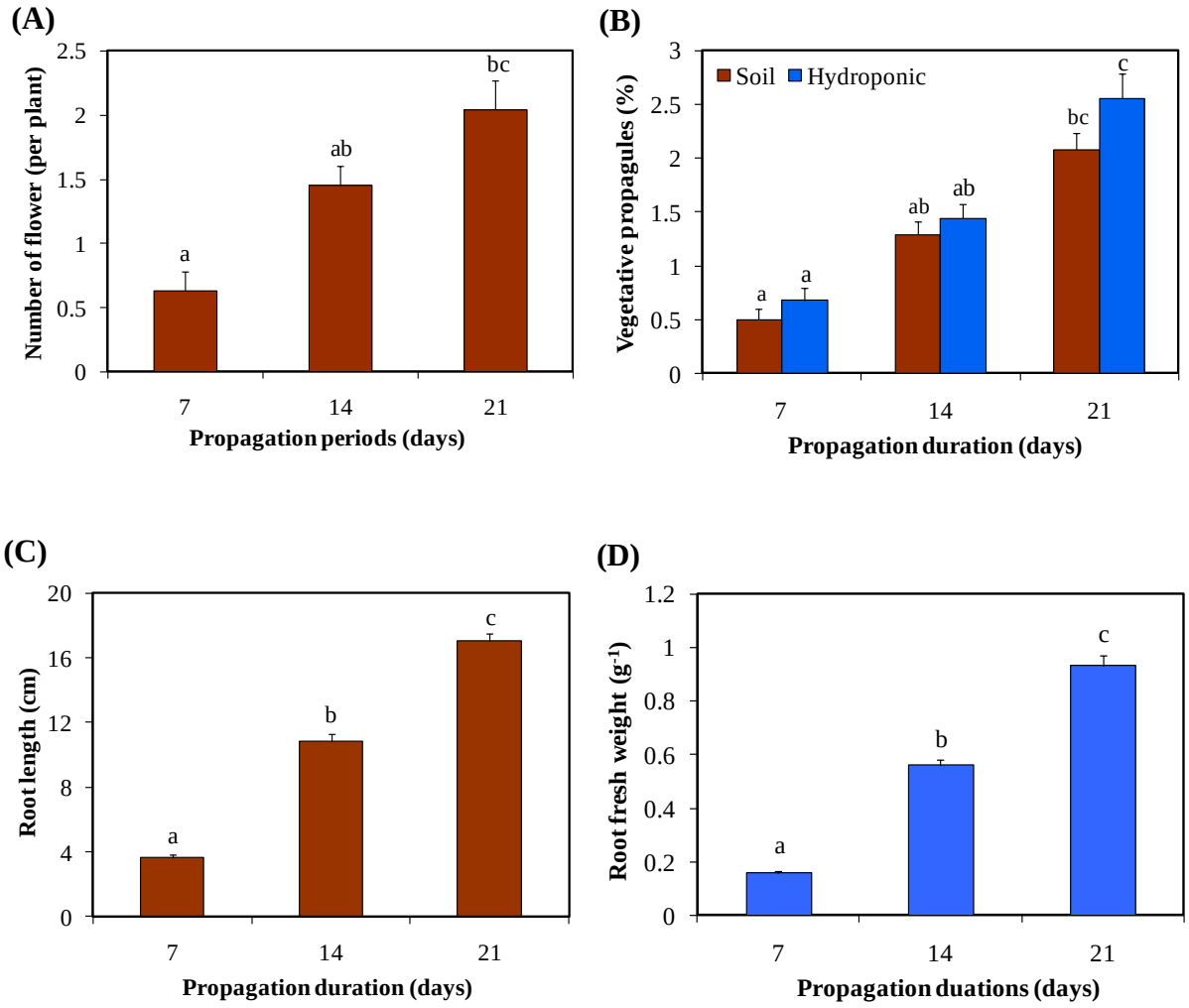

Fig. 7 Number of flowers in soil conditions **(A)**, vegetative propagules in propagated stem cutting in soil and hydroponic media **(B)**, adventitious root length in hydroponic media **(C)** and adventitious roots fresh weight in hydroponic media **(D)** after after 7, 14 and 21 days. Mean values (± S.E.) of three replicate (n= 8) denoted by different letters are significantly different ($P \leq 0.05$) between each other.

Table 6 Dose and duration symmetric scheme for selecting the treatment concentration and durations on the basis of visible observations: Y- healthy; LS- less stress; HS- high stress; X- Lethal.

	Treatment durations (days)												
$Pb(NO_3)_2$ (mM)	1	2	3	4	5	6	7	8	9	10	11	12	13
0.00	Y	Y	Y	Y	Y	Y	Y	Y	Y	Y	Y	Y	Y
0.05	Y	Y	Y	Y	Y	Y	Y	Y	S	S	HS	HS	X
0.10	Y	Y	Y	Y	Y	Y	LS	LS	LS	HS	HS	HS	X
0.20	Y	Y	Y	Y	Y	LS	LS	LS	LS	HS	HS	HS	X
0.30	Y	Y	Y	Y	Y	LS	LS	LS	HS	HS	HS	X	
0.40	Y	Y	Y	Y	LS	LS	LS	HS	HS	HS	HS	X	
0.50	Y	Y	Y	Y	LS	LS	LS	HS	HS	HS	X		
0.75	Y	Y	Y	Y	LS	LS	LS	HS	HS	X			
1.00	Y	Y	Y	LS	LS	HS	HS	HS	X				
1.25	Y	Y	Y	LS	LS	HS	HS	HS	X				
2.50	Y	Y	LS	LS	HS	HS	HS	X					
3.75	Y	Y	LS	HS	X	X							
5.00	Y	Y	LS	HS	X	X							

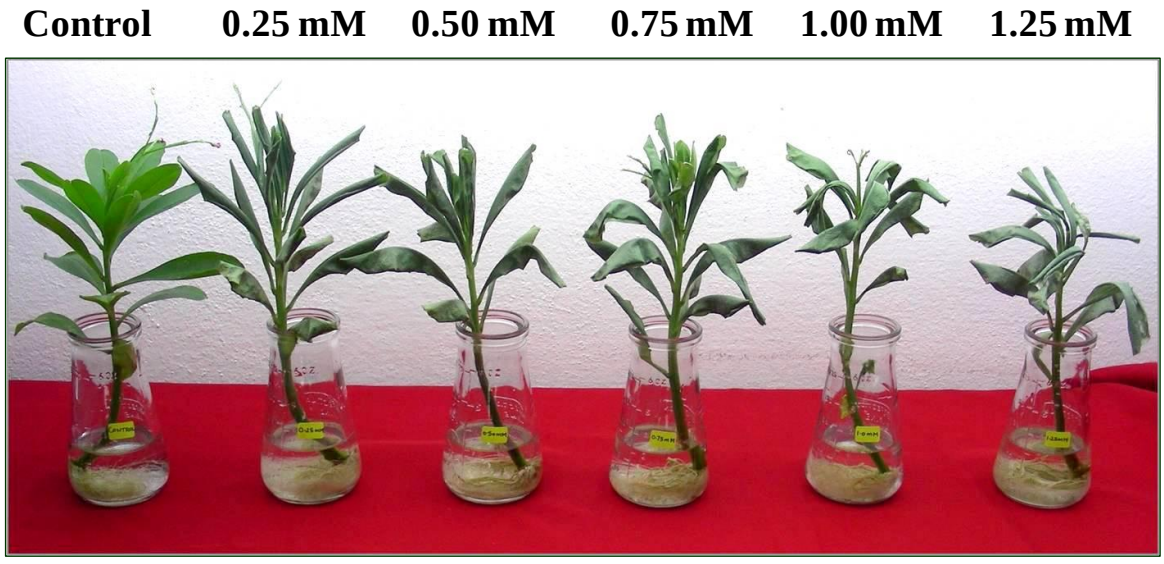

Fig. 8 Aspect of *T. triangulare* plant grown in Hoagland's solution containing different concentration of $Pb(NO_3)_2$ for 7 days.

Discussions

T. *triangulare* and other members of this genus are considered as rock outcrop plants because different species of this genus grow on granite, serpentine, sandstone, and limestone rocks (Black and Murdy 1972; Ware and Pinion 1990). During the experiment potted plants were observed daily to understand their ability to acclimatize in soil. Results of our observation confirmed that *T. triangulare* plants are mostly multiplied through vegetative propagation and produced numerous vegetative propagules on their senescing stem tips. The number of flowers and vegetative propagules were increased and directly dependent on propagation periods (**Fig. 7**). Shoot tip explants are routinely used for the propagation of ornamental plants, including *Ardisia japonica* (Roh et al. 2005), *Begonia tuberous*, *Ranunculus asiaticus* L., *Dianthus caryophylus* L., *Jasminum officinale* L. (Jain and Ochatt 2010), *Ebenus cretica* (Hatzilazarou et al. 2001), *Pelargonium hortorum* (Druege et al. 2007), *Rosa hybrida* L. (Bredmose and Hansen 1995) and *Zantedeschia albomaculata* (Chang et al. 2003). The sustainable growth of *T. triangulare* makes continuous demands on soil properties and it is necessary to restore the nutrients and increase the sustainability of soil by the application of nutrients and organic manure. Soil multiplication is a powerful tool for large-scale propagation of ornamental plants and further, having application for phytoremediation. Phytoremediation is a cost-effective, nonintrusive technique and an emerging green technology that uses the ability of certain plant species to remove toxic metals or substances from the soil. It has been reported that *Portulaca oleracea*, another member of the family Portulacaceae (previously include genus *Talinum*), can survive for a longer periods in spite of accumulating more toxic metals than reported hyperaccumulators such as *Helianthus annus* and *Brassica juncea* in the presence of electroplating industrial effluents (Jenita et al. 2010).

In laboratory conditions, *Talinum* plants can be maintained effortlessly in hydroponic media. Plants were observed with adventitious roots in hydroponic media (**Fig. 6C,D**). The higher percentage of survival of cuttings showed that plants grew easily in hydroponic media. The root primordia at the base of stem cuttings were observed within one week of culture. Root parameters such as length and fresh weight of adventitious roots were enhanced and increased exponentially over time (**Fig. 6C and 7C,D**). Almost no variation in the root diameter was observed. The above parameters (vegetative propagules, root length and root fresh weight) of stem cuttings in hydroponic media showed minimum values after 7 days indicating that the initial week is required for acclimatization of plants stem cuttings under such conditions. Our results suggested that the formation of any vegetative propagules and adventitious roots in *T. triangulare* cuttings was promoted by hydroponic media and growth conditions.

The growth of *T. triangulare* plants is directly dependent on the growth of roots in hydroponic media because the growth and survival of terrestrial plants are related to the potential ability of roots to absorb water and nutrient elements from the soil or growth media (Eapen et al. 2005). The advantages of water culture are that plant roots are suspended only in water medium containing inorganic and organic form of nutrient elements. The plant growths not only avoid soil but also soil containing salts and soil-borne microorganisms. They may interrupt nutrient uptake and plant growth by precipitating salts or affecting the pH of the solution. On the other hand, hydroponic culture provides only liquid nutrient medium to plants and a generous availability of nutrients promote rapid plant growth. Additionally, in hydroponic conditions plant are growing bit fast and gives extensive adventitious roots, which are easy to harvest at any time of plant growth.

Hydroponically cultivated adventitious roots of several terrestrial plants were used for rhizofiltration, a process used for absorbing or precipitating toxic metals effectively from a

polluted site (Dushenkov et al. 1995). Adventitious roots of *T. triangulare* plants have the potential to absorb heavy metals and might be useful for a new rhizofiltration system. *Talinum* plants could absorb heavy metals and were used for absorption experiments of heavy metals i.e. Pb, Cd, Ni, Cu (Rajkumar et al. 2009). Absorption of heavy metal content induces some ultrastructure modifications in root tissues concerning the increase in cell wall thickness (Probst et al. 2009). The methods of propagation in hydroponic media have a significant influence on the production of adventitious roots and new leaves. Very rapid development of adventitious roots in *Talinum* plants indicates that a one week period required for the establishment of a potential plant propagation system for rhizofiltration. Furthermore, with the help of adventitious roots we can study the effect of foliar retention, absorption of heavy metals and also various aspects of abiotic stresses in root tissues.

Conclusions

In the present study, stem cuttings of *T. triangulare* were successfully propagated in soil and hydroponic media. However, we conclude that in vitro (vegetative) propagation through stem cuttings is a key tool for rapid expansion and multiplication of *T. triangulare*. The property of growing both in soil and hydroponic media, *T. triangulare* plant can be used as an indoor and outdoor ornamental plant. The main advantage we observed was extensive growth of adventitious roots in a short period of time. Hydroponically grown shoots, with adventitious roots can serve as an ideal experimental system for for plant research or toxicity bioassays. Furthermore, Pb concentration at 0, 0.25, 0.50, 0.75, 1.00 and 1.25 mM for a maximum of 7 days treatment duration were selected for Pb toxicity bioassays with *T. triangulare* in hydroponic conditions.

Objective 2

Pb uptake and changes in morpho-physiological and biochemical parameters

Introduction

Lead (Pb), a non-essential element, widely present in the various ecosystems as a result of natural and technogenic activities of human being. Various industrial activities introduced large amount of Pb in the form of liquid, solid and gas waste in to the environments. Pb is extremely persistent in the soil, air, water and foodstuffs with no biological significance, has been a global concern (Anonymous-ATSDR 2007; Anonymous-INSA 2011).

Pb-induced phytotoxicity and photoxidative damage

Lead is a non-redox active metal and a known environmental toxicant for plants and other biota, which can easily, absorbed and accumulated in plants tissues. In plant, Pb cells cause molecular damage either directly or indirectly through the formation of reactive oxygen species (ROS) (Sharma and Dubey 2005; Wang et al. 2010; Pourraut et al. 2011a; Shu et al. 2012). The ROS changes membrane structure and function by attacking on the polyunsaturated fatty acid of membrane lipids, initiating lipid peroxidation and altered cell biochemical activities (Reddy et al. 2005; Sun et al. 2010; Maldonado-Magaña et al. 2011). Pb is a non-essential for plant metabolism and exhibit varied degrees of phytotoxicity including adverse effects to photosynthesis (Tang et al. 2009). Pb accumulation in different parts of plant is not only depends upon the exogenous concentration, but also on the phytochemistry and soil physico-chemcial conditions (Reddy et al. 2005; Mishra et al. 2006). As a non-redox active metal, Pb can replace essential metals or cofactors at enzyme active site causing imbalance in cellular redox status. Plants exposed to Pb showed changes in photosynthetic rate due to distortion of chloroplast ultrastructure, impairments of chlorophyll synthesis, imbalance in plastoquinone, reduced minerals uptake and obstructed electron transport (Sharma and Dubey 2005; Sengar et al. 2008; Cenkci et al.

2010; Pourraut et al. 2011a). Chlorophylls and total carotenoid are considered as simple and reliable indicators of Pb–induced phytotoxicity in higher plants (Krupa et al. 1996). ROS production in higher plants not only affects the chlorophylls but also changes the lipids such as sulphoquinovosyldiacyl-glycerol (SQDG) compositions. SQDG is the deacylation product of sulpholipid and comprises up to 24% of the four major chloroplast lipids. In higher plants approximately 40% of the thylakoid SQDG was tightly associated with LHC II (Harwood and Okanenko, 2003). SQDG is implicated in regulation of light energy distribution between the two photosystems via the phosphorylation of the mobile antennae (Larsson and Andersson 1985).

HMs affects on chlorophyll fluorescence

Lead and other HMs cause the changes in fluorescence parameters of higher plants as a results of harmful effects caused by these toxicants, as the inhibition of photosynthetic pigment biosynthesis, damage of oxygen evolving complex (OEC), decrease of photosystem (PS) II and I activity and inhibition of energy transfer to PSII-reaction center (RC) and inhibition of electron transport between OEC and PSII-RC (Kalaji and Loboda 2007; Subrahmanyam 2008; Gupta et al. 2009; Cenkci et al. 2010; Drążkiewicz and Baszyński 2010). The analysis of PSII function from higher plants could provide a great opportunity to build a system for HMs toxicity bioassays. Pb has been reported to affect the light harvesting complexes of PSII and PSI and the chloroplast coupling factor (Miles et al. 1972). Chlorophyll (Chl) fluorescence and photosynthetic Chl fluorescence are competitive processes and have opposite mechanism with each other (Mallick and Mohn 2003). The measurement of Chl fluorescence through Pulse Amplitude Modulated (PAM) fluoremeter is a noninvasive technique, which can analyze through the without disrupting the integrity of the tissue/cell and give an extact idea about the Pb affect in photosynthetic mechaniry (Maxwell and Johnson 2000).

Protective role of non-enzymatic antioxidants from HMs-induced oxidative stress

Plant cells are protected against ROS by enzymatic and non-enzymatic antioxidative defense systems. Non–enzymatic antioxidative system, involves carotenoids, phenols, flavonoids and glutathione etc., are known to play an important role in scavenging ROS. Anthocyanins (in vacuole) and α-tocopherol (membrane associated) are major secondary metabolites found in the plants against oxidative stresses (Araceli et al. 2009; Hernández et al. 2009). Their antioxidant activities are due to by capturing free radical ions by donation of phenolic hydrogen atoms and protect the plant cells from adverse effects of abiotic stresses (Hernández et al. 2009). Another important property of anthocyanins is that they react with alkaloids, other flavonoids, organic acids, biomolecules and metals forming complexes and stabilizing the colour in plants (Araceli et al. 2009). The most active form of vitamin E is α-tocopherol, which is capable of scavenging free oxygen radicals and lipid peroxides. It has been reported that abiotic stress factors might alter tocopherol levels in plant tissues (Collin et al., 2008; Yusuf et al., 2010). In addition to flavonoids, glutathione is widely distributed in living cells and the oxidized form of glutathione (GSSG) is readily converted in to reduced form (GSH) by the enzyme glutathione reductase (GR) (Wang et al. 2010; Maldonado–Magaña et al. 2011; Anjum et al. 2012).

Talinum species have been used to investigate a variety of environmental problems. Moreover, toxicity and tolerance on various biological parameters have been investigated in a number of experimental model systems (Sharma and Dubey 2005; Sengar et al. 2008). In this study, *Talinum triangulare* grown hydroponically were exposed to different concentrations of Pb (0, 0.25, 0.50, 0.75, 1.0 and 1.25 mM) to investigate the oxidative damage and associated biomarkers of toxicity and tolerance mechanisms. Further, analysis carried out to understand the mechanisms of actions of Pb to the photosystems the relation of Chl contents, Chl fluorescence and photosynthetic electron transport was investigated.

Materials and methods

Hydroponic experiment and Pb treatment

T. triangulare was propagated through stem **c**uttings (5.0–7.0 mm diameter and 17–22 cm height) in conical flask containing 100 mL of modified Hoagland's media in plant growth chamber at 16/8 h (day/night) and at 28 ± 2 °C (Hoagland and Arnon 1950) for 3 weeks. After 3 weeks of acclimatization, uniform stem cuttings with adventitious roots and leaves were treated separately with $Pb(NO_3)_2$ at different Pb concentrations of 0 (control), 0.25, 0.5, 0.75, 1.0 and 1.25 mM for maximum 7 days under above conditions. Roots, leaves and stems were separated from treated plants after 1, 3, 5 and 7 days were used for the study of various parameters. All the treatments were repeated at least three times.

Quantification of Pb accumulation in plant

Metal treated plants roots were washed thoroughly with 0.1 M HNO_3 to remove metals adsorbed to the surface. Roots, stems and leaves were separated and oven dried at 80 ºC for two days. Dried plant materials were acid digested with 4 mL of $HNO_3/HClO_4$ (3:1 v/v) and the digested material was dissolved in the 10 mL of 0.1 N HNO_3. This solution was analyzed for Pb content using Atomic Absorption Spectrophotometer (AAS, GBC 932 plus, Australia). The standard reference material of Pb (Sisco Research Laboratories Pvt. Ltd. Mumbai, India) was used for caliboration of instrument for every batch. Recovery of the Pb from the tissue was found to be more than 84.81±0.07% as determined by spiking sample popular and *Phragmites australis* (riet) with known amount of Pb.

Detection of relative water content (RWC)

Plant leaves were freshly weight (fw) and were kept in water at 4 ºC for 2 hours to know turgid weight (tw). After that leaves were oven dried at 60 ºC till completely dry

followed by the estimation of dry weight (dw). The relative water content (RWC) was calculated according to Gao et al. (2010) : **RWC (%)** = [(fw–dw/tw–fw)] × 100

Detection of cell death

To determine changes in viability of cells after Pb treatment, 0.1 g of freshly harvested leaves were stained with 0.25% (w/v) aqueous solution of Evans blue for 15 min (Baker and Mock 1994) with slight modifications. After staining leaves were washed with miliQ water for 30 min, followed by soaked in 3 mL of N, N-dimethylformamide for 1 h at room temperature. The absorbance of released Evans blue was measured at 600 and 652 nm and was expressed as A_{600} after correction for chlorophyll.

Elemental analysis by energy dispersive X- rays spectroscopy (EDS)

Energy-dispersive X-ray spectroscopy (EDS) is an analytical technique used for the elemental/chemical analysis of specimen. Thin transverse sections were prepared from leaves of *T. triangulare* treated with 0, 0.25 and 1.25 mM of Pb. Sectioned tissues were dehydrated, mounted on aluminium stubs, coated with gold-palladium and elemental analyses were done with EDS (Oxford instruments) coupled with field emission scanning electron microscope (FESEM, Ultra 55- Carl Zeiss) and wavelength dispersive X-ray spectroscopy (WDS, Oxford instruments). The EDS analysis was carried out at an operating voltage of 20 KV and working distance of 8.5 mm. With the help of the INCA software, X-ray emission based spectral peaks were analyzed. Electron-induced X-rays were detected by Si drift detector (Oxford Instruments) by measuring typical spectrum (contains characteristic peaks) intensities. A typical spectrum contains characteristic peaks for present elements, which are superimposed on a slowly varying background. This background contribution is carefully subtracted from the spectrum. Once these intensities have been determined, a comparison is then made with standards of known composition

with the INCA software applications, which uses filtered least squares (FLS) technique for this filtering and fitting. The energy resolution of EDS detector is 70 to 130 eV (depending on the elements) imposes a limit on the separation of peaks. When peaks overlap, it is still possible to interacted individual peak area, provided that the corresponding peak shapes are accurately known. The differences in analyzed elements energies are more than 130 eV. Thus, there were no overlapping of the peaks and the elements were detected easily.

Lipid peroxidation

Lipid peroxidation in leaves was determined as a function of malondialdehyde (MDA) content following the method of Heath and Packer (1968) with slight modifications. Leaves (0.2 g) were homogenized in 3 mL 0.1 M tris buffer containing 0.3 M sodium chloride. After that 2 mL of 20% trichloroacetic acid (TCA) containing 0.5% 2-thiobarbituric acid (TBA) and 2 mL 20% TCA. Mixture was heated at 95 °C for 30 min. After heating the homogenate mixture were kept in ice for cooling followed by centrifugation at 10,000 g for 5 min. Absorbance of the supernatant was taken at 532 nm. MDA was calculated by using extinction coefficient of 155 mM^{-1} cm^{-1}.

Chlorophylls and carotenoids estimation

Extraction and estimation of chlorophyll and carotenoid contents were carried out by the method of Arnon (1949) and Duxbury and Yentsch (1956), respectively. *T. triangulare* leaves (0.1 g) were ground in 5 mL chilled 80% acetone in dark. After centrifugation at 5,000 g for 10 min at 4 ºC, absorbance of supernatant was taken at 480, 645 and 663 nm. Chlorophylls and carotenoids were calculated by using the following equation:

Chlorophyll *a* = $12.3 \times A_{663} - 0.86 \times A_{645}$

Chlorophyll *b* = $19.3 \times A_{645} - 3.60 \times A_{645}$

Carotenoids = $A_{480} + 0.114 \times A_{663} - 0.638 \times A_{645}$

The chlorophylls and carotenoids were calculated in mg g^{-1} fw and represented in mg g^{-1} dw based on the relative water content in leaves (Tang et al. 2009).

Sulphoquinovosyl diacylglycerol estimation

Plant leaves (0.2 g) were homogenized with 0.5 g glass powder and 0.5 g $Na_2(SO_4)$. The homogenate was transferred to a glass column and 3 mL acetone was added for filtration. To the filtrate 1 mL hexane: benzene (4:1 v/v) and 2 mL H_2O was added and centrifuged at 5,000 g for 5 min at room temperature (RT). After centrifugation 1 mL of the bottom layer was added to 1 mL of 0.01% azure (prepared in acetone) and 2 mL benzene, and again centrifuged at 5,000 g for 5 min at RT. The upper layer was collected and absorbance was measured at 610 nm. The calculation of SQDG was based on the standard curve of sodium dodecylsulphate according to Kean (1968).

Chlorophyll fluorescence and P700 analysis

Prior to simultaneous assessment of Chl fluorescence and P700 measurements, *T. triangulare* leaves were dark-adapted for 45 min to obtain oxido-reduction equilibrium of PSII-PSI electron transport carriers. The Dual-Pulse Amplitude Modulated fluorometer (Dual-PAM-100, Heinz Walz GmbH, Germany) was used to measure the rapid polyphasic Chl fluorescence and P700 kinetic during 800 ms induction by a saturation pulse of 6,000 μmol photons m^{-2} s^{-1}. The actinic photon flux density was 339 μmol m^{-2} s^{-1}. The measurements were performed at room temperature (25 °C) in the dark (Strasser and Strasser 1995; Force et al. 2003).

Anthocyanins estimation

Anthocyanins were extracted from 0.5 g of leaves with 10 mL of mixture of n-propanol: HCl: H_2O (18: 1: 81, v/v/v). The samples were heated in boiling water bath for

30 min and then they were incubated for 24 h in the dark at 4 ºC. Extracts were filtered and absorbance was taken at 535 and 650 nm. Anthocyanins contents were calculated according to Lange et al. (1971) and Bette and Kutschera (1996) and were expressed as A_{535} g^{-1} fresh weight after correction for chlorophyll:

$$\mathbf{A_{535}} = A_{535} - 0.22\times A_{650}$$

α-Tocopherol estimation

Concentration of α-tocopherol was measured in leaves as described by Szymańska and Kruk (2008) with some modifications. Fresh leaves (1.0 g) were homogenized in mortar with 20 mL of ice chilled methanol (HPLC grade). The extracts were centrifuged at 10,000 g for 15 min at 4 ºC. The supernatant were collected and was filtered through 0.2 µm millipore filter and stored in ice in dark. The α-tocopherol content in filtrate was determined by using High Performance Liquid Chromatography (HPLC) with a C_{18} reverse-phase column (250 x 4.60 mm 5 microns Phenomenax, UK) at a flow rate of 1 mL min^{-1}, using isocratic solvent system of methanol: ethyl acetate (1:4 v/v) as an eluant. Thirty microliters of the samples were injected by a microliter syringe and α-tocopherol content was quantified by UV-visible detector system at 295 nm (LC-10 AT VP Shimadzu, Japan). Peak identification of analyzed leaf extract was performed by comparing with the retention time of standard α-tocopherol. Chromatogram peak area of leaf sample was integrated and the concentration of α-tocopherol was calculated with regard to the peak area of the corresponding standard α-tocopherol.

Glutathione estimation

The GSH and GSSG estimation was done fluorometrically by following the method of Hissin and Hilf (1976) with slight modification. Control and treated leaves (0.5 g) were

homogenized in 4 mL of 0.1 M sodium phosphate-EDTA buffer (pH 8.0) containing 25% H_3PO_3. The homogenate was centrifuged at 15000 g for 20 min at 4 ºC. After centrifugation supernatants were collected and used for GSH and GSSG content. For GSH assay 0.5 mL supernatant was diluted with 4.5 mL sodium phosphate-EDTA buffer (pH 8.0) and mixed well. From diluted mixture 100 µL of supernatant was collected and mixed with 1.8 mL sodium phosphate-EDTA buffer (pH 8.0) and 100 µL *o*-phthaldialdehyde (OPT) followed by dark incubation for 15 min at room temperature (RT). GSSG contents were measure by incubating the 0.5 mL supernatant with 200 µL of 0.04 M N-ethylmaleimide for 30 min at RT. After incubation mixed 4.3 mL sodium hydroxide (0.1 N) and mixed well. After mixing 100 µL of mixture was mixed with 1.8 mL 0.1 N sodium hydroxide solution and 100 µL of OPT and incubated for 15 min in dark at RT. Fluorescence intensity from GSH and GSSG were determined in incubated samples at 420 nm after excitation at 350 nm with FluoroMax 3 fluorescence spectrophotometer. GSH, and GSSG in roots were calculated from the standard curve. The content of GSH, GSSG total glutathione was expressed as µ mol g^{-1} fw.

Statistical analysis

The experiments were repeated three times and the data presented corresponds to the mean values ± S.E. (standard errors) of three replicates (Microsoft Office 2003). One-way and two-way and two way analysis of variance (ANOVA) were done with all the data to confirm the variability of data and validity of results, and performed Duncan's multiple range test (DMRT) by using SIGMASTAT software (version 11.0) to determine the significant difference between treatment group. Correlation analysis was performed wherever required. *P* values ≤ 0.05 were considered significantly different with each other and denoted by different letters.

Results

Visible Symptoms

Our study showed that Pb treatment caused visible chlorotic mottling of leaves after 7 days of Pb exposure (**Fig. 9**). In all Pb treated plants, especially 1.00 and 1.25 mM, the visible damages, chlorosis and irreversible necrosis have observed on the leaf edges.

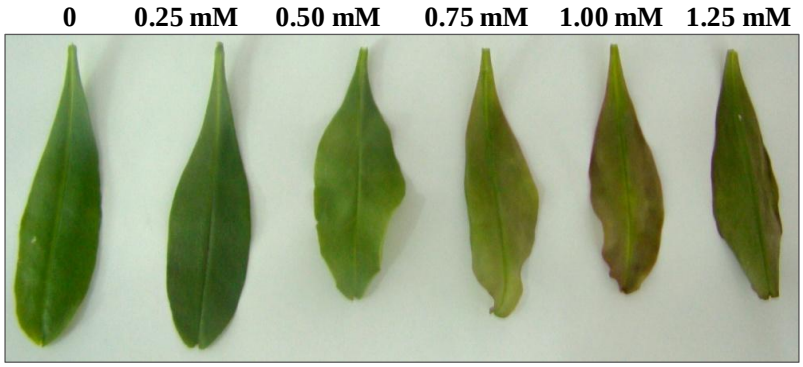

Fig. 9 Visual symptoms observation, chlorosis, in *T. triangulare* leaves after 7 days under different Pb treatment.

Lead accumulation in plant

T. triangulare was found to be sensitive to Pb exposure and the Pb accumulation was calculated in tissues on dry weights (dw) basis. When the *T. triangulare* cuttings were raised under increasing concentration of Pb, the Pb accumulation in plant parts increased significantly as compared to control (**Table 7**). Roots were the main accumulation site as they absorbed much higher quantities (19.9 mg g^{-1}dw) than stems (2.67 mg g^{-1}dw) while in leaves, Pb accumulation has been observed below detectable limit after 7 days of treatment. The translocation factor (TF) of root to stem was calculated by the Pb contents in stem/ Pb content in root. Result showed that TF values are always below 1.0 and it

decreased as the Pb treatment increased from 0.25 to 0.75 mM Pb (**Fig. 10A**). Further the TF value more or less stabilized at 1.0 and 1.25 mM Pb treatment.

Lead-induced changes in relative water content

Relative water content in the leaves of *T. triangulare*, after 7 days of Pb treatment, decreases gradually (**Fig. 10B**). RWC significantly decreased by approximately 6% at 0.25 mM to 19% at 1.25 mM of Pb, respectively in comparison to control. The water imbibition rates also decreased steadily with increasing Pb concentration.

Lead-induced cell death

Pb-induced oxidative damage in *T. triangulare* leaves were confirmed by the staining with Evans blue (**Fig. 10C**). A dose-dependent response for cell death was also evident for treatments with different concentrations of Pb. There was no significant difference between control and 0.25 mM Pb treated plant leaf. Evans blue accumulation in leaf was significantly increased maximum by 137% at 1.25 mM Pb treatment in respect to control.

Lead-induced lipid peroxidation

Experimental results of MDA estimation, an indicator of lipid peroxidation, showed that the MDA concentrations were significantly ($P \leq 0.05$) increased than control after Pb treatment and were directly related to the treatment concentrations. MDA concentration in leaves of *Talinum* plants were elevated after 7 days due to Pb toxicity and the magnitude of elevation ranged from 1.4 to 2.1 folds at 0.25 to 1.25 mM of Pb more than controls, respectively (**Fig. 10D**). Seven days of Pb treatment prompted a greater increase in the level of MDA at 1.25 mM and was 1.5 fold increased in compare to 0.25 mM of Pb.

Table 7 Lead accumulation in roots and stem of *T. triangulare* grown for 7 days at different doses of $Pb(NO_3)_2$.

Pb concentration (mM)	Concentration of Pb taken up by plant (mg g^{-1} dw)	
	Roots	**Stem**
0	ND	ND
0.25	3.14 ± 0.3^{a}	0.81 ± 0.04^{a}
0.50	7.85 ± 1.2^{b}	1.18 ± 0.28^{ab}
0.75	13.5 ± 1.4^{c}	1.70 ± 0.17^{b}
1.0	15.5 ± 1.6^{c}	1.88 ± 0.16^{c}
1.25	19.9 ± 0.9^{d}	2.67 ± 0.07^{d}

In a column, means followed by different letter(s) are significantly differ ($P \leq 0.05$) according to DMRT; ND: not detectable.

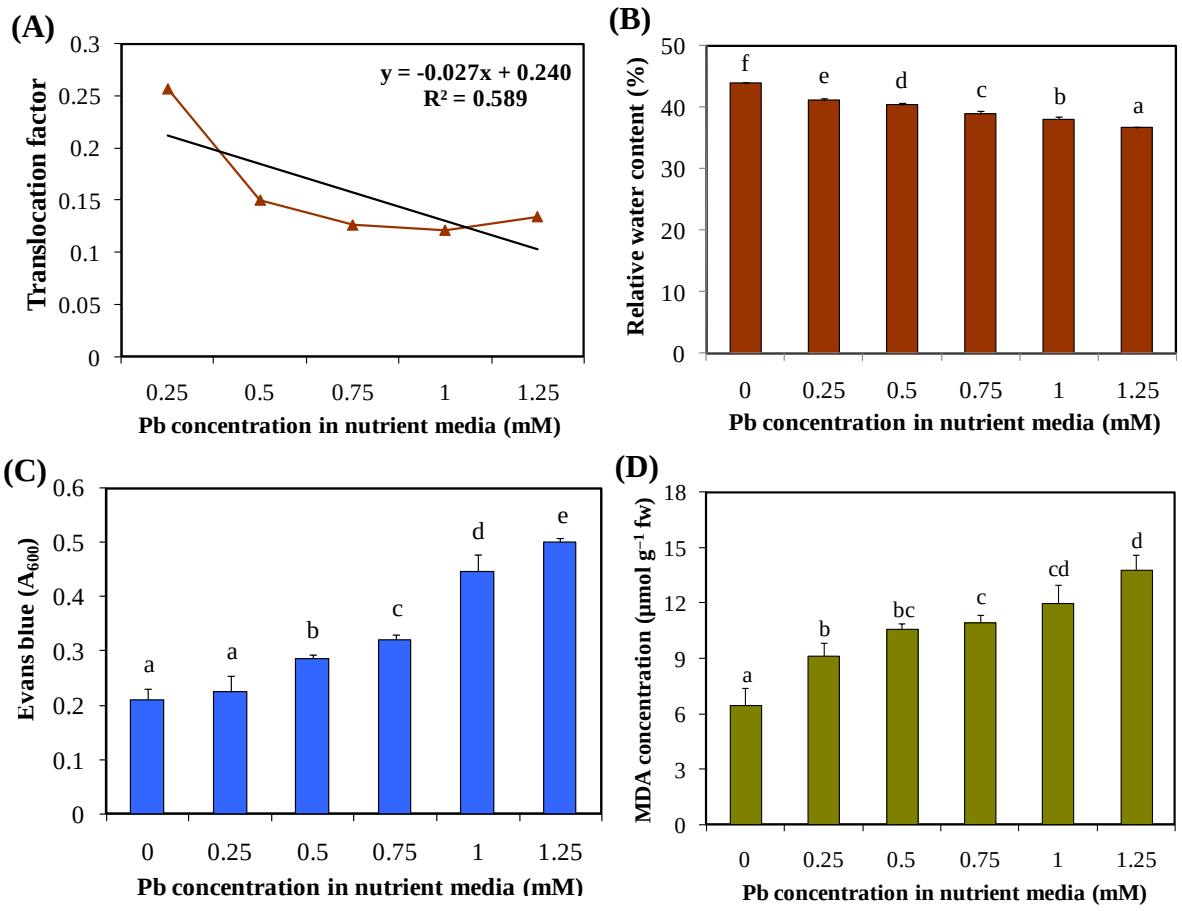

Fig. 10 Translocation factor of Pb from root to stem **(A),** relative water content **(B)**, Cell death through Evans blue staining **(C)** and lipid peroxidation through MDA content measurement **(D)** in *T. triangulare* leaves after 7 days of Pb treatment. Mean values (± SE) denoted by different letters are significantly different ($P \leq 0.05$) between each other.

Elemental analysis by EDS

Results of energy dispersion spectroscopy give the atomic or chemical characteristics of analyzed tissue. As a first barrier to metals toxicity, most plants accumulate metals and nutrients in the roots and restrict its transport to the shoots and leaves. Microanalysis of elements was performed at the same site in 0, 0.25 and 1.25 mM of Pb-treated plant samples. In all sample the Pb concentration was below the EDS detectable limit (**Fig. 11A-C**). The other elements such as oxygen (O), potassium (K), magnesium (Mg), chlorine (Cl), sodium (Na), silicon (Si) and copper (Cu) were detected in leaf tissues (**Fig. 11A-C**). In analyzed sample, O and K were contributed as major elements. Trace elements include Mg, Cl, Na, Si, Cu and Ca. X-ray microanalysis of untreated samples showed high spectral peak for all elements, except for O, in comparison to treated (at both 0.25 and 1.25 mM of Pb) plant. Only calcium (Ca) was observed in leaf sample treated with 1.25 mM of Pb (**Table 8**). Qualitative percentage composition analysis revealed that the percentages of all elements were decreased in both treated plant leaves except O which was increased in Pb treated plant leaves.

Table 8 Analysis of atomic percentage (%) of elements by energy dispersive spectroscopy (EDS) in leaves of *T. triangulare* treated with 0 (control), 0.25 and 1.25 mM of Pb for 7 days.

	Atomic % of elements in leaves of *T. triangulare*		
Elements	**Control**	**0.25 mM Pb**	**1.25 mM Pb**
O	71.33	75.14	76.13
K	20.3	19.47	18.45
Mg	3.61	1.76	1.58
Cl	3.11	3.01	3.0
Si	0.58	0.29	0.38
Cu	0.4	0.33	ND
Na	0.67	ND	ND
Ca	ND	ND	0.46

ND: not detectable

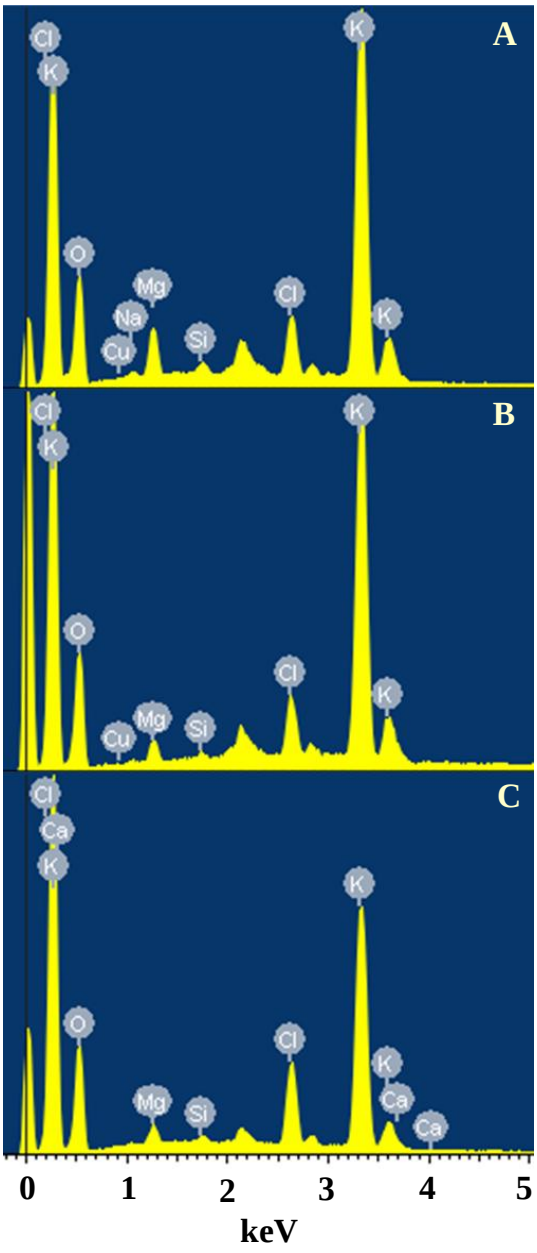

Fig. 11 Energy dispersive X-ray spectral line profile of transverse section of *T. triangulare* leaf: control **(A)**, 0.25 mM Pb **(B)** and 1.25 mM Pb **(C)**. EDS micrograph showed elemental atomic percentage of the imaged area for the samples using FESEM/EDS.

Lead-induced changes in chlorophyll contents

Chlorophylls concentrations showed an inverted U-shaped curve with the increasing Pb concentrations after 1 day of treatment period. Moreover, chlorosis of leaves was observed after 5 days at higher Pb concentrations, which was further increased with subsequent treatment period. In leaves decreased chlorophylls contents were observed at higher concentrations (0.75, 1.0 and 1.25 mM) of Pb (**Fig. 12**). The highest concentration of Chl *a, b* and total chlorophyll were found at 0.5 mM after 1 day and at 0.25 mM after 3, 5 and 7 days of Pb treatment. Contents of Chl *a, b* and total chlorophyll were significantly ($P \leq 0.05$) increase by approximately 17%, 37% and 24% over control at 0.50 mM of Pb after 1 day, respectively. After 7 days at 1.25 mM of Pb concentration, there were approximately 19%, 8% and 14.8% decrease in Chl *a, b* and total chlorophyll in comparison to control, respectively (**Fig. 12**).

Lead-induced changes in SQDG concentration

The SQDG concentration significantly ($P \leq 0.05$) increased at 0.25, 0.5 and 0.75 mM and decreased at 1.0 and 1.25 mM of Pb treatment in comparison with control after 1 day (**Fig. 13**). The tendencies to decrease the SQDG concentrations were observed at 1.0 and 1.25 mM of Pb after all treatment periods. However, after 5 and 7 days the SQDG concentration showed dose-dependent reduction at higher concentration of Pb. After 1 day at 1.0 and 1.25 mM of Pb, SQDG concentrations were decreased and at control level, but in the subsequent period increase in SQDG concentrations have been observed. After 7 days SQDG concentrations at 0.75, 1.0 and 1.25 mM of Pb significantly ($P \leq 0.05$) decreased to approximately 55%, 70% and 68% in compare to control, respectively, but in compare with 0.5 mM of Pb concentration decreased to approximately 37%, 38% and 13%, respectively (**Fig. 13**).

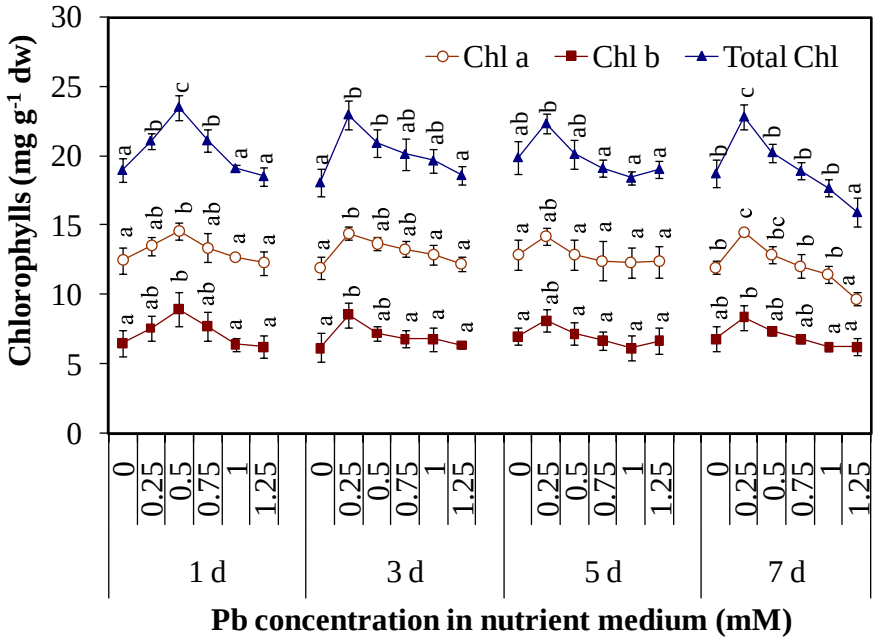

Fig. 12 Changes in chlorophyll *a*, chlorophyll *b* and total chlorophyll contents in *T. triangulare* treated with different Pb concentrations. Mean values (± SE) denoted by different letters are significantly different ($P \leq 0.05$) between each other in each group.

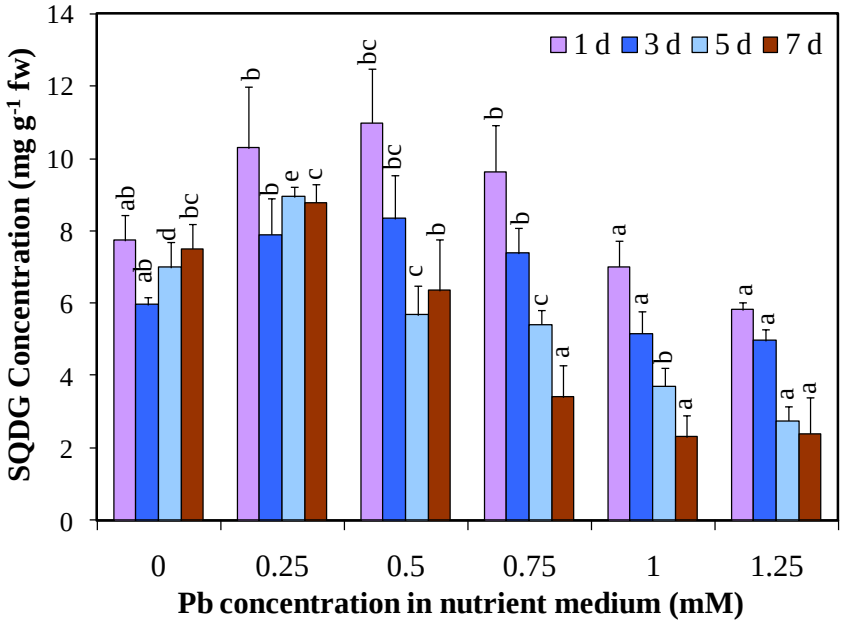

Fig. 13 Changes in sulphoquinovosyl diacylglycerol (SQDG) contents in leaves of *T. triangulare* treated with different Pb concentrations. Mean values (± SE) denoted by different letters are significantly different ($P \leq 0.05$) between each other in each group.

Lead-induced changes in chlorophyll fluorescence and P700

Results of Chl fluorescence showed that maximal fluorescence yield (F_m) was decreased in Pb treated leaf (**Fig. 14A**). Pb caused linear significant (R^2= 0.856; $P \leq 0.05$) dose-dependent reduction during 0.25, 0.50, 0.75, 1.0 and 1.25 mM Pb treatments that accounted for ca. 19%, 34%, 39%, 42% and 45% as compared to control, respectively (**Fig. 14A**). Experimental findings of maximal quantum yield (F_v/F_m) and effective quantum yield (Φ_{PSII}) were showed the linear decrease for F_v/F_m (R^2= 0.962, **Fig. 14B**) and Φ_{PSII} (R^2= 0.882, **Fig. 14C**) during all Pb treatment. The highest significantly ($P \leq 0.05$) decrease in F_v/F_m were observed at 0.75 (8.8%), 1.0 (16.2%) and 1.25 mM Pb (19%) with control, respectively. The significant decline in the Φ_{PSII} in 0.25, 0.50, 0.75, 1.0 and 1.25 mM Pb treated leaf of *T. triangulare* were ca. 23%, 37%, 44%, 49%, 53% in comparison to control, respectively.

The tendency of photochemical quenching (*q*P) was almost similar to that of F_v/F_m values (R^2= 0.940; **Fig. 14D**). The *q*P in leaf decreased significantly ($P \leq 0.05$) at 0.50–1.25 mM of Pb, which was accounted for 30.5% and 50% in comparsion to control. Result of non-photochemical quenching (*q*N) showed significant ($P \leq 0.05$) increase value at 0.25–1.25 mM Pb in comparison to control, respectively (**Fig. 14E**). The maximum increase in *q*N was observed at 1.25 mM Pb by 21.2% when compared to control.

On the other hand, linear increase of quantum yields of regulated energy dissipation [Y(NPQ)] (R^2= 0.983) and non-regulated energy dissipation [Y(NO)] (R^2= 0.966) were observed in Pb treated leaves (**Fig. 15A, B**). In comparison to control, the value of Y(NPQ) significantly ($P \leq 0.05$) increased to ca. 22.5%, at 1.25 mM Pb. In terms of Y(NO), it is significantly increased by ca. 35%, 42% and 52% during 0.75, 1.0 and 1.25 mM Pb treatment with respective control (**Fig. 15A, B**).

PAM results revealed that photosynthetic electron transport rate (ETR) of both PSII and PSI were decreased, with a negative linear correlation of (R^2= 0.981) and (R^2= 0.919), after 7 days of Pb treatment, respectively (**Fig. 15C,D**). ETR of PSII was observed to decreased significantly at 0.75 (45%), 1.0 (49%) and 1.25 (62.5%) mM Pb in comparison to control leaf (**Fig. 15C**). Similarly, photosynthetic ETR of PSI also observed significantly decrease by 37.8% and 41% at 1.0 and 1.25 mM Pb treated leaves (**Fig. 15D**). The ETR of PSII is showed good correlation (R^2= 0.841) with ETR of PSI.

PAM results of P700 or PSI showed that maximal P700 change (P_m) and photochemical quantum yield [Y(I)] were decreased in *T. triangulare* leaves (**Fig. 15E,F**) with a positive linear correlation of (R^2= 0.987) and (R^2= 0.968) after 7 days of Pb treatment, respectively. A significant decrease in Pm values was observed at 0.50–1.25 mM Pb after 7 days of Pb treatment, which is ranged from 21.2% to 51.2% in comparison to control, respectively (**Fig. 15E**). The level of Y(I) was not significantly affected up to 0.75 mM of Pb. Maximum significant depletions in Y(I) were observed by ca. 37% and 46% in plant leaves treated with 1.0 and 1.25 mM Pb when compared to control, respectively (**Fig. 15F**).

Lead-induced changes in carotenoids contents

The analysis of carotenoids contents were performed after 1, 3, 5 and 7 days of Pb treatments. In leaves decrease in carotenoid contents were observed at higher concentrations (0.75, 1.0 and 1.25 mM) of Pb. The carotenoid contents were significantly different ($P \leq 0.05$) at 0.25, 0.5 and 0.75 mM Pb among all treatment periods in comparison to control. After 1 and 3 days of treatment at 0.5 and 0.25 mM of Pb, carotenoid content was significantly increased up to 26% and 40% in comparison to control, respectively (**Fig. 16A**).

Lead-induced changes in anthocyanins concentration

Anthocyanins accumulation was performed 1, 3, 5 and 7 days of Pb treatments. In our experiment, anthocyanins accumulation was higher at 0.25 mM of Pb compared with control after all treatment periods (**Fig. 16B**). In comparison to control 1.7 fold reductions in anthocyanins have been observed at 1.25 mM of Pb treatment after 1 day. But interestingly after 7 days of Pb exposure, anthocyanins were increased and almost at the control level. Significant (at 0.25 mM of Pb) and insignificant (at 0.5-1.25 mM of Pb) increases in anthocyanins were observed after 3 days of treatment periods. The concentrations of anthocyanins were (significant, $P \leq 0.05$) increased at 0.5 and 0.75 mM of Pb treatment after 5 and 7 days of treatment period. Pb-induced an intense anthocyanins accumulation, especially after the seventh day of treatment. The maximum concentrations of anthocyanins were observed at 0.5 and 0.75 µM of Pb and were 1.7 and 1.6 fold increased than control, respectively (**Fig. 16B**).

Lead-induced changes in α-tocopherol concentration

The HPLC analysis of leaf extracts were calculated by comparison of retention time and UV absorption spectra with those obtained for corresponding standards. Peaks were observed at 3.42 ± 0.025 min for α-tocopherol in standard and leaf extract (**Fig. 17A**). Results showed that the α-tocopherol content gradually increased in treated plants in compare to control. But after 7 days significant ($P \leq 0.05$) increase in the α-tocopherol level has been observed at higher (0.75– 1.25 mM) doses of Pb. The levels of increased α-tocopherol ranges from 1.2 to 2.2 fold at 0.25 to 1.25 mM of Pb in comparison to control (**Fig. 17B**).

Lead-induced changes in glutathione

The level of reduced (GSH) and oxidized (GSSG) glutathione directly point towards the induction of oxidative stress by Pb (**Fig. 18A,B**). GSH content in plant leaves were found to increase at all Pb treatment except that 1.25 mM of Pb. The level of GSH was not significantly affected at 0.25 and 1.25 mM of Pb. GSH level showed a maximum value at 0.50 mM of Pb which was about 23% higher than control. Maximum depletion in GSH content was observed by ca. 12.5% in plant treated with 1.25 mM of Pb when compared to control (**Fig. 18A**). On the other hand, GSSG level was found to gradually increased at concentration in comparison to control (**Fig. 18B**). Maximum GSSG content was found at 1.25 mM which was ca. 172% higher than control. However, the ratio of GSH to GSSG significantly decline and was inversely related to the Pb treatments (**Fig. 18C**).

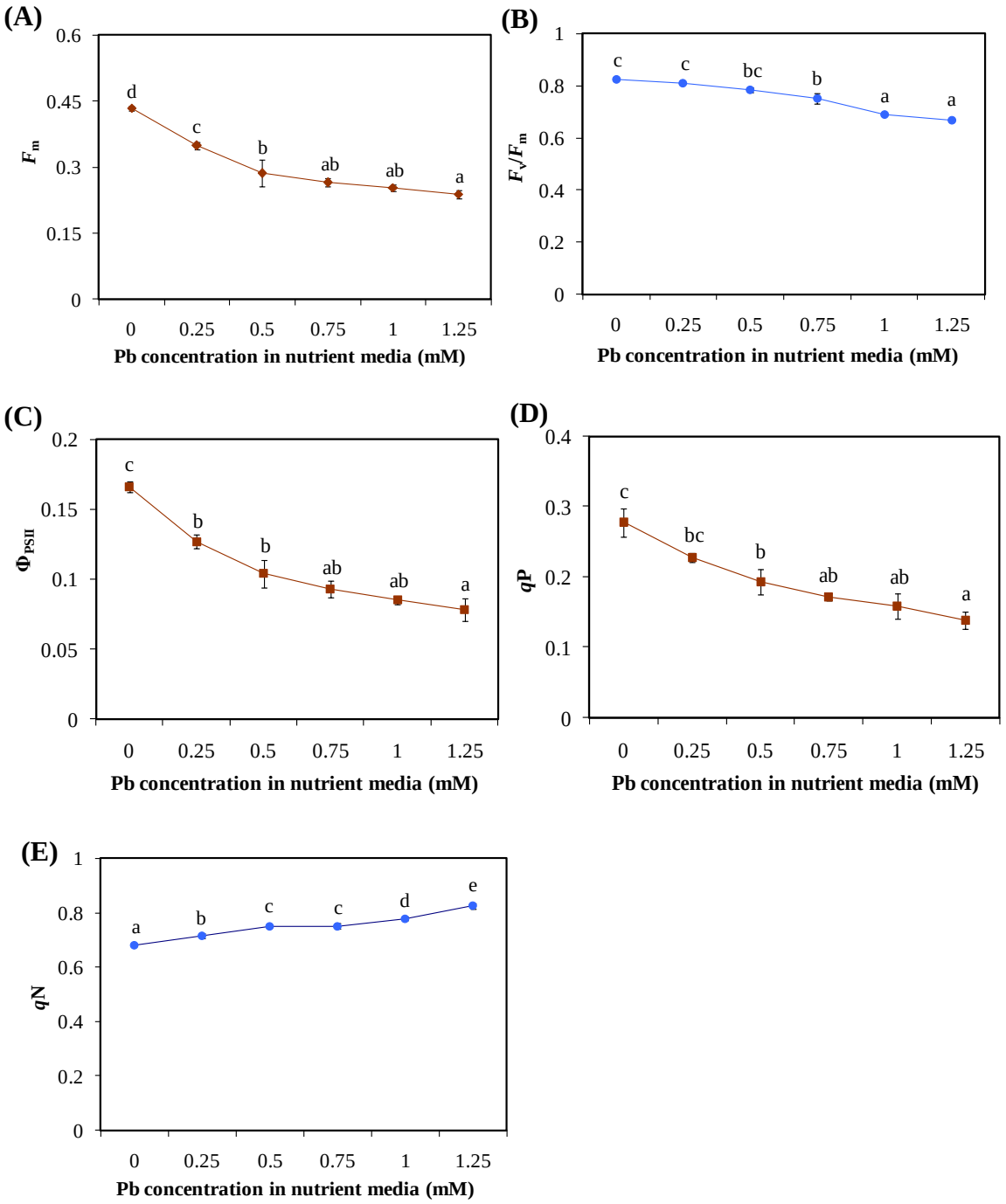

Fig. 14 Changes in chlorophyll fluorescence: (A) maximal fluorescence yield (F_m), **(B)** maximal PSII quantum yield (F_v/F_m), **(C)** effective PSII quantum yield (Φ_{PSII}), **(D)** coefficient of photochemical quenching (*q*P) and **(E)** coefficient of non-photochemical quenching (*q*N) in *T. triangulare* leaves treated with different Pb concentrations. Mean values (± SE) denoted by different letters are significantly different ($P \leq 0.05$) between each other.

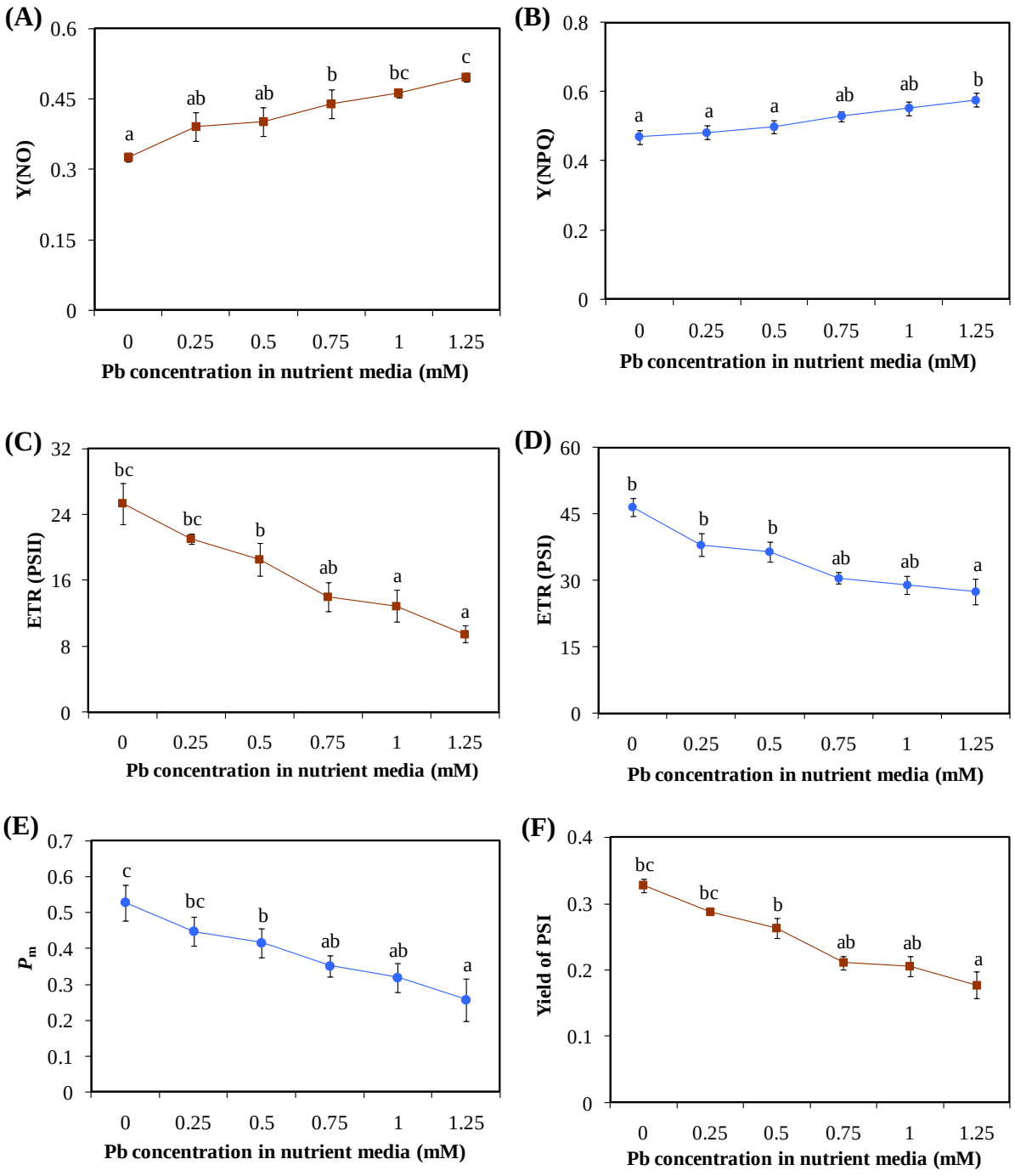

Fig. 15 Changes in quantum yields of **(A)** non-regulated energy dissipation [Y(NO)] and **(B)** regulated energy dissipation of PSII; **(C)** electron transport rate (ETR) of PSII, **(D)** ETR of PSI; **(E)** maximal P700 change (P_m); **(F)** photochemical quantum yield of PSI [Y(I)] in *T. triangulare* leaves treated with different Pb concentrations. Mean values (± SE) denoted by different letters are significantly different ($P \leq 0.05$) between each other.

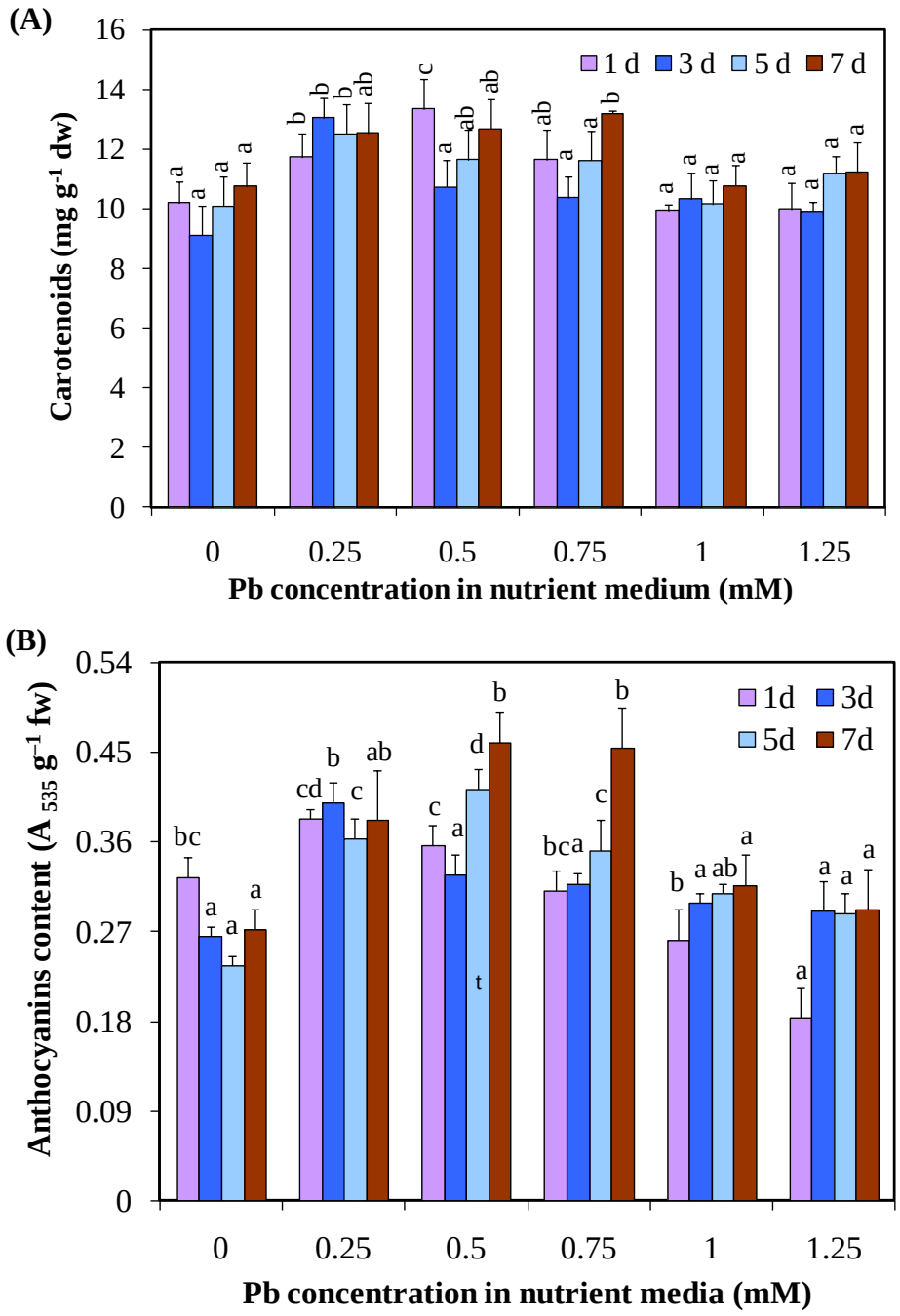

Fig. 16 Changes in carotenoids contents **(A)** and accumulation of anthocyanins **(B)** in *T. triangulare* leaves treated with different Pb concentrations. Mean values (± SE) denoted by different letters are significantly different ($P \leq 0.05$) between each other in each group.

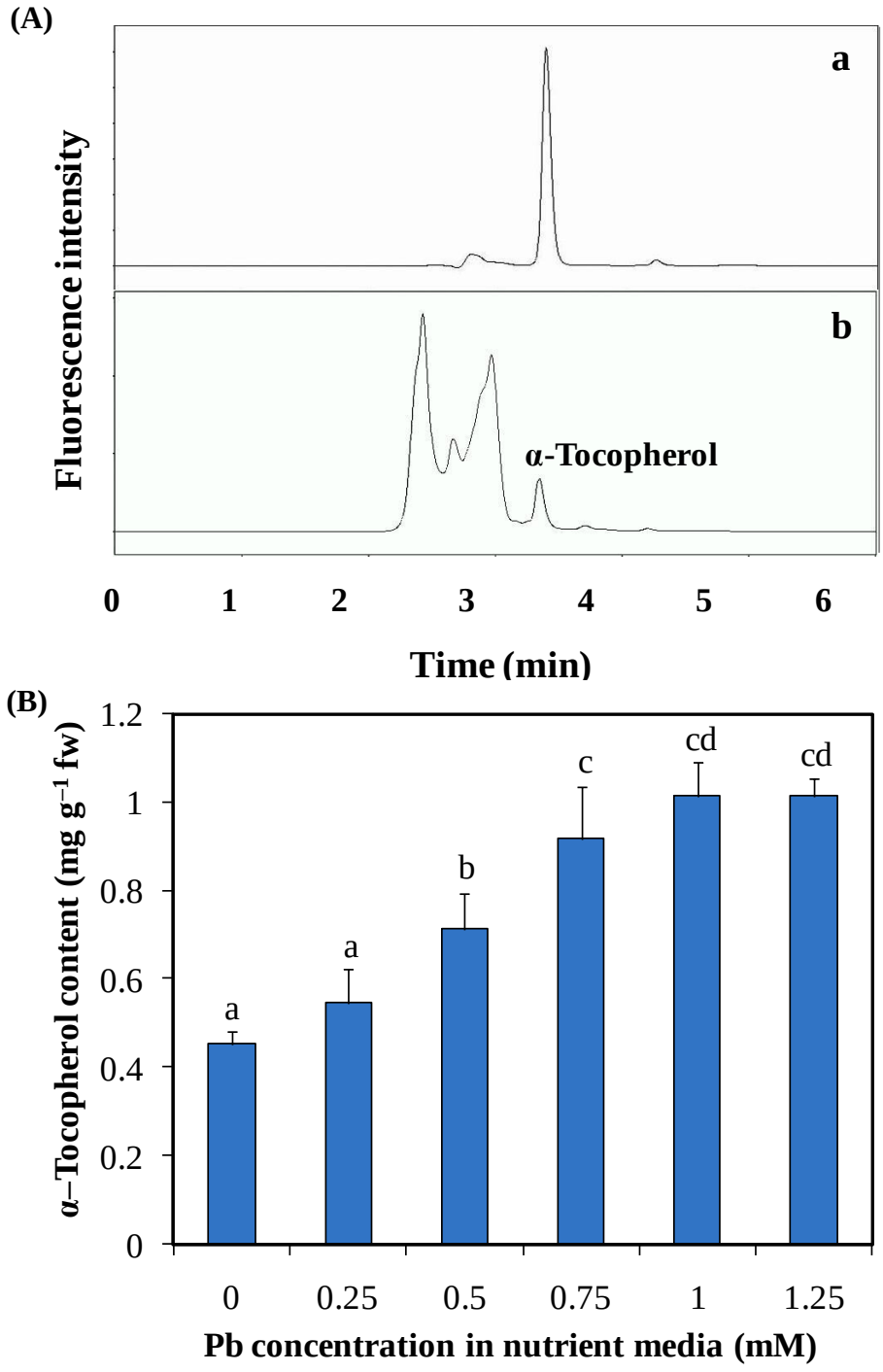

Fig. 17 α-Tocopherol estimation through high performance liquid chromatography: **(A)** chromatograms of α-tocopherol (**a**) standard solution (**b**) leaf extract. **(B)** α-Tocopherol concentration in *T. triangulare* leaves treated with different Pb concentrations. Mean values (± SE) denoted by different letters are significantly different ($P \leq 0.05$) between each other.

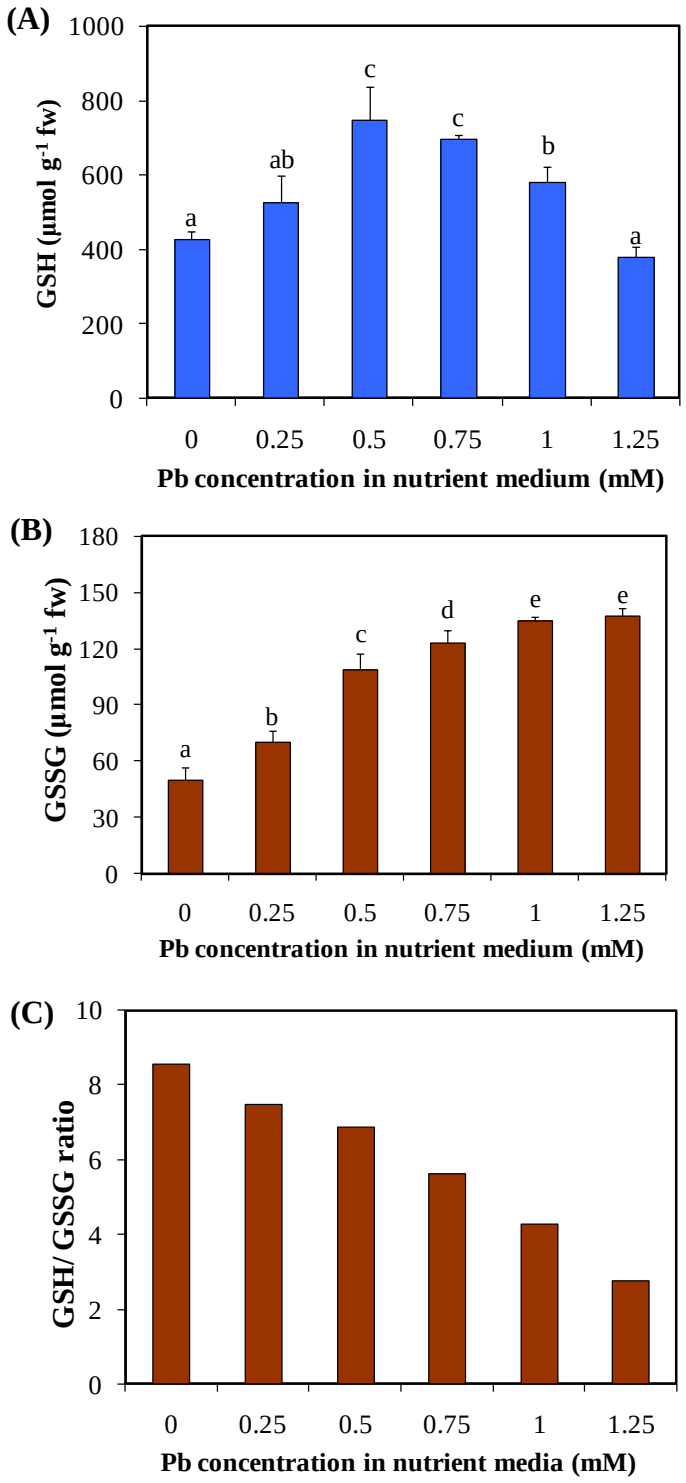

Fig. 18 Levels of reduced glutathione (GSH) **(A)** and **(B)** oxidized glutathione (GSSG) and **(C)** GSH/GSSG ratio in *T. triangulare* leaves treated with different Pb concentrations. Mean values (± SE) denoted by different letters are significantly different ($P \leq 0.05$) between each other.

Discussion

In the present study, the Pb accumulation in the tissues increased as the exogenous Pb concentration increased. The efficiency of metal uptake by plants depends on several processes for metal uptake by roots and its translocation from root to the shoot. Roots absorbed high amount of Pb than stem (**Table 7**). Probst et al. (2009) also reported that *Vicia faba* roots absorbed more metals than stems and leaves. The order of metal accumulation was root > leaf > stem for all HMs except for Pb and Cd where the order was root > stem > leaf for *Vicia faba* (Probst et al. 2009). This order may vary in different plant and different experimental conditions. In our experimental system, Pb was not detected in the leaves of treated plants. Lower intensity of Pb in the stems (**Table 7**) and below detectable limit in leaves of Pb treated plants confirmed the decreased translocation of Pb within the plants (**Fig. 10A**). It is confirmed by Tian et al. (2011) that Pb is rather immobile within the plants, and accumulated mostly in the vascular bundles of the plant tissues and it could not re-translocated in the tissues even after treatment with a metal chelating agent i.e. EDTA (ethylenediaminetetraacetic acid). The immobilization of Pb^{+2} on *T. triangulare* roots could represent a new and attractive characteristic for the development of phytoremediation strategies requiring that the large amount of the toxic substances remain tightly bound to plant tissues. In our experimental system Pb bioaccumulation in roots and stems through Hoagland's solution represents the Pb accumulation capacities of *T. triangulare* that are almost equivalent to those of efficient root accumulators of HMs such as *Lathyrus sativus* (Brunet et al. 2008), and *Brassicae juncea* (Meyers et al. 2008) or less than *Sedum alfredii* (Tian et al. 2011). It is found that hydroponically cultivated adventitious roots of several terrestrial plants were used for rhizofiltration, a process used for absorbing or precipitating toxic metals effectively from a polluted site (Dushenkov et al. 1995).

Relative water content has been known as phytotoxicity indicator of HMs stress in plants. HMs generally causing a loss of leaf water potential than in non-treated plants (Prasad 1997; Gao et al. 2010). The results showed that Pb caused phytotoxicity to the plants, which was evidenced by the significant decrease of water content in treated leaves (**Fig. 10B**). In the present experiment, RWC decreased with increasing Pb concentrations, and this could be due to decreased water uptake and transport from root to leaf. The damage of membrane integrity was detected by uptake of a non-permeable dye (Evans blue) into the leaf cells, which has been used as an indicator of cell death. Evans blue staining showed that Pb is able to cause death of plant leaf cells (**Fig. 10C**). This could be possible due to decline in water content and decrease in nutrient elements contents in leaf of treated plants in comparison to control.

The X-ray microanalysis can semi-qualitatively analyze and quantify the total amounts of elements present in tissues. Elemental microanalysis is becoming an important way to understand individual component within tissues deposits, which may be difficult to analyze by other methodology (Nagata 2004; Shillito et al. 2009). Results of our EDS study showed the notable reduction of elements in Pb treated plants in comparison to control (**Table 8**). From the results, it was shown that X-ray microanalysis using semi-thin sections observed by intermediate high voltage SEM at 20 KV was very useful resulting for quantifying some trace elements in biological specimens. The large decreases observed in Na and Mg along with Pb concentrations suggests a barrier in transport through the stele or may be due to the damage of the transport system in the plant. Our result is verifying that changes in the other biological parameters are due to metal stress or due to decreasing percentage of nutrients.

Lead exerts adverse effects on the morphology, growth and photosynthetic processes of plants (Sharma and Dubey 2005; Sengar et al. 2008; Cenkci et al. 2010; Pourraut et al. 2011a). In our experiments we observed that the lower concentrations of Pb (0.25 and 0.5

mM) significantly increasing the chlorophylls content over the control at all duration (**Fig. 12**). Exposure of low concentration of Pb has an opposite effects on high concentration exposure. In some cases, lower concentrations stimulate metabolic processes through increased the activities of enzymes involved in biosynthetic pathways of photosynthetic pigments, on the other hand long term exposure could reduced the plant growth by inhibiting such pathways (Parys et al. 1998). Inhibition of the photosynthetic pigment biosynthesis is one of the primary events in plants during HMs stress and decreases in photosynthetic pigment content have also been reported in many plants under Pb stress (Shakya et al. 2008; Cenkci et al. 2010). It was suggested that HMs could interfere with Chl biosynthesis either through the direct inhibition of enzymatic steps or through the substitution of the central Mg ion (Prasad 1997, 2000, Prasad et al. 2006; Sengar et al. 2008; Cenkci et al. 2010; Pourraut et al. 2011a). Carotenoid serves as antioxidant against free radicals and photochemical damage (Sengar et al. 2008). Thus less effect on carotenoid might represent its supportive role against oxidative stress after 7 days (**Fig. 16A**). It is possible that at higher Pb concentrations affected the plant water status, causing water deficit, and finally reduced the Chl content.

The SQDG defined the chlorophylls orientation in membrane and the changes in sulpholipid (SQDG) quantity under HMs stress as a marker of oxidative stress is known phenomenon and studies on stress responses have shown quantitative and qualitative changes in SQDG (Harwood and Okanenko 2003). In our experiment, higher (0.75–1.25 mM) Pb concentration causes a decrease in SQDG concentration (**Fig. 13**). The similar results with decrease of SQDG concentrations were observed with influence various concentrations of Pb on wheat seedling, leaves and roots which grew in hydroponic cultures (Okanenko et al. 2003). It has also been reported that Cd concentration induced a decrease in SQDG concentration in *Brassica napus* leaves (Youssef et al. 1998). The most HMs tested cause a decrease of SQDG concentration (Youssef et al. 1998; Pádua et al.

2003). It is possible that under stress conditions competitive use of sulfur for synthesis of sulfur containing *cys*–rich peptides. It is suppose that the influence of HMs can utilize sulfur preferentially for the synthesis of essential metabolites, such as glutathione and metal binding proteins (phytochelatins and metallothioneins), rather than for SQDG synthesis.

Measurement of Chl fluorescence and activities of PSII and PSI under different Pb concentrations provides simple and reliable information about photoinhibition due to given Pb treatments (**Fig. 14 and 15**). The effects of Pb on fluorescence parameters such as F_m, F_v/F_m, Φ_{PSII}, ETR, *q*P, *q*N, Y(NPQ) and Y(NO) of PSII and *P*m, ETR and Y(I) of PSI are well documented in different plant species during past decades (Vassilev and Manolov 1999; Maxwell and Johnson 2000; Mallick and Mohn 2003; Sigfridsson et al. 2004; Verney et al. 2008; Sbubrahmanyam 2008; Drążkiewicz and Baszyński 2010).

Results showed that Pb^{2+} alter the fluorescence parameters and has negative impact on photosynthesis and activity of both PSII and PSI. Our study revealed that Pb treatment declined the Chl fluorescence induction curves, which is well explained by the decrease values of maximal Chl fluorescence intensity when all PSII-RC are closed (F_m) (Kalaji and Loboda, 2007). Different Pb treatments caused the decrease in F_m intensity in comparison to control, which is directly related to altered values of Φ_{PSII} and *q*P. The F_m can be assessed after dark adaptation when all PSII-RC are open and maximal photochemical quenching is observed. The decrease in F_m, expresses the inhibition on the donor side of PSII when all molecules of Q_A are in reduced condition, is due to the unavailability of electrons to provide for the accumulation of photoreduced Q_A (Govindjee 1995; Mallick and Mohn 2003). Similar trend of results were observed in our study during Pb treatment (**Fig. 14A**). It has been reported that Pb causes dissociation of 23 KDa polypeptide and cofactors from OEC and inhibit the activity of water oxidizing enzymes (Rashid et al. 1994).

The structure of the thylakoid membrane is directly affected by ROS through peroxidation and oxidative stress, altering the lipid composition of the thylakoid membranes and leads to structural disorganization of granna (Mohanty and Mohanty 1988; Zheng et al. 2012), which resulted in to the functional inactivation of oxygen-evolving centers and impaired electron transport (Sanitádi Toppi et al. 2003). Vernay et al (2008) reported that the decline in F_m in Cr treated *Datura innoxia* was associated with the structural alteration in the PSII pigment-protein complexes as well as changes in the ultrastructure of the thylakoid membrane. A similar tendency of decreased in F_m value by 68% was also observed in the response to Ni stress in maize plants (Drążkiewicz and Baszyński 2010). However, change in F_m in Pb treated plant leaves were mainly resulted from the reduced maximal fluorescence, as found in the Pb, Hg and Cu treated spinach (Boucher and Carpentier 1999) and Cr treated duckweed (Oláh 2010) leaves. Like other HMs such as Cd, Pb was found to inhibit the PSII function to a much greater extent than that of PSI (Miles et al. 1972; Joshi and Mohanty 2004). The decrease in F_m intensities caused a decrease in F_v/F_m, known as the most sensitive indicator for photoinhibition under various stresses conditions including HMs, which further corroborated with decrease in Φ_{PSII} (Boucher and Carpentier 1999; Verney et al. 2008; Ekmekçi et al. 2008). Pb-treated *T. triangulare* leaves showed the decline in F_v/F_m (**Fig. 14B**) and Φ_{PSII} (**Fig. 14C**), and the maximum significantly reductions were approximately 19% for F_v/F_m and 53% for Φ_{PSII} in comparison to the control, respectively. The decrease in F_v/F_m ratio may be explained by the negative effects of Pb on the photochemical reactions, which affected the efficiency of PSII photochemistry. It is suggested that F_v/F_m may decrease due to the limited reoxidation of Q_A, which is resulted due to the decrease rate of electron transport from PSII to PSI (Mallick and Mohn 2003). Also, decreased F_v/F_m resulted in a decrease in the Φ_{PSII}, which showed a significant reduction at 0.50–1.25 mM Pb treatment. Likewise, a gradual decrease in F_v/F_m and Φ_{PSII} were observed in *D. innoxia* under Cr treatment

(Vernay et al. 2008), while Ni treated maize seedlings showed the slight reduction in F_v/F_m and further affected the electron transport system by inhibiting PSII donor and acceptor side (Drążkiewicz and Baszyński 2010). Along with F_v/F_m and Φ_{PSII} other activities like photochemical quenching *q*P (at 0.50–1.25 mM Pb) were also found to significantly decrease (**Fig. 14D**) but in *q*N significant induction was observed during Pb treatment in *T. triangulare* leaves (**Fig. 14E**). Similar trend of results were observed in maize cultivars treated with different Pb concentrations (Ekmekçi et al. 2008). The decline values of *q*P well represent about the increased number of reduced (closed/inactive) PSII-RC at Pb-treated plant leaves. High number of closed RC signified that light absorption exceeds the capacity of ETR and CO_2 fixation and further increases the *q*N (Vassilev and Manolov 1999). It is reported that Cr treatment caused the simultaneous decrease in *q*P values and increase in *q*N in *Triticum aestivum* (Sbubrahmanyam 2008) and *D. innoxia* (Vernay et al. 2008), indicating the utilization of NADPH was inhibited under reduced CO_2 assimilation caused by Cr stress (Vernay et al. 2008). The increase in *q*N is due to an increased rate constant of thermal dissipation of excitation energy, which down regulate photosynthetic electron transport mechanism (Vernay et al. 2008; Sbubrahmanyam 2008). Pb treatment caused a significant increase in Y(NO) at 0.75–1.25 (**Fig. 15A**) and Y(NPQ) at only 1.25 mM Pb (**Fig. 15B**), which is strong accordance with the decrease in F_m that were used to calculate these parameters. The Y(NO) reflects the part of energy dissipated as fluorescence and heat, due to closed PSII-RC. Increased Y(NO) and Y(NPQ) values, can compensate for a decrease of Φ_{PSII}, under different Pb treatment that accounted the Pb-induced damages of the photosynthetic systems, often represents the suboptimal capacity of photoprotective reaction (Handbook of operation with Dual-PAM 2008; Klughammer and Schreiber 2008).

Our experimental results showed that Pb causes a significant decline in ETR values in both PSII (at 0.75–1.25 mM) and PSI (1.0–1.25 mM) reaction centers (**Fig. 15C,D**). The

Pb treatment of 1.25 mM affects the ETR of PSII (62.5%) much extent than that of ETR of PSI (41%). It is suggest that down regulation of ETR of PSII is due to avoidance of over-reduction of primary electron acceptor Q_A and to decrease the load on the electron transport chain. Several studies have reported about altered rate of electron transfer in PSII and PSI under influence of Pb and other HMs (Miles et al. 1972; Sbubrahmanyam 2008; Ekmekçi et al. 2008; Vassilev and Manolov 1999). However, previous study reported that Pb^{2+} was found to decrease the activity of ETR in PSI to some extent in isolated chloroplast of *Zea mays* (Wong and Govindjee 1976). On the other hand, in another study with isolated chloroplast from Cd treated *Z. mays* showed that Cd decreased ferredoxin (Fd)-dependent $NADP^+$ photo-reduction but had not affected the ETR from 2,6-dichlorophenolindophenol to methyl viologen, which suggested about the metal interference in electron transport at the reducing side of PSI (Siedlecka and Baszyński 1993).

P700 parameters analysis was carried out by using the automated induction curve provided by the Dual PAM software, with repetitive application of saturation pulses (SP), from which the quantum yields of PSI were derived. In plants, the PSI pigment-protein complex converts light energy into a trans-membrane charge separation, which finally leads to the carbon dioxide reduction. As foresaid, PSI activity has been observed to be less sensitive than PSII caused by Pb stress (Sárvári 2005; Mobin and Khan 2007). The P_m values, represents the maximal change of the P700 signal upon quantitative transformation of P700 from the fully reduced to the fully oxidized state, were observed decreased significantly ($P \leq 0.05$) at 0.50–1.25 mM Pb. Different concentration of Pb treatment caused the decrease in P_m (**Fig. 15E**), Y(I) (**Fig. 15F**) and nonphotochemical quantum yield [Y(ND)] (data not presented) of PSI in *T. triangulare* leaves. The Y(ND) values, represents the fraction of overall P700 that is oxidized in a given state, is a determinant of donor side limitation of PSI. The changes in Y(ND) values was accompanied by changes

in Y(NA), the nonphotochemical quantum yield of PS I, represents the fraction of overall P700 that cannot be oxidized by a SP in a given state due to a lack of acceptors. It may suggest that in Pb treated plant leaves, weak acceptor-side limitation develop as reflected by decreased Y(ND) values (0.73 to 0.38 in the control leaf), which may be explained as an failure of adaptation to the donor-side limitation of PS I (Schreiber and Klughammer 2008). The decreased level of P_m and Y(I) also point towards the inhibition of the PSI reaction center by Pb.

Results suggested that in plants, the synthesis of anthocyanins makes it an effective strategy against ROS generation due to Pb stress, but interestingly lower concentrations of Pb (0.25– 0.75 mM) stimulated synthesis of anthocyanins more than higher concentrations (1.0 and 1.25 mM) of Pb (**Fig. 16B**). This indicates that there is a strong correlation between the level of anthocyanins and the presence of HMs in the environment, which further corroborates the results obtained in *Zea mays* demonstrating that accumulation of anthocyanins increased under HMs stress (Krupa et al. 1996). Anthocyanins not only scavenge free radicals, but they also have the ability to bind HMs and are biosynthesized through the phenylpropanoid pathways, the first enzymatic step of the conversion of phenylalanine to trans-cinnamic acid that catalyzed by phenylalanine ammonium lyase (PAL) (Kitamura et al. 2002). It is suggested that PAL, a key enzyme in the flavonoids synthesis, to be the target of HMs inhibitory influence and finally inhibition of anthocyanins synthesis (Dube et al. 1993). However, it seems to be possible that 0.5 and 0.75 mM of Pb concentration stimulate PAL activity resulting in to increased production of anthocyanins which may further bind with metals or metal inducing ions in vacuole and detoxify them from cell. Higher concentration of Pb i.e. 1.0 and 1.25 mM are is toxic and lethal to the plant cell, leading to an inhibition of PAL and thus decrease of the biosynthesis of anthocyanin. The initial increase followed by a decline of PAL activity was also observed under different concentration of Cd in *Azolla imbricate* (Dai et al. 2006).

HPLC data showed that Pb treatment to *T. triangulare* plant resulted in the enhancement of α-tocopherol level in leaves (**Fig. 17**). Probably, the gradual increase in α-tocopherol concentration can be associated with the increased oxidative stress, which supports it as a potential biomarker against oxidative stress. Results showed that tocopherol might be involved in the adaptation of plants against Pb stress. The important function of tocopherol is that to scavenging free radicals and protects polyunsaturated fatty acids (PUFAs) and inhibiting the lipid peroxides in membranes. Abiotic stress factors such as HMs have been found to initiate lipid peroxidation and start a chain reaction which further induces the tocopherols biosynthesis. Previous experimental results also showed that increase in tocopherol content in *Arabidopsis thaliana* exposed to Cd and Cu treatment (Collin et al. 2008) and *Brassica juncea* exposed to Cd (Yusuf et al. 2010), which confers with induced tolerance to plants against HMs stress. After 7 days at higher concentration of Pb, an increase in α-tocopherol concentrations was found in proportion with decrease in chlorophylls content. Previous report suggested that may be the partial degradation of chlorophyll induced the tocopherol content because chlorophyll derived phytol is acting as substrate for tocopherol biosynthesis (Rise et al. 1989).

In parallel with increase α-tocopherol content, lipid peroxidation was also stimulated by Pb stress (**Fig. 10D**). Lipid peroxidation is a biochemical marker of the Pb-induced free radical mediated oxidative damage in *Talinum* plants. Pb ions are known to induce lipid peroxidation, increasing unsaturated fatty acids and decreasing saturated fatty acids in plants (Mishra et al. 2006; Wang et al. 2010; Maldonado-Magaña et al. 2011; Pourraut et al. 2011a). However, the percent increase in MDA content was relatively less (**Fig. 10D**). Generally, free radical generation and membrane damage would be low in tolerant plants and thereby formation of lower levels of MDA content. Therefore, relatively lower degree of increase in MDA content in *Talinum* due to Pb stress may support its tolerant nature (Sharma and Dubey 2005; Pourraut et al. 2011a).

The result of GSH and GSSG estimation in Pb treated plants indicate an alteration in GSH content, and simultaneous increase in GSSG showed a true indication of oxidative stress. Glutathione is one of the major cellular safeguards, maintains the cellular redox status, which plays a protective role as a key antioxidant and a chelating bioligand responsible for detoxification of HMs (Gupta et al. 1995; Mishra et al. 2006; Maldonado-Magaña et al. 2011; Pourraut et al. 2011a). In this study a significant increase in GSH content has been observed in leaves of *T. triangulare* followed by depletion at higher concentration (**Fig. 18B**). At lower concentration induction of GSH accumulation and maintenance of high GSH/GSSG ratio might be attributed to Pb-induced GSH synthesis (Piechalak et al. 2002). Increase in GSSG and decline in GSH seems to be correlated. Ratio of GSH/GSSG decline when Pb concentrations increased, this is evidently due to induction in GSH biosynthesis and rapid reduction of GSSG by the enzyme GR at lower concentration of Pb (Maldonado-Magaña et al. 2011). GSH, as a substrate, synthesize PC due to a reaction catalyzed by phytochelatin synthase (PCS) an enzyme activated by HMs ions including Pb. Decline in GSH at higher concentrations might be attributed to high consumption rate of GSH as antioxidant to combat oxidative stress or for the synthesis of PC. Pb-induced changes in GSH have been reported in *Acacia farnesiana* (Maldonado-Magaña et al. 2011), *Ceratophyllum demersum* L. (Mishra et al. 2006), *Vicia faba*, *Phaseolus vulgaris* (Piechalak et al. 2002). During the depletion of GSH content, under high Pb stress, formation of Pb–GSH complexes and Pb-induced PC synthesis reduces free Pb concentration in cytoplasm and contributes to suppress the activation of the stress-related responses in plant metabolism (Mishra et al. 2006).

Conclusions

It is concluded that *T. triangulare* plants grown hydroponically and exposed to Pb showed that the roots were the main accumulating site as they accumulated more Pb than

stem and were below detectable level in leaves. This confirmed that Pb immobilization or decreased translocation within the plants, which represent an attractive aspect for the development of defense strategies. It can be suggest that Pb accumulation potential of *T. triangulare* were almost equivalent to efficient accumulators. The decrease in RWC, due to decreased water transport to leaf, elements atomic % and increased cell death showed that analyzed Pb concentrations have potential to cause oxidative damage in leaf through increase production of lipid peroxides. Photosynthetic pigments and SQDG contents have been increased at 0.25 and 0.5 mM Pb at early treatment period, which were declined at further concentration and treatment durations. In vivo assay of Pb toxicity using the PAM fluorometric analysis may provide a quick and sensitive method for assessing phytotoxic agents (HMs) and their sites of action. Though F_m, F_v/F_m, Φ_{PSII}, ETR, *q*P and *q*N found to be much sensitive tool to evaluate the impact of Pb stress in *T. triangulare* leaves. The reduction in *q*P shows that Pb interference in the utilization of ATP and NADPH generated during light reaction. Interference in *q*N values resulted in to the changes in ETR of PSII and reduced the quantum yield. Moreover, the PSI photochemical reaction and their yields and ETR were reduced during different Pb treatment condition. Pb treatments affects or inhibited PSII function to a much greater extent than that of PSI.

Furthermore, increase level of anthocyanins, duration dependent, and α-tocopherol showed their involvement in the adaptation mechanisms in Pb treated plants. Alteration in glutathione levels showed that GSH maintained an important antioxidant system for the plant to accumulate higher concentration of toxic Pb and survive for longer period. These findings confirm the key role of the toxicity and tolerance strategy of *T. triangulare* and analyzed defense parameters suggesting that these might be the potential biomarkers for detecting Pb toxicity. Further research on the molecular mechanism(s) of Pb toxicity and its micro-localization and detoxification mechanism is required to improve our understandings.

Objective 3

Pb-induced oxidative damage, genotoxicity and function of enzymatic and non-enzymatic antioxidants

Introduction

Plants and microbes play important roles in detoxifying and stabilizing hazardous substances in the environment through the process of remediation (Rajkumar et al. 2012). Pb is a traditional metal with modern applications, but could lead to multiple toxic effects in plants by inducing ROS (Hu et al. 2007; Gupta et al. 2009; Lamhamdi et al. 2011). ROS being highly unstable, plays a dual role in i) damaging cellular components and ii) acting as an important secondary messenger for inducing plant defense system. Cells are equipped with enzymatic and non-enzymatic defense mechanisms to counteract this damage. Some are constitutive and others were activated only when a stress-specific signal is perceived. HMs, in particular Pb stress caused reduction of molecular oxygen and produced intermediate products, which are more toxic and reactive than O_2 (Sharma and Dubey 2005; Lamhamdi et al. 2011; Kaur et al. 2013). These active molecules are involved in the free radicals chain reaction of membrane lipids and proteins, causing oxidative decomposition of them (**Fig. 19**) (Kanoun-Boule et al. 2009; Ann et al. 2011).

Lipid peroxidation and enzymatic system during HMs stress

Plasma membranes are considered as primary target for metal toxicity in both leaves and roots. Membrane damage was deduced from the analysis of TBA (thiobarbituric acid) active products level, after reaction using TBA assay. This is one of the basic methods of research process to determine lipid peroxidation in the biological systems (**Fig. 19**). Measurement of the level of thiobarbituric acid reactive substances (TBARS) in tissues is widely used as an index of lipid peroxidation. Malondialdehyde (MDA) is one such thiobarbituric acid reactive substance. Various results testified that under action of HMs, plants often activate processes of lipid peroxidation (Dazy et al. 2009; Iqbal et al. 2010; Ann et al. 2011; Yusuf et al. 2012). Lipid peroxidation is a biochemical marker for the free

radical mediated injury by production of ROS. The investigations with increasing Pb concentration showed the Pb-induced lipid peroxides and oxidative stress in rice (Verma and Dubey 2003). Stimulation process of lipid peroxidation might be activated by lipoxigenase (LOX) with the formation of hydroperoxide, because the early stress reactions occur at the membranes level (Huang et al. 2012). The major targets of the lipid peroxidation on the membranes were unsaturated fatty acids. The process of lipid peroxidation is usually correlated with activities of plants major antioxidant enzymes. The changes in enzymes activities determine the intensity and function of cells and organism as a whole, and also their viability in the environment conditions.

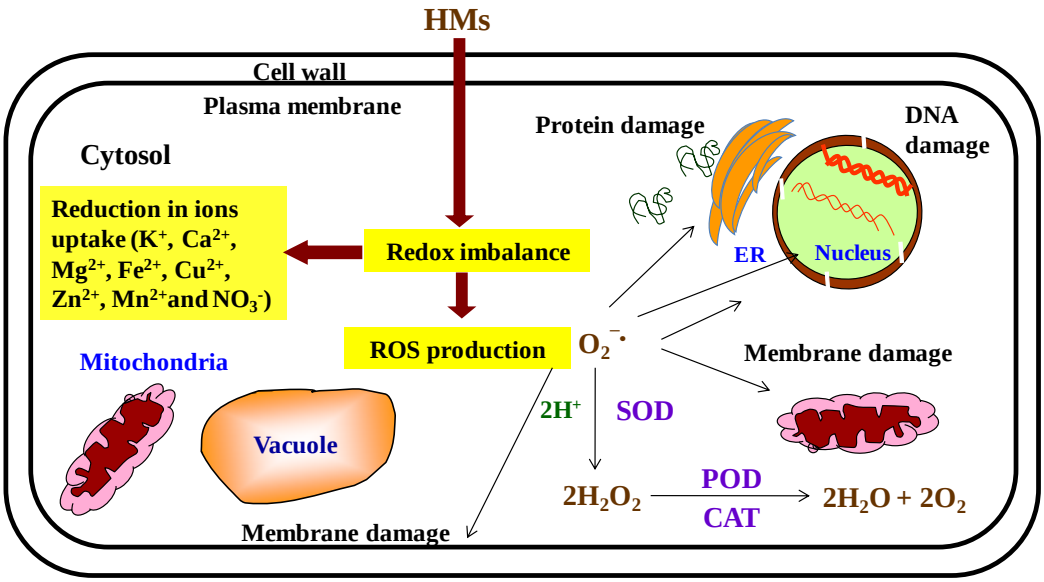

Fig. 19 Heavy metal uptake, induced oxidative stress and tolerance mechanisms in plant cell: CAT, catalase; ER, endoplasmic reticulum; H, hydrogen molecule; HMs, heavy metals; H_2O_2, hydrogen peroxide; H_2O, water; O_2, oxygen molecule; $O_2^{\bullet-}$, superoxide radicals; POD, peroxidases; ROS, reactive oxygen species; SOD, superoxide dismutase.

In the past for many years ROS were considered as unsafe molecules which must be maintained at low level in cells. However, recently this point of view has been changed. It has been shown that ROS can also play an important role in plant defense against oxidative explosion and can serve as markers of the certain stages of development, such as formation

of tracheids and the cross-link in cell walls, lignifications, and programmed cell death and also serve as signaling/alarm molecules in regulation of gene expression process (Schütenzendübel and Polle 2002). Due to diverse functions of the active oxygen species, cells must strictly control the level of ROS. This controlling system is composed of antioxidants including enzymes such as superoxide dismutase (SOD, E.C. 1.15.1.1), catalase (CAT, E.C. 1.11.1.6), glutathione reductase (GR, E.C. 1.6.4.2), peroxidase (POD, E.C. 1.11.1.7), ascorbate peroxidase (APX, E.C. 1.11.1.11) and guaiacol peroxidases (GPX, E.C. 1.11.1.7). Experiments with two ecotypes of *Sedum alfredii* showed Pb-induced increased production of ROS in root cells. Furthermore, ROS caused increased enzyme activities of SOD, CAT, APX, POD and lipoxygenase (LOX, E.C. 1.13.11.12). High concentrations of Pb aggravated ultrastructural damage to leaf cells including disruption of chloroplasts, mitochondrial cristae, nuclear membrane and nucleoli and disappearance of chloroplast envelopes, vacuolation of mitochondria and condensation of chromatin. Changes in antioxidative enzymes activities and damage to fine structure are the results of Pb-induced ROS accumulation (Hu et al. 2007). Concomitant changes in CAT, POD and SOD activities are responsible for removal and destruction of ROS, and hence referred as antioxidative enzymes, however, they have got important bearings on the oxidative damage of membranes in organisms under oxidative stress conditions (Ghnaya et al. 2009). Pb and other HMs such as Cd, Cu and Zn caused significant changes in SOD and CAT activities, which are resulted due to increased lipid peroxidation level. Moreover, the SOD activity and MDA level often presented clear linear relationships with a wide range of HMs concentrations.

Proline response during metal stress condition

The biochemical collision of metal ions on the cells is as diverse as their chemical nature. Plants respond to HMs stress by operating various defense strategies such as

exclusion and formation of complexes and switching on certain metabolic events associated with the biosynthesis of amino acids particularly proline, histidine and cystein (Sharmila and Saradhi 2002). Among all amino acids, proline is most studied molecules in the perspective of plants responses to HMs stress. The accumulation of soluble proline under various environmental stresses paricularly HMs, and has been reported in wide variety of experimental organisms including bacteria, algae to various higher plants (Sharmila and Saradhi 2002; Sharma and Dietz 2006). Sun et al. (2007) compared the accumulation of proline in the newly discovered Cd-hyperaccumulator *Solanum nigrum* with *Solanum melongena* under different Cd concentrations. Authors reported that enhanced concentrations of free proline in both leaves and roots of *S. nigrum*. While there were no significant differences in free proline levels in roots of *S. melongena* (Sun et al. 2007). Hunag et al. (2010) reported that the contents of proline increased in the leaves of *Kandelia candel* and *Bruguiera gymnorrhiza* leaves when exposed with multiple metals (Pb, Cd and Hg) together. Proline accumulation is mediated by either increased biosynthesis from glutamate or ornithine (Yang et al. 2011). Zhen and Ma (2009) reported that the glutamate pathway, rather than the ornithine pathway, plays a vital role in proline accumulation in plants when exposed to environmental stresses. However, in two cultivars of *Tritium aestivum* i.e. Xihan and Ningchun treated with Pb showed that the accumulation of proline is due to the induced activities of ornithine-δ-aminotransferase (OAT) and r-glutamyl kinase (GK) enzymes in Xihan seedlings, and only to the increase of GK activity in *Ningchun* leaves (Yang et al. 2011).

HMs-induced protein oxidation

ROS can interact with biomolecules such as polypeptides of plant proteins and result in increasing carbonyl groups, the levels of which were explained as metal-catalyzed proteins oxidation (Pena et al. 2008) and were often taken as presumptive confirmation of oxidative

modification in protein (Levine et al. 1994; Franco et al 2009). Oxidation of proteins can be regarded either as a negative consequence of a stressing condition (especially, irreversible protein oxidative modifications such as carbonylation, oxidation of cysteines to sulphonic acids, oxidation of tryptophan) or a specific signal for the cell to respond to such a stress (for review see Rinalducci et al. 2008). The relation between plant physiological responses and oxidation of cellular proteins was explained by Qin et al. (2009), that carbonylation of mitochondrial proteins can contribute to fruit senescence by altering biological functions or inducing loss of specific enzyme activities (Qin et al. 2009). Proteolytic system in plants under various HMs stress conditions in sunflower leaves (Pena et al. 2008), castor beans (Nguyen and Donaldson 2005), have been studied.

A brief review of HMs-induced plant genotoxicity or DNA damage

In the presence of HMs, particularly Pb, in the growth media, even at low concentrations, plants usually experience harmful effects along with various physiological impacts such as micronucleus induction, mitosis disturbance (Wierzbicka 1999), chromosomal abnormalities (Siddiqui 2012), microsatellites (simple sequence repeats) instability (Rodriguez et al. 2013) damage of cytoskeleton, nucleus and DNA (Gichner et al. 2008). Agents that cause DNA damage are considered as genotoxic agents or mutagens that are capable of damaging the nuclear and extranuclear genetic material of cells. Many of the HMs, particular Pb is a genotoxic agent. Pb is considered as a potential human carcinogen, IARC, EPA and ATSDR (Patra et al. 2004; Anonymous 2005, 2007, 2011; Shahid et al. 2011). Pb is considered as an effective mitotic poison (turbagens) at particular concentrations, due to their known affinity for thiol groups and induces various types of spindle disturbances (Patra et al. 2004). The relationship between Pb toxicity and genotoxicity has, however, not been established unequivocally (Shahid et al. 2011). Pb exhibited toxic effects of mitotic index or on cell cycle progression of root tip cells, which

resulted in to inhibitory effect of root lengthening in *V. mungo* (Eun et al. 2000; Wozny and Jerczynska, 1991). ROS was not only responsible for oxidative damage through damage of polyunsaturated fatty acid of membrane lipid but they also damage proteins and DNA (Sharma and Dubey 2005; Pourraut et al. 2011; Kaur et al. 2012; Hu et al. 2012). Majority of the studies for evaluation of metal genotoxicity was carried out in animal and microbial systems. The genotoxic effects depend on the oxidation state of the metal, its concentration and duration of its exposure. The use of cost effective and short-term bioassays, especially comet assay, to assess the potential of environmental pollutants has gained special attention over the last decades. These assays are quite easy to conduct, capable of predicting the genotoxic potential of the pollutant under investigation by measuring gene mutations and damage to chromosomes and DNA (Kumaravel et al. 2000; Panda and Panda 2002). The ethidium bromide (EtBr) staining technique used here has often been the technique of choice for comet assay in developing courtiers (García et al. 2004).

Lead uptake, bio-accumulation, toxicity and tolerance have been investigated in a number of terrestrial plants such as *Brassica campestris* (Singh et al. 2011), *Tritium aestivum* (Lamhamdi et al. 2011; Kaur et al. 2012), *Potamogeton crispus* (Hu et al. 2007), *Zea mays* (Gupta et al. 2009), *Pisum sativum* (Malecka et al. 2009) and *Oryza sativa* (Li et al. 2012). Previous studies have reported that *T. trianglare* accumulate heavy metals (HMs) from contaminated media (Rajkumar et al. 2009). Our earlier study investigated Pb induced oxidative stress in leaf of *T. triangulare*. The aims of the present study were: (1) to investigate early symptoms of the Pb toxicity and relationship between Pb tolerance and antioxidant metabolism in roots in hydroponic condition; and (2) to examine the Pb-induced DNA damage, changes in structural integrity and nutrient contents in *T. triangulare*.

Materials and methods

Plant description and treatment in hydroponic experiment

T. *triangulare* was propagated through stem cuttings (5.0–7.0 mm diameter and 17–22 cm height) in conical flask containing 100 mL of modified Hoagland's nutrient media in plant growth chamber at 16/8 h (day/night) at 28 ± 2 °C for 3 weeks. After 3 weeks of acclimatization, uniform stem cuttings with adventitious roots and leaves were selected and treated with $Pb(NO_3)_2$ at different Pb concentrations of 0 (control), 0.25, 0.50, 0.75, 1.0 and 1.25 mM for 7 days under above conditions. Roots excised after 7 days of treatment were processed for analysis of various endpoints described as follows.

Estimation and visualization of H_2O_2 in root tissue

Fresh roots (0.5 g) were homogenized in ice bath with 5 mL of 0.1% (w/v) trichloroacetic acid (TCA). The homogenate was centrifuged at 12,000 g for 15 min at 4 °C, and 0.5 mL of the supernatant was added to 0.5 mL of 10 mM potassium phosphate buffer (pH 7.0) and 1 mL of 1 M potassium iodide. H_2O_2 concentration was estimated at 390 nm based on the absorbance of a standard curve and was expressed nmol g^{-1} FW Velikova et al. (2000).

In situ H_2O_2 visualization in control and Pb treated roots was determined by 2´,7´-dichlorodihydrofluorescein diacetate (H_2DCFDA) fluorescent dye. Plant root tips were excised and wash with DDW two times. After that root tips were dipped in to 5µM H_2DCFDA dye prepared in dimethyl sulphoxide (DMSO) for 30 min. After staining with fluorescent dye roots were again washed with DDW two times and mounted on the clean glass slides. Fluorescent images were captured with using confocal microscope (Leica TCS SP2 AOBS Microscope, Germany) at 480 nm excitation and 520 nm emission wavelengths.

Estimation of cell death

Fresh roots (0.1 g) were stained with 0.25% (w/v) aqueous solution of Evans blue for 15 min. After washing with miliQ water for 30 min, roots were excised and soaked with 3 mL of N,N-dimethylformamide for 1 h at room temperature. The absorbance of released Evans blue was measured and represented at 600 nm (Baker and Mock 1994).

Estimation of lipid peroxidation

Lipid peroxidation in control and Pb treated roots were determined as a function of malondialdehyde (MDA) content following the method of Heath and Packer (1968) with slight modifications. The detail procedures for lipid peroxidation are described in **objective 2** (**Page number 52**).

Estimation of lipoxygenase activity (LOX, E.C. 1.13.11.12)

Fresh root (0.5 g) was homogenized in 50 mM sodium phosphate buffer (pH 7.0), 1 mM EDTA, 0.1 mM phenylmethanesulfonylfluorid (PMSF), 2% (w/v) polyvinylpoly-pyrrolidone (PVPP), 1% (v/v) glycerol and 0.1% (v/v) tween-20. The homogenate was centrifuged at 12,000 g for 20 min. The reaction was initiated by addition of 1 mM linoleic acid in 0.1 M sodium acetate buffer (pH 5.6) to the supernatant. The increase in the activity of LOX was measured at 234 nm (extinction coefficient = 25 mM^{-1} cm^{-1}). One unit of activity was defined as the amount of enzyme catalyzing the synthesis of 1 μmol of hydroperoxide (HPOD) min^{-1} (Ederli et al. 1997).

Estimation of antioxidative enzymes activities

Plant roots samples (1 g) were homogenized in 50 mM sodium phosphate buffer (pH 7.8) for SOD enzyme, and (pH 7.0) for CAT enzymes activity respectively containing 2%

PVPP. Homogenates were centrifuged at 13,000 g for 20 min at 4 °C. The protein content in the supernatant was determined according to the method of Lowry et al. (1951) using a bovine serum albumin as a standard.

Superoxide dismutase (SOD, E.C. 1.15.1.1)

SOD activity was determined according to the method of Beauchamp and Fridovich (1971). The required reaction mixture was prepared with 50 mM sodium phosphate buffer (pH 7.8), 13 mM methionine, 75 μm nitroblue tetrazolium (NBT), 0.1 mM ethylenediamminetetraacetic acid (EDTA), and 2 μM of riboflavin (added at last) and 50 μg of protein. After mixing, samples were illuminated for 15 min using comptalux bulbs (40 W). The reaction mixture containing sample protein were kept in dark and served as blank, while the reaction mixture without sample protein that were kept under light served as positive control. The absorbance was taken at 560 nm. One unit of SOD activity is the amount of protein required to inhibit 50% photochemical reduction of NBT under light.

Catalase (CAT, E.C. 1.11.1.6)

CAT activity was measured of consumption of H_2O_2 (extinction coefficient = 39.4 mM^{-1} cm^{-1}) according to the method of Aebi (1984). The reaction mixture for measuring CAT activity contained 50 mM sodium phosphate buffer pH 7.0, 10 mM H_2O_2 and 100 μg of protein in a final volume of 3 mL. The activity was determined by the oxidation of H_2O_2 at 240 nm.

Estimation of protein oxidation

Equal amount of proteins were precipitated with equal volume of 20% TCA. The tubes were centrifuged at 12,000 g for 10 min and the pellet obtained was allowed to react with 500 μL of 10 mM 2,4-dinitrophenylhydrazine (DNPH) in 2 M HCl and incubated at room

temperature for 1 h with regular vortexing. The samples were again precipitated with 500 µL of 20% TCA, centrifuged at 12,000 g for 5 min. The resultant pellet was washed with ethanol: ethyl acetate (1:1). The precipitated protein was redissolved in 0.6 mL of 6 M guanidine-HCl. The optically clear solutions were obtained after two to three times repeated centrifugation at 6,000 g at 4 °C. Carbonyl concentration was calculated from the difference in absorbance recorded at 380 nm against a blank treated with 2 M HCl instead of DNPH (extinction coefficient = 22,000 M^{-1} cm^{-1}) and expressed in nmol of DNPH incorporated mg^{-1} protein (Reznick and Packer 1994).

Estimation of proline content

Free proline content was measured following the method of Bates et al. 1973. Plant root (0.5 g) was homogenized in 5 mL of 3% aqueous sulfosalicylic acid and the homogenate filtered through Whatman # 2 filter paper. One mL of filtrate was reacted with 1 mL of freshly prepared acid ninhydrin reagent (0.625 g ninhydrin in 15 mL glacial acetic acid and 10 mL of 6 M phosphoric acid) and 1 mL glacial acetic acid. Reaction mixture was heated at 100 °C for 1 h and then kept in an ice bath to stop the reaction. The developed color was extracted with addition of 2 mL of toluene and the toluene-chromophore absorbance was measured at 520 nm using toluene as a blank. Proline content was determined by using a proline standard curve and expressed as n mol g^{-1} fw.

Estimation of DNA damage by alkaline comet assay

For alkaline comet assay (Patnaik et al. 2011), rooted stem cuttings were taken out from treatment solutions and thoroughly washed with distilled water. The whole schematic representation of comet assay analysis is described in **Fig. 22**. Roots excised were placed in a 60 mm Petri dish and placed on ice. With the help of new razor blades, the roots were sliced in the medium containing 100 to 200 µL of chilled 0.4 M Tris-HCl buffer pH 7.4,

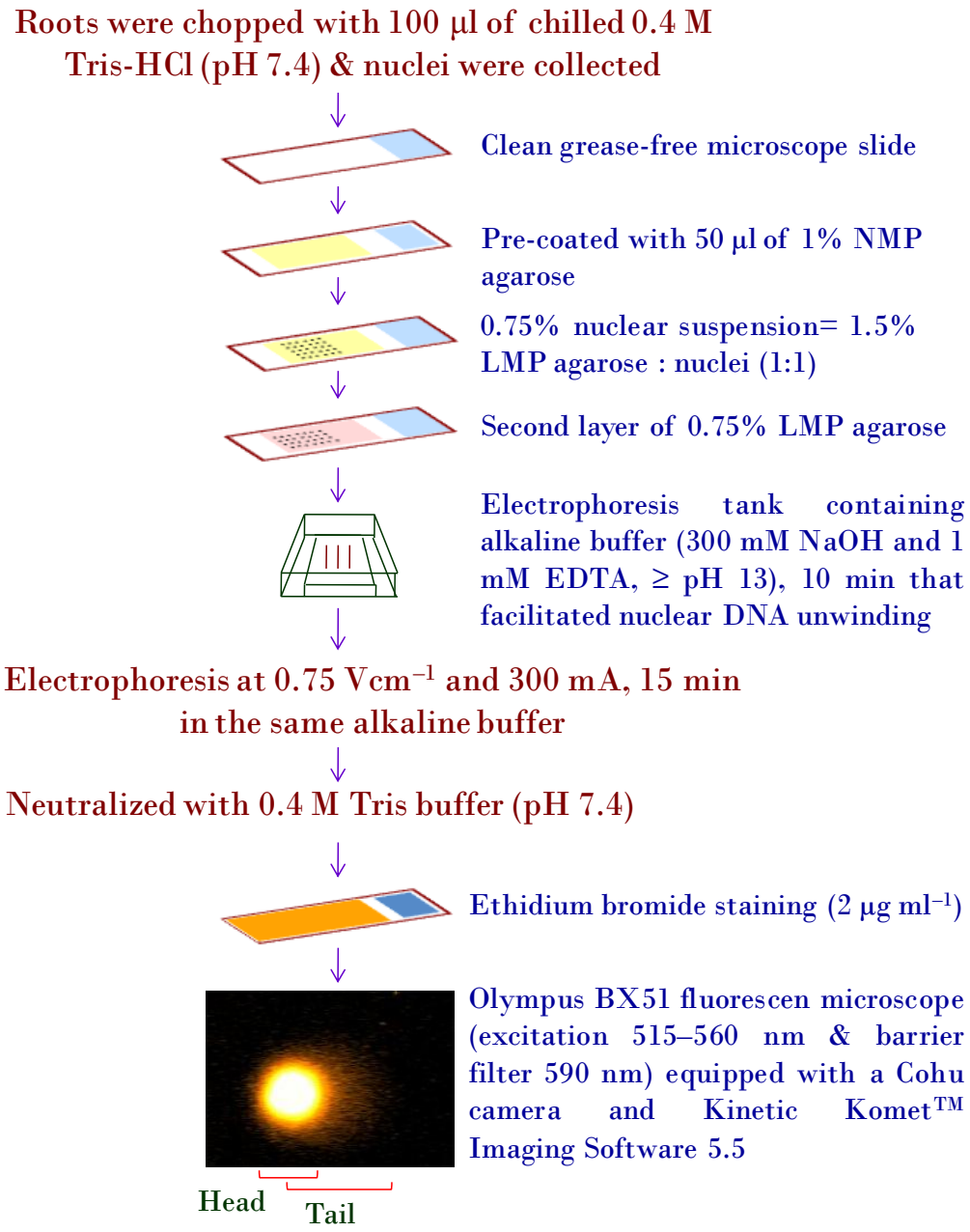

Fig. 20 Schematic representations for methodology of alkaline comet assay analysis for DNA damage evaluation. Head: DNA amounts that still remain in the nuclear matrix. Tail: DNA fragments migrating from the nuclei. NMP: normal melting point agarose. LMP: low melting point agarose.

and the nuclei were collected in to a micro-centrifuge tube with same buffer and kept at 4 °C. Before proceeding to the next step, nuclear suspension in 0.75% low melting point

region. (LMP type VII, Sigma-Aldrich, USA) was prepared by mixing the above collected nuclei with equal volume (1:1) of 1.5% LMP dissolved in Tris-HCl buffer at 37 °C. Clean grease-free microscope slides pre-coated with 50 µL of 1% normal melting point agarose (NMP type, I Sigma-Aldrich, USA) dissolved in distilled water were kept dry over night at room temperature and labeled. Onto the above slides, 80 µL of the aforesaid nuclear suspension was layered at 37 °C with the aid of a cover slip (20 × 40 mm). After gelling of the agarose layer, the slides were kept over a chilled metal plate for 5 min, the cover slip from the top of the agarose layer containing the nuclei was gently removed. A second layer of 80 µL 75% LMP agarose was spread over the nuclear layer, which was allowed to gel once again for 5 min. After removing of the cover slips, the slides with agarose-embedded nuclei were placed in a horizontal electrophoresis tank containing alkaline buffer (300 mM NaOH and 1 mM EDTA, ≥ pH 13) for 10 min that facilitated nuclear DNA unwinding, followed by electrophoresis at 0.75 Vcm^{-1} and 300 mA for 15 min in the same alkaline buffer at 4 ºC. Slides were then washed in distilled water and neutralized with 0.4 M Tris buffer (pH 7.4). After a 5 min wash in distilled water, nuclei were stained by spreading 200 µL ethidium bromide solution (2 µg mL^{-1}) over the gel on the slide. Analysis of comets was carried out employing an Olympus BX51 microscope with a fluorescence attachment (using the excitation filter 515–560 nm and barrier filter 590 nm) equipped with a Cohu camera and Kinetic Komet™ Imaging Software 5.5 (Andor™ Technology, www.andor.com). Two slides were prepared for each treatment. At least, 50 comets were scored from each slide. The comet images were visualized and captured at 100 × magnification. Out of a number of parameters available in the software, comets were analyzed on the basis of the Olive tail moment (OTM) = Tail DNA% × Tail moment length (the distance between the intensity centroids of the head and the tail along the x-axis of the comet). This parameter allows us to detect variations in DNA distribution within the tail. Therefore, OTM is considered as an absolute parameter with a measurement unit µm

(Kumaravel 2009). The entire process of comet assay was carried out in dim or yellow light.

Structural and elemental analysis

Structural analyses were done by environmental scanning electron microscope (ESEM, Philips XL-30) for root (tip) and stem transverse section (T.S.) of *T. triangulare* treated with 0, 0.25 and 1.25 mM Pb concentration. Elemental/chemical analyses were done with energy-dispersive X-ray spectroscopy (EDS, Oxford instruments) coupled with field emission scanning electron microscope (FESEM). Samples for ESEM and FESEM/EDS were prepared by primary fixation using 3% gluteraldehyde in 0.05 M phosphate buffer for 90 min followed by secondary fixation in 2% osmium tetroxide in 0.01 M sodium cacodylate buffer for 30 min followed by dehydration with a graded ethanol series, mounted on aluminium stubs and coated with gold-palladium. The EDS analysis in roots was performed followed similar procedure as for EDS in leaves (for detail see **objective 2**, **page number 51**).

Statistical analysis

The experiments were repeated at least three times and the data presented corresponds to the mean values ± S.E. (standard errors) of three replicates (Microsoft Office 2003). One-way analysis of variance (ANOVA) were done with all the data to confirm the variability of data and validity of results, and performed Duncan's multiple range test (DMRT) by using SIGMASTAT software (version 11.0) to determine the significant difference between treatment group. Correlation analysis was performed wherever required. $P \leq 0.05$ were considered significantly different with each other and denoted by different letters (Gomez and Gomez 1984).

Results

H_2O_2 estimation and visualization

Spectrophotometric estimation together with histochemical visualization of H_2O_2 in the root tissue clearly indicated that Pb significantly induces a dose-dependent H_2O_2 production (**Fig. 21**). Confocal results revealed that maximum fluorescence was observed at 1.25 mM Pb treated root, which directly signify the maximum H_2O_2 production at this treatment (**Fig. 21A**). While no difference in autoflorescense was observed between control and 0.25 mM Pb treated roots, which is corroborated with the H_2O_2 result observed spectrophotometrically (**Fig. 21B**). However, the significant ($p \leq 0.05$) increase in H_2O_2 production was reported at 0.5–1.25 mM Pb.

Lead-induced cell death

Lead-induced oxidative damage in *T. triangulare* roots tissue were measured by Evans blue staining method (**Fig. 22A**), that showed a positive linear correlation (R^2= 0.831) with dose-dependent H_2O_2 generation. Evans blue uptake by root tissue were significantly ($P \leq 0.05$) increased by 125% and 205% at 1.0 and 1.25 mM Pb treatment, and no significant difference between treatments was observed below 0.75 mM Pb.

Lead-induced lipid peroxidation

Lipid peroxidation in Pb treated *T. triangulare* roots was measured by the estimation of MDA contents, a degradation product of membrane unsaturated fatty acid, that reflected the extent of cell membrane damage in response to ROS. The increase in MDA contents presented a positive correlation (R^2= 0.986; **Fig. 22B**) with the increasing Pb concentration in the treatment solutions. Pb induces significant ($P \leq 0.05$) lipid peroxidation at 1.0 and

1.25 mM concentrations that accounted for 150.3% and 180.3% increased as compared to control, respectively.

Lead-induced LOX activity

Lead enhanced the LOX enzyme activity in a concentration-dependent fashion (**Fig. 22C**). However, similar to MDA, the increase was significant ($P \leq 0.05$) at 0.75–1.25 mM. The increased LOX activities ranged between 9.5% to 43.6% in response to Pb treatment (0.25 to 1.25 mM), with respect to control.

Lead-induced changes in protein turnover

Experimental finding with the total protein content estimated at a range of concentrations of Pb in root tissue of *T. triangulare* indicated a concentration-dependent (R^2= 0.89; **Fig. 22D**) decrease in the protein content. The decrease of the protein content was significant ($P \leq 0.05$) at 0.5 mM onwards.

Lead-induced changes in antioxidant enzymes activities

A linear increase in SOD activity was observed with increasing concentration of Pb (R^2= 0.983; **Fig. 23A**). However, the SOD activity remained unchanged up to 0.50 mM of Pb treatment. The highest SOD activities were observed at 0.75 (67.5%), 1.0 (89.4%) and 1.25 (105.3%), which were significantly ($P \leq 0.05$) when compared to control, respectively.

Similar to SOD, CAT activity presented a dose-dependent response in Pb treated roots (**Fig. 23B**). The CAT activity in roots increased significantly at 0.25–1.25 mM of Pb compared to control. The highest CAT activity was observed at 1.0 mM of Pb, which increased 137.5% in comparison to control. CAT activity was found to slight decrease at 1.25 mM of Pb (127.3%) in comparison to 1.0 mM of Pb.

Lead-induced protein oxidation

This assay was based on the reaction of carbonyls resulting from free radicals modification of proteins and DNPH. Protein oxidation is a measure of Pb-induced production of carbonyl contents. The accumulation of carbonyl contents was observed in Pb treated roots (R^2= 0.938; **Fig. 23C**). In comparison to control, the amount of carbonyls significantly increased ($P \leq 0.05$) to approximately 36%, 38% and 42% at 0.75, 1.0 and 1.25 mM Pb, respectively. Pb-induced protein oxidation showed a positive linear correlation (R^2= 0.960) with H_2O_2 contents.

Lead-induced changes in proline accumulation

Our experimental results showed that the free proline content was increased at 0.25–0.75 mM Pb, but decreased at 1.0–1.25 mM Pb when compared to control root, respectively (**Fig. 23D**). A moderate increase in free proline level was observed in the roots subjected to 0.25–0.75 mM of Pb over control root. The accumulation of proline increased as the stress prolonged and attained significant ($P \leq 0.05$) maximal levels at 0.25 mM of Pb (49.5%) after 7 days experiment. There was a marginal decrease in the accumulated proline upto 0.75 mM of Pb treatment. However, the decrease in proline was as much as 39.2%, even on continuing the treatment 1.25 mM of Pb.

Lead-induced DNA damage

Evidences from the OTM values (**Fig. 24**), comet assay revealed that the Pb at concentrations in the range 0.5–1.0 mM significantly ($P \leq 0.05$) induced DNA damage compared to the control in roots cells of *T. triangulare*. In our experimental conditions, Pb treatments at 0.25 mM induced very slight DNA damage, which was not significantly different from control. Pb treatment of 1.25 mM was observed toxic and caused nuclear

necrosis, and thus it was not possible to analyze the comet images at this concentration. After 7 days, DNA damage was significantly enhanced ($P \leq 0.05$) at doses of 0.50, 0.75 and 1.0 mM Pb treatment in comparison to control, respectively.

Lead-induced structural modification and elemental analysis

The SEM analysis revealed that 0.25 and 1.25 mM of Pb treatment altered the root anatomical surfaces (**Fig. 25A-F**), vascular tissues and internal structure of the stem (**Fig. 26A-C**). SEM images of roots showed that Pb toxicity is able to rupture the root integrity, pore formation on surface and modification of root tip. However, at 1.25 mM Pb, roots surface were highly porous in nature and the pore size was larger in size than 0.25 mM Pb treated root. SEM micrograph of stem showed that Pb caused disruption of vascular bundles especially xylem vessels, which reduces nutrient and water transport to the aerial part of the plant.

Results of EDS showed the atomic% and chemical characteristics of tissue. Microanalysis of root elements was performed at the root tip of the 0, 0.25 and 1.25 mM of Pb treated plant samples. X-ray microanalysis revealed the presence of Pb spectral peak in both Pb treated roots (**Fig. 27A-C**), which support the presence of Pb in the sample. Semi-quantitative estimation of other elements such as oxygen (O), potassium (K), sodium (Na), calcium (Ca), magnesium (Mg), chlorine (Cl), arsenic (As), silicon (Si), aluminium (Al), sulfur (S) and copper (Cu) in control root tissues (**Table 9**). Qualitative percentage composition analysis showed that only high spectral peak for O, K and Pb were observed in 0.25 and 1.25 mM Pb treated root in comparison to control root, respectively. Other elements were detected less or below detectable level in Pb treated roots than in control root.

Table 9 Analysis of atomic percentage (%) of elements by energy dispersive spectroscopy (EDS) in roots of *T. triangulare* treated with 0 (control), 0.25 and 1.25 mM of Pb for 7 days.

	Atomic% of elements in roots of *T. triangulare*		
Elements	**Control**	**0.25 mM Pb**	**1.25 mM Pb**
O	82.88	84.50	84.69
K	7.33	6.91	11.18
Na	3.74	3.50	0.55
Ca	2.08	1.95	0.67
Mg	1.83	1.82	1.50
Cl	0.91	0.83	0.78
Si	0.72	ND	ND
S	0.23	0.20	ND
Cu	0.28	ND	0.22
Pb	ND	0.29	0.41

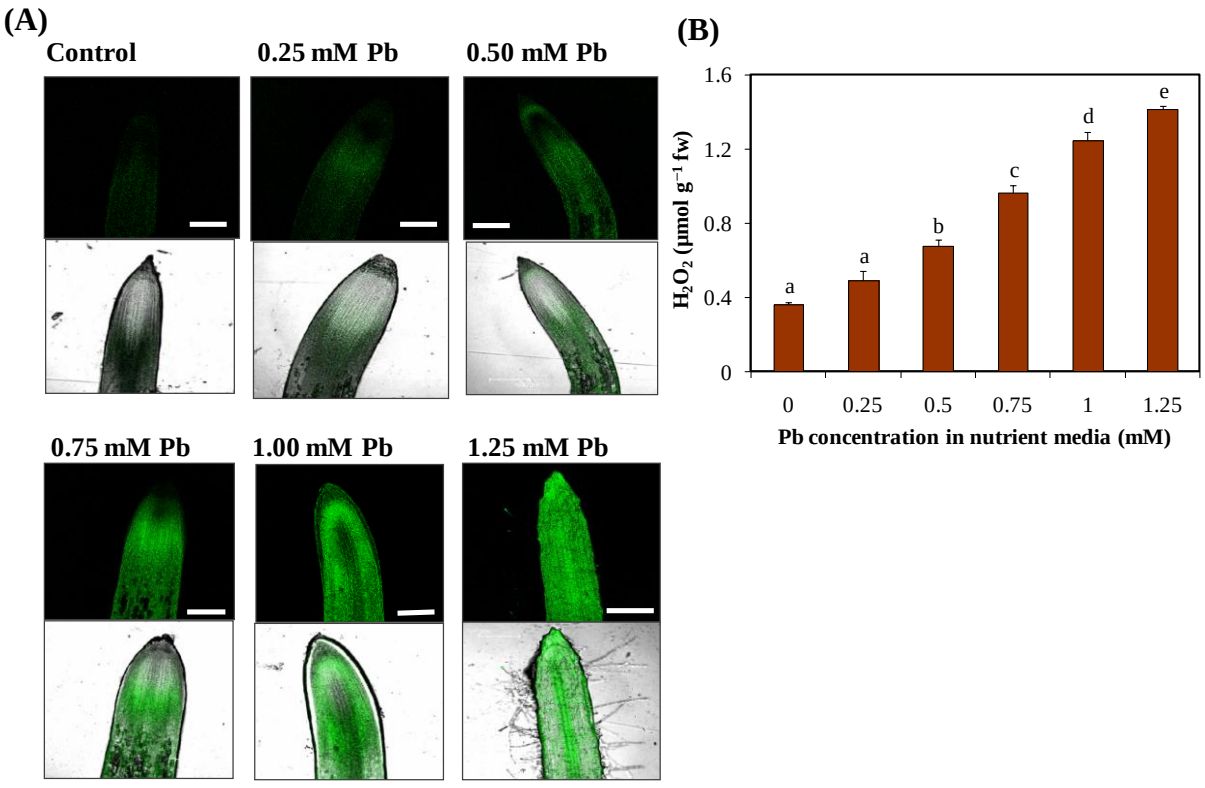

Fig. 21 (A) H_2O_2 production in *T. triangulare* roots after 7 days of Pb treatment. Mean values (± SE) are denoted by different letters indicating significantly different values ($P \leq 0.05$) between each treatment. **(B)** Fluorescence micrograph of histochemical visualization of ROS (H_2O_2) in root tip of Pb treated plant. (Bar = 300µm).

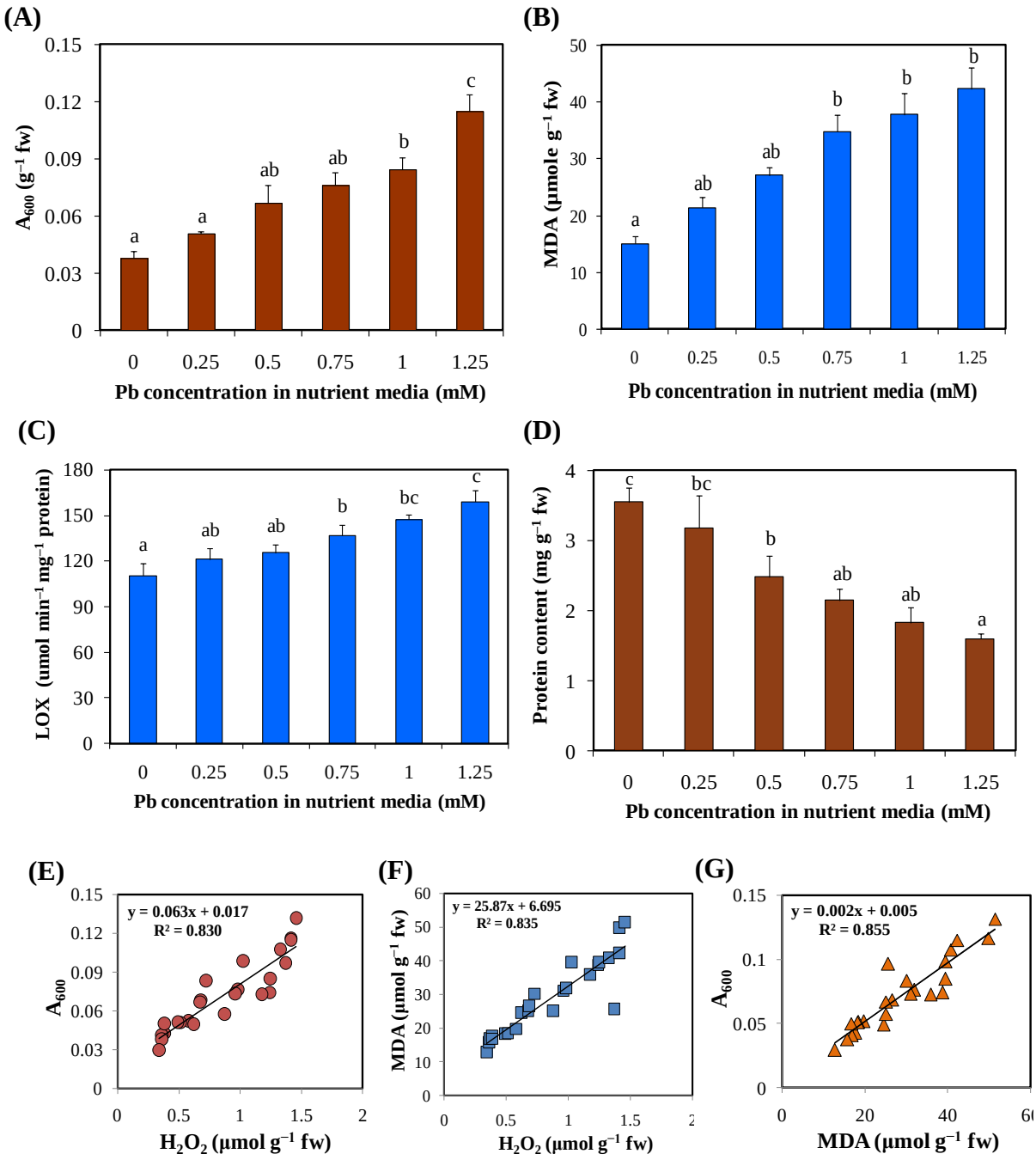

Fig. 22 Cell death measurements by Evans blue uptake **(A)**, malondialdehyde (MDA) contents **(B)**, lipoxygenase (LOX) activities **(C)** and total protein contents **(D)** in *T. triangulare* roots after 7 days of Pb treatment. Mean values (± SE) denoted by different letters are significantly different ($P \leq 0.05$) between each other. **(E)**, **(F)** and **(G)** represent the correlation analysis between H_2O_2-Cells death, MDA-H_2O_2, Cell death-MDA, respectively.

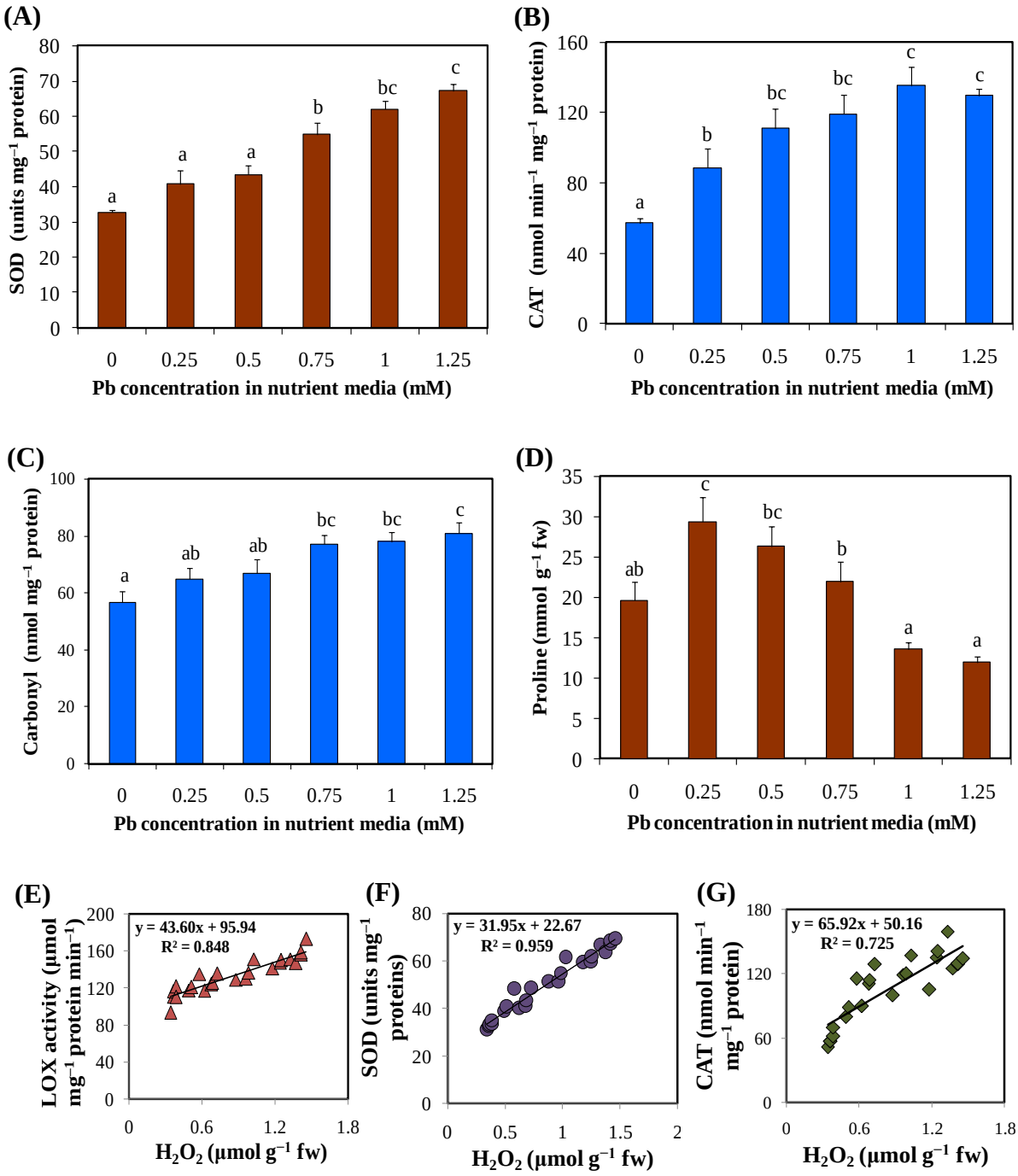

Fig. 23 Superoxide dismutase (SOD) activity **(A)**, catalase (CAT) activity **(B)**, carbonyl content as indicator of protein oxidation **(C)** and proline accumulation **(D)** in *T. triangulare* roots after 7 days of Pb treatment. Mean values (± SE) denoted by different letters are significantly different ($P \leq 0.05$) between each other. **(E)**, **(F)** and **(G)** represent the correlation between LOX, SOD and CAT with increase in H_2O_2 generation.

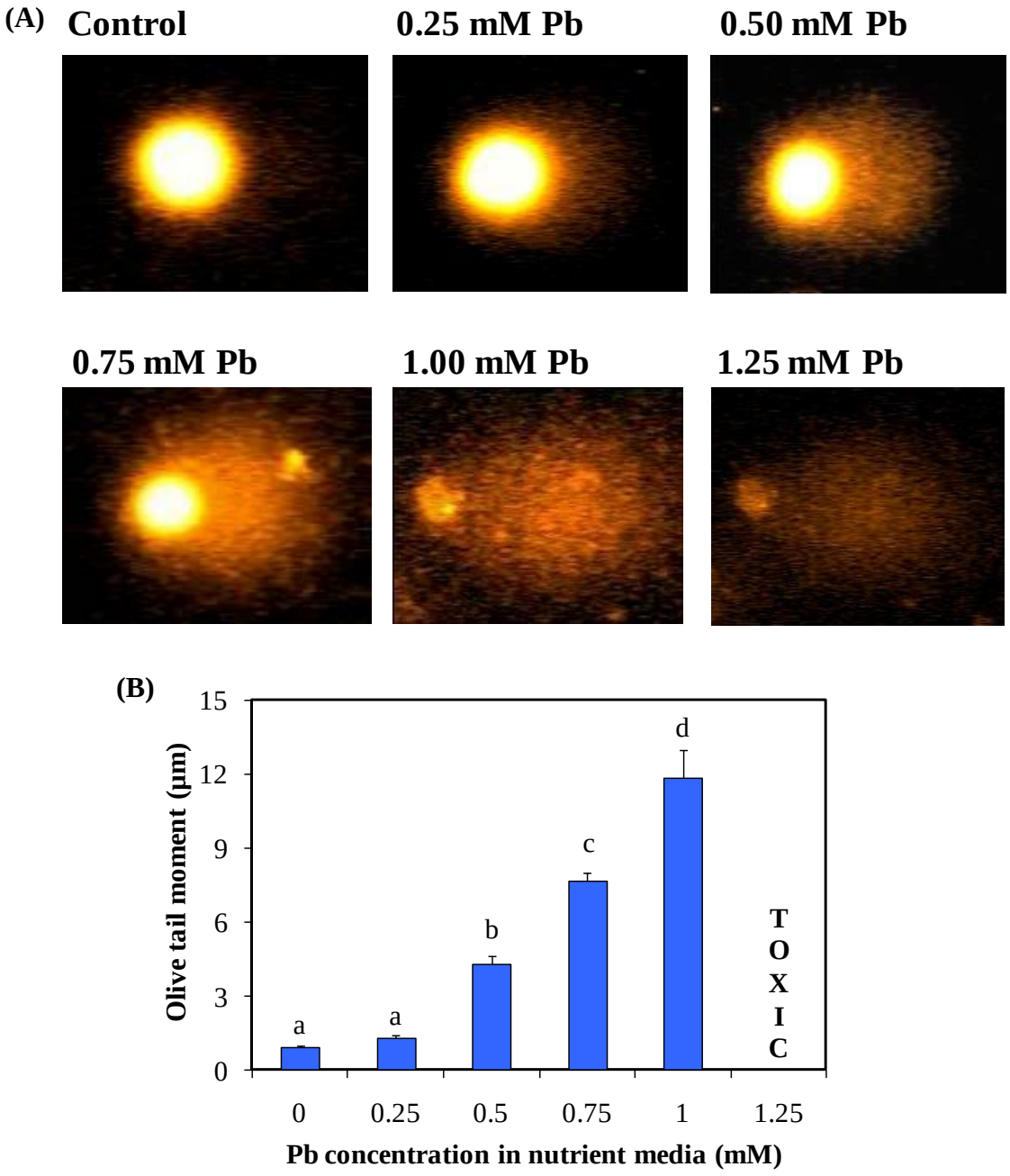

Fig. 24 Pb-induced DNA damage evaluated by comet assay on the basis of OTM. **(A)** Comets in root cells of *T. triangulare* representing Pb-induced DNA damage. **(B)** Dose dependent induction of DNA damage in root of *T. triangulare* after 7 days of Pb treatment. Mean values (± SE) denoted by different letters are significantly different ($P \leq 0.05$) between each other.

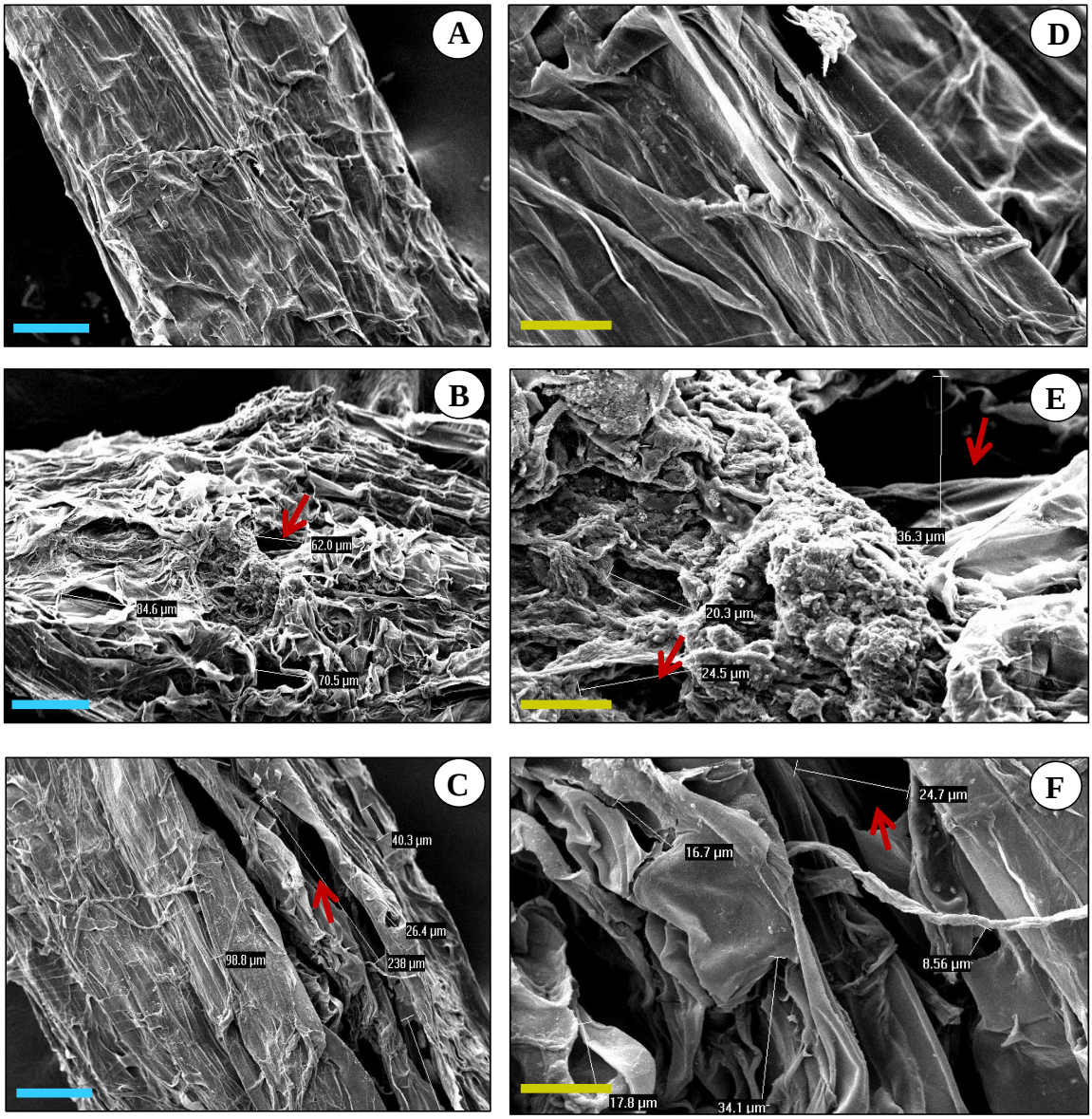

Fig. 25 Scanning electron micrographs showing the root surface: control **(A, D)**, 0.25 mM Pb **(B, E)** and 1.25 mM Pb **(C, F)**. Electron micrographs **A**, **B** and **C** are at 200 X magnification (Bar = 100 µm). Electron micrographs **D**, **E** and **F** are at 1000 X magnification (Bar = 20 µm). Arrow represents the rupture the root integrity and pore formation on root surface.

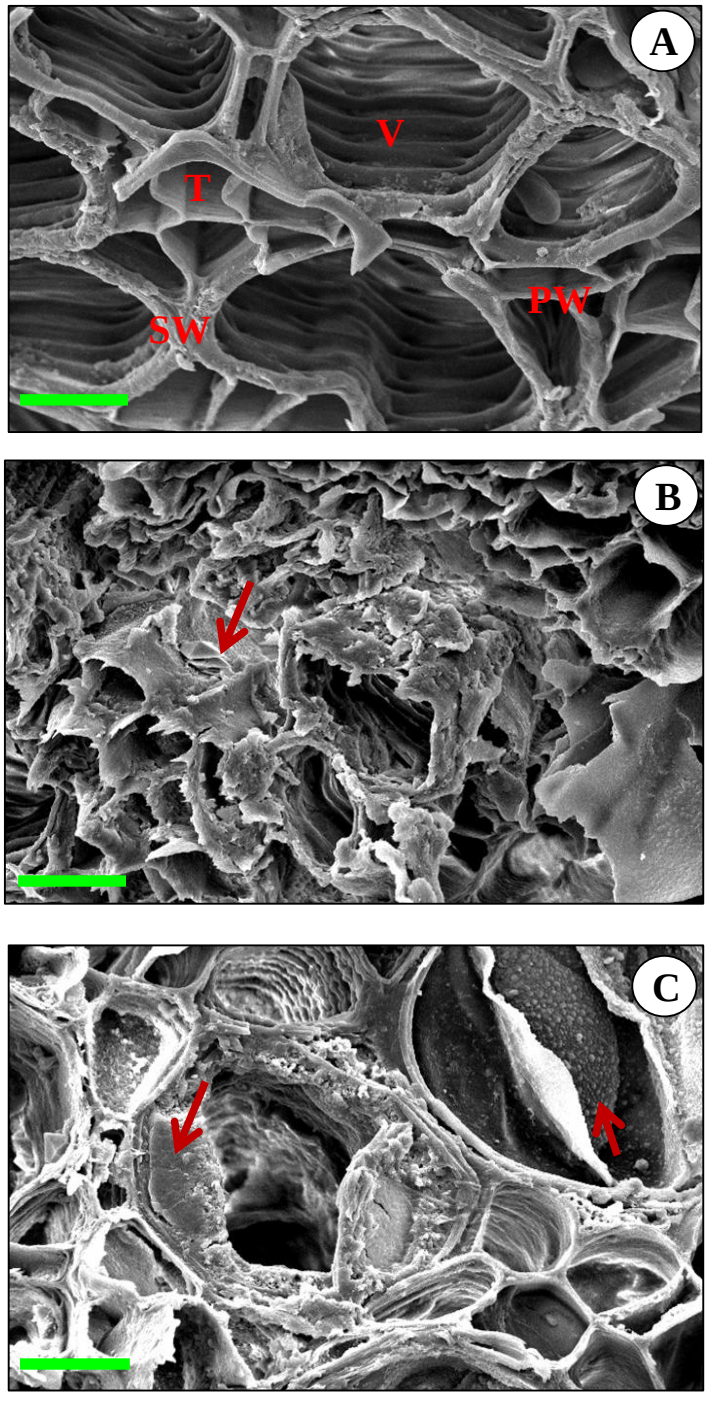

Fig. 26 Scanning electron micrographs showing the stem transverse sections: control **(A)**, 0.25 mM Pb **(B)** and 1.25 mM Pb **(C)**. Electron micrographs are at 1000 X magnification (Bar = 20 µm). E and F showed damage of internal structures and clotted depositions along the cell walls of vascular bundles represented by arrow.

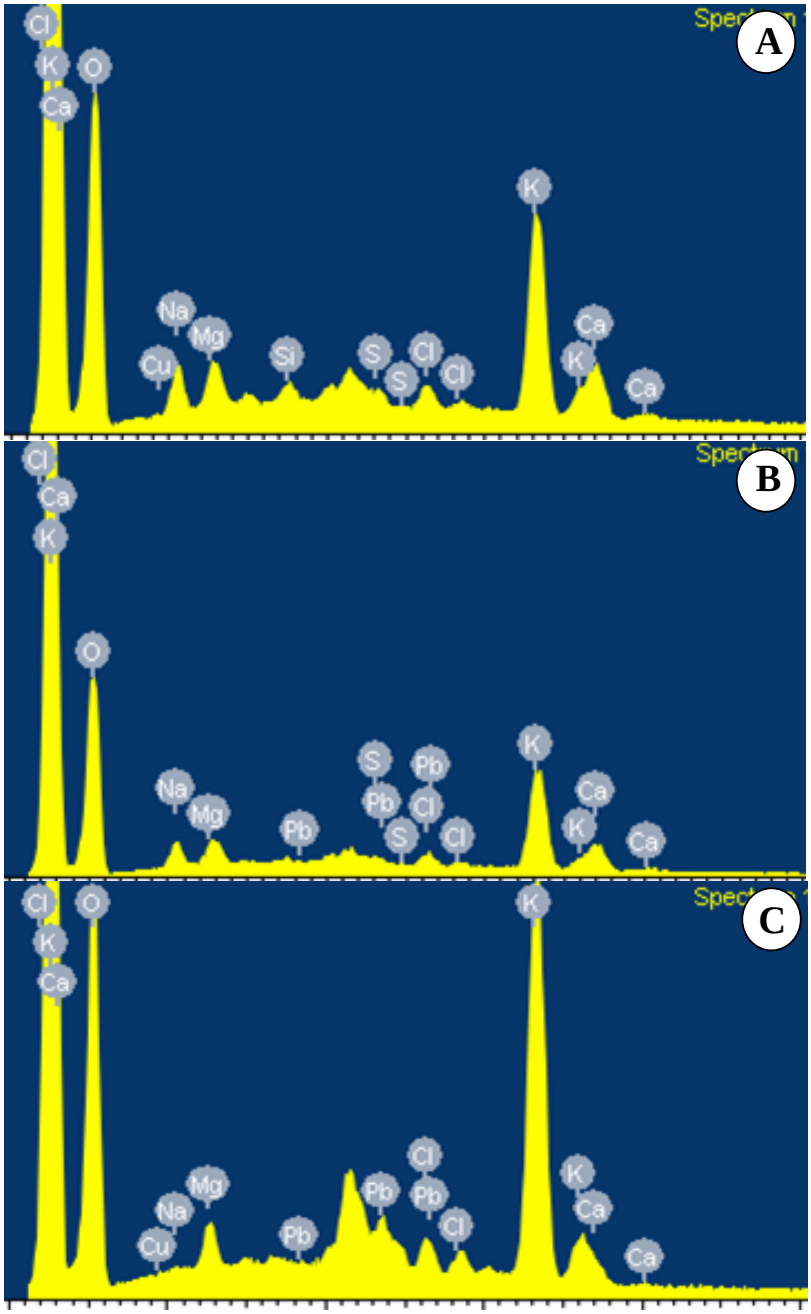

Fig. 27 Energy dispersive X-ray spectral line profile of *T. triangulare* roots: control **(A)**, 0.25 mM Pb **(B)** and 1.25 mM Pb **(C)**. EDS micrograph showing elemental atomic percentage of the imaged area for the *T. triangulare* roots samples using FESEM/EDS.

Discussion

In the present study, extracellular H_2O_2 production increased after 7 days of Pb treatment with respect to control. With confocal laser scanning microscopic images we could visualize that Pb significantly increased the H_2O_2 production in treated roots when compared to control root. The dose-dependent increase in histochemically visualized cellular H_2O_2 generation was in good agreement with extracellular H_2O_2 generation in root tissue of *T. triangulare* (**Fig. 21A**). Our result is in good accordance with previous studies reporting higher H_2O_2 generation in *Wolffia arrhiza* (Piotrowska et al. 2009), *Pisum sativum* (Malecka et al. 2009), *Triticum aestivum* (Kaur et al 2012), *Oryza sativa* (Li et al. 2012) and *Sedum alfredii* (Huang et al. 2012) upon Pb exposure. It has been reported that the disturbance in electron transport chain in the membrane is the major cause for ROS generation (Sharma and Dubey 2005; Pourraut et al. 2011). From our study, we can suggest that *in vivo* H_2O_2 analyses through histochemical visualization under Pb treatment was sensitive, fast, and reliable. HMs stress in plants causes oxidative damage to membrane lipid and proteins through generation of ROS (Pena et al. 2008; Aravind et al. 2009; Huang et al. 2012). It was reported that ROS play an important role as signal transduction that regulates plant defense responses to HMs stress (Aravind and Prasad 2003).

Our previous objective showed that Pb taken up by *T. triangulare* is mostly accumulated in roots, lesser in shoots and least in leaves (below detection limit). The present results indicated that Pb accumulation leads to cell death in root tissue evaluated by Evans-blue staining, a measure of disintegration of membrane integrity (Baker and Mock 1994). The measure of cell death showed a significant correlation with H_2O_2 (R^2= 0.831; **Fig. 22F**) generation, lipid peroxidation (R^2= 0.855; **Fig 22G**) as well as with LOX activity (R^2= 0.874) in the root tissue of *T. triangulare* following exposure with Pb in the present

study. Pb-induced lipid peroxidation have been reported in a number of plants: *Potamogeton crispus* (Hu et al. 2007), *Wolffia arrhiza* (Piotrowska et al. 2009), *Acacia farnesiana* (Maldonado-Magaña et al. 2011), *Triticum aestivum* (Lamhamdi et al. 2011), *Salsola passerine* and *Chenopodium album* (Hu et al. 2012) and *Sedum alfredii* (Huang et al. 2012). Membrane lipid peroxidation is a very sensitive reaction caused by HMs stress and is initiated by ROS and/or by the enzyme LOX, which is the key enzyme that produces hydroperoxide and oxy-free radicals by catalyzing the peroxidation of unsaturated fatty acids of biomembranes (Aravind et al. 2009). Increased LOX activity in the present study showed good correlation with H_2O_2 generation (R^2= 0.848; **Fig. 23E**) and lipid peroxidation (R^2= 0.855). LOX mediated lipidperoxides accumulation was reported in Pb treated *Sedum alfredii* (Huang et al. 2012). It is possible that the Pb induces the LOX activity, which through production of hydroperoxide derivative attacks the cell membrane and causes oxidative stress in *T. triangulare* root cells.

The dose-dependent decline in protein content of Pb treated roots observed in the present study (**Fig. 22D**) could be due to inhibition of protein synthesis and/or protein oxidation. Pb treatment induces a substantial increase in the formation of oxidation product of proteins measured as protein carbonyls content (**Fig. 23C**), which was reflected as a decrease in the total protein content. Carbonyls containing oxidative products are formed as a result of hydroxyl radical ($^{\bullet}OH$) attack on susceptible amino acids or peptide side chain of proteins (Aravind and Prasad 2003; Pena et al. 2008). Protein degradation is the process to prevent accumulation of the unfolded, damage, abnormal and oxidized protein regulating protein processing and maintain intracellular protein levels (Buchanan et al. 2000; Shringarpure et al. 2003; Pena et al. 2008). Thus, the intracellular levels of oxidized proteins imitate the equilibrium between the rate of protein oxidation and the rate of oxidized protein degradation (Pena et al. 2008). Cu-induced proteins oxidation has been mainly investigated by measuring protein carbonyl contents spectrophotometrically.

Higher levels of protein derived carbonyls were found in corkwing wrasse (*Symphodus melops*) captured near a disused Cu mine where water and sediments were contaminated with various HMs (Almroth et al. 2008). Our result is in accordance with the concept that oxidatively modified proteins may be selectively degraded, though degradation may not be a necessary consequence but rather protein carbonylation may represent a regulatory mechanism to finely tune the oxidative stress response.

A variety of proteins function as scavengers of ROS, including SOD and CAT measured here that represent biomarkers of antioxidative response to Pb stress (Reddy et al. 2005; Wang et al. 2011; Huang et al. 2012). In contrast to protein concentration, SOD and CAT activities were gradually increased and were negatively correlated (R^2= 0.569 and R^2= 0.479, respectively) with the total protein contents. SOD is considered to play most significant role and first line of defense in active oxygen species scavenging because its action prevents the accumulation of $O_2^{\bullet-}$ radical, which could lead to generation of toxic $OH^{\bullet}$ (Reddy et al. 2005; Hu et al. 2007; Shaw et al. 2006). SOD is the key enzyme in plant cells that dismutates superoxide radical ($O_2^{\bullet-}$) to form H_2O_2 and O_2. Increase in SOD activity showed good correlation with Pb-induced membrane damage (R^2= 0.851) and increased ROS (R^2= 0.959; **Fig. 23F**) production, respectively. CAT is an important H_2O_2 scavenging enzyme, which detoxifies H_2O_2 directly in the cell (Sharma and Dubey 2005). Increase in CAT activity could possibly be due to the result of both a direct effect of Pb and an indirect effect mediated via an increase in H_2O_2 (R^2= 0.725; **Fig. 23G**) level through SOD (R^2= 0.795). It is observed that the tendencies of LOX, SOD and CAT activities showed positive correlation with the concentration of Pb in treatment solution.

Studies of Pb with *Potamogeton crispus* (freshwater plant) showed that the high peroxidases activities and MDA content were observed with an increase in Pb concentration, whereas SOD and CAT activities firstly decreased and then increased. Pb-dependent increase in activities of SOD and CAT from wheat seedling extracts was

observed at 0.15, 0.30, 1.5, and 3.0 mM of Pb concentration (Lamhamdi et al. 2011). This suggested that these enzymes could be used as environmental biomarkers of HMs pollutions (Dazy et al. 2009). The responses of antioxidative enzymes activities in leaf of accumulating ecotype (AE) and non-accumulating ecotype (NAE) of *S. alfredii* have showed that accumulating ecotype was more tolerant to excessive Pb levels in growth medium (Liu et al. 2008). Under such conditions the activities of SOD and CAT were elevated in leaves of AE. However, in NAE, only SOD activity was increased while CAT activity was declined after Pb treatment comparing to the control plants. With increase in Pb level, MDA content increased significantly in both ecotypes of *S. alfredii,* indicating that Pb toxicity leads to lipid peroxidation and membrane damage, but MDA content in leaves of NAE was higher than in AE plants (Liu et al. 2008; Huang et al. 2012).

Proline is a multi-functional amino acid which is reported to accumulate in plant cells in response to various stresses including HMs stress (Szabados and Savouré 2010). It is suggested that accumulation of compatible amino acids like proline seems to be one of the means by which plant cells combat non-enzymatically against Pb generated free radicals (Sharmila and Saradhi 2002). Proline followed an inverted U-shaped dose response curve, which was enhanced at 0.25–0.75 mM Pb suggesting the hermetic, low dose induction and high dose reduction, response against increasing Pb concentrations (**Fig. 23D**). The increased accumulation of proline at low Pb doses suggests that proline accumulation is essential to maintain the osmotic uptake of water into root cells. Similar results were observed by the Rodriguez et al. (2013) in lupin roots treated with 0.5 and 1.0 mM Pb. Result of carbonyl contents showed that Pb at 0.75, 1.0 and 1.25 mM caused the significantly high rate of protein carbonylation that might be resulted in dysfunction in cellular proteins or enzymes (Aravind and Prasad 2003). Accumulation of this compatible organic acid is believed to protect plants against osmotic stress by regulating osmotic potential, from enzyme denaturation, protect macromolecules against denaturation and

stabilization of protein synthesis machinery, scavenging toxic oxygen species and act as a reservoir of carbon and nitrogen sources (Alia and Saradhi 1991; Raymond and Smirnoff 2002; Sharmila and Saradhi 2002; Sun et al. 2007; Hunag et al. 2010; Yang et al. 2011). It is possible that Pb at higher concentrations have declined the 1-pyrroline-5-carboxylate synthase (P5CS) and ornithine aminotransferase (OAT) enzymes activities and interfered enzymatic synthesis of proline (monocarboxylic acid) or may be due to increased proline catabolism/degradation by activating the enzymes PDH at those Pb concentrations (Sharmila and Saradhi 2002; Rodriguez et al. 2013), but it needs further studies. Obtained data may imply that enzymatic synthesis of proline Rodriguez et al. (2013was strongly affected by the metal ions.

DNA damage in control and Pb treated roots was estimated using the alkaline comet assay, which is a quick and sensitive fluorescent method that allows measurement of DNA strand damage in individual cells (Patnaik et al. 2011). Visual examinations gave a fairly good indication of DNA damage (**Fig. 24A**), which showed an individual isolated nucleus comprising a head and a tail. The head corresponds to the DNA amounts that still remain in the nuclear matrix region, whereas the tail reveals the DNA fragments migrating from the nuclei (Kumaravel et al. 2009). Alkaline comet assay detects DNA damage as single stranded and/or double stranded DNA breaks at the level of eukaryotic genome. Pb is known to potential genotoxic agent, which directly destroy microtubules of the mitotic spindle causing characteristic c-mitosis (Wierzbicka, 1994 and Eun et al., 2000) or DNA strand breaks which lead to chromosome fragments through the production of ROS molecules. ROS attack to DNA causes either altered bases or damaged sugars or both that undergo fragmentation and resulted in to strand break. This involves $^{\bullet}OH$ addition to double bonds, while sugar damage mainly results from hydrogen abstraction from deoxyribose leads to single strand break (Dizdaroglu 1993). This occurred through deletion of the C4' hydrogen atom from deoxyribose gives rise to deoxyribose radicals that further

react to produce DNA strand break, which may have serious consequences for the cell injuries such as inhibition of replication and failure of DNA repair (Evans et al. 2004; Roldan-Arjona and Ariza 2009).

Pb can inhibit the DNA synthesis or may even block the cells in the G2 phase of cell cycle preventing the cells from entering the mitosis (Sudhakar et al., 2001). It has been reported that Pb may also have inhibitory effects on nuclear proteins involved in DNA-repair or DNA topoisomerase II involve in chromosome segregation either by alteration in protein functional structure or by inhibiting the protein synthesis at transcription level (Panda and Panda 2002; Siddiqui 2012). Ability of Pb to cause DNA damage in root cells of *Lupinus luteus* was first demonstrated by Rucińska et al. (2004). Subsequently, comet assay using *Nicotiana tabacum* and *Solanum tuberosum* plants was successfully applied to monitor genotoxicity of soils heavily contaminated with Cd, Cu and Pb (Gichner et al. 2006), respctively. It has been reported that Pb binds strongly to a large number of molecules like amino acids, several enzymes, DNA and RNA; thus it disrupts many metabolic pathways (Patra et al. 2004). In the present study, the Pb treatment significantly increased the frequency of DNA damage at the 0.50–1.0 mM (**Fig. 24B**) that followed a dose-response (Shahid et al. 2011), which perhaps was mediated through the generation of ROS. The potential of genotoxicity was reported in root cells of *Vicia fava* upon Pb exposure (Lamhamdi et al. 2011).

Structural modification in roots and stem of *T. triangulare* plants due to uptake and accumulation of Pb were investigated by using SEM. In our experiment, we have noticed that given Pb treatment resulted in gradual changes in root morphology and stem internal structure, leading to a deformed structural organization compared to respective control. Pb treatment developed longitudinal ruptures in root resulted in formation of pores, when compared to respective control (**Fig. 25A-F**). Rupture in root's rhizodermis and outer cortex has been reported in cowpea (*Vigna unguiculata*) exposed to aluminum (Al), Cu

and lanthanum (La) (Kopittke et al. 2008). Certainly, the rupture on the Pb treated roots appears to be more or less similar to those formed in Al, Cu and La treated cowpea roots (Kopittke et al. 2008). Further analysis of stem T.S. revealed that most of the Pb was accumulated within the xylem vessels (**Fig. 26B, C**). The increase number of vacuoles and the loss of cell shape and decrease in intercellular spaces have also been observed in the Pb treated plant over the control plant, which may inhibit the translocation or uptake of nutrient elements, Pb and water from roots to stems and aerial part of the plant. This is confirmed in our previous study by the significant decrease in relative water content and atomic percentage of nutrient elements in leaves of *T. triangulare*. However, 1.25 mM Pb concentration resulted in higher amount of morphological and structural modification in roots and stems in comparison to control and 0.25 mM Pb treated plants, respectively.

The EDS analysis of intercellular elements distribution in the *T. triangulare* root revealed that, Pb amount was higher in the 1.25 mM Pb treated group compared to the 0.25 mM Pb. Similarly, the atomic% of O and K were also found to increase in 1.25 mM Pb treated sample (**Table 9; Fig. 27**). In contrast to the elements described above, the atomic% of other elements in Pb treated root tissues declined, which suggested the avoidance of the elemental uptake. It was noted that in *Brachiaria decumbens* (signal grass), *Chloris gayana* (Rhodes grass) (Kopittke et al. 2007) and *Spirodela polyrhiza* (Qiao et al. 2012) toxic levels of Pb caused reductions in the most of the nutrients concentrations in shoot tissue. A similar result was observed for Na, Ca, Mg, Cl, Si, S and Cu atomic% in the present study. The study showed that Pb treatment had negative effects on the nutrient elements in the *T. triangulare* root. Atomic% of Si and S analyzed by EDS were below detection limit in both 0.25 and 1.25 mM Pb treated roots. Metal transporters belonging to the CaCA (Ca-calmodulin) superfamily have been identified as being able to transport H^+, Ca^{2+}, Na^+ and K^+ (Manara 2012). The integral component of Ca^{2+} cycling systems that involve the efflux of Ca^{2+} across membranes against a concentration gradient, which

further is achieved by using a counter electrochemical gradient of other ions such as H^+, Na^+ or K^+ (Emery et al. 2012). The Na or K/Ca ratio is crucial for water balance in plants. Competition interference with such transporters may form the basis of the negative interactions between nutrient elements and Pb in plants. Furthermore, essential metals Na, Mg, Cu and Ca are acts as catalyst for many of the enzymatic processes that are necessary for plant growth, development and metabolic processes (Sharma and Dubey 2005). Thus, we may postulate that decreased in the nutrients atomic% in the present study were more effective in the direct or indirect role of altered plant growth and metabolic characteristics.

Conclusions

Considering our results we can conclude that accumulated Pb in the root tissue causes oxidative stress and genotoxicity, which is manifested through increased ROS production, cell death, and increased MDA content and increased LOX activity in comparison to control. *T. triangulare* showed good tolerance mechanism against Pb toxicity through the increased activity of SOD, CAT and APX and accumulation of free proline in Pb treated roots. The increase in Pb treatment caused reduction in total protein contents, which may be possible due to increased protein oxidation. Result of genotoxicity concluded that the comet assay is an efficient bioassay technique, which demonstrates the Pb-induced DNA damage and cell death in *T. triangulare* roots. SEM analyses revealed that Pb treatment developed ruptures in root surface, which resulted in formation of pores on root; Pb accumulation within the xylem vessels, and the loss of the cell integrity in stem. The atomic% of elements in Pb treated root tissues declined, supporting the idea of an avoidance mechanism.

Objective 4

Pb-induced responses of ascorbate-glutathione, related metabolites and enzymes

Introduction

HMs contamination in the environment poses threat to all forms of life. Studies have revealed the phytotoxic effects of elevated concentrations of HMs, particular Pb, on growth, water potential, physiological, biochemical and molecular processes of plants (Myśliwa-Kurdziel and Strzałka 2002; Malec et al. 2009; Prasad et al. 2006). Despite the toxicity of these HMs, several plants growing in metals polluted soil, are able to exclude, accumulate or hyperaccumulate HMs and acquire a wide range of adaptive strategies (Sharma and Dietz 2006; Anjum et al. 2012; Ahmad and Prasad 2012). However, sensitive plants develop visible symptom of phytotoxicity due to metal exposure. Some of the well established HMs phytotoxic manifestations includes, generation of ROS as well as replacement of enzyme cofactors and transcription factors, inhibitions of antioxidative enzymes, cellular redox and ionic transport imbalance leading to oxidative damage (Cenkci et al. 2009; Potters et al. 2010; Ann et al. 2011; Huang et al. 2012).

HMs-induced oxidative stress: dynamics of cellular redox status and ROS

The HMs effect on living organisms depends on their chemical and physical properties. It is possible to select three different molecular mechanisms of Pb toxicity: a) ROS production via the auto-oxidation or via Fenton reaction; b) blocking of essential functional groups in biomolecules; c) substitution of necessary metal ions from biomolecules (Schützenendübel and Polle 2002). The cellular redox state maintains normal cell homeostasis and is a key determinant of metal phytotoxicity. Pb ions are well known causing agents for altering cellular redox balance (Potters et al. 2010). Influence of Pb on the cellular redox balance is connected with development of oxidative stress and damage in plants. In these conditions the ability of plants to resist oxidative stress with using antioxidant systems is limited. Many studies showed that ample amount of HMs leads to

reduction of redox active enzymes activities (Sharma and Dubey, 2005; Potters et al. 2010; Ahmad and Prasad 2012; Lamhamdi et al. 2013). The cellular redox state is made of the individual redox active molecules in cells and for each of them redox state can be defined as the ratio between reduced and oxidized molecules within a pool (Potters et al. 2010; Huang et al. 2012). Major components maintaining cellular redox state are ascorbate (ASC), glutathione (GSH or GSSG) and pyridine nucleotides nicotinamide adenine dinucleotide (NAD^+)/nicotinamide adenine dinucleotide phosphate ($NADP^+$) (Ann et al. 2011).

Importance of non-enzymatic antioxidants during HMs-induced oxidative stress

Plants exposure to Pb stress affects the reactions of the antioxidant systems which depends on plant type, tissues exposed, type of the metals used and the dose intensity. Along with enzymatic system, plant cells posses a non-enzymatic antioxidative defense system against ROS, which includes glutathione, phenols and flavonoids and other primary and secondary metabolites. Plant phenolic compounds such as flavonoids and lignin precursors have been recognized largely as beneficial antioxidants which can scavenge harmful active oxygen species. Phenolic compounds which could be also substrates for different peroxidases were the first line of defense against Cu stress in experiment with red cabbage (Posmyk et al. 2009). It was shown in experiment with *Raphanus sativus* that phenolic acids as well as the total and reduced ascorbate content increased with the intensification of Cu treatment. Non-enzymatic antioxidants such as ascorbic acid (AsA), glutathione (GSH) and secondary metabolites to suppress the Pb-induced ROS molecules (Shu et al. 2012). These non-enzymatic antioxidants are intermediates of ascorbate-glutathione cycle (AGC) which plays a major role in H_2O_2 scavenging pathway operating in the chloroplasts as well as the cytosol. Operations of the AGC not only maintain the

reduced active forms of AsA and GSH on an appropriate level, thereby adjusting the cellular redox potential, but also participate in ROS detoxification (Potters et al. 2010).

Glutathione metabolism during HMs-induced oxidative stress

Excessive amounts of HMs trigger a wide range of cellular responses including changes in gene expression and synthesis of metal-detoxifying peptides. Plants exposed to HMs, synthesize a set of diverse metabolites that include specific amino acids, such as proline and histidine, peptides such as glutathione, phytochelatins (PCs) and the amines (Sharma and Dietz 2006; Estrella-Gómez et al. 2009). Glutathione is widely distributed redox active molecule in living cells and the tripeptide GSH (γ-Glu-Cys-Gly) is playing a key role in scavenging ROS and protecting membrane to damage by these ROS. The oxidized form of glutathione (GSSG) is readily converted to reduced form (GSH) by the enzyme glutathione reductase (GR). GR also plays a key role in the antioxidant defense processes, by reducing GSSG, thus allowing a high GSH/GSSG ratio to be maintained. Study on maize plantlets after 6 days action of low Cd concentration showed to increase in GR and glutathione peroxidase (GP) activity (Syshchikov 2009). Glutathione metabolism tightly regulates biosynthesis of PCs in plants through the regulation of GSH and helps metal sequestration (Thangavel et al. 2007). The PCs consist of repeating units of γ-glutamylcysteine followed by a single C-terminal glycine, with the number of repeating units ranging from 2 to 11 (Grill et al. 1986; Cobbett 2000; Anjum et al. 2012). PCs are synthesized enzymatically by PC synthase (PCS) by the transfer of γ-Glu-Cys moieties to glutathione (GSH) (Estrella-Gómez et al. 2009; Zhao et al. 2010). PCS was purified from a variety of plant species and was found to be produced constitutively in the absence of metal induction (Grill et al. 1986). PCs link HMs, the complexes formed with them are then transported to tonoplast which transfers to the vacuole, where they get stored and detoxified from cells. The important mechanism of detoxification includes metal

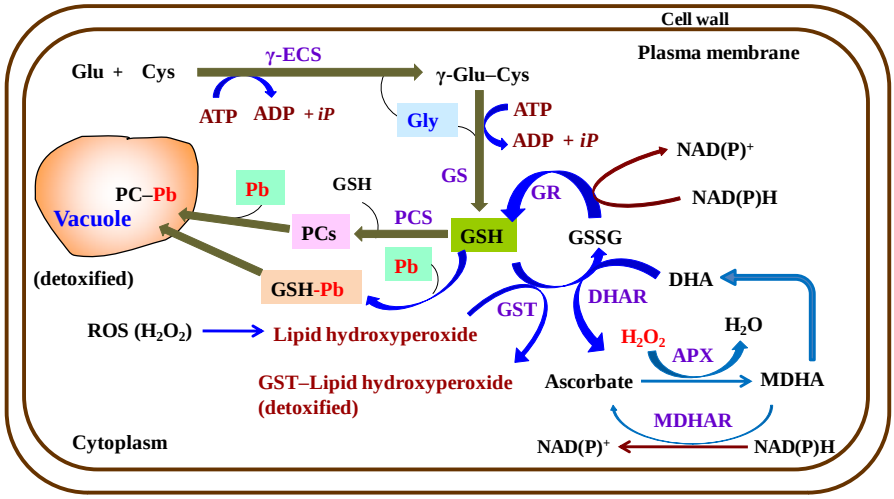

Fig. 28 Mechanisms of Pb detoxification and ascorbate-glutathione metabolisms: ADP, adenosine dinucleotide phosphate; APX, ascorbate reductase; ATP, adenosine triphosphate phosphate; Cys- cysteine; DHA, dehydroascorbate; DHAR, dehydroascorbate reductase; γ-ECS, γ- glutamylcysteine synthetase; Glu, glutamine; Gly, glycine; GR, glutathione reductase; GS, glutathione synthetase; GSH, glutathione (reduced); GSSG, glutathione (oxidized); GST, glutathione-S-transferase; H_2O_2, hydrogen peroxide; MDHA-monodehydroascorbate; MDHAR, monodehydroascorbate reductase; $NAD(P)^+$, nicotinamide adenine dinucleotide phosphate; NAD(P)H, NAD(P) reduced; iP, inorganic phosphate; PCs, phytochelatins; PCS, phytochelatin synthase; ROS, reactive oxygen species.

complexation with glutathione, amino acids, synthesis of phytochelatins and sequestration into the vacuoles. A schematic representation of the integrated Pb detoxification mechanisms and corresponding glutathione metabolism is illustrated in **Fig. 28**. Excessive stresses induce a cascade, MAPK (mitogen-activated protein kinase) pathway and synthesis of metal-detoxifying ligands, which will be of considerable interest in the field of plant biotechnology.

Thus, the available literatures provide convincing evidence, as presented above, suggesting the crucial roles of enzymatic and non-enzymatic antioxidants in different plants under HMs stress conditions. There is a lack of reports on extensive molecular aspects of HMs influence on the redox state of such compounds as such as glutathione,

ascorbate, and their redox couple in plants. Much progress has been done on different aspects of PCs and glutathione metabolisms and its related enzymes, taking into consideration their significance in HMs uptake, distribution and detoxification mechanisms in plants. But a number of questions such as the regulation of thiols and molecular characterization of sulfur, phenolics and flavonoids in economically important plant species growing under the influence of various HMs are yet to be answered. The aim of the present study is to analyzed the i) responses of non-enzymatic antioxidants, ascorbate-glutathione related metabolites and enzymes, and ii) functional group involved in Pb binding to understand the Pb tolerance and detoxification mechanisms in roots.

Materials and methods

Plant description and treatment in hydroponic experiment

T. *triangulare* was propagated through stem cuttings (5.0–7.0 mm diameter and 17–22 cm height) in conical flask containing 100 mL of modified Hoagland's nutrient media in plant growth chamber at 16/8 h (day/night) at 28 ± 2 °C for 3 weeks. After 3 weeks of acclimatization, uniform stem cuttings with adventitious roots and leaves were selected and treated with $Pb(NO_3)_2$ at different Pb concentrations of 0 (control), 0.25, 0.50, 0.75, 1.00 and 1.25 mM for 7 days under above conditions. Roots excised after 7 days of treatment were processed for analysis of various endpoints described as follows.

Non-protein thiols (NPSH)

NPSH in *T. triangulare* roots were analyzed according to Sedlak and Lindsay 1(968) and Bulaj et al. (1998). Fresh root (0.5 g) was homogenized in 4 mL of 0.1 M Tris-EDTA buffer (pH 8.0) under ice cold conditions. The homogenate was centrifuged at 15000 g for 20 min at 4 ºC. After centrifugation, NPSH content was measured in the supernatant by mixing with 2 mM 5,5'-dithio-bis-(2-nitrobenzoic acid) (DTNB) reagent. DTNB regent was prepared by mixing the 100 mM sodium acetate buffer with 4 mM DTNB (1:1). The 1 mL of reaction mixture containing 100 µL 0.1M Tris-EDTA, 50 µL DTNB reagent, 800 µL milliQ water and 50 µL supernatant. Mix well, incubate 5min at 37°C and the absorbance was measured at 412 nm (extinction coefficient = 13,600 M^{-1} cm^{-1}).

Molecular cysteine

Cysteine content in plant sample was estimated following the method of Gaitnode (1967). Plant material (500 mg) was homogenized in 5% chilled perchloric acid and

centrifuged at 10000 g for 10 min at 4 °C. Cysteine content was measured in supernatant using acid-ninhydrin reagent. For preparation of each 10 mL of acid-ninhydrin reagent, 250 mg of ninhydrin was dissolved in 6 mL glacial acetic acid and 4 mL HCL. Reaction mixture (3 mL) contained 1.0 mL each of supernatant, glacial acetic acid and acid ninhydrin reagent. Mixture was heated for 15 min, and then cooled rapidly and absorbance was recorded at 560 nm. Cysteine content was calculated by using the standard curve prepared from cysteine (Sigma-Alderich) and expressed as n mol g^{-1} fw.

Glutathione estimation

The GSH and GSSG estimation in control and Pb treated roots (0.5 g) were done fluorometrically by following the method of Hissin and Hilf (1976) with slight modification. The detail procedures for the analysis are described in **Objective 2** (**Page number 54**).

Estimation of enzymes activities

Control and Pb treated plant roots samples (1.0 g) were homogenized in 50 mM sodium phosphate buffer (pH 7.0) containing 2% PVPP. Homogenates were centrifuged at 13000 g for 20 min at 4 °C. After centrifugation supernatant were collected and the protein content in the supernatant was determined according to the method of Lowry et al. (1951) using a bovine serum albumin as a standard.

γ-Glutamylcysteine synthetase (γ-ECS, EC 6.3.2.2)

The assay was performed following the methodology of Reugsegger et al. (1992). The reaction mixture for assaying γ-ECS contained 50 µL each of 0.2 M sodium glutamate, 0.2 M L-amino butyrate, 40 mM Na_2-EDTA, 0.4% BSA, 100 µL each of 0.2 M $MgCl_2$, 50 mM Na_2-ATP and 500 µL of 0.2 M Tris-HCl (pH 8.2). It was pre-incubated for 2 min at RT

and the reaction was started by addition of 50 µg protein. The reaction mixture was incubated at 37 ^{o}C for 30 min and the reaction was stopped by the addition of 100 µL of TCA. The mixture was centrifuged and the supernatant was used for the estimation of phosphate content by phosphomolybdate estimation at 660 nm (Fiske and Subbarow, 1925) as previously described.

Glutathione-S-transferase (GST, E.C. 2.5.1.18)

The estimation of GST enzyme activity was performed according to Habig and Jacoby (1981). The reaction mixture for assaying GST consisted of 500 µL of 0.2 M sodium phosphate buffer (pH 7.0), 100 µL of 10 mM GSH, 10 µL of 0.1 M 1-chloro,2,4-dinitrobenzene (CDNB) and 390 µL of distilled water. The reaction was started by the addition of 50 µg of protein. The reaction proceeded by conjugation of CDNB to GSH and the increase in absorbance was measured at 340 nm for 1 minute. Activity of the enzyme was calculated using the extinction coefficient = 9.6 mM^{-1} cm^{-1}, and the values represented as unit of µ mol mg^{-1} protein min^{-1}.

Glutathione reductase (GR, E.C. 1.6.4.2)

The activity of enzyme GR was analyzed according to Jiang and Zhang (2001). The reaction mixture contained 500 µL of 0.2 M sodium phosphate buffer (pH 7.0), 100 µL each of 10 mM GSSG, 1 mM NADPH and 180 µL of distilled water. The components were added in the same order as they mentioned and the reaction was started by addition of 50 µg proteins. NADPH oxidation was recorded as the changes in absorbance at 340 nm for 1 min. The rate of enzyme activity was calculated using extinction coefficient = 6.2 mM^{-1} cm^{-1} and were expressed as unit µ mol mg^{-1} protein min^{-1}.

Ascorbate peroxidase (APX, E.C. 1.11.1.11)

The activity of APX was assayed by the method of Nakano and Asada (1981). The reaction mixture contained 50 mM sodium phosphate buffer (pH 7.0), 0.2 mM EDTA, 0.5 mM ascorbic acid, 250 mM H_2O_2 and 50 μg of protein. The activity was recorded as decrease in the absorbance at 290 nm for 1 min and the amount of ascorbate oxidized was calculated using extinction coefficient = 2.8 mM^{-1} cm^{-1}.

Cellular ascorbic acid (AsA) content

Ascorbate (AsA) was measured according to Logan et al. (1998) with minor modifications as per Ma and Cheng, (2003). Control and treated (1.0 g) root samples were homogenized in 1 mL of ice cold 6% (v/v) $HClO_4$. The extract was centrifuged at 10000 g at 4 ^oC for 10 min and supernatant was immediately assayed for total AsA. For the analysis 100 μL of extract was neutralized with 30 μL of 2 mM Na_2CO_3 and incubated for 30 min at room temperature with equal volume of 20 mM GSH in 100 mM Tricine-KOH (pH 8.5) and the absorbance was recorded spectrophotometrically at 265 nm (extinction coefficient = 14 mM^{-1} cm^{-1}).

Functional groups analysis by Fourier Transform Infra-red (FTIR) spectroscopy

Determination of chemical nature of functional groups, which are involved in roots tissue, were done by Fourier Transform Infra-red (FTIR) spectroscopy (JASCO FTIR-5300) as described by Wei et al. (2009) with slight modifications. FTIR analysis has done only for two samples i.e. control and 1.25 mM Pb treated roots. After 7 days, both control and Pb treated roots (1.0 g) were washes with DDW two times, followed by homogenization with DDW. Water was evaporated from homogenized sample and make them fine powder. The powdered sample were mixed with KBr and made KBr tablets,

which were directly used for FTIR analysis. Spectral Wavenumber was recorded in the ranges of 400−4000 cm^{-1}.

Statistical analysis

The experiments were repeated at least three times and the data presented corresponds to the mean values ± S.E. (standard errors) of three replicates (Microsoft Office 2003). One-way analysis of variance (ANOVA) were done with all the data to confirm the variability of data and validity of results, and performed Duncan's multiple range test (DMRT) by using SIGMASTAT software (version 11.0) to determine the significant difference between treatment group. Correlation analysis was performed wherever required. *P* values < 0.05 were considered significantly different with each other and denoted by different letters.

Results

Lead-induced changes in NPSH content

Results of our NPSH contents analysis showed that NPSH content were slight increased at low Pb concentration and thereafter declined (**Fig. 29A**). Moreover, the responses of NPSH against increasing Pb concentration showed a negative linear graph with a R^2= 0.924. Pb-induces NPSH content very slightly during 0.25 mM Pb by 3.5% in comparison to control. But the Pb treatment of 0.50–1.25 mM declined the NPSH contents in *T. triangulare* roots. The maximum significant ($P \leq 0.05$) reduction in NPSH contents were observed by 35.0%, 40.4% and 64.9% at 0.75, 1.0 and 1.25 mM Pb in comparison to control sample, respectively.

Lead-induced changes in cysteine content

This assay was based on the reaction of acid-ninhydrin reagent with present amino acid cysteine. The accumulation of cysteine contents was dose-dependent responses in *T. triangulare* roots (R^2= 0.912; **Fig. 29B**). A gradual increase in cysteine accumulation was observed in the roots subjected to 0.25–1.25 mM of Pb over control root. The accumulation of cysteine increased in stress responses and attained significant maximum accumulation during 1.25 mM Pb in comparison to control, the amount of cysteine significantly ($P \leq 0.05$) increased to approximately 21%, 28%, 33%, 39% and 46% during 0.25, 0.50, 0.75, 1.0 and 1.25 mM Pb, respectively.

Lead-induced changes in glutathione

The level of reduced (GSH) and oxidized (GSSG) glutathione directly point towards the induction of oxidative stress by Pb (**Fig. 30A**). GSH content in *T. triangulare* roots was

give very interesting result, which was first increased and then decreased. The regression analysis showed that as the Pb concentration increased in treatment media the GSH content declined with a R^2= 0.934 (**Fig. 30A**). The significant ($P \leq 0.05$) induction in GSH content was observed at only 0.25 mM Pb treatment, which accounted for 7.7% in comparison to control. The significant ($P \leq 0.05$) maximum declined (68.8%) in GSH content was observed during 1.25 mM Pb. On the other hand, GSSG level was found to gradually increased as the external Pb concentration increased (R^2= 0.956; **Fig. 30B**). The significant inductions in GSSG contents were observed at concentration 0.25–1.25 mM Pb and that accounted for 83.0%–236.5% in comparison to control, respectively. Total glutathione contents were calculated from the addition of GSH and GSSG contents (**Fig. 30C**). However, the total glutathione contents followed the same pattern as GSH (R^2= 0.860). In contrast to GSSG contents, the GSH/GSSG ratio also significantly ($P \leq 0.05$) decline and was inversely related to the increasing Pb treatments (R^2= 0.860; **Fig. 30D**). The correlation analysis between GSH and NPSH showed a positive linear correlation with a R^2= 0.821 (**Fig. 30E**), whereas the analysis of GSH and GSSG showed a negative relationship (R^2= 0.771) between these two values (**Fig. 30F**).

Lead-induced changes in γ-glutamyl cystein synthetase (γ-ECS) activity

A linear decline in γ-ECS activity was observed with increasing Pb concentration in *T. triangulare* roots (R^2= 0.874; **Fig. 31A**). However, the γ-ECS activity was slight induced at 0.25 mM Pb by 6.5%, but it was insignificant with the control value. The maximum declined in γ-ECS activities were observed at 0.75 (32.7%), 1.0 (42.7%) and 1.25 (45.5%), which were significantly ($P \leq 0.05$) in comparison to control, respectively. The γ-ECS followed the same pattern as free thiols and GSH did and showed a positive correlation with NPSH (R^2= 0.727; **Fig. 31D**) and GSH (R^2= 0.903; **Fig. 31E**).

Lead-induced changes in glutathione-S-transferase (GST) activity

Evidences from our spectrophotometric result showed that the activities of GST enzymes increased as the Pb concentration increased in the nutrient media (**Fig. 31B**). The increased in GST activities were strongly correlated (R^2= 0.947) with the increased in Pb concentration. In our experimental conditions, Pb treatments at 0.25 and 0.50 mM induced very slight GST activities, which were not significantly different from control. After 7 days, the maximum significantly ($P \leq 0.05$) induction in GST activities were observed at 0.75 (71.4%), 1.0 (89.1%) and 1.25 (91.3%) when compared to control, respectively. The increased in GST activity showed a positive correlation (R^2= 0.644) with increased in H_2O_2 contents in *T. triangulare* roots (**Fig. 31F**).

Lead-induced changes in glutathione reductase (GR) activity

Our results showed that GR activity was not much affected with Pb treatment in *T triangulare* roots (**Fig. 31C**). Pb treatment causes a slight insignificant induction in GR activity was observed during 0.25 and 0.50 mM Pb, which was declined at subsequent treatment concentrations. Interestingly, the induction and declined were not significant ($P \leq 0.05$) with the respective control. The maximum declined in GR activity was observed during 1.25 mM Pb stress which was accounted for 10.8% in comparison to control.

Lead-induced changes in total ascorbate content

The Spectrophotometric analysis of *T. triangulare* root extracts showed that Pb treatment caused dose-dependent reduction in total ascorbate content in comparison to control (**Fig. 32A**). Total ascorbate contents were negatively correlated (R^2= 0.965) with increase in Pb treatment concentration. The significant decline in the total ascorbate contents were observed during 0.25, 0.50, 0.75, 1.0 and 1.25 mM Pb treated *T. triangulare*

roots, which were accounted for reduction of 23%, 37%, 44%, 49%, 53% in comparison to control, respectively. The tendencies of total ascorbate contents were almost similar to that total glutathione contents and both were showed a strong positive correlation (R^2= 0.810; **Fig. 32C**) with each other.

Lead-induced changes in ascorbate peroxidase (APX) activity

Our results showed that 0.25 and 0.50 mM Pb slightly enhanced APX activity in comparison to control, respectively, which declined at further Pb concentrations in comparison to control (**Fig. 32B**). APX activity significantly ($P \leq 0.05$) decreased at only 1.0 and 1.25 mM of Pb in respect to control, respectively. The maximum increase and decrease in APX activities were observed at 0.50 mM (34%) and at 1.25 mM (55.8%), respectively.

Functional groups analysis by Fourier Transform Infra-red (FTIR) spectroscopy

The FTIR spectra of the control and 1.25 mM Pb treated root tissues were recorded in the range of 400–4000 Wavenumber (cm^{-1}) to obtain the information about the stretching and bending vibration and reduction in transmittance of characteristic functional group peak. FTIR spectra revealed that Pb treatment caused reductions in characteristics peaks when compared with control spectra (**Fig. 33**). In **Fig. 33** wavenumber for characterstic peaks were presented in numerical values (not decimal values). However, the detail about %transmittance and exact Wavenumber are listed in **Table 10**. The major reductions in peaks transmittance values were observed at 3391, 2922, 1643, 1381 and 1055 cm^{-1}. The region below 1000 cm^{-1} are considered as fingerprint zone and the binding of functional groups cannot be assigned to any perticular functional group due to complex interacting vibration system.

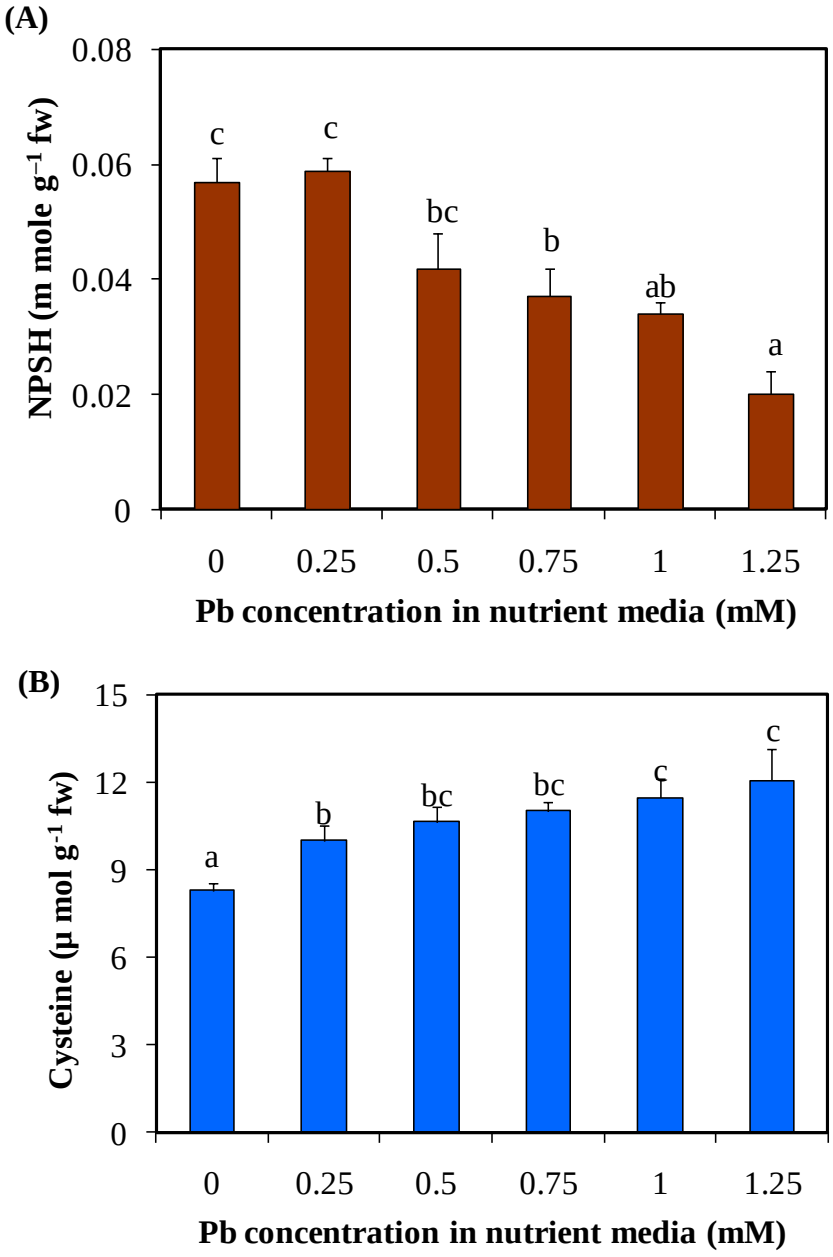

Fig. 29 Non-protein thiols (NPSH) **(A)** and amino acid cysteine **(B)** contents in *T. triangulare* roots after 7 days of Pb treatment. Mean values (± SE) denoted by different letters are significantly different ($P \leq 0.05$) between each other.

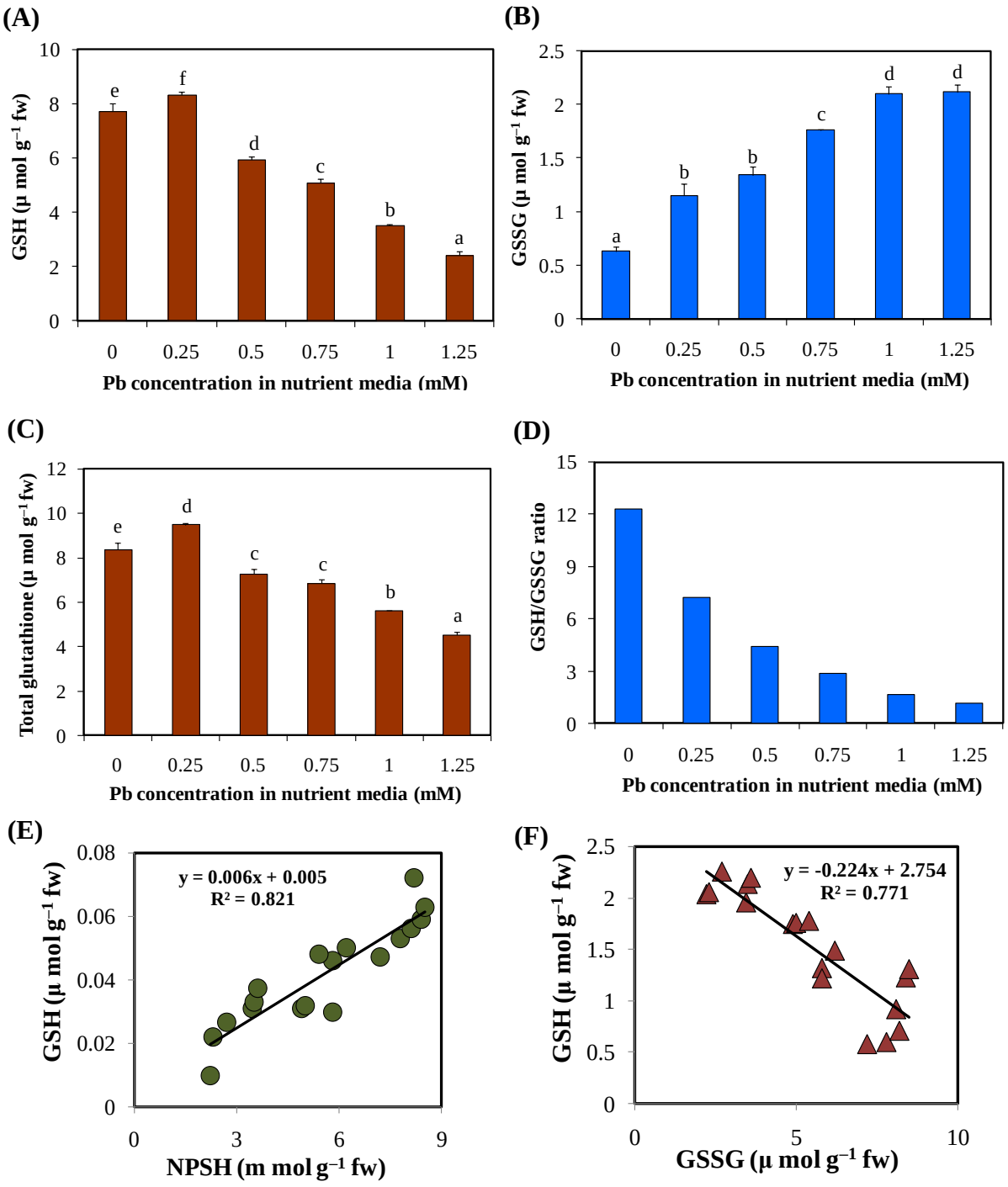

Fig. 30 Reduced glutathione (GSH) content **(A)**, oxidized glutathione content **(B)**, total glutathione contents **(C)** and GSH/GSSG ratio **(D)** in *T. triangulare* roots after 7 days of Pb treatment. Mean values (± SE) denoted by different letters are significantly different ($P \leq 0.05$) between each other. **(E)** and **(F)** represent correlation analysis of GSH-NPSH and GSH-GSSG, respectively.

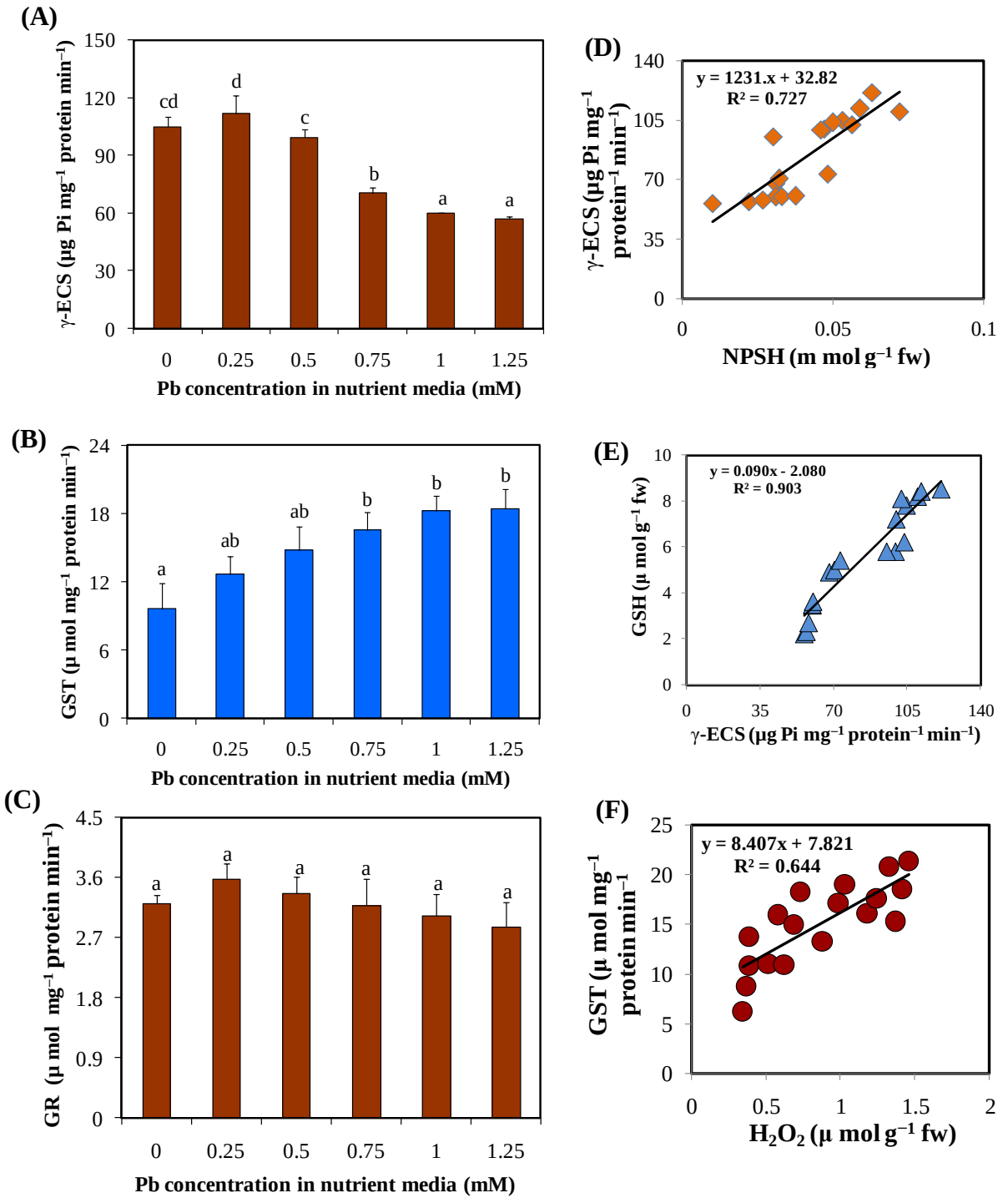

Fig. 31 Activities of **(A)** γ-Glutamyl cystein synthetase (γ-ECS), **(B)** glutathione-S-transferase (GST), **(C)** glutathione reductase (GR) activities in *T. triangulare* roots after 7 days of Pb treatment. Mean values (± SE) denoted by different letters are significantly different ($P \leq 0.05$) between each other. **(D)**, **(E)** and **(F)** represent the correlation analysis of γ-ECS–NPSH, GSH–γ-ECS and GST–H_2O_2, respectively.

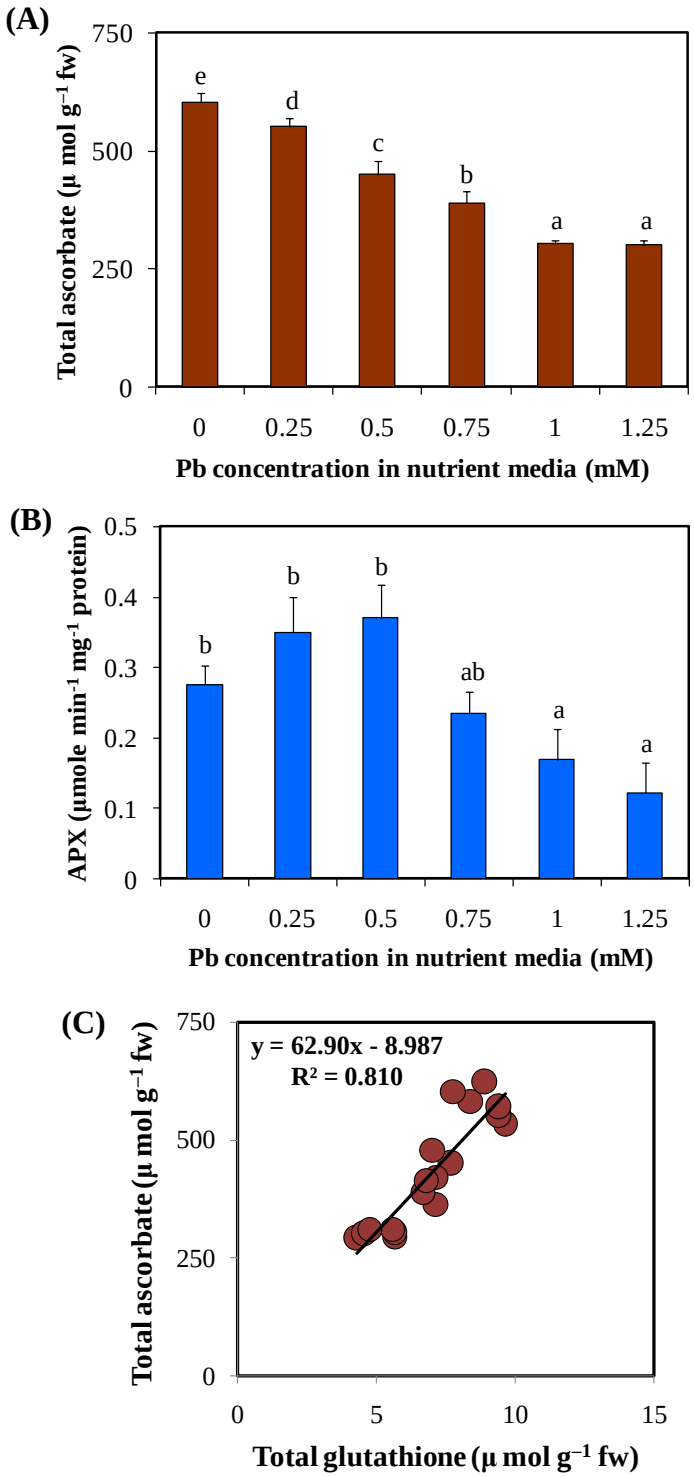

Fig. 32 Total ascorbate contents **(A)** and ascorbate peroxidase (APX) activity **(B)** in *T. triangulare* roots after 7 days of Pb treatment. Mean values (± SE) denoted by different letters are significantly different ($P \leq 0.05$) between each other. **(C)** Represent the correlation analysis between total ascorbate and total glutathione contents.

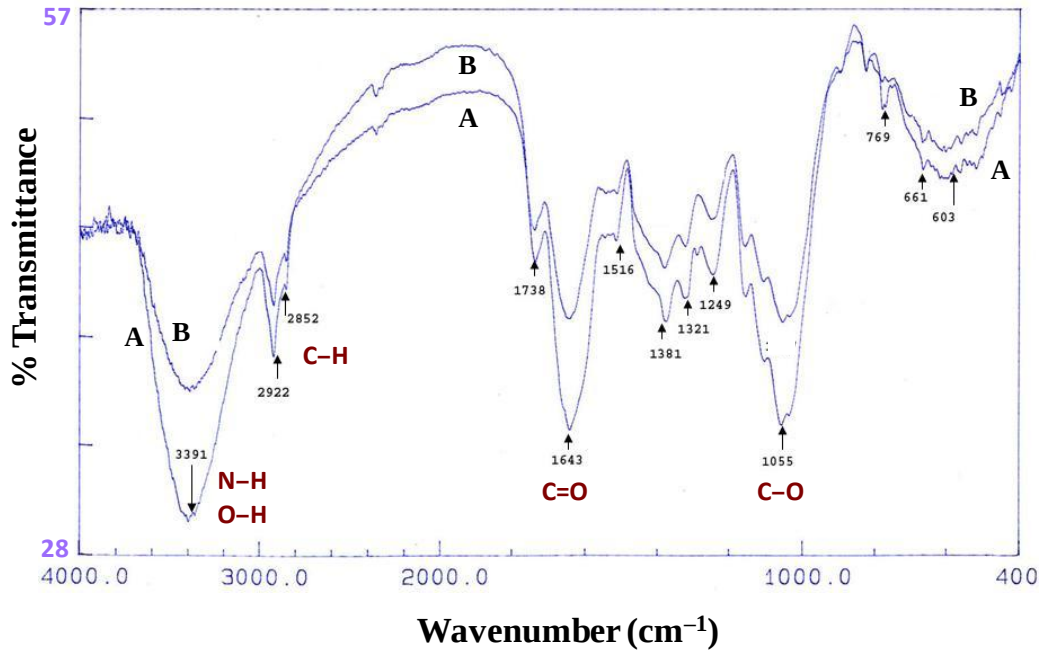

Fig. 33 Stretching, bending and changes in %transmittance of functional groups involved in binding and detoxification of Pb and Pb-induced free radicals by Fourier Transform Infrared Spectroscopy (FTIR) in roots: control sample **(A)** and 1.25 mM Pb treated **(B)** samples spectra.

Table 10 Changes in %transmittance of peaks representing the characteristic functional group involved in binding and detoxification of Pb and Pb-induced toxic radicals or metabolites.

Wavenumber	**% Transmittance**		**Difference in %transmittance**
	Control	**1.25 mM Pb**	
3391.16	36.7	27.8	8.9
2922.42	41.3	38.6	2.7
2852.98	43.6	42.1	1.5
1738.02	45.3	43.6	1.7
1643.50	40.6	32.6	8.0
1516.19	47.2	44.7	2.5
1381.16	43.2	40.4	2.8
1321.36	44.4	41.7	2.7
1249. 99	45.8	42.9	2.9
1055.16	40.4	32.9	7.5
769.67	53.3	52.0	1.3
661.64	50.0	48.5	1.5
603.77	49.4	48.6	0.8

Discussion

Our study showed that *T. triangulare* plant is efficient to accumulate Pb in its tissue as we observed in our previous objectives. The accumulated Pb has potential to caused oxidative stress in *T. triangulare*, which was evident by increased accumulation of free radicals, such as H_2O_2. The analyzed antioxidative systems could able to detoxify the Pb-induced directly or free radicals mediated injury by activating its enzymatic and non-enzymatic antioxidants. In relation with non-enzymatic antioxidants AGC metabolites always play an important role in stress alleviation as reported by various researchers (Ref).

In our present study, plant treated with Pb showed a variety of responses viz. alteration in AGC metabolites, related metabolites and enzymes. Pb treatment caused reduction in NPSH and induction in cystein accumulation in responses to Pb-induced oxidative stress in *T. triangulare* roots. It has been suggested that during HMs stress condition the stimulate sulfate absorption (Nocito et al. 2002; Anjuman et al. 2011) and other associated enzymes related with sulfate reduction such as ATP sulfurylase (ATP-S), APS reductase and cystein synthase (Rausch and Wachter 2005; Singh et al. 2010). Maximum reduction in NPSH was observed during 1.25 mM Pb treatment. Similar response was also reported in *Najas indica* treated with different Pb concentration for maximum 7 days (Singh et al. 2010). It has been observed that 0.1 mM Pb treatment for 7 days caused significant reduction in NPSH contents, whereas the same concentration declined the cystein content due to decreased activity of cystein synthase in *Najas indica* (Sing et al. 2010). The declined in NPSH in our study might be related with the incorporation of sulfur in to organic molecules such as sulfur containing amino acid (cys-residues) and peptides such as GSH and PCs, which further involved in metal binding and detoxification mechanisms. Treatment of Cd to *Egeria densa* (water weed) resulted in both a formation of thiol-enriched Cd complexing peptides and a synthesis of low-molecular-weight metal chelators (Malec et al. 2009).

Additionally, this peptide was characterized by a broad absorption band specific to mercaptide bonds and Cd-sensitive fluorescence emission of aromatic amino acid residues (Malec et al. 2009).

Cysteine, a –SH containing amino acid and is a key constituent of phytochelatins, which plays an important role in metal detoxification. The increased in cysteine content is initiated by sulfur assimilation, which is catalyzed by enzyme ATP-S, a rate limiting enzyme in sulfur assimilation, regulates cysteine (and thus GSH) biosynthesis. Cysteine itself acts as precursor for various sulfur containing metabolites, including GSH (Anjum et al. 2011). Khan et al. (2009) reported that increased ATP-S activity, cysteine and GSH content helped the mustard plant to tolerate against high Cd-induced oxidative stress. In our experimental condition the increase in cysteine content might be related to the level of plant tolerance mechanisms against Pb-induced oxidative stress (Chandra et al. 2009). An increase in cystein content could be due to the increased in cystein synthase activity (Singh et al. 2010). Pb-induced increase in cysteine content was reported in *Hydrilla verticillata* (Gupta et al. 1995) *Salix acmophylla* (Ali et al. 2003). Vadas and Ahner (2009) observed that pretreatment of cysteine and glutathione to *B. napus* and *Z. mays* facilitate increased accumulation of Pb and Cd in the plant tissues. Cysteine-mediated uptake rates of Pb and Cd were much higher than those for without pretreatment with cysteine in both plant species (Vadas and Ahner 2009). It has suggested that Pb or Cd may bind to cysteine or glutathione, which accelerate the roots metal accumulation via a biological mechanism that has been confirmed with an inhibitor and through observation of changing kinetics in pre-exposure experiments in both the plant (Vadas and Ahner 2009).

Glutathione is one of the major cellular safeguards and usually the most abundant intracellular non-protein thiols, maintains the cellular redox status. GSH plays a protective role as a key antioxidant and a chelating bioligand responsible for detoxification of HMs (Gupta et al. 1995; Mishra et al. 2006; Anjum et al. 2012).

Our results showed of GSH and GSSG estimation showed that Pb treatment declined GSH and stimulated GSSG contents. The increase in GSSG showed a true indication of oxidative stress. In this study, significant slight induction in GSH and total glutathione have been observed during 0.25 mM Pb treated roots followed by depletion at higher concentration (**Fig. 30**). The contents of NPSH and cysteine and the activity of γ-ECS were also increased at this concentration. Further the responses of GSH showed a good correlation with NPSH (R^2= 0.903; **Fig. 30E**) and γ-ECS (R^2= 0.903; **Fig. 31E**) activity. At 0.25 mM Pb, induction of GSH accumulation might be attributed to Pb-induced GSH synthesis via increased in NPSH content and activation of γ-ECS (Piechalak et al. 2002). On the other hand at higher Pb concentration (0.50–1.25 mM Pb) declined in NPSH contents as well as reduction in γ-ECS activity observed, suggested that these factors possibly responsible for the reduction in GSH and total glutathione contents at those Pb concentrations in *T. triangulare* roots. Furhermore, a significant reduction in γ-ECS activity was observed during 0.75–1.25 mM Pb stress in *T. triangulare* roots. γ-ECS (EC 6.3.2.2) catalyses the first step of glutathione (GSH) synthesis, producing gamma-glutamylcysteine (γ-EC) from L-glutamate and cysteine. The reduction in γ-ECS activity was also correlated (R^2= 0.727; **Fig. 31D**) with NPSH. It may suggest that decrease in NPSH content and γ-ECS activity might be a possibly cause for the reduction in GSH contents.

GSH, as a substrate, synthesize PC through a reaction catalyzed by phytochelatin synthase (PCS) an enzyme activated by HMs ions including Pb (Cobbett 2000). In most cases, HMs cause decline of glutathione in plant tissues. Such reaction is usually observed after actions of HMs and predefined the growing consumption of glutathione, which is used for the synthesis of PCs (Anjum et al. 2012; Zhao et al. 2010; Cobbett 2000). PC synthesis is induced by a variety of HMs (Schützendübel and Polle 2002; Shaw et al. 2004, 2006; Mishra et al. 2006 and 2009; Ahmad et al. 2012). Decline in GSH at higher

concentrations might be attributed to high consumption rate of GSH as antioxidant to combat oxidative stress or for the synthesis of PC. It might be also possible that during high Pb stress, the depletion of GSH content facilitate formation of Pb–GSH complexes and Pb-induced PCs synthesis with the help of enzyme PCS. PCS further bind to Pb and carry to vacuole and detoxify them. Furthermore, PCs synthesis reduces free Pb concentration in cytoplasm and contributes to suppress the activation of the stress-related responses in plant metabolism (Mishra et al. 2006). It has been reported that the expression level of the *Salvinia minima*, Pb-hyperaccumulator aquatic fern, PCS gene (*SmPCS*) was evaluated in response to Pb^{2+} treatment in both roots and leaves (Estrella-Gómez et al. 2009). Results suggested that the accumulation of PC in *S. minima* was a directly connected to Pb accumulation in tissues, where phytochelatins do participate as one of the mechanism to cope with Pb-induced stress (Estrella-Gómez et al. 2009).

GSH is widespread in bacteria, plants and animals and has been shown to exhibit high affinity for majority of metals. Additionally, GSH is a vital part of the antioxidant armory of plant cells against oxidative stress, and plays multifaceted roles by contributing to the cellular redox status (Anjum et al. 2011). Moreover, Malecka et al. (2009) has reported that Pb concentration of 0.5 mM for 4 days caused significantly declined the GSH level in *Pisum sativum* roots. Similar type of response was also observed in *Spirodela polyrhiza* treated with 0.4 mM Pb for 7 days (Qiao et al. 2012). Wang et al. (2012b) also reported declined in GSH content during 0.75 μM Pb treatment, in a duration dependent manner, where maximum reduction was observed after 6 days of Pb treatment. Pb-induced changes in GSH have been reported in *Helianthus annuus* (Strubińska and Hanaka 2012), *Acacia farnesiana* (Maldonado-Magaña et al. 2011), *Vicia faba* and *Phaseolus vulgaris* (Piechalak et al. 2002), *Zea mays*, *Hydrilla verticillata* and *Vallisneria spiralis* (Gupta et al. 1995, 1999, 2009).

The reduction in GSH and induction in GSSG contents are seems negatively correlated (R^2= 0.771; **Fig. 30F**) with each other. In *T. triangulare* roots Pb treatment cause a significant ($p \leq 0.05$) induction in GSSG content, which was maximum increased by 237% during 1.25 mM Pb stress (**Fig. 30B**). The studies with pea plant showed that during Pb stress, the amount of GSSG increased and reaching maximum after 4 days of Pb treatment, which could be due to decrease in a rate limiting factor, GSH, for the synthesis of GSSG (Malecka et al. 2009). Cytoplasmic pool of GSSG may be increased as a result of oxidation of glutathione due to oxidative stress, transported from apoplast to cytosol, where it is reduced once more to GSH through GR and NADPH (Foyer et al. 2001). The GSSG is get converted in to GSH by the reaction catalyzed by enzyme GR. GR is a member of flavoenzyme family which catalyzes the NADPH dependent reduction of GSSG to GSH. In our study we noted that Pb treatments have declined the GR activity in *T. triangulare* roots, but the responses were not significant different with control (**Fig. 31C**). The increase in GSSG content could be possibly due to decreased or no GR activity in reaction catalyzing reduction of GSSG to GSH. This reaction maintains a proper GSH/GSSG ratio in cells (Singh et al. 2010; Anjum et al. 2012). For example, in rice seedlings Pb toxicity causes an increase in GSH/GSSG ratio and the total glutathione pool suggested that this is evidently due to induction in GSH biosynthesis and rapid reduction of GSSG by the enzyme GR after Pb treatment (Verma and Dubey 2003) reported that GR activity increased which suggests possible involvement of GR in regenerating GSH from GSSG under Pb ions action.

On the other hand, results showed that Pb treatment caused declined in GSH/GSSG ratio (**Fig. 30D**). The reduction in GSH/GSSG ratio is only due to the rapid reduction in GSH and induction in GSSG contents during Pb treatments. Our results showed insignificant decrease in GR activity in Pb treated *T. triangulare* roots suggests that GR enzyme is not involved in regeneration of GSH from GSSG under Pb toxicity conditions

and further resulted in to decrease GSH/GSSG ratio and the total glutathione pool. In contrast, The analysis of roots of *Vallisneria natans* have consistently shown that GR activity increases in response to Pb treatment, in order to detoxify H_2O_2 or to produce glutathione for the synthesis of phytochelatins (Wang et al. 2012b). It has been suggested that the high GSH/GSSG ratio is necessary to achieve optimal protein synthesis in cells and thus plays a bridging role between primary and secondary responses of plant against metal toxicity (Nagalakshmi and Prasad 2000).

Glutathione-S-transferases (GSTs) are major phase II, GSH-dependent ROS-detoxifying enzymes mainly found in cytosol of the plant cell. GST involved in GSH-metabolism and thus plays important roles in the cellular antioxidant defense mechanisms of plants (Yan et al. 2008; Anjum et al. 2012). GSTs are catalyzing the removal of lipid peroxides and nucleophilic conjugation of GSH to a wide variety of hydrophobic and electrophilic organic molecules. The conjugation of GSH to a wide range of electrophilic metabolites of xenobiotics converted them in to inactive or non-toxic product, and further the conjugates are transported to the vacuoles for sequestration and/or subsequent metabolism (Coleman et al. 1997; Reddy et al. 2005; Moons 2005). Our result showed that increase in GST activity during Pb treatment may be attributed that this enzyme has potential role in ROS detoxification in roots of *T. triangulare* (**Fig. 31B**). The increased GST activity might also support or catalyze the conjugation of GSH with Pb or other toxic electrophiles and strengthen the plant against Pb-induced oxidative stress. Similarly, Cd-induced increased GST activity was observed in leaves and roots of *P. sativum* (Dixit et al. 2001) and in roots of *Orazy sativa* and *Phragmites australis* (Iannelli et al. 2002). Reddy et al. (2005) has reported about the Pb-induced increased GST activity by 3–4 fold in leaves and roots of *Macrotyloma uniflorum* and *Cicer arietinum* plants. However, the GST activity was relatively more in *M. uniflorum* than in *C. arietinum* (Reddy et al. 2005).

Ascorbate is the key metabolites and APX is a key enzyme of Halliwell–Asada enzyme pathway. Ascorbate is ubiquitous antioxidant, present in all cellular component, which reacts directly with ROS molecules as well as act as a secondary antioxidant (Wang et al. 2012b). Result of our study showed that total ascorbate contents in roots were significantly ($P \leq 0.05$) declined during Pb treatment when compared to control (**Fig. 32A**). The maximum reduction of 53% in ascorbate content was observed at 1.25 mM Pb treatment. In present study, the decrease in ascorbate content attributed to the oxidation of ascorbate in to MDHA with the activity of APX with concomitant detoxification of H_2O_2 in to water molecule (Sharma and Dubey 2005). MDHAR converted in to DHA, which further catalyzed by enzyme DHAR and converted in to ascorbate (Mishra et al. 2006). The reduction of DHA to ascorbate is very important for plant, because the half life of DHA is very sort and it would be lost if it remain in same form. Ascorbate considered as strong ROS scavenger due to its ability for donating electrons in number of enzymatic and non-enzymatic reactions (Mishra et al. 2006; Bhaduri and Fluker 2012). The study of *V. natans* treated with 0.75 mM Pb also showed significant decline in ascorbate content, with simultaneous induction in DHA content (Wang et al. 2012b). Like GSH/GSSG ratio, ascorbate/DHA ratio is also very important to sense the stress condition and maintain the cellular redox balance (Gill and Tuteja 2010; Bhaduri and Fluker 2012). Furthermore, being a metabolite of AGC, it also plays a key role in maintaining the activities of other metabolites and enzymes. The decrease in total ascorbate content showed good correlation (R^2= 0.810; **Fig. 32C**) with decrease in total glutathione content. Pb-induced declined in ascorbate contents were also observed in *Allium cepa* (Verma and Dubey 2003) and in *N. indica* (Singh et al. 2010). Similar to CAT, the increased APX activity may catalyze the oxidation of excess H_2O_2 caused by Pb and thus may play a detoxifying role. However, APX activity initiated to decline as the concentration of Pb rose to 0.75 mM (**Fig. 32B**), suggesting that the antioxidative potential of APX had reached maximum level to maintain

the stability of the antioxidative system (Sharma and Dubey 2005; Malecka et al. 2009; Pourraut et al. 2011a). Pb-dependent increase in activities of CAT and APX from wheat seedling extracts was observed at 0.15, 0.30, 1.5, and 3.0 mM of Pb concentration (Lamhamdi et al. 2011). Pb-induced APX activity has been reported in pea roots (Malecka et al. 2009), *Wolffia arrhiza* (Piotrowska et al. 2009) and *Pluchea sagittalis* (Rossato et al. 2012).

The FTIR spectral analysis is important to identify some characteristic functional groups, which were responsible for tolerance against Pb-induced oxidative stress and detoxification of Pb and Pb-induced toxic free radicals and metabolites. The spectral peak analysis showed that reductions in %transmittance of peaks during 1.25 mM Pb treatment in comparison to control peaks were observed (**Fig. 33**). Out of all peaks values few major %transmittance reductions values were observed at 3391, 2922, 1643, 1381 and 1055 cm^{-1} (**Table 10)**. In this study, very less stretching in characteristic peaks observed after Pb. In Pb treated root, a broad reduction in 8.9 %transmittance observed at 3400–3200 cm^{-1}, when compared with characteristic control peak, representing the –OH (alcoholic or hydroxyl) and N–H (amide) functional group (Yalçın et al. 2012; Naik et al. 2012; Singha and Das 2012). Alcoholic or hydroxyl group might be donated from phenolic, alcoholic, carboxylic and amino acids, whereas amide was from amino acids, which were involved in the binding of the metal ion (Nahar and Tajmir-Riahi 1996). Additionally, a strong reduction of 8.0 %transmittance noted in peak of 1.25 mM Pb treated sample at 1643 cm^{-1} representing the C=O (corboxylic) functional group of amide I or carboxylic side of amino acid or peptides (Nahar and Tajmir-Riahi 1996), representing the involvement in removal of Pb or Pb-induced toxic substances (Naik et al. 2012). Furthermore, reduction in 7.5 %transmittance has observed at 1055 cm^{-1}, representing the C–O (ester or amide) functional group. This might be possibly donated by amino acid or peptide or lipid. Along with these peakes, minor reductions for few more peakes were observed (**Table 10**), which

showed that these groups were less or not involved in the tolerance and detoxification process. Thus, the FTIR analysis revealed that during Pb stress condition, phenolic, alcoholic, carboxylic, amino acids and lipid are majorly, consist in establishing links with large organic molecules, involved in detoxification of Pb and Pb-induced toxic electrophiles (Nahar and Tajmir-Riahi 1996; Marmiroli et al. 2005).

Conclusions

Our results concluded that Pb treatment declined the NPSH, GSH, total ascorbate and total GSH contents in similar pattern. The contrary was true regarding cystein and GSSG contents and GST activity, whose values increased after Pb treatment. Decline in GSH at higher Pb might be attributed to high GSH consumption as an antioxidant to combat oxidative stress or for the synthesis of other metal binding ligands i.e. phytochelatins or metallothioneins. The GSH/GSSG ratio was declined in a dose dependent manner, which was evident by the gradual reduction in GR and γ-ECS enzyme activities. The increased activity of GST involved in active binding and detoxification of lipid hydro-peroxide, support the active tolerance mechanisms of *T. triangulare.* We can suggest that ascorbate-glutathione and other related metabolites and enzymes cumulatively form an efficient defense system against ROS in addition to their significance for the detoxification, and compartmentalization of HMs in plant. FTIR analysis, performed for characterization of functional groups involved in binding mechanisms of ions showed that amino, phenolic, carboxylic acids and other alcoholic, amide and ester containing bio-molecules were have key role in detoxification of Pb or Pb-induced toxic metabolites.

Objective 5

Proteomic approach for root proteins identifications exposed to Pb stress

Introduction

Environmental changes can modify physiological and biochemical state of plants that trigger several signaling pathways for adaptation to unfavorable conditions. It is known that metal sensitivity and toxicity to plants are influenced by the concentration and the toxicant types. Plants are key components of the biota, as they often directly receive chemical pollutants and thus represent fundamental tools in an ecotoxicological perspective (Luque-Garcia et al. 2011). However, plants are still quite neglected organisms for 'omic' approaches to environmental toxicology. Proteomics, with its high resolution for protein separation by two-dimensional polyacrylamide gel electrophoresis (2D-PAGE) coupled to protein identification by mass spectrometry (MS) and database searches (Lopez 1999; Newton et al. 2004), has been applied to various fields of biology including, the efficient analysis of (differentially) expressed proteins and identification of proteins involved in cellular processes. Thus, use of proteomic-based approaches in various areas of plant biology research came up with stunning rapidity over past decade (Kosová et al. 2011). Proteomics also proves to be a powerful means for investigating the molecular mechanisms of plants responses against various stage of development. The technology is based on high-throughput biotechnological approaches for the separation and identification of proteins, allowing an essential study of many proteins at the same time being used to address the biological function of plant proteins in different biotic or abiotic responses (Agrawal et al. 2002; Kim et al. 2005; Sengupta et al. 2011). Large-scale proteomics is a powerful approach for studies of complex biological processes in which a number of proteins take part in various physiological, biochemical and molecular mechanisms (Hashiguchi et al. 2010).

Importance of comparative proteomic approach for stress response studies

Plant response against abiotic stress factors includes changes in protein expression and post-translational modification of proteins to activate their defense mechanism. Comparative quantitative analysis of proteins is able to provide accurate information about molecular changes allowing the establishment of a range of specific mechanisms, leading to the identification of major players in the considered pathways. Research on plant proteomes has provided advantageous information for a comprehensive understanding of the protein networks in plants in response to external stress factors. In particular, proteins being the most abundant cell components (70%) (Davies 2005), interest in redox modifications of proteins is of paramount interest in environmental toxicology because it can provide fundamental insights both into toxicity mechanisms and biomarker discovery. For the proteomics analysis the separation of desired protein mixture can be performed with the two-dimensional gel electrophoresis followed by mass spectrometry. Several plants proteomics studies have been performed on the responses of various abiotic stresses (Cho et al. 2006, Sengupta et al. 2011). To begin with few examples, an investigation made with Cu treatment with rice seedlings showed various physiological and biochemical responses and their correlation with a total of 25 proteins that were identified and differentially expressed in response to Cu stress (Ahsan et al. 2007). Bah et al. (2010) reported about the *Typha angustifolia* leaf proteome in response to 1 mM Cr, Cd and Pb for 90 days and 130 days to analyze and identify the stress-responsive proteins. More than 1600 protein spots were reproducibly detected and were differentially expressed over the control, whereas Pb caused up-regulation of carbohydrate metabolic pathway enzymes of fructokinase and APX along with other chloroplast proteins (Bah et al. 2010). Proteome analysis of gametophores identified up-regulation of *Physcomitrella patens* metallothionein type 2 (*PpMT2*) involved in various abiotic stress responses such as Cu,

Cd, cold, indole-3-acetic acid, and ethylene, when treated during culturing (Cho et al. 2006).

Root proteomics-based approaches in plant under different HMs stress conditions

Plants have different sensitivity to HMs. Roots being the below-ground or merged (in case of aquatic plants) portion of plants, are the sole access point to metal and as such they play a vital role in plant metal accumulation and translocation to the aerial part of the plants. Root systems, though genetically determined, are very plastic and can be affected by a number of environmental factors, including metals. The regulation of root proteins under HMs-stress response may act to re-establish root system homeostasis, and may be considered as molecular markers for bioengineering new plants in phytoremediation projects (Elisa et al. 2007). The expression pattern of terrestrial and crop plants in responses to various HMs have been described by various authors. Arsenic-induced differentially expressed proteins profiles have been described by Requejo and Tena (2005) for maize root and by Ahsan et al. (2008) for rice roots. Ahsan et al. (2007) reported about the identified proteins in rice roots against Cu excess were related to antioxidants or stress regulatory proteins that might work together to establish a new homeostasis in response to Cu as well as other HMs stress (Ahsan et al. 2007). On the other hand, proteome analysis of rice root tissues showed that 10 μM Cd treatment strongly induced the expression of regulatory proteins and some metabolic enzymes, but it mainly activated defence mechanisms by the induction of transporters and proteins involved in the degradation of oxidatively modified proteins (Aina et al. 2007). Furthermore, the exposure to 100 μM Cd concentrations, strongly affect rice physiology and significantly altering DNA sequence and protein pattern of roots, with important changes to regulatory proteins (Aina et al. 2007).

Plants have a variety of mechanisms by which they reduce their susceptibility to HMs-induced toxicity, one of which is the production of HM-binding factors and proteins. A few research groups have conducted proteome analysis in plant roots under different HMs stress conditions (Aina et al. 2007; Elisa et al. 2007; Wang et al. 2011; Sharmin et al. 2012. Comparative proteomic analysis in roots of two genotypes of soybean i.e. Al-tolerant (PI 416937) and Al-sensitive (Young) has been studied for Al stress. Al-induced a distinct protein profile changes in both soybean genotypes. Al stress up-regulated the citric acid cycle enzymes resulted in to increased synthesis of citrate, having key role in Al detoxification in PI 416937 genotype only. The comparative proteome analysis revealed that the tolerance mechanism in root was also developed due to up-regulation of novel proteins for DNA damage control, cell cycle regulator, and transcription factor (Duressa et al. 2011). Furthermore, it has shown that 150 ppm Cu stress in *Cannabis sativa* roots caused morphological and proteomic changes (Elisa et al. 2007).

Since proteins are directly involved in plant stress response, analysis of roots protein expression during HMs stress can significantly unravel the possible relationships between protein abundance and plant stress acclimation. A proteomic analysis of the Ni hyperaccumulator plant *Alyssum lesbiacum* was carried out to identify proteins that may play a role in the exceptional degree of Ni tolerance. Out of the 816 polypeptides detected in root tissue by 2-D SDS-PAGE, eleven were up-regulated which having important role in the sulphur metabolisms and ROS detoxification (Ingle et al. 2005). Alterations in the root proteome of hydroponically grown *A. thaliana* plants treated with 10 mM Cd^{2+} for 24 h showed that identified proteins were related with different classes and having wide role in Cd-tolerance mechanisms (Roth et al. 2006). The results obtained with Al-responsive proteins in rice roots indicated that the protein regulation occurred at the transcriptional level. The proteins identified were related to ion transport and sulphur metabolism, which could have major roles in Al adaptation or tolerance in rice (Zhang et al. 2007).

Toxic levels of Pb in growth medium inhibit growth and cause substantial reduction in plant yields. Pb-tolerant cultivars detoxify Pb through multiple mechanisms that are currently not well understood at genetic and molecular levels. Total protein analysis of the proteins expressed by the genome, is not only a powerful molecular tool for reveling complete proteomes at the point organelle, cell, organ or tissue level but also, for evaluating proteomes as affected by different physiological conditions, such as those resulting due to Pb or other stressful environmental factors. However, little information is available in the field of plant proteomics under HMs or Pb stress conditions. Moreover, inadequate reports have been published on root proteome analysis subjected to HMs stress. To the best of our knowledge, to date, there is no report of the proteomic analysis of Pb treated *T. triangulare*. To investigate the Pb stress-responsive proteins in and their key role in response against Pb stress in adventitious roots, through proteomic approach has been adopted.

Materials and methods

Plant description and treatment in hydroponic experiment

T*. triangulare* was propagated through stem cuttings in 100 mL of modified Hoagland's nutrient media in plant growth chamber at 16/8 h (day/night) at 28 ± 2 °C for 3 weeks. After 3 weeks of acclimatization, uniform stem cuttings with adventitious roots and leaves were selected and treated with $Pb(NO_3)_2$ at Pb concentrations of 0 (control) and 1.25 mM for 7 days under above conditions. Roots excised after 7 days of treatment were processed for proteomic study.

Protein extraction and two-dimensional electrophoresis (2-DE)

After 7 days of Pb treatment, whole roots from both control and stressed plants were collected, washed thoroughly with DDW and immediately frozen in liquid nitrogen and stored at –80 ºC till protein extraction. Total root proteins were extracted according to Sarvanan and Rose (2004) with minor modifications. The methodology for proteomic analysis is breefed in **Fig. 34**. Frozen root tissues (2.0 g) of control and 1.25 mM Pb were ground to fine powder in liquid nitrogen and suspended in 5 mL of the extraction buffer containing 0.5 M Tris-HCl (pH 7.5), 0.7 M sucrose, 0.1 M potassium chloride, 50 mM EDTA, 2% β mercaptoethanol and 1 mM PMSF. After thorough mixing, equal volume of commercially available Tris-saturated phenol (pH 7.5) was added to the extract suspension and further mixed for 30 min at 4 ºC using a rotospin cyclomixer.

The Tris-saturated phenol mixed extract suspension was centrifuged at 8,000 g for 30 min at 4 ºC. The upper phenolic phase was collected carefully in centrifuge tubes with the help of micro pipette and an equal volume of extraction buffer was added to it. The above step was repeated and the upper phenolic phase was re-extracted. To the final collected phenolic phase, four volumes of 0.1 M ammonium acetate in methanol was added and

incubated overnight at –20 ºC for protein precipitation. The samples were then centrifuged at 10,000 g at 4 ºC for 30 min and the precipitate was washed thrice in ice cold methanol, twice in ice cold acetone and air dried for few minutes. The final pellet was solubilized in 200 µL of the rehydration solution containing 8 M (w/v) urea, 2M (w/v) thiourea, 4% (w/v) CHAPS, 30 mM DTT, 1.5% (v/v) IPG buffer pH range 4–7 (GE, Healthcare). The protein concentration was determined according to Bradford (1976) protein assay using BSA as standard.

One-dimensional IEF and two- dimensional SDS–PAGE

Aliquots of 800 µg protein of control and 1.25 mM Pb treated roots were mixed with rehydration solution containing 8 M urea, 2 M thiourea, 4% CHAPS, 30 mM DTT, 0.8% IPG buffer pH range 4–7 and 0.004% bromophenol blue to a final volume of 320 µL (Sengupta et al. 2011). Further, active rehydration of mixed protein (800 µg) was done on immobilized pH gradient (IPG) strips (18 cm, 4–7 pH linear gradient; Amersham, GE) for 12 h at 50 V. Rehydration and isoelectric focusing (IEF) was carried out in Ettan IPGphor II (GE Healthcare) at 20 ºC, using the following program: 30 minutes at 500 V, 3 h to increase from 500 to 10000 V and 6 h at 10000 V (a total of 60000 Vh). After IEF, strips were equilibrated with two different equilibrium buffers for 30 min each with gentle rocking at RT (25 ± 2 ºC). The first equilibration was performed in a solution containing 50 mM Tris-HCl buffer (pH 8.8), 6 M urea, 2% (w/v) SDS, 30% (w/v) glycerol and 2% DTT and the second equilibration was performed by using 2.5% (w/v) iodoacetamide by replacing DTT. The proteins were separated in the second dimension by 12% SDS-PAGE (vertical polyacrylamide slab gels) at 10 mA gel^{-1} for 1 h and then 38 mA gel^{-1} for 6 h, using an EttanDalt6 chamber (GE Healthcare). The gels were stained with modified

colloidal coomassie staining (Wang et al. 2007; Sengupta et al. 2011). Protein spots in the gels were recorded as digitized images using a calibrated densitometric scanner (GE, Healthcare) and analyzed (normalization, spot matching, expression analyses, and statistics) using Image Master 2-D Platinum version 6 image analysis software (GE, Healthcare).

In-gel trypsin digestion and MALDI-TOF MS analysis

After spot analysis in gel digestion and matrix-assisted laser desorption/ionization time of flight mass spectrometric (MALDI-TOF MS) analysis was conducted with a MALDI-TOF/TOF mass spectrometer (Bruker Autoflex III smartbeam, Bruker Daltonics, Germany) following the method explained by Shevchenko et al. (1996) with slight modifications (Sengupta et al. 2011). Colloidal coomassie stained protein spots were manually excised from three reproducible gels. The excised gel pieces were collected in centrifuge tubes. To remove ammonium acetate, used in staining dye the gel pieces were first washed with 200 µL of 25 mM ammonium bicarbonate (NH_4HCO_3) solution. Then, the gel pieces were destained with 100 µL of 50% acetonitrile (ACN) in 25 mM NH_4HCO_3 for four times and then, treated with 10 mM DTT in 25 mM NH_4HCO_3 and incubated at 55 ºC for 1 h. After that gel pieces were treated with 55 mM iodoacetamide prepared in 25 mM NH_4HCO_3 for 1 h at room temperature, followed by washing with 25 mM NH_4HCO_3 and ACN, dried in speed vac and rehydrated in 20 µL of 25 mM NH_4HCO_3 solution containing 12.5 ng μL^{-1} trypsin (sequencing grade, Promega). The above mixture was incubated on ice (4 ºC) for 10 min and kept overnight for digestion at 37 ºC. After digestion, a short spin for 10 min was given and the supernatant was collected in a fresh centrifuge tube. The gel pieces were re-extracted with 50 µL of trifluoroacetic acid (TFA)-ACN extraction solution, containing 0.1% trifluoroacetic acid (TFA) and ACN in ratio of 1:1, for 15 min with frequent vortexing. The supernatants were pooled together and dried

using speed vac and were reconstituted in 5 µL of TFA-ACN extraction solution. An aliquot (2 µL) of the above sample was mixed with 2 µL of freshly prepared α-cyano-4-hydroxy-cinnamic acid (CHCA) matrix in 50% ACN and 1% TFA (1:1) and 1 µL was spotted on target plate for MALDI analysis.

Peptide mass fingerprinting and MS/MS analysis

Identification of protein samples were performed by database searches on the basis of peptide mass fingerprinting (PMF) and (MS/MS) using MASCOT program (http://www.matrixscience.com) employing biotools software (Bruker Daltonics, Germany). The similarity search for mass values was done with existing digests and sequence information from NCBInr and SwissProt database. The taxonomic category was set to *Viridiplantae* (green plants) and other search parameters were fixed modification of carbamidomethyl (C), enzyme trypsin, peptide charge of 1^+ and monoisotropic. According to the MASCOT probability analysis ($P \leq 0.05$), only significant hits were accepted for protein identification.

Statistical analysis

Three biological replicates were performed for proteomic analysis for both control and 1.25 mM Pb treated root proteins. Each replication comprising of approximately fifteen pooled plants were considered and the spots were analyzed using Image Master 2-D Platinum image analysis software (GE, Healthcare) and statistical one-way factor ANOVA ($P \leq 0.05$) was performed considering the values (n = 3) of the best matched replicate gels from the three independent experiments. The normalized volume (% vol) of each spot was automatically calculated by the software as a ratio of the volume of a particular spot to the total volume of all the spots present on the gel.

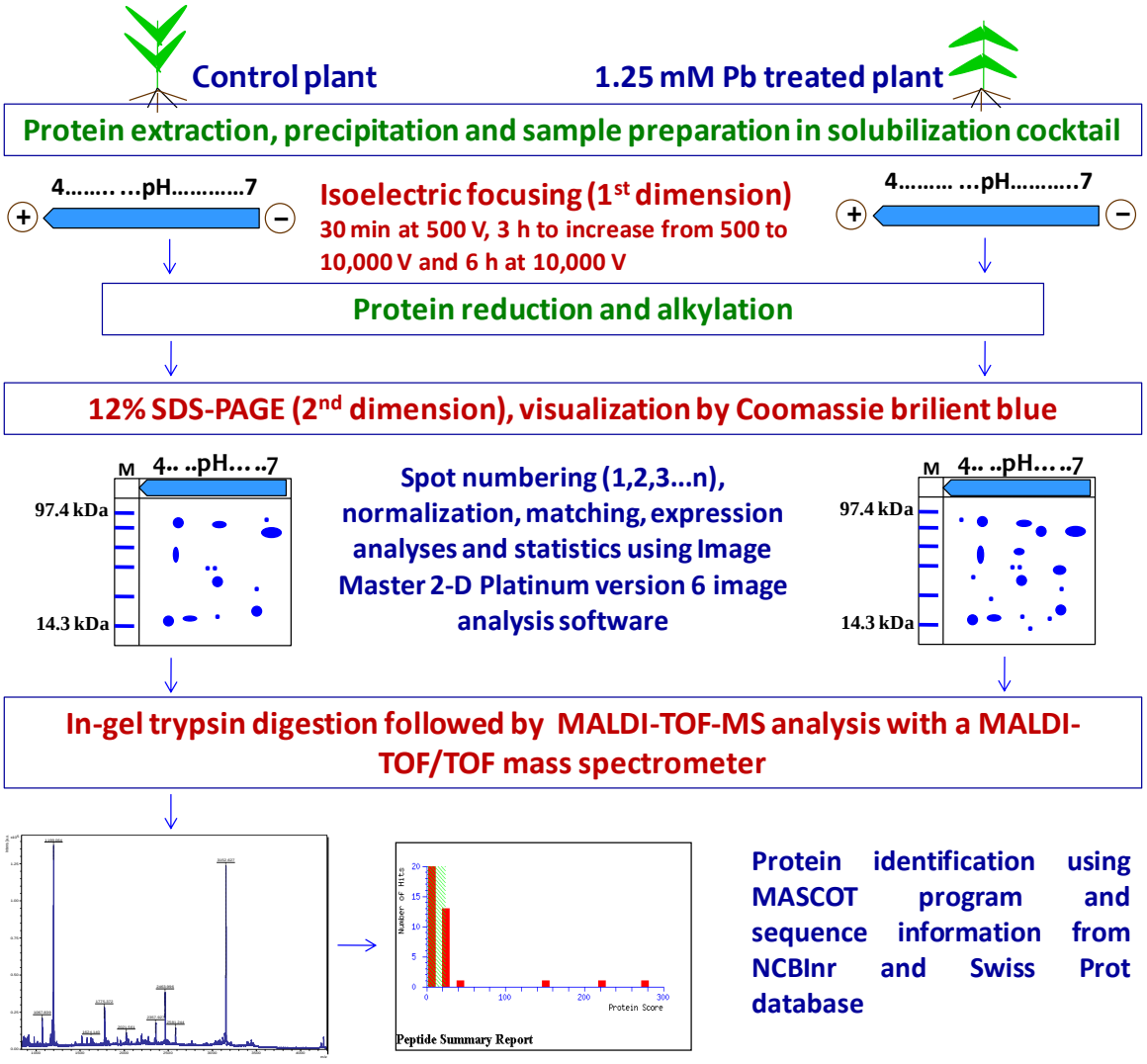

Fig. 34 Schematic overview of the process of the protein extraction, focusing, SDS-PAGE resolution, visualisation, digestion and protein identification using advanced spectrometry and bioinformatics tools (Qureshi et al. 2007).

Results

2-DE and protein expression profiling

To investigate the expression patterns total root protein in *T. triangulare* plant exposed to 1.25 mM Pb concentration against respective control plant. Total proteins were extracted from roots of control and 1.25 mM Pb treated plants and separated by 2-D polyacrylamide gel. The 2-D electrophoresis (2-DE) gels were reproducible and clearly revealed separated protein spots. Triplicate gels were obtained from three independent experiments, and the representative gels are illustrated in **Fig. 35A and B**. The 2-DE gels were stained with colloidal coomassie, revealed more than 500 well resolved protein spots. The spots were reproducibly detected in the gels with Image Master 2D Platinum software and all gels showed highly similar distribution patterns in 2D image.

Overall analysis of all the gels revealed that out of the number of matched spots between control and Pb stress, approximately 61 spots were significantly up-regulated (>1.8 fold). The criteria were used to identify and explained the Pb-responsive proteins among hundreds of protein spots resolved by 2-DE gel are that expression fold should at least 1.8 in case of up-regulated spots and new spots only present in Pb treated gel. A total of 33 major spots, 27 up-regulated spots and 6 new spots only visible in Pb stress, which were distinct, well-separated but not in complexes and of considerable intensity were selected for protein identification by MALDI-TOF analysis. Out of 33 selected spots 23 proteins were successfully identified, which include 20 up-regulated under Pb stress in compared to control and 3 new spots visible only in Pb stress gel. Positions of the 23 identified proteins were numbered and depicted accordingly in the master gel (**Fig. 36A**) and the rest eleven did not show any significant hits in the database and hence not considered. The 20 up-regulated spots were marked in numerical values such as 1 to 20 and newly detected spots were marked as N1, N2 and N3. Few of the identified spots were

enlarged in **Fig. 36B** to visualize their expression patterns during 1.25 mM Pb stress. Relative spot volumes for each spot were expressed as %Spot Vol indicating the normalized values of the ratio of the individual spot to the total volume of all the spots in the gel (**Fig 37**).

Identification of differentially expressed proteins during Pb stress

To identify the up-regulated and newly expressed proteins, the spots were excised from the gel, in-gel digested using trypsin and analyzed via MALDI-TOF MS. In order to avoid complexity, we first grouped the 23 identified proteins spots as up-regulated and newly detected during 1.25 mM Pb treatment was analyzed. Each of the 23 spots contained only one protein. The relative spot intensities during control and 1.25 mM Pb stress, matched peptide sequence, accession number, source organism, sequence coverage, experimental and theoretical molecular weight and pI and the MS/MS score of each individual protein were shown in **Table 11**. In some cases, more than one spot were identified as the same protein. For example, ATP synthase subunit β (spot 10 and 13) and Chalcone-flavanone isomerase (spot 3 and N1). Usually, this phenomenon results from the presence of different isoforms, post-translational modification or degradation.

The 23 identified proteins could be categorized into 5 major groups based on their biological function i.e 1) ROS-detoxification and defense, including Cu-Zn SOD, aldo-keto reductase, peroxidase, glutathione-S-transferase and monodehydroascorbate reductase; 2) Protein synthesis/energy metabolism related which includes two isozymes of ATP synthase subunit β, ATP synthase β chain, ATP synthase subunit α and Heat Shock Protein-70 (HSP 70); 3) Cell signaling/cell metabolism, including two isomers of chalcone-flavanone isomerase, triosephosphate isomerase, 2,3-bisphospho-glycerate-independent phosphoglycerate mutase 1, adenosylhomocysteinase, probable receptor-like protein kinase and DNA-directed RNA-polymerase subunit β; 4) Root morphology related

proteins, including actin and auxin transport protein and finally 5) Transport related proteins which includes aquaporin NIP1-1 (**Fig 38**). Auxin transport, one isozymes of chalcone-flavanone isomerase and DNA-directed RNA-polymerase subunit β were detected as newly appeared proteins in Pb stress gel.

The analysis of the expression patterns of these proteins showed that the spot 1 is highly up-regulated by a values of 23.3 fold, while spot 12 was least up-regulated which was accounted for 1.8 fold in comparison to control spot (**Fig 37**). The identified proteins highlight their possible role in the plant's overall Pb stress-response mechanisms. The results also showed that an inter-relationship and existence of coherence among the identified groups of proteins.

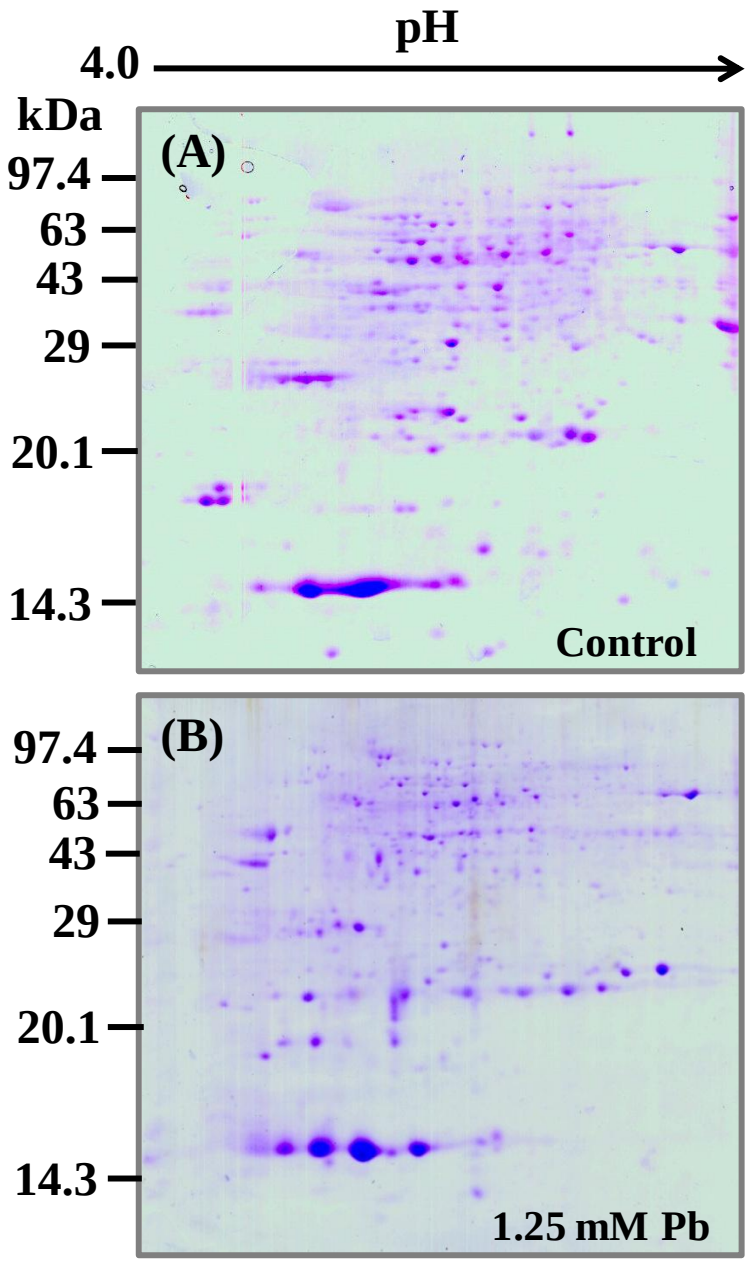

Fig. 35 2-D protein profile of *T. triangulare* roots grown under control **(A)**, and 1.25 mM Pb **(B)**.

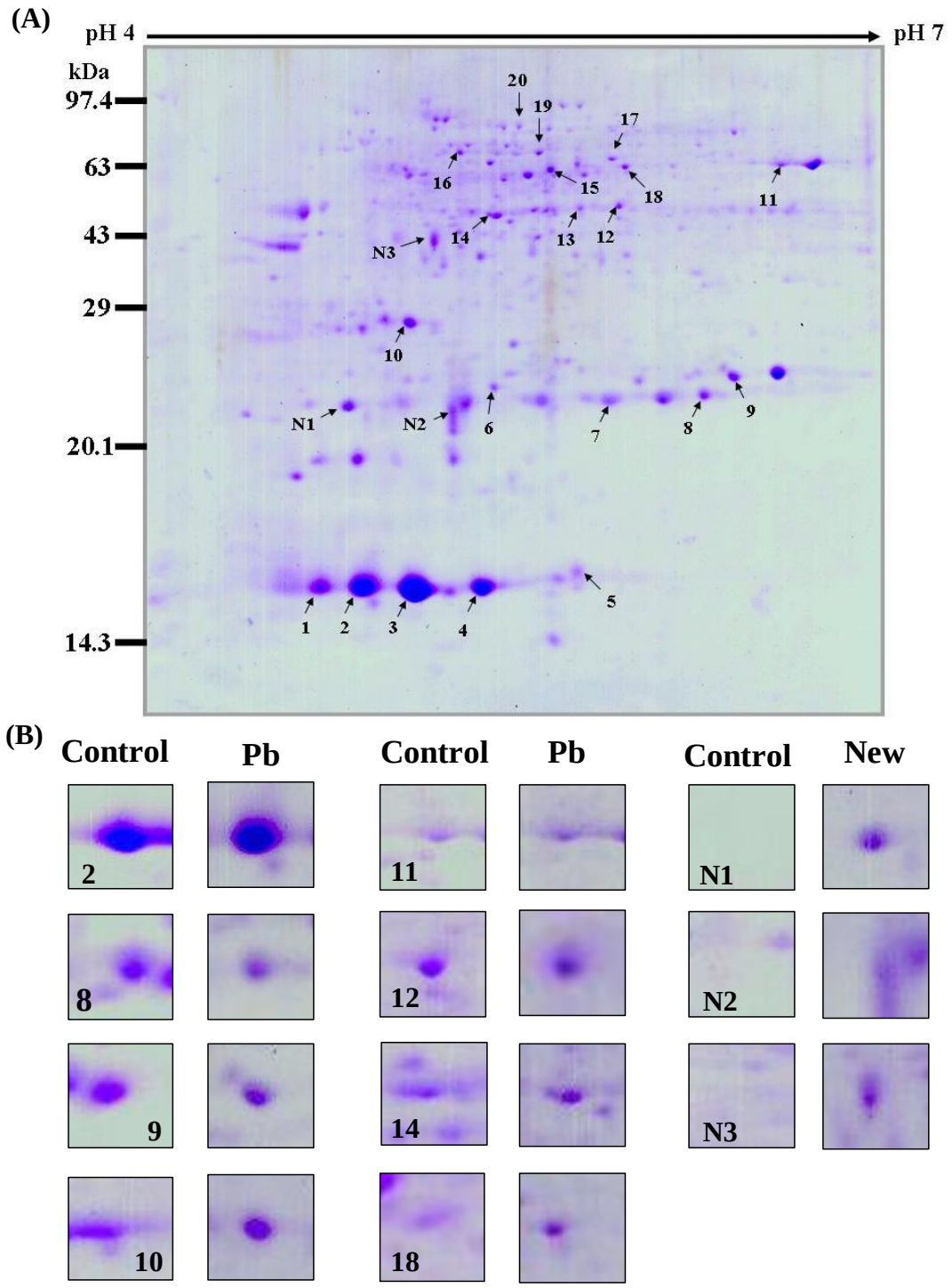

Fig. 36 Two-dimensional electrophoresis master gel from the 1.25 mM Pb treated root sample illustrating 23 identified proteins **(A)**. The spot numbering in the master gel shown corresponds to the spot numbers given in Table 5.1. Enlarged view of the expression patterns of few spots during control and 1.25 mM Pb stress conditions **(B)**.

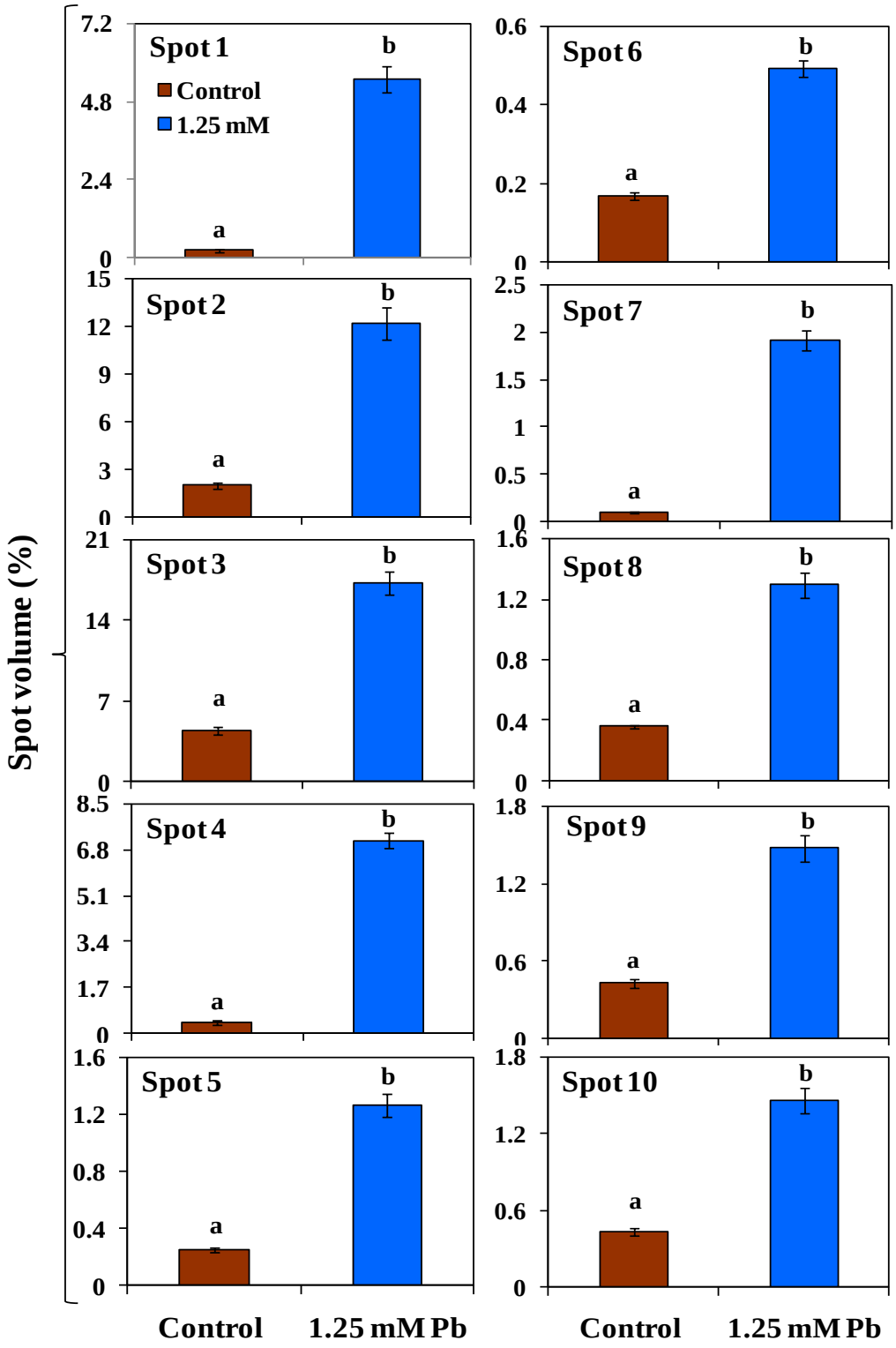

Fig. 37 Percentage volumes of the spots on the gel for understanding the expression pattern. Data are presented in mean value ± SE (n =3) denoted by different letters are significantly different ($P \leq 0.05$) between each other.

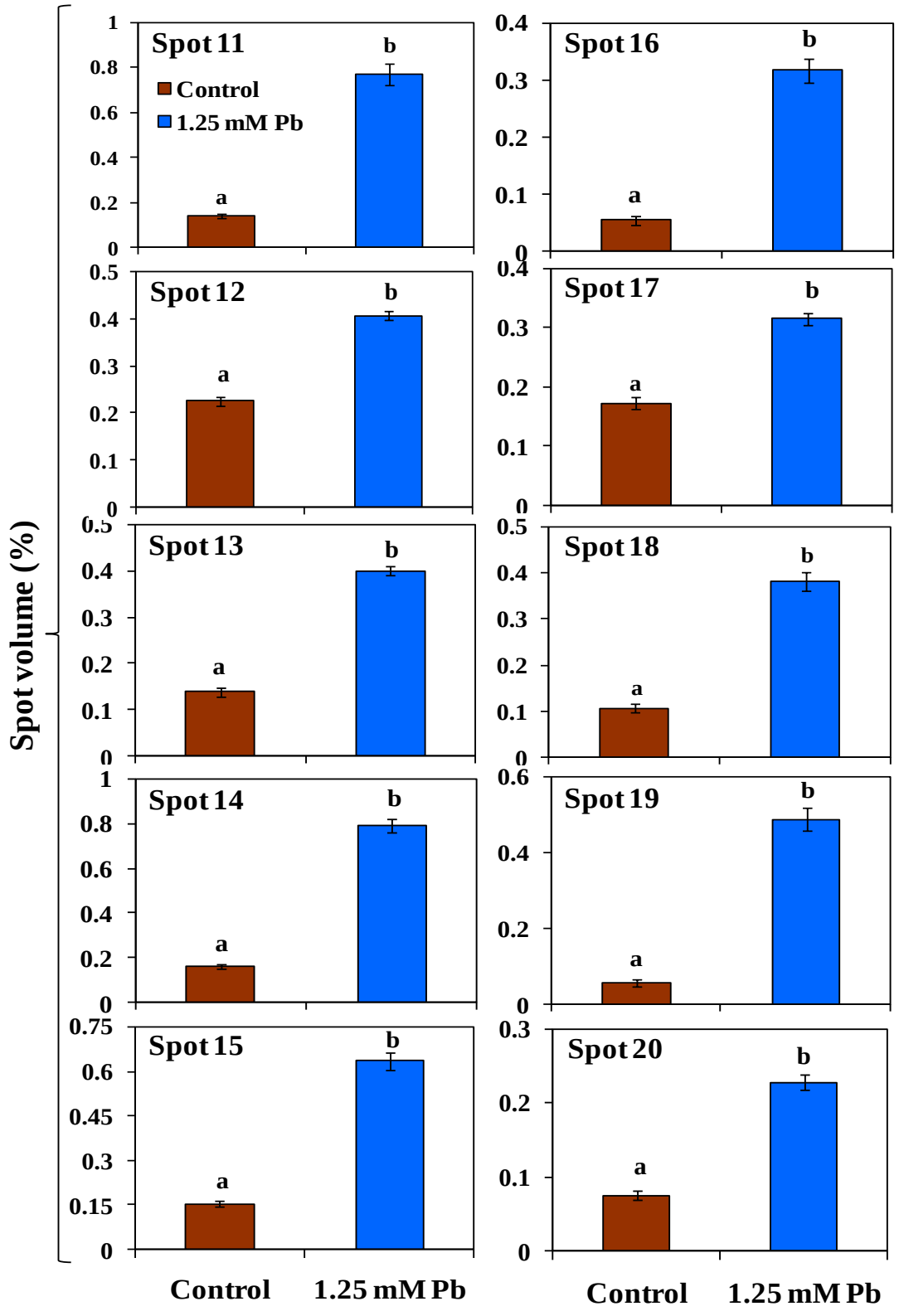

Fig. 37 continuation.

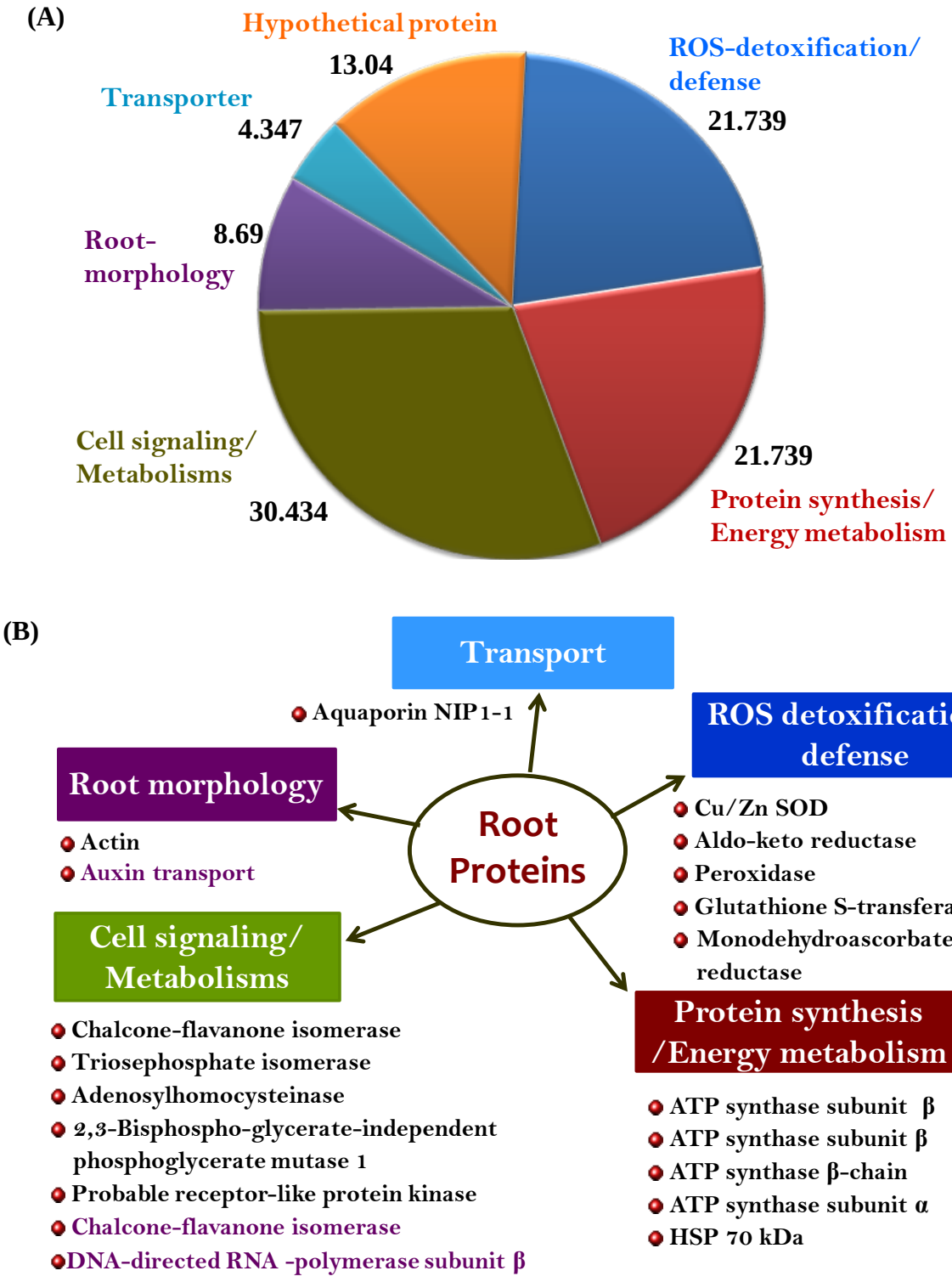

Fig. 38 Functional categorization and percentage contribution **(A)** and list of identified proteins in their respective groups **(B)**.

Table 11 Major up-regulated and newly identified root proteins of *T. triangulare* during 1.25 mM Pb stress.

Spot No.	Protein identified	Peptide Sequences matched	Mr(kDa)/pI		Accession no.	SC (%)	Reference organism	MS-MS Score
			Theoretical	Observed				
1	Probable aldo-keto reductase	LTPEEMVELEAIAQPDFVK MVELEAIAQPDFVK	36.72/ 5.4	17/ 4.8	AKR6_ARATH	5	*Arabidopsis thaliana*	49
2	Glutathione S-transferase	MATIKVHGVPMSTATMR ATIKVHGVPMSTATMR VHGVPMSTATMRVLAAL-YEK	24.32/ 6.3	17/ 5.0	gi|297824877	11	*Arabidopsis lyrata*	57
3	Chalcone-flavonone isomerase	FMQVTMILPLTGQQYSEK-VSENCVAIWK HLGIYTDEEGK DQTFPPGSSILFTVLPK	23.99/ 5.7	17/ 5.1	CFI2_LOTJA	25	*Lotus japonicus*	48
4	Hypothetical protein SORBIDRAFT	EEIVYNYFKGILGTPFQR GLRQGDPISPMLFVIVMES-LNSLFKEADR EVVLIDSQADR	43.34/ 10.0	17/ 5.4	gi|242050434	15	*Sorghum bicolor*	98
5	Superoxide dismutase (Cu-Zn)	HAGDLGNITVGDDGTATF-TIIDSQIPLTGPNSIVGR VGDDGTATFTIIDSQIP-LTGPNSIVGR	15.27/5.4	18/ 5.7	SODC1_MESCR	23	*Mesembryant-hemum crystallinum*	30
6	Peroxidase (Fragments)	LSPTFYATSXPNVXXTR PTFYATSXPNVXXTR	9.4/ 4.7	25/ 5.4	PER_GINBI	19	*Ginkgo biloba*	30
7	Hypothetical protein	MDVENVKVDDNDVK DLHFDLLTLHFIELVR LQQEQGGK	23.9/5.3	24/5.9	gi|302770993	18	*Selaginella moellendorffii*	58

8	**Triosephosphate isomerase**	**EAGSTMEVVAEQTKAIADKQAQEVHANLR**	**27.13/ 5.2**	**25/ 6.3**	**TPIS_SECCE**	**11**	***Secale cereale***	**49**
9	**Aquaporin NIP1-1 (homolog)**	**EEFADQGCAAMVVSVPFIQKIIAEIFGTYFLMFAGCGAVTINASK**	**29.65/ 8.5**	**26/ 6.4**	**NIP11_MAIZE**	**15**	***Zea mays***	**30**
10	**ATP synthase subunit β, mitochondrial**	**VVDLLAPYQR IPSAVGYQPTLATDLGGLQER**	**61.95/ 4.9**	**28/ 5.1**	**gi|5852203**	**5**	***Chlamydomonas reinhardtii***	**87**
11	**Heat shock 70 kDa protein**	**ATAGDTHLGGEDFDER ARFEELCMDLFR**	**71.29/5.2**	**67/ 6.6**	**HSP70_CHLRE**	**4**	***Chlamydomonas reinhardtii***	**25**
12	**Monodehydroasc-orbate reductase**	**LPGFHVCVGSGGER SVEEYDYLPYFYSR**	**47.47/ 5.9**	**51/ 5.9**	**gi|146432261**	**6**	***Vitis vinifera***	**125**
13	**ATP synthase subunit β**	**GYIVQIIGPVLDVAFSPGMMPSIYNALVVQGR HNQEPNVTCEVQQLLGNNR TVLIMELINNIAK**	**54.13/ 5.2**	**50/ 5.7**	**ATPB_CUSGR**	**12**	***Cuscuta gronovii***	**49**
14	**Actin-1**	**AVFPSIVGRPR NYELPDGQVITIGAER TTGIVLDSGDGVSHTVPIYEGYALPHAILR**	**42.2/ 5.6**	**49/ 5.4**	**gi|113217**	**15**	***Daucus carota***	**277**
15	**ATP synthase β-chain**	**VVDLLAPYQR AHGGFSVFAGVGER YDEGLPPILTALEVLDNDIR**	**59.05/ 5.9**	**63/ 5.6**	**gi|226493589**	**7**	***Zea mays***	**61**
16	**Probable receptor-like protein kinase**	**INIGGDLISPKIDPLSR DAPMDEGHVSTAVKGSFGYLDPEYFR**	**93.03/ 5.9**	**70/ 5.3**	**Y5613_ARATH**	**5**	***Arabidopsis thaliana***	**31**

17	**Adenosylhomocysteinase**	**DQADYISVPVEGPYKPAHYR LSKDQADYISVPVEGPYKP-AHYR**	**53.77/ 5.7**	**67/ 5.8**	**SAHH_MESCR**	**4**	***Mesembryanthemum crystallinum***	**32**
18	**ATP synthase subunit α, mitochondrial**	**EAFPGDVFYLHSR ATSESETLYCVYVAIGQKR**	**55.47/ 5.8**	**63/ 5.9**	**ATPAM_NICPL**	**6**	***Nicotiana plumbaginifolia***	**104**
19	**Hypothetical protein**	**SEVHVDENVAAPSPR TCMFTLVFQDAAESSQR**	**68.4/ 6.03**	**70/ 5.6**	**gi|302811229**	**5**	***Selaginella moellendorffii***	**35**
20	**2,3-Bisphospho-glycerate-independent phosphoglycerate mutase 1**	**ALEYEDFDKFDR ALEYEDFDKFDRVR**	**60.77/ 5.3**	**80/ 5.5**	**PMG1_ARATH**	**2**	***Arabidopsis thaliana***	**70**
N1	**Chalcone-flavonone isomerase**	**VMENCVAHMKSVGTYGDA-EAAAIEK FAEAFKNVNFQPGATVFYR**	**23.84/ 5.3**	**22/ 4.6**	**CFI_PUEML**	**19**	***Pueraria montana***	**30**
N2	**Auxin transport**	**EQTMGKSAPAVQEK LLGVVKVTSILSSR**	**574.5/ 5.6**	**21/ 5.3**	**BIG_ARATH**	**0**	***Arabidopsis thaliana***	**38**
N3	**DNA-directed RNA polymerase subunit beta**	**ENIASSPFLFHNK SISNNDSNNFQLAK**	**139.6/ 9.47**	**42/ 5.2**	**RPOC2_CRYJA**	**2**	***Cryptomeria japonica***	**53**

Discussion

Protein network and mechanisms of Pb-induced stress response in roots of *T. triangulare* have been well explained in the present study. Comparative proteomic analysis was performed here to explain the dynamic role of root proteins involved in different cellular functions of *T. triangulare*. Though *T. triangulare* was known to be a remarkable accumulator of HMs, not much is known about its physiological and biochemical responses under elevated metal concentrations. Our present root proteome analysis of *T. triangulares* suggests that 1.25 mM Pb concentration seems to be the threshold value over which *T. triangulare* cannot contrast Pb toxicity. In general, the analysis of protein expression showed that defence mechanisms were activated in *T. triangulare* roots treated with 1.25 mM Pb with concomitant changes in various physiological and biochemical mechanisms. Out of the 33 major spots showing significant up-regulation (≥ 1.8 fold), selected for MALDI-TOF MS analysis, only 23 spots were successfully identified. Based on their function we categorized them under various functional groups which will be discussing in the subsequent categories.

ROS detoxification and defense

In the present study, ROS detoxification and defense related proteins constituted around 21.739 % of the total identified proteins. Five spots (spot1, 2, 5, 6 and 12) were identified in this group including aldo-keto reductase, glutathione-S-transferase, Cu-Zn SOD, peroxidase and MDHAR proteins, respectively. Our previous objectives showed that Pb treatment of 1.25 mM concentration caused significant oxidative stress in roots of *T. triangulare*. In general, plants are known develop ROS scavenging mechanisms including various detoxification and antioxidative pathways to cope with the oxidative stress (Sharma and Dubey 2005). Superoxide dismutase (SOD), is the key enzyme in plant cells

which plays crucial role in ROS detoxification by preventing the accumulation of $O_2^{\bullet -}$ radicals and form H_2O_2 and O_2. The up-regulation of Cu-Zn SOD (spot 5) in our study, has given an indication about increased defense mechanism of *T. triangulare* against oxidative stress. The over-expression of Cu-Zn SOD was also observed in *Vigna radiata* roots under water deficit condition (Sengupta et al. 2011). Proteomic response of *Arabidopsis* seeds constitutively over-expressing Cu-Zn SOD during germination in response to Cu stress (Gill et al. 2012). Another enzyme peroxidase (fragment) was also up-regulated (spot 6) in 1.25 mM Pb treatment. Peroxidases are well known for detoxification of H_2O_2 molecules and catalyzed them in to H_2O. Peroxidases not only play an important role in regulating H_2O_2 molecules but it also involve in H_2O_2 signaling in plant cell (Møller and Sweetlove 2010). Highest up-regulation (26.13 fold) was observed for spot 1 which was identified as probable aldo-keto reductase protein with a relative molecular weight (Mr) of 16 KDa and 4.7 isoelectric point (pI). Aldo-keto reductase are a group of enzymes related to nicotinamid adenine dinucleotide phosphate [NADP(H)] dependent oxidoreductases. This group of enzymes facilitates the interconversion of hydrogen molecules between aldehydes or ketones with the reduction of nicotinamid adenine dinucleotide (NAD^+ to NADH) and is known to detoxify the highly cytotoxic lipid-peroxidation derived reactive aldehydes. Therefore, significantly high induction levels of a probable aldo-keto reductase protein in *T. trangulare* roots under Pb stress indicate that detoxification pathways are highly crucial to ameliorate Pb-induced toxicity. Similar response was also observed in the *Cannabis sativa* roots under Cu stress condition (Elisa et al. 2007).

Plant root responses to Pb-induced oxidative stress and Pb detoxification are often mediated by up-regulating the glutathione metabolic enzymes. Sopts 2 and 12 were identified as GST (EC 2.5.1.18) and MDHAR, respectively. Both enzymes were up-regulated at 1.25 mM Pb stress that accounted for 6.0 and 1.8 fold, respectively. GSTs are

important enzymes involved in GSH-metabolism and thus play significant roles in conjugation of GSH to a wide variety of exogenous and endogenous electrophilic metabolites of xenobiotics and the reduction of H_2O_2 formed during oxidative stress (Reddy et al. 2005; Yan et al. 2008; Anjum et al. 2012). The conjugation of GSH with toxic substances forming S-glutathionylated reaction productes, are later transported to the vacuoles for sequestration and/or subsequent metabolism that are non-toxic to the plant cell (Coleman et al. 1997; Moons 2005; Yan et al. 2008; Anjum et al. 2012). Almost all of the cytocolic GSTs have been known to occur as homo- or hetero- dimers of subunits with moleculer weights of 23–29 kDa, which is quite similar to the 17 kDa protein as identified in our experiment. Both SOD and GST were up-regulated in roots of *Agrosttis* grass under moderate and severe heat stress conditions (Xu and Huang 2008). The increased GSTs expression has been identified in various plants root proteomic studies under several stress conditions such as; during combined effect of heat and drought in maize (Liu et al. 2012), in soybean under Al stress (Duressa et al. 2011); in tomato under Cd stress (Rodrígues-Celma et al. 2010); in rice under Cu stress (Ahsan et al. 2007).

MDHAR is an important enzyme of ascprbate-glutathione cycle (AGC), which has a major H_2O_2 scavenging pathway and operate both in the chloroplast and cytosol (Hausladen and Kunert 1990; Zhang and Kirkham 1996; Sharma and Dubey 2005). The APX enzyme catalyzes on the H_2O_2 and reduces it in to H_2O molecules in the presence of ascorbate with concomitant changes in ascorbate to monodehydroascorbate (MDHA) an ascorbyl radical (Prasad 1997; Sharma and Dubey 2005). The conversion of MDHA in to ascorbate is done by the enzyme MDHAR in the presence of NAD(P)H. MDHAR enzyme maintaining the level of ascorbate in the cell, an important component of AGC, which participate in ROS detoxification and adjust the cellular redox potential (Potters et al. 2010).

Protein synthesis/energy metabolism

Protein synthesis is one of the major metabolic pathways to be affected by HMs stress. The peptides identified in spot 11 matched to HSP70 of *Chlamydomonas reinhardtii* with two matched peptide covering 4% of the protein sequence. The heat-shock proteins are commonly induced under stressful conditions and plays crucial protecting role against stress by re-establishing normal protein confirmation and thus cellular homeostasis (Wang et al. 2004; Timperio et al. 2008). Members of HSP70 family were reported to be up-regulated in response to various abiotic stresses including salt, heat, drought and HMs (Leborgne-Castel et al. 1999; Lin et al. 2001; Kim et al., 2005). HSP70 act as a molecular chaperon and has wide range of functions including protein folding, assembly, translocation, degradation, transport of various proteins across membranes and preventing protein from arbitrary aggregation under stress conditions through binding to hydrophobic residues of protein (Wang et al. 2004, 2006b; Wang et al. 2011; Timperio et al. 2008). It has been suggested that the up-regulation of HSP70 under various HMs in different plants such as rice (Ahsan et al. 2007), *Thlaspi caerulescens* (Tuomainen et al. 2010), wheat roots (Wang et al. 2011), soybean roots (Duressa et al. 2011) and *Miscanthus sinensis* (Sharmin et al. 2012) was probably related to cellular protection against HM-induced damage..

Spots number 10, 13 were identified as ATP synthase subunit β, spot 15 representing ATP synthase β chain and spot 18 was confirmed as ATPase synthase subunit α, which were up-regulated by 3.3, 2.8, 4.1 and 3.6 folds, respectively in 1.25 mM Pb stress when compared to control. These proteins belong to bioenergetics metabolism and were expressed in similar manner. The enzymes ATP synthase was associated with the production of energy in the form of adenosine tri phosphate (ATP) from phosphorylation of adenosine di phosphate (ADP) with inorganic phosphate (iP). ATP synthase also act as

transporter of ions and transport protons across the membrane electrochemical gradient. Additionally, the up-regulation of four different subunits of ATP synthase enzymes during 1.25 mM Pb revealed that during Pb stress high energies are required to cope with the stress in *T. triangulare* roots. The increased energy production might be related to enhanced utilization of energy in the synthesis of defense related metabolites required for combating against Pb-induced toxicity and oxidative stress. ATP-dependent synthase or protease plays vital roles in controlling the availability of regulatory proteins and in eliminating abnormal or damaged proteins (Bah et al. 2010). Such data suggest that a high electrochemical proton gradient across the membrane may be used by secondary active antiporters responsible for higher accumulation of Pb in the vacuole and further in root tissues. It have been reported that arsenic (As) treatment caused increased expression/up-regulation of ATP synthase protein in maize roots (Requejo and Tena 2005) and *Pteris vittata* roots (Bona et al. 2011). Furthermore, similar responses were also reported in wheat roots under Cd treatment (Wang et al. 2011). On the other hand interestingly, no changes in ATP synthase were observed in Cd treated poplar (Kieffer et al. 2009) and down-regulation in Cd treated tomato roots (Rodríguez-Celma et al. 2010).

Cell signaling/cell metabolism

In response to Pb stress increased expression of two proteins for carbohydrate metabolisms and glycolysis have been observed in root of *T. triangulare*. Spot 8 and 20 identified as triosephosphate isomerase (TPI, EC 5.3.1.1,) and 2,3-bisphospho glycerate independent phosphoglycerate mutase 1 (2,3 BPG) were up-regulated by 3.5 and 3.1 fold, respectively, in *T. triangulare* roots treated with 1.25 mM Pb when compared to the control. These proteins catalyze the fifth and eight step of glycolysis, respectively and were expressed in almost similar fashion. TPI catalyzes the reversible interconversion of dihydroxyacetone phosphate and D-glyceraldehyde-3-phosphate, while 2,3 BPG catalyzes

the interconversion of 3-phosphoglycerate to 2-phosphoglycerate and leading towards the final product of glycolysis i.e. pyruvate. The proteomic up-regulation of glycolysis enzymes suggest that glycolysis might have important role in plant root cells under Pb stress condition to adjust and accomplish the energy requirement and supply of pathway intermediates for synthesis of various metabolites useful for stress acclimatization (Wang et al 2011). It have been reported that several of the glycolysis metabolic enzymes such as glucose phosphate isomerase, aldolase, glyceraldehyde 3-phosphate dehydrogenase, enolase, were affected when exposed to various abiotic stress such as drought (Sengupta et al. 2011), salt (Minhas and Grover 1999) as well as HMs (Wang et al. 2011; Rodríguez-Celma et al. 2010; Labra et al. 2006; Roth et al. 2006).

Spot 17 identified as S-adenosylhomocysteinase was found to be up-regulated by 3.8 fold during 1.25 mM Pb stress when compared to control. S-adenosylhomocysteinase catalyzes the lysis of S-adenosylhomocysteine to form homocysteine with the elimination of adenosine (Jakubowski and Guranowski, 1978). The intermediate homocysteine can either synthesize methionine, with the activity of methionine synthase or form cysteine with the help of two subsequent enzymes, cystathionine-β-synthase and cystathionine-γ-lyase (Palmer and Abeles 1979; Ravanel et al. 2004). Methionine is a sulfur-containing amino acid which serves as component of the universal activated methyl donor S-adenosyl methionine and the building block in proteins synthsis (Sengupta et al. 2011). It has been suggested that the accumulation of methionine along with other amino acids in plant cells, under HMs stress indicates a significant protective role as well as regulatory function (Pearce and Sherman 1999; Sharma and Dietz 2006; Herrera-Rodríguez et al. 2007). In addition, amino acid cysteine is required for the synthesis of methionine and GSH/PCs and also plays a central role in antioxidant defense and metal sequestration (Sharma and Dietz 2006; Singh et al. 2010). The adenosine produced as the action of S-adenosylhomo-cysteinase may also act as the precursor for purine nucleotide biosynthesis, which serves

multiple roles in the plant cells (Stasolla et al. 2003). Thus, it can be suggested that the protein S-adenosylhomo-cysteinase might be a key regulator of various plant metabolic pathways which ensures an optimum plant performance during Pb-induced oxidative stress.

Sensitivity of cells to sense the stress signal and subsequent changes in gene expression, cell metabolism, and physiology were the key events in plant adaptation response to a stress factor (Bisseling 1999; Lindsey et al. 2002). In our experiment, spot 16 is identified as probable receptor like protein kinase (RLPK) of *A. thaliana*. RLPK membrane protein belongs to Serine/Threonine protein kinase superfamily and containg one protein kinase domain. This superfamily belongs to the family of transferase and recognized as largest class of transmembrane sensors in *A. thaliana* (Wigniewska et al. 2003; Liu et al. 2012). It has been considered that *Arabidopsis* genome has at least 340 receptor like kinases, but only few of them are known for their biological functions (Anonymous 2000; Torii 2000; Matsubayashi et al. 2002; Wigniewska et al. 2003). The up-regulation of RLPK might have relevance in Pb-induced oxidative stress signal. It is possible that RLPK play crucial roles in communication between cells or organs that control the defence mechanisms in response to Pb stress in cells of *T. triangulare* roots.

Flavonoids are considered as large family of plant secondary metabolites, and are well known antioxidants. Through MALDI-TOF-MS analysis we confirmed spot 3 as a chalcone-flavanone isomerase (CFI), which belongs to the family of isomerases. This enzyme catalyzes the isomerization of chalcones to their corresponding flavanones in flavonoids biosynthesis pathway (Moustafa and Wong 1976). In the present study CFI was up-regulated by 3.8 fold under Pb stress conditions. Flavanones are a type of flavonoids which are a group of plant polyphenolic secondary metabolites, known to be involved in various plant growth and developmental processes (Hernández et al. 2009). Thus, synthesis of flavonoids was considered to be an effective plant defense strategy against ROS, as

flavonoids have the ability to capture free radical ions by donation of phenolic hydrogen atoms, which protect plant cells from adverse effects of abiotic stresses (Hernández et al. 2009). It was reported that most of the flavonoids possesses comparatively higher antioxidants capacities than some of the well known antioxidants including, ascorbate and α-tocopherol (Hernández et al. 2009). Also, a temporal correlation has been suggested between flavonoid accumulation and oxidative stress (Kirakosyan et al. 2003). Thus, the present up-regulation of CFI in roots of *T. triangulare* against high Pb concentrations demonstrates that rapid isomerization of chalcones to flavanones is an important defense strategy of *T. triangulare* to detoxify Pb-induced ROS.

Root morphology/Cell structure

The expression of spot 14 was identified as actin 1 (cytoskeleton protein) through MALDI-TOF-MS and its accumulation increased by approximately 5 fold during Pb stress when compared to control. Apart from being the essential housekeeping gene actin also performs certain special cellular functions, including cell division and cytokinesis, cell signaling, vesicle and organelle movement and the maintenance of cell junctions and cell shape. Actin is also known to have dynamic plasticity with respect to its structure under different abiotic stress conditions (Chitteti and Peng 2007; Xu et al. 2010; Sengupta et al. 2011; Duressa et al. 2011). Its abundance was increased in soybean roots (Duressa et al. 2011), and declined in rice cultivars (Zhang et al. 2007) during Al treatment. It has been also reported about increased expression of actin in Cd treated tomato roots (Rodríguez-Celma et al. 2010) in Cu treated *Cannabis sativa* roots (Elisa et al. 2007). A recent proteomic study also showed that Cd stress reduced actin accumulation in *Solanum torvum* roots (Wu et al. 2012), while it had up-regulated the actin expression in Cd treated wheat roots (Wang et al. 2011). The response of actin protein to Pb stress may be related with cellular adaptive strategies to structural modification and cellular damage involving cell

rupture and formation of pores, as we observed in our previous SEM study of *T. triangulare* roots under different Pb treatment.

Transporters

Aquaporins are channel proteins that facilitate the transport of water and small neutral molecules across cell membranes of most of the living organisms (Dynowski et al. 2008; Maurel et al. 2009). Compared with control, spot 9 was identifies as aquaporin NIP1-1 protein and was up-regulated by 3.5 fold during 1.25 mM Pb stress. Plant aquaporins can be divided into four subfamilies: Among them, nodulin-26-like intrinsic proteins (NIPs) are unique to plants, with nine and 10 members being present in *A. thaliana* and rice, respectively (Wallace et al. 2006; Mitani-Ueno et al. 2011). NIPs are further subdivided into three subgroups (NIP I, II, and III) based on the sequence similarity of the aromatic/arginine (ar/R) constriction region (Wallace et al. 2006; Mitani-Ueno et al. 2011; Maurel et al. 2009). NIPs are involved in the transport of wide variety of solutes, but the mechanisms controlling the selectivity of transport substrates are poorly understood (Mitani-Ueno et al. 2011). It has been reported that Pb treatment down-regulate the aquaporin PIP1-6 (Plasma membrane Intrinsic Protein) homolog in maize roots (Shen et al. 2013), which probably related to the inhibition in the plant water transport. Whereas drought stress significantly up-regulated the expression of PIP1-1 and did not affect the expression of PIP2-2 (Vandeleur et al. 2009) and abscissic acid up-regulated the expression of PIP2-5 under heat and combined drought and heat stress in maize root (Liu et al. 2012). Bienert et al. (2008) suggested that aquaporin homologues facilitate the rapid transport of two metalloids, As and antimonite (Sb), in plants. On the otherhand, the active efflux of As(III) by roots have potential role in As detoxification mechanism in plants suggested the potential strategy to decrease As accumulation in plants (Tripathi et al. 2007; Duan et al. 2012). However, in rice aquaporin also involved in bi-directional As(III)

transport (Zhao et al. 2010). Furthermore, the transgenic study of *A. thaliana* mutants with independent mutations in *AtNIP1;1* showed decrease in As contents in comparison to wild type confirmed that NIP1;1 is the key determinant of As(III) uptake and transport (Kamiya et al. 2009). Yet, number of studies demonstrated the involvement of aquaporin transporter in transport and uptake of As (III) in *Pteris vittata* (Mathews et al. 2011) and aquaporin *NIP2;1* in rice (Ma et al. 2008).

Newly identified proteins

In our experimental conditions, we have analyzed six new spots which appeared/expressed only during 1.25 mM Pb stress conditions. Out of six, we could have identified only three spots as they marked by N1, N2 and N3 in 2DE gel (Fig.). Spot N1, N2 and N3 represents chalcone-flavanone isomerase, auxin transport and DNA directed RNA polymerase subunit β proteins, respectively. As we already discussed about the chalcone-flavanone isomerase, up-regulated during Pb stress when compared to control, was also identified as a new spot during 1.25 mM Pb stress. But the Mr/pI of this protein is 23.84/5.3, confirming the different isoform of the enzyme, having important role in ROS detoxification. Furthermore, another protein DNA directed RNA polymerase subunit β is known to be involved in the transcription of DNA to mRNA that further translated in to peptide with the help of various translation factors. The two isoform of DNA directed RNA polymerase subunit β were expressed in cobalt treated *Pseudomonas putida* (Ray et al. 2013). Certainly, the up-regulation of transcription factor, RNA polymerase subunit β, during Pb stress in our experiment indicates that Pb possibly promote specific protein synthesis in *T. triangulare* roots, which may reveal a key secret of its tolerance mechanisms to Pb stress.

The phytohormone auxin has well established functional roles in embryogenesis, cell divison and elongation, phototropism, lateral root formation and other physiological

processes of plants (Friml et al. 2003, Campanoni and Nick 2005, Kimura and kagawa 2006, Dubrovosky et al. 2008). Auxin is synthesized in the leaves and then transported to the roots via vascular tissues and inter-cellular auxin transport is mediated through various auxin-transport proteins along with the diffusive flux of auxin across apoplast (Titapiwatanakun and Murphy 2009). Modulations in the expression of auxin transport proteins was highly crucial as the concentration gradient created by directional auxin movement could be strongly correlated to the plant morphological adaptations to the environment along with the establishment of plant axial polarity and organ patterning (De Smet and Jurgens 2007). In the present study, an auxin transport protein (spot N2) was found to be newly induced in *T. triangulare* roots subjected to 1.25 mM Pb concentrations. It is known that in hydroponic culture, high metal concentrations results in osmotic stress to the plant due to reduced amount of available water for uptake through roots and under such conditions, plants try to modulate their root morphology for maximizing the water conductivity. Thus, based on our results, we can hypothesize that *T. triangulare* induced auxin transport protein in response to high Pb concentrations for altering its root morphology through lateral root formation in order to tolerate Pb-induced osmotic stress. Moreover, we have also observed a significant up-regulation of water conducting protein channel, aquaporin (spot 9) in *T. triangulare* roots at similar Pb concentrations, which further establishes plant's defense strategy to enhance water conductivity during Pb-induced water-limitations.

Hypothetical proteins

Spot no. 4, 7 and 19 were identified as hypothetical proteins and hence no defined role could be assigned to these spots. Since these proteins exhibited increased expression during 1.25 mM Pb when compared to control, possibility existed that these hypothetical proteins might be involved in tolerance to Pb-induced oxidative stress.

Conclusions

In conclusion, we have successfully identified major Pb-induced proteins in *T. traingulare* roots. Significant induction of proteins involved in ROS detoxification and defense, protein synthesis/energy metabolism, cell signaling/metabolism, root morphology and root conductivity provides an interesting insight into the root system dynamics against Pb-induced toxicity. Under high concentrations of Pb, *T. triangulare* primarily regulate its water conductivity through induction of water conducting aquaporins and root morphology-related proteins including actins and auxin transporters. While to alleviate Pb-induced oxidative stress, induction of various ROS detoxifying enzymes and proteins involved in energy metabolism, protein synthesis and cell signaling was observed.

Summary & Conclusions

Summary and conclusions

Stem cuttings of *T. triangulare* were successfully propagated in soil and hydroponic media with convincing growth of vegetative propagules, adventitious roots and leaves in a short period of time. Stem cuttings of *T. triangulare* grown in hydroponic media, initiated adventitious roots within 7 days, which gives extensive adventitious roots in cultureing periods of 21 days. Hydroponically grown shoots, with adventitious roots can serve as an ideal experimental system for toxicity bioassays. Thus, uniform stem cuttings (acclimatized for 21 days) with extensive adventitious roots and leaves were treated with 0, 0.25, 0.50, 0.75, 1.00 and 1.25 mM of $Pb(NO_3)_2$ for a maximum of 7 days treatment duration for Pb toxicity bioassays with *T. triangulare*. Pb accumulation level and changes in morpho-physiological and biochemical parameters in *T. triangulare* leaves have been studied under increasing external concentration of Pb. Our experimental data showed that roots were absorbed much higher quantities (85–87%) than stems (12–14%) while in leaves it was below detectable limit after 7 days of treatment, which was confirmed by due to the decreased translocation of Pb within the plants.

Pb treatment resulted in gradual changes in morphology leading to developed longitudinal ruptures and formation of pores in treated root and damage of the vascular transport system in stem when compared to control. The EDS analysis detected the presence of Pb in treated roots, while it was not detected in leaf samples. The atomic% of nutrient elements was declined during Pb treatment over control sample in both leaf and root, which suggested the decreased translocation and avoidance of the elemental uptake, respectively. Thus, we may postulate that decreased in the nutrients atomic% were directly or indirectly altered the plant growth and metabolic characteristics.

Pb is phytotoxic, which was evidenced by the significant decrease of RWC and dose-dependent increase of cells death and lipid perxidation in leaves of Pb-treated plants. In continuation with toxic symptoms, we observed that Pb treatment for 7 days caused

significant reductions in Chl and SQDG contents when compared to control. Exposure of low Pb concentration caused induction in Chl and SQDG contents and had opposite effects when compared to high Pb concentration exposure. *In vivo* assay of chlorophyll fluorescence using the PAM fluorometric analysis showed that both PSII and PSI functions were affected under Pb stress in *T. triangulare* leaves. The reduction in F_m and *q*P shows the interference in the electron transport chain of photosystems, which resulted in to increased *q*N and decreased F_v/F_m, Φ_{PSII} of PSII. Pb treatments affects or inhibited PSII function to a much greater extent than that of PSI. Carotenoid, antocyanins, α-tocopherol, glutathione serves as antioxidant in leaves against free radical mediated cellular injury, which supports the existence of an effective defense strategy in *T. triangulare* and also a potential biomarker against ROS generation and Pb-induced oxidative stress.

Pb in the root tissue causes oxidative stress, which was manifested by increased ROS production, MDA content along with increasing LOX activity in comparison to control. Increase in LOX could be responsible for oxidative stress in root cells which produces hydroperoxide by catalyzing the peroxidation of unsaturated fatty acids present in biomembranes. Pb induces a substantial increase in the formation of oxidative product of proteins measured as protein carbonyls content, which was reflected as a decrease in the total protein content in Pb treated roots. In contrast to total protein contents, a variety of proteins such as SOD, CAT, APX and GST activities measured here proved their key role in ROS detoxification. SOD dismutates superoxide radical to form H_2O_2 and O_2, CAT APX and GST are the important H_2O_2 scavenging enzymes. The increased activity of GST involved in active binding and detoxification of lipid hydro-peroxide. Amino acid cystein content increased gradually against Pb treatment, while amino acid proline showed an inverted U-shaped dose response possibly due to increased inhibition in proline biosynthesis or proline catabolism at higher Pb concentrations. Pb treatment increased the

frequency of DNA damage analyzed through alkaline comet assays, followed a dose-response, which perhaps was mediated through the generation of ROS.

Pb treatment declined the NPSH, GSH, total ascorbate and total GSH contents in similar pattern, while it induced the GSSG content in dose-dependent manner. Decline in GSH at higher Pb might be attributed to high GSH consumption as an antioxidant to combat oxidative stress or for the synthesis of other metal binding ligands i.e. phytochelatins or metallothioneins. Pb treatment for 7 days caused gradual reduction in GSH/GSSG ratio, which was evident by the reduced activities of GR and γ-ECS enzyme. FTIR results showed that Pb or Pb-induced active species are mostly bound to amino, phenolic, carboxylic acids and other alcoholic, amide and ester containing bio-molecules.

Comparative analysis of proteins provides accurate information about specific mechanisms, and identification of major players in the considered pathways. Overall analysis of control and 1.25 mM Pb treated gels, showed that out of the number of matched spots approximately 61 spots were up-regulated. A total of 20 major up-regulated spots (> 1.8 fold) and 3 new spot (appeared only in 1.25 mM Pb) were identified by MALDI-TOF, which showed the up-regulation different sets of proteins during 1.25 mM Pb stress. Root proteins involved in root architecture, energy metabolism, ROS detoxification, cell signaling, primary and secondary metabolisms and transport were differentially up-regulated during Pb stress. Expression patterns of proteins belonging to different functional groups are highly correlated with other morphological, physiological and biochemical parameters.

Literature cited

References

Adeniyi AA (1996) Determination of cadmium, copper, iron, lead, manganese, and zinc in water leaf (*Talinum triangulare*) in dumpsites. Environ Inter 22:259–262.

Aebi H (1984) Catalase in vitro. Meth Enzymol 105:121–126.

Agrawal GK, Rakwal R, Yonekura M, Kubo A, Saji H (2002) Proteome analysis of differentially displayed proteins as a tool for investigating ozone stress in rice (*Oryza sativa* L.) seedlings. Proteomics 2:947–959.

Ahamad M, Verma S, Kumar A, Siddiqui MKJ (2005) Environmental exposure to lead and its correlation with biochemical indices in children. Sci Total Environ 346:48–55.

Ahmad P, Prasad MNV (2012) (Eds) Abiotic stress responses in plants: metabolism, productivity and sustainability. Springer, New York. ISBN 978-1-4614-0633-4.

Ahsan N, Lee D-G, Lee S-H, Kang KY, Lee JJ, Kim PJ, Yoon H-S, Kim J-S, Lee B-H (2007) Excess copper induced physiological and proteomic changes in germinating rice seeds. Chemosphere 67:1182–1193

Ahsan N, Lee DG, Alam I, Kim PJ, Lee JJ, Ahn YO, et al. (2008) Comparative proteomic study of arsenic-induced differentially expressed proteins in rice roots reveals glutathione plays a central role during As stress. Proteomics 8:3561–7356.

Aina R, Labra M, Fumagalli P, Vannini C, Marsoni M, Cucchi U, Bracale M, Sgorbati S, Citterio S (2007) Thiol-peptide level and proteomic changes in response to cadmium toxicity in *Oryza sativa* L. roots. Environ Exp Bot 59:381–392.

Aitkenhead-Peterson JA, Dvorak BD, Volder A, Stanley NC (2011) Chemistry of growth medium and leachate from green roof system in South-central Texas. Urban Ecosyst. 14:17–33.

Ajibesin KK, Ekpo BA, Bala DN, Essien EE, Adesanya SA (2008) Ethnobotanical survey of Akwa Ibom State of Nigeria. J Ethnopharmacol 115:387–408.

Ali MB, Vajpayee P, Tripathi RD, Rai UN, Singh SN, Singh SP (2003) Phytoremediation of lead, nickel, and copper by *Salix acmophylla* Bioss: role of antioxidants enzymes and antioxidant substances. Bull Environ Conta Toxicol 70:462–469.

Alia P, Saradhi P (1991) Proline accumulation undr heavy metal stress. J Plant Physiol 138:554–558.

Allabi AC, Busia K, Ekanmian V, Bakiono F (2011) The use of medicinal plants in self-care in the Agonlin region of Benin. J Ethnopharmacol 133:234–243.

Almroth BC, Sturve J, Stephensen E, Holth TF, Forlin L (2008) Protein carbonyls and antioxidant defenses in corkwing wrasse (*Symphodus melops*) from a heavy metal polluted and a PAH polluted site. Mar Environ Res 66:271–277.

Al-Saleh I, Al-Enazi S, Shinwari N (2009) Assessment of lead in cosmetic products. Regulat Toxicol Pharmacol 54:105–113.

Andarwulan N, Batari R, Sandrasari DA, Bolling B, Wijaya H (2010) Flavonoid content and antioxidant activity of vegetables from Indonesia. Food Chem 121:1231–1235.

Anjum NA, Umar S, Iqbal M, Ahmad I, Pereira ME, Khan NA (2011) Protection of growth and photosynthesis of *Brassica juncea* genotype with dual type sulfur transport system against sulfur deprivation by coordinate changes in the activities of sulfur metabolism enzymes and cysteine and glutathione production. Russ J Plant Physiol 58:892–898.

Anjum NA, Ahmad I, Mohmood I, Pacheco M, Duarte AC, Pereira ME, Umar S, Ahmad A, Khan NA, Iqbal M, Prasad MNV (2012) Modulation of glutathione and its related enzymes in plants' responses to toxic metals and metalloids- a review. Environ Exp Bot 75:307–324.

Ann C, Karen S, Jos R, Kelly O, Els K, Tony R, Nele H, Nathalie V, Suzy VS, Frank VB, Yves G, Jan C, Jaco V (2011) The cellular redox state as a modulator in cadmium and copper responses in *Arabidopsis thaliana* seedlings. J Plant Physiol 168:309–316.

Anonymous (1989) Environmental health criteria 85: Lead- environmental aspects. World Health Organization (WHO). http://www.inchem.org/pages/ehc.html.

Anonymous (1995) Lead. Hazardous Substances Data Bank (HSDB). National Library of Medicine. http://toxnet.nlm.nih.gov.

Anonymous (2000) The *Arabidopsis* Genome Initiative. Analysis of the genome sequence of the flowering plant *Arabidopsis thaliana.* Nature 408:798–815.

Anonymous (2003) Annual report 2003-2004. Ministry of Coal and Mines, Government of India (MoCM, GOI), India. Pp 94. Web Site Address: http://www.mines.nic.in

Anonymous (2004) Estimation of relative bioavailability of lead in soil and soil-like materials using in vivo and in vitro methods. Washington, DC: U.S. Environmental Protection Agency (EPA). OSWER 9285777.

Anonymous (2005) Lead in drinking water. Washington, DC: U.S. Environmental Protection Agency (EPA). http://www.epa.gov/safewater/lead/leadfacts.html. April 19, 2005.

Anonymous (2007) Air quality and emissions-progress continues in 2006. United State Environmental Protection Agency (EPA). http://www.epa.gov/airtrends/econ-emissions.html. June 14, 2007.

Anonymous (2007) Lead. Hazardous Substances Data Bank (HSDB). National Library of Medicine. http://toxnet.nlm.nih.gov.

Anonymous (2007) Toxicological profile for lead. Atlanta, GA: U.S. Department of Health and Human Services, Public Health Service, Agency for Toxic Substances and Disease Registry (ATSDR).

Anonymous (2008) Handbook of operation with Dual-PAM Heinz Walz, Germany.

Anonymous (2011) Hazardous metals and minerals pollution in India. In: Indian National Science Academy (INSA). A Position Paper, pp 1–24.

Anonymous (2011a) Detailed data table for the 2011 priority list of hazardous substance. Atlanta, GA: Division of Toxicology and Environmental Medicine, Agency for Toxic Substances and Disease Registry (ATSDR).

Anonymous (2011b) Division of Toxicology and Environmental Medicine Atlanta, GA: Support document to the 2011 priority list of hazardous substances. Division of Toxicology and Environmental Medicine, Agency for Toxic Substances and Disease Registry (ATSDR).

Anonymous (2011) Lead and lead compounds. In: Report on Carcinogens (ROC), National Toxicology Program, Department of Health and Human Services. pp 251–255.

Anonymous (2011) Monthly summary on non-ferrous minerals and metals, December-2011. Ministry of Mines Government of India (MoM, GOI), India, 16 pp.

Anonymous (2011) Hazardous metals and minerals pollution in India. Indian National Science Academy (INSA). A Position Paper, pp 1–24.

Antosiewicz DM (2005) Study of calcium-dependent lead-tolerance on plants differing in their level of Ca-deficiency tolerance. Environ Pollut 134:23–34.

Araceli C-O, Ma de Lourdes P-H, Ma Elena P-H, Rodríguez JA, Carlos Andrés G-V (2009) Chemical studies of anthocyanins: Review Food Chem 13:859–871.

Aravind P, Prasad MNV (2003) Zinc alleviates cadmium-induced oxidative stress in *Ceratophyllum demersum* L.: a free floating freshwater macrophyte. Plant Physiol Biochem 41:391–397.

Aravind P, Prasad MNV, Malec P, Waloszek A, Strzałka K (2009) Zinc protects *Ceratophyllum demersum* L. (free-floating hydrophyte) against reactive oxygen species induced by cadmium. J Trace Ele Med Biol 23:50–60.

Arazi T, Sunkar R, Kaplan B, Fromm H (1999) A tobacco plasma membrane calmodulin-binding transporter confers Ni^{2+} tolerance and Pb^{2+} hypersensitivity in transgenic plants. Plant J 20:171–182.

Arias JA, Peralta-Videa JR, Ellzey JT, Ren M, Viveros MN, Gardea-Torresdey JL (2010) Effects of *Glomus deserticola* inoculation on *Prosopis*: enhancing chromium and lead uptake andtranslocation as confirmed by X-ray mapping, ICP-OES and TEM techniques. Environ Exp Bot 68:139–148.

Arnon DI (1949) Copper enzymes in isolated chloroplasts: polyphenoloxidases in *Beta vulgaris*. Plant Physiol 24:1–15.

Arshad M, Silvestre J, Pinelli E, Kallerhoff J, Kaemmerer M, Tarigo A, Shahid M, Guiresse M, Pradere P, Dumat C (2008) A field study of lead phytoextraction by various scented *Pelargonium* cultivars. Chemosphere 71:2187–2192.

Bah AM, Sun H, Chen F, Zhou J, Dai H, Zhang G, Wu F (2010) Comparative proteomic analysis of *Typha angustifolia* leaf under chromium, cadmium and lead stress. J Hazard Mater 184:191–203.

Baker CJ, Mock NM (1994) An improved method for monitoring cell death in cell suspension and leaf disc assays using Evans blue. Plant Cell Tissue Org Cult 39:7–12.

Bates LE, Waldren RP, Teare ID **(**1973) Rapid determination of free proline for water stress studies. Plant Soil 39**:**205–207.

Beauchamp C, Fridovich I (1971) Superoxide dismutase: improved assays and an assay applicable to acrylamide gels. Anal Biochem 44:276–287.

Bette A, Kutschera U (1996) Pigment accumulation and photosynthesis in developing rye coleoptiles. Bot Acta 109:194–198.

Bhaduri AM, Fulekar MH (2012) Antioxidant enzyme responses of plants to heavy metal stress. Rev Environ Sci Biotech 11:55–69.

Bi X, Feng X, Yang Y, Li X, Shin GPY, Li F, Qiu G, Li G, Liu T, Fu Z (2009) Allocation and source attribution of lead and cadmium in maize (*Zea mays* L.) impacted by smelting emissions. Environ Poll 157:834–839.

Bienert GP, Thorsen M, Schüssler MD, Nilsson HR, Wagner A, Tamás, MJ et al. (2008) A subgroup of plant aquaporins facilitate the bi-directional diffusion of $As(OH)_3$ and $Sb(OH)_3$ across membranes. BMC Biol 6:26.

Bindu T, Sumi MM, Ramasamy EV (2010) Decontamination of water polluted by heavy metals with Taro (*Colocasia esculenta*) cultured in a hydroponic NFT system. Environmentalist 30:35–44.

Bisseling T (1999) The role of plant peptides in intercellular signalling. Cur Plant Biol 2:365–368.

Black CB, Murdy WH (1972) The evolutionary origin of *Talinum teretifolium* pursh. Botanical Gazette 133:405–410.

Bona E, Marsano F, Massa N, Cattaneo C, Cesaro P, Argese E, Sanità di Toppi L, Cavaletto M, Berta G (2011) Proteomic analysis as a tool for investigating arsenic stress in *Pteris vittata* roots colonized or not by arbuscular mycorrhizal symbiosis. J Proteomics 74:1338–1350.

Boucher N, Carpentier R (1999) Hg^{2+}, Cu^{2+}, and Pb^{2+}-induced changes in Photosystem II photochemical yield and energy storage in isolated thylakoid membranes: A study using simultaneous fluorescence and photoacoustic measurements. Photosynth Res 59:167–174.

Braconi D, Bernardini G, Santucci A (2011) Linking protein oxidation to environmental pollutants: redox proteomic approaches. J Proteomics 74:2324–2337.

Bradford MM (1976) Rapid and sensitive method for the quantitation of microgram quantities of protein utilizing the principle of protein-dye binding. Anal Biochem 72: 248–254.

Bredmose N, Hansen J (1995) Regeneration, growth and flowering of cut rose cultivars as affected by propagation material and method. Scient Horticul 64:103–111.

Brunet J, Repellin A, Varrault G, Terryn N, Fodil YZ (2008) Lead accumulation in the roots of grass pea (*Lathyrus sativus* L.): a novel plant for phytoremediation systems? C R Biol 331:859–864.

Buchanan BB, Gruissem W, Jones RL (2000) Biochemistry and Molecular Biology of Plants. American Society of Plant Physiology, United States of America.

Bulaj G, Kortemme T, Goldenberg DP (1998) Ionization-reactivity relationships for cysteine thiols in polypeptides. Biochemistry 37:8965–8972.

Burzynski M, Kolbus G (2004) Changes of photosynthetic parameters in cucumber leaves under Cu, Cd, and Pb stress. Photosynthetica 42:505–510.

Cenkci S, Cigerci IH, Yildiz M, Ozay C, Bozdag A, Terzi H (2010) Lead contamination reduces chlorophyll biosynthesis and genome template stability in *Brassica rapa* L. Environ Exp Bot 67:467–473.

Chandra R, Bharagava RN, Yadav S, Mohan D (2009) Accumulation and distribution of toxic metals in wheat (*Triticum aestivum* L.) and Indian mustard (*Brassica campestris* L.) irrigated with distillery and tannery effluents. J Hazard Mater 162:1514–1521.

Chang HS, Chakrabarty D, Hahn EJ, Paek KY (2003) Micropropagation of calla lily (*Zantedeschia albomaculata*) via *in vitro* shoot tip proliferation. In Vitro Cellular Devlop Biol- Plant 39:129–34.

Chaudhury S, Panda SK (2005) Toxic effects, oxidative stress and ultrastructural changes in moss *Taxithelium nepalense* (Schwaegr.) broth under chromium and lead phytotoxicity. Water Air Soil Pollut 167:73–90.

Chitteti BR, Peng Z (2007) Proteome and phosphoproteome differential expression under salinity stress in rice (*Oryza sativa*) roots. J Proteome Res 6:1718–1727.

Cho SH, Hoang QT, Kim YY, Shin HY, Ok SH, Bae JM, Shin JS (2006) Proteome analysis of gametophores identified a metallothionein involved in various abiotic stress responses in *Physcomitrella patens*. Plant Cell Rep 25:475–488.

Cobbett CS (2000) Phytochelatin biosynthesis and function in heavy-metal detoxification. Curr Opin Plant Biol 3:211–216.

Coleman JOD, Blake-Kalff M, Davies E (1997) Detoxification of xenobiotics by plants: chemical modification and vacuolar compartmentation. Trends Plant Sci 2:144–151.

Collin VC, Eymery F, Genty B, Rey P, Havaux M (2008) Vitamin E is essential for the tolerance of *Arabidopsis thaliana* to metal-induced oxidative stress. Plant Cell Environ 31:244–257.

Campanoni P, Nick P (2005) Auxin-dependent cell division and cell elongation. 1-Naphthaleneacetic acid and 2,4-dichlorophenoxyacetic acid activate different pathways. Plant Physiol 137:939–948.

Dai L-P, Xiong Z-T, Huang Y, Li M-J (2006) Cadmium-induced changes in pigments, total phenolics, and phenylalanine ammonia-lyase activity in fronds of *Azolla imbricate*. Environ Toxicol 21:505–512.

Davies MJ (2005) The oxidative environment and protein damage. Biochim Biophys Acta 1703:93–109.

Dazy M, Masfaraud JF, Ferard JF (2009) Induction of oxidative stress biomarkers associated with heavy metal stress in *Fontinalis antipyretica* Hedw. Chemosphere 75:297–302.

De Smet I, Jurgens G. 2007. Patterning the axis in plants: auxin in control. Curr Opin Genetic Develop 17:337–343.

Dixit V, Pandey V, Shyam R (2001) Differential antioxidative responses to cadmium in roots and leaves of pea (*Pisum sativum* L. cv. Azad). J Exp Bot 52:1101–1109.

Dizdaroglu M (1993) Chemistry of free radical damage to DNA and nucleoproteins. In: Halliwell B, Aruoma OI (Eds) DNA and free radicals, Ellis Horwood, London, U.K., Pp 19–39.

Drążkiewicz M, Baszyński T (2010) Interference of nickel with the photosynthetic apparatus of *Zea mays*. Ecotoxicol Environ Saf 73:982–986.

Druege U, Baltruschat H, Franken P (2007) *Piriformospora indica* promotes adventitious root formation in cuttings. Scientia Horticul 112:422−426.

Duan G, Kamiya T, Ishikawa S, Arao T, Toru F (2012) Expressing *ScACR3* in rice enhanced arsenite efflux and reduced arsenic accumulation in rice grains. Plant Cell Physiol 53:154–163.

Dube A, Bharti S, Laloraya MM (1993) Inhibition of anthocyanin synthesis and phenylalanine ammonium lyase activity by Co^{2+} in the leaf disks of *Terminalia catappa*. Physiol Plant 88:237–242.

Dubrovsky JG, Sauer M, Napsucialy-Mendivil S, Ivanchenko MG, Friml J, Shishkova S, Celenza J, Benkova E (2008) Auxin acts as a local morphogenetic trigger to specify lateral root founder cells. Proceed Nat Acad Sci, USA 105:8790–8794.

Duressa D, Soliman K, Taylor R, Senwo Z (2011) Proteomic analysis of soybean roots under aluminum stress. Int J Plant Genomics. DOI:10.1155/2011/282531.

Dushenkov V, Kumar PBAN, Motto H, Raskin I (1995) Rhizofiltration: the use of plants to remove heavy metals from aqueous streams. Environ Sci Tech 29:1239−1245.

Dutta I, Mookerjee A (1981) Lead in soil and grasses along roadsides in Delhi. Pro Ind Nat Sci Acad B 47:58–64.

Duxbury AC, Yentsch CS (1956) Plankton pigment monograph. J Mar Res 15:93–101.

Dynowski M, Mayer M, Moranb O, Ludewig U (2008) Molecular determinants of ammonia and urea conductance in plant aquaporin homologs. FEBS Letters 582:2458–2462.

Eapen D, Barroso ML, Ponce G, Campos ME, Cassab GI (2005) Hydrotropism: root growth responses to water. Trends Plant Sci 10:44−50.

Ederli L, Pasqualini S, Batini P, Antonielli M (1997) Photoinhibition and oxidative stress: effects on xanthophyll cycle, scavenger enzymes and abscisic acid content in tobacco plants. J Plant Physiol 151:422–428.

Ekmekçi Y, Tanyolac D, Ayhan B (2008) Effects of cadmium on antioxidant enzyme and photosynthetic activities in leaves of maize cultivars. J Plant Physiol 165:600–611.

Elisa B, Marsano F, Cavaletto M, Berta G (2007) Copper stress in *Cannabis sativa* roots: morphological and proteomic analysis. Caryologia 60: 96–101.

Emery L, Whelan S, Hirschi KD, Pittman JK (2012) Phylogenetic analysis of Ca^{2+}/cation antiporter genes and insights into their evolution in plants. Front Plant Sci. DOI:10.3389/fpls.2012.00001.

Estrella-Gómez N, Mendoza-Cózatl D, Moreno-Sánchez R, González-Mendoza D, Zapata-Pérez O, Martínez-Hernández A, Santamaría JM (2009) The Pb-hyperaccumulator aquatic fern *Salvinia minima* Baker, responds to Pb^{2+} by increasing phytochelatins via changes in *SmPCS* expression and in phytochelatin synthase activity. Aqua Toxicol 91:320–328.

Eun SO,Youn HS, LeeY (2000) Lead disturbs microtubule organization in the root meristem of *Zea mays*. Physiol Plant 110:357–365.

Evans MD, Dizdaeoglu M, Cooke MS (2004) Oxidative DNA damage and disease: induction, repair and significance. Mutat Res 567:1–61.

Fasuyi OA (2007) Bio-nutritional evaluations of three tropical leaf vegetables (*Telfairia occidentalis*, *Amaranthus cruentus* and *Talinum triangulare*) as sole dietary protein sources in rat assay. Food Chemistry 103:757−765.

Finster ME, Gray KA, Binns HJ (2004) Lead levels of edibles grown in contaminated residential soils: a field survey. Sci Total Environ 320:245–257.

Fiske CH, Subbarow Y (1925) The colorimetric determination of phosphorus. J Biol Chem 66:375–400.

Force L, Critchley C, van Rensen JJS (2003) New fluorescence parameters for monitoring photosynthesis in plants. Photosynth Res 90:1–19.

Foxcraft CL, Richardson DM, Wilson JRU (2008) Ornamental plants as invasive aliens: problems and solutions in Kruger National park, South Africa. Environ Manag 41:32–51.

Foyer C, Theodoulou FL, Delrot S (2001) The functions of inter- and intracellular glutathione transport systems in plants. Trends Plant Sci 6:486–487.

Franco R, Sanchez-Olea R, Reyes-Reyes EM, Panayiotidis MI (2009) Environmental toxicity, oxidative stress and apoptosis: menageatrois. Mutat Res 674:3–22.

Friml J, Vieten A, Sauer M, Weijers D, Schwarz H, Hamann T, Offringa R, Jurgens G (2003) Efflux-dependent auxin gradients establish the apical-basal axis of *Arabidopsis*. Nature 426:147–153.

Gaitonde MK (1967) Spectrophotometric method for the direct determination of cysteine in the presence of other naturally occurring amino acids. Biochem J 104:627–633.

Gao S, Ou-yang C, Tang L, Zhu J, Xu Y, Wang S, Chen, F (2010) Growth and antioxidant responses in *Jatropha curcas* seedling exposed to mercury toxicity. J Hazar Mater 182:591–597.

García O, Mandina T, Lamadrid AI, Diaz A, Remigio A, Gonzalezd Y, Piloto J, Gonzalez JE, Alvarez A (2004) Sensitivity and variability of visual scoring in the comet assay. Results of an inter laboratory scoring exercise with the use of silver staining. Mutat Res 556:25–34.

Gbolade A (2012) Ethnobotanical study of plants used in treating hypertension in Edo State of Nigeria. J Ethnopharmacol 144:1–10.

Ghnaya AB, Charles G, Hourmant A, Hamida JB, Branchard M (2009) Physiological behavior of four rapeseed cultivar (*Brassica napus* L.) submitted to metal stress. C R Biol 332:363–370.

Ghnaya T, Zaier H, Baioui R, Sghaier S, Lucchini G, Sacchi GA, Lutts S, Abdelly C (2013) Implication of organic acids in the long-distance transport and the accumulation of lead in *Sesuvium portulacastrum* and *Brassica juncea*. Chemosphere 90:1449–1454.

Gichner T, Patkova Z, Szakova J, Demnerova K (2006) Toxicity and DNA damage in tobacco and potato plants growing on soil polluted with heavy metals. Ecotoxicol Environ Saf 65:420–426.

Gichner T, Znidar I, Száková J (2008) Evaluation of DNA damage and mutagenicity induced by lead in tobacco plants. Mutat Res Genet Toxicol, Environ Mutagen 652:186–190.

Gill T, Dogra V, Kumar S, Ahuja PS, Sreenivasulu Y (2012) Protein dynamics during seed germination under copper stress in *Arabidopsis* over-expressing *Potentilla superoxide dismutase*. J Plant Res 125:165–172.

Gill SS, Tuteja N (2010) Reactive oxygen species and antioxidant machinery in abiotic stress tolerance in crop plants. Plant Physiol Biochem 48:909–930.

Gomez KA, Gomez AA (1984) Statistical procedures for agricultural research. Wiley, New York, 2nd edition. Paperback, 680 pp.

Govindjee (1995) Sixty-three years since Kautsky: Chlorophyll *a* fluorescence. Aust J Plant Physiol 22:131–160.

Gopal R, Rizvi AH (2008) Excess lead alters growth, metabolism and translocation of certain nutrients in radish. Chemosphere 70:1539–1544.

Grill E, Loffler S, Winnacker EL, Zenk MH (1986) Phytochelatins, the heavy-metal-binding peptides of plants, are synthesized from glutathione by a specific γ-glutamylcysteine dipeptidyl transpeptidase (phytochelatins synthase). Proc Natl Acad Sci USA 86:6838–6842.

Gupta DK, Nicoloso FT, Schetinger MRC, Rossato LV, Pereira LB, Castro GY, Srivastava S, Tripathi RD (2009) Antioxidant defense mechanism in hydroponically grown *Zea mays* seedlings under moderate lead stress. J Hazard Mater 172:479–484.

Gupta M, Tripathi RD, Rai UN, Chandra P (1995) Lead induced changes in glutathione and phytochelatin in *Hydrilla verticillata*. Chemosphere 30:2011–2020.

Gupta M, Tripathi RD, Rai UN, Chandra P (1999) Lead induced synthesis of metal binding peptides (Phytochelatins) in submerged macrophyte *Vallisneria spiralis* L. Physiol Mol Biol Plants 5:173–180.

Habig, WH, Jakoby WB (1981) Assay for differentiation of glutathione-S-transferase. In: Jakoby WB (Ed), Methods in Enzymology. Vol 77, Academic press, New York, pp 398–405.

Han WY, Shi YZ, Ma LF, Ruan JY, Zhao FJ (2007) Effect of liming and seasonal variation on lead concentration of tea plant (*Camellia sinensis* (L.) O. Kuntze). Chemosphere 66:84–90.

Harris FS, Martin CE (1991) Plasticity in the degree of CAM cycling and its relationship to drought stress in five species of *Talinum* (Portulacaceae). Oecologia 86:575−584.

Hartmann HT, Kester DE, Davies FT, Geneve RL (2002) Plant Propagation: principles and practices (7th Edn), Prentice Hall, New Jersey, pp 363−365.

Harwood JL, Okanenko AA (2003) Sulphoquinovosyl diacylglycerol (SQDG)- The sulpholipid of higher plants. Kluwer Academic Publisher, pp 189–221.

Hashiguchi A, Ahsan N, Komatsu S (2010) Proteomics application of crops in the context of climatic changes. Food Res Int 43:1803–1813.

Hatzilazarou S, Economou A, Antoniou T, Ralli P (2001) Propagation of *Ebenus cretica* L. by tissue culture. Propagat Ornament Plants 1:25−27.

Hausladen A, Kunert KJ (1990) Effects of artificially enhanced levels of ascorbate and glutathione on the enzymes monodehydroascorbate reductase, dehydroascorbate reductase, and glutathione reductase in spinach (*Spinacia oleracea*). Physiol Plant 79:384–388.

HEI (2004) Special report 15, Health effects of outdoor air pollution in developing countries of Asia. A literature review. Health Effects Institute, Cambridge, MA.

Heath RL, Packer L (1968) Peroxidation in isolated chloroplasts 1. Kinetics and stoichiometry of fatty acid peroxidation. Arch Biochem Biophys 125:189–198.

Hernández I, Alegre L, Breusegem FV, Munné-Bosch S (2009) How relevant are flavonoids as antioxidants in plants? Trends Plant Sci 14:125–132.

Herrera-Rodrígues MB, Pérez-Vicente R, Maldonado JM (2007) Expression of asparagines synthetase genes in sunflower (*Helianthus annus*) under various environmental stresses. Plant Physiol Biochem 45:33–38.

Hickey M, King C (1981) 100 Families of flowering plants, Cambridge University Press, London, 76 pp.

Hissin PJ, Hilf R (1976) A fluorometric method for determination of oxidized and reduced glutathione in tissues. Anal Biochem 74:214–226.

Hoagland DR, Arnon DI (1950) The water-culture method for growing plants without soil. California Agricultural Experiment Station Circular 347:1−32.

Howe HE (1981) Lead. In: Kirk-Othmer Encyclopedia of Chemical Technology, 3rd edition, vol 14. New York: John Wiley & Sons, pp 98–139.

Hu JZ, Shi GX, Xu QS, Wang X, Yuan QH, Du KH (2007) Effects of Pb^{2+} on the active oxygen-scavenging enzyme activities and ultrastructure in *Potamogeton crispus* leaves. Russ J Plant Physiol 54**:**414**–**419.

Hu R, Sun K, Su X, Pan Y, Zhang Y, Wang X (2012) Physiological responses and tolerance mechanisms to Pb in two xerophils: *Salsola passerina* Bunge and *Chenopodium album* L. J Hazard Mater 205–206:131–138.

Huang G-Y, Wang Y-S (2010) Physiological and biochemical responses in the leaves of two mangrove plant seedlings (*Kandelia candel* and *Bruguiera gymnorrhiza*) exposed to multiple heavy metals. J Hazard Mater 182:848–854.

Huang H, Li T, Tian S, Gupta DK, Zhang X, Yang X (2008) Role of EDTA in alleviating lead toxicity in accumulator species of *Sedum alfredii* H. Biores Tech 99:6088–6096.

Huang H, Gupta DK, Tian S, Yang X, Li T (2012) Lead tolerance and physiological adaptation mechanism in roots of accumulating and non-accumulating ecotypes of *Sedum alfredii*. Environ Sci Pollut Res 19:1640–1651.

Iannelli MA, Pietrini F, Fiore L, Petrilli L, Massacci A (2002) Antioxidant response to cadmium in *Phragmites australis* plants. Plant Physiol Biochem 40:977–982.

Ingle RA, Smith JAC, Sweetlove LJ (2005) Responses to nickel in the proteome of the hyperaccumulator plant *Alyssum lesbiacum*. BioMetals 18:627–641.

Iqbal N, Masood A, Nazar R, Syeed S, Khan NA(2010) Photosynthesis, growth and antioxidant metabolism in mustard (*Brassica juncea* L.) cultivars differing in Cd tolerance. Agri Sci China 9:519–527.

Islam E, Yang X, Li T, Liu D, Jin X, Meng F (2007) Effect of Pb toxicity on root morphology, physiology and ultrastructure in the two ecotypes of *Elsholtzia argyi*. J Hazard Mater 147:806–816.

Israr M, Jewell A, Kumar D, Sahi SV (2011) Interactive effects of lead, copper, nickel and zinc on growth, metal uptake and antioxidative metabolism of *Sesbania drummondii*. J Hazard Mater 186:1520–1526.

Jain SM, Ochatt SJ (2010) Protocols for In Vitro Propagation of Ornamental Plants. Methods in Molecular Biology (Vol 589), Humana Press, U.S., 324 Pp.

Jakubowski H, Guranowski A (1978) Adenosylhomocysteinsae: Adenosine complex. Bochem Biophys Res Commun 84:1060–1068.

Jarvis MD, Leung DWM (2002) Chelated lead transport in *Pinus radiata*: an ultrastructural study. Environ Exp Bot 48:21–32.

Jathar VS, Pendharkar PB, Raut SJ, Pandey VK (1981) Intake of food in India. J Food Sci Tech, India 18:240–242.

Jenita KZ, Kalaivani P, Sathyavathi S, Doble M (2010) *Portulaca oleracea*, a potential candidate for contaminated soil? In: Proceedings of the 7th International Phytotechnologies conference, 26−29 September 2010 Parma, Italy, Servizio Editoria e Fotoriproduzione- Settore economato e provveditorato, University of Parma, Italy, 188 pp.

Jiang M, Zhang J (2001) Effect of abscissic acid on active oxygen species, antioxidative defense system and oxidative damage in leaves of maize seedlings. Plant Cell Physiol 42:1265–1273.

Jiang W, Liu D (2010) Pb-induced cellular defense system in the root meristematic cells of *Allium sativum* L. BMC Plant Biol 10:40–40.

Joshi MK, Mohanty P (2004) Chlorophyll *a* fluorescence as a probe of heavy metal ion toxicity in plants. In: Papageorgiou GC (Ed): Chlorophyll *a* Fluorescence: A Signature of Photosynthesis, Advances in Photosynthesis and Respiration. Springer, Dordrecht, pp 637–661.

Ju S, Zhang Y, Zhang Yi, Xuec P, Wang Y (2011) Clean hydrometallurgical route to recover zinc, silver, lead, copper, cadmium and iron from hazardous jarosite residues produced during zinc hydrometallurgy. J Hazard Mater 192:554–558.

Kadukova Jana, Kalogerakis N (2007) Lead accumulation from non-saline and saline environment by *Tamarix smyrnensis* Bunge. European J Soil Biol 43:216–223.

Kalaji HM, Loboda T (2007) Photosystem II of barley seedlings under cadmium and lead stress. Plant Soil Environ 53:511–516.

Kamiya T, Tanaka M, Mitani N, Ma JF, Maeshima M, Fujiwara T (2009) NIP1;1, an aquaporin homolog, determines the arsenite aensitivity of *Arabidopsis thaliana*. J Biol Chem 284:2114–2120.

Kaul PP, Shyam S, Srivastva R, Misra D, Salve PR, Srivastva SP (2003) Lead levels in ambiant air and blood of pregnant mothers from the general population of Lucknow (U.P.) India. Bull Environ Conta Toxicol 71:1239–1243.

Kaur G, Singh HP, Batish DR, Kohli RK (2012) A time course assessment of changes in reactive oxygen species generation and antioxidant defense in hydroponically grown wheat in response to lead ions (Pb^{2+}). Protoplasma 249:1091–1100.

Kean, E., 1968. A rapid sensitive spectrophotometric method for quantitative determination of sulfatides. J. Lipid Res. 9:319–329.

Khan NA, Anjum NA, Nazar R, Iqbal N (2009) Increased activity of ATP-sulfurylase and increased contents of cysteine and glutathione reduce high cadmium-induced oxidative stress in mustard cultivar with high photosynthetic potential. Russ J Plant Physiol 56:670–677.

Kieffer P, Planchon S, Oufir M, Ziebel J, Dommes J, Hoffmann L, Hausman JF, Renaut J (2009) Combining proteomics and metabolite analyses to unravel cadmium stress-response in poplar leaves. J Proteome Res 8:400–417.

Kim DW, Rakwal R, Agrawal GK, Jung YH, Shibato J, Jwa NS, Iwahashi Y, Iwahashi H, Kim DH, Shim IS, Usui K (2005) A hydroponic rice seedling culture model system for investigating proteome of salt stress in rice leaf. Electrophoresis 26:4521–4539.

Kimura M, Kagawa T (2006) Phototropin and light-signaling in phototropism. Curr Opin Plant Biol 9:503–508.

King M, Ramachandran V (1995) Lead. In: Kirk-Othmer encyclopedia of chemical technology. 4th edition. New York, NY: John Wiley & Sons, pp 69–113.

Kirakosyan A, Seymour E, Kaufman PB, Warber S, Bolling S, Chang S (2003) Antioxidant capacity of polyphenolic extracts from leaves of *Crataegus laevigata* and *Crataegus monogyna* (Hawthorn) subjected to drought and cold stress. J Agric Food Chem 51:3973–3976.

Kitamura Y, Ohta M, Ikenaga T, Watanabe M (2002) Responses of anthocyanin-producing and non-producing cells of *Glehnia littoralis* to radical generators. Phytochemistry 59:63–68.

Klughammer C, Schreiber U (2008) Complementary PS II quantum yields calculated from simple fluorescence parameters measured by PAM fluorometry and the saturation pulse method. PAM Appl No 1:27–35.

Kohda H, Yamaoka Y, Morinaga S, Ishak M, Darise M (1992) Saponins from *Talinum triangulare*. Chemical and Pharmaceutical Bulletin 40:2557−2558.

Kopittke PM, Blamey FPC, Menzies NW (2008) Toxicities of soluble Al, Cu, and La include ruptures to rhizodermal and root cortical cells of cowpea. Plant Soil 303:217–227.

Kopittke PM, Asher CJ, Kopittke R, Neal W. Menzies (2007a) Toxic effects of Pb^{2+} on growth of cowpea (*Vigna unguiculata*). Environ Pollut 150:280–287.

Kopittke PM, Asher CJ, Blamey FPC, Menzies NW (2007b) Toxic effects of Pb^{2+} on the growth and mineral nutrition of signal grass (*Brachiaria decumbens*) and Rhodes grass (*Chloris gayana*). Plant Soil 300:127–136.

Kosová K, Vítámvás P, Prášil IT, Renaut J (2011) Plant proteome changes under abiotic stress−Contribution of proteomics studies to understanding plant stress response. J Proteomics 1301–1322.

Krupa Z, Bańanowska M, Orzoł D (1996) Can anthocyanin be considered as a heavy metal stress indicator in higher plants? Acta Physiol Plant 18:147–151.

Kumar A, Gottesfeld P (2008) Lead content in household paints in India. Sci Total Environ 407:333–337.

Kumaravel TS, Vilhar B, Faux SP, Jha AN (2009) Comet Assay measurements: a perspective. Cell Biol Toxicol 25:53–64.

Labra M, Gianazza E, Waitt R, Eberini I, Sozzi A, Regondi S, Grassi F, Agradi E (2006) *Zea mays* L. protein changes in response to potassium dichromate treatments. Chemosphere 62 1234–1244.

Lakshminarayana R, Raju M, Krishnakantha TP, Baskaran V (2007) Lutein and zeaxanthin in leafy greens and their bioavailability: Olive oil influences the absorption of dietary lutein and its accumulation in adult rats. J Agri Food Chem 55:6395−6400.

Lamhamdi M, Bakrim A, Aarab A, Lafont R, Sayah F (2011) Lead phytotoxicity on wheat (*Triticum aestivum* L.) seed germination and seedlings growth. C R Biol 334:118–126.

Lamhamdi M, Galiou OE, Bakrim A, Nóvoa-Muňoz JC, Arias-Estévez M, Aarab A, Lafont R (2013) Effect of lead stress on mineral content and growth of wheat (*Triticum aestivum*) and spinach (*Spinacia oleracea*) seedlings. Saudi J Biol Sci 20:29–36.

Lange H, Shropshire W, Mohr H (1971) An analysis of phytochrome–mediated anthocyanins synthesis. Plant Physiol 47:649–655.

Larsson UK, Andersson B (1985) Different degrees of phosphorylation and lateral mobility of two polypeptides belonging to the light-harvesting complex of photosystem II. Biochim Biophys Acta 809:396–402.

Latha A, Pavanaguru R (2010) Genesis of Bandalamottu laed deposit, Agnigundala, Guntur district, A.P. J Appl Geochem 12:186–195.

Leborgne-Castel N, Jelitto-Van DEP, Crofts AJ, Denecke J (1999) Overexpression of *BiP* in tobacco alleviates endoplasmic reticulum stress. Plant Cell 11:459–470.

Levine RL, Garland D, Oliver CN, Amici A, Climent I, Lenz A, Ahn B, Shaltiel S, Stadtman ER (1990) Determination of carbonyl content in oxidatively modified proteins. Method Enzymol 106:464–478.

Li X, Bu N, Li Y, Ma L, Xin S, Zhang L (2012) Growth, photosynthesis and antioxidant responses of endophyte infected and non-infected rice under lead stress conditions. J Hazard Mater 213:55–61.

Liang D, Zhou Q, Gong W, Wang Y, Ni Z, He H, Li J, Wu J, Wu C, Zhang J (2012). Studies on the antioxidant and hepatoprotective activities of polysaccharides from *Talinum triangulare*. J Ethnopharmacol 136:316–321.

Lin BL, Wang JS, Liu HC, Chen RW, Meyer Y, Barakat A, Delseny M (2001) Genomic analysis of the Hsp70 superfamily in Arabidopsis thaliana. Cell Stress Chaperones 6:201–208.

Lindsey K, Casson S, Chilley P (2002) Peptides: new signaling molecules in plants. Trends Plant Sci 7:78–83.

Liu D, Li TQ, Yang XE, Islam E, Jin XF, Mahmood Q (2008) Effect of Pb on leaf antioxidant enzyme activities and ultrastructure of the two ecotypes of *Sedum alfredii* Hance. Russ J Plant Physiol 55:68–76.

Liu N, Lin Z, Mo H (2012) Metal (Pb, Cd, and Cu)-induced reactive oxygen species accumulations in aerial root cells of the Chinese banyan (*Ficus microcarpa*). Ecotoxicology. DOI10.1007/s 10646-012-0935-y.

Liu T, Zhang L, Yuan Z, Hu X, Lu M, Wang W, Wang Y (2012) Identification of proteins regulated by ABA in response to combined drought and heat stress in maize roots. Acta Physiol Plant. DOI 10.1007/s11738-012-1092-x.

Logan BA, Grace SC, Adams WW, Adams BD (1998) Seasonal differences in xanthophylls cycle characteristics and antioxidants in *Mahonia repens* growing in different light environments. Oecologia 116:9–17.

López MF (1999) Proteome analysis. I. Gene products are where the biological action is. J Chromatogr B Biomed Sci Appl 722:191–202.

López ML, Peralta-Videa JR, Benitez T, Gardea-Torresdey JL (2005) Enhancement of lead uptake by alfalfa (*Medicago sativa*) using EDTA and a plant growth promoter. Chemosphere 61:595–598.

Lowry OH, Rosebrough NJ, Farr AL, Randall (1951) R Protein measurement with the Folin-phenol reagent. J Biol Chem 193:265–275.

Luque-Garcia JL, Cabezas-Sanchez P, Camara C (2011) Proteomics as a tool for examining the toxicity of heavy metals. Trends Anal Chem 30:706−716.

Ma JF, Yamaji N, Mitani N, Xu XY, Su YH, McGrath SP, Zhao FJ (2008) Proc Natl Acad Sci USA. 105:9931–9935.

Maldonado-Magaña A, Favela-Torres E, Rivera-Cabrera F, Volke-Sepulveda TL (2011) Lead bioaccumulation in *Acacia farnesiana* and its effect on lipid peroxidation and glutathione production. Plant Soil 339:377–389.

Malec P, Maleva MG, Prasad MNV, Strazałka K (2009) Identification and characterization of Cd-induced peptides in *Egeria densa* (water weed): Putative role in Cd detoxification. Aquatic Toxicol 95:213–221.

Malecka A, Piechalak A, Tomaszewska B (2009) Reactive oxygen species production and antioxidative defense system in pea root tissues treated with lead ions: the whole roots level. Acta Physiol Plant 31:1053–1063.

Mallick N, Mohn FH (2003) Use of chlorophyll fluorescence in metal-stress research: a case study with the green microalga *Scenedesmus*. Ecotoxic Environ Saf 55:64–69.

Manara A (2012) Plant responses to heavy metal toxicity. In: Furini A (Ed), Plants and Heavy Metals, Springer Briefs in Biometals, pp 27–53.

Maric M, Antonijevic M, Alagic S (2012) The investigation of the possibility for using some wild and cultivated plants as hyperaccumulators of heavy metals from contaminated soil. Environ Sci Pollut Res. doi.10.1007/s11356-012-1007-9

Marmiroli M, Antonioli G, Maestri E, Marmiroli N (2005) Evidence of the involvement of plant ligno-cellulosic structure in the sequestration of Pb: an X-ray spectroscopy-based analysis. Environ Pollut 134:217–227.

Marschner H (1995) Mineral nutrition of higher plants. Academic Press, Cambridge.

Maurel C, Santoni V, Luu D-T, Wudick MM, Verdoucq L (2009) The cellular dynamics of plant aquaporin expression and functions. Curr Opin Plant Biol 12:690–698.

Mathews S, Rathinasabapathi B, Ma LQ (2011) Uptake and translocation of arsenite by *Pteris vittata* L.: Effects of glycerol, antimonite and silver. EnvironPollu 159:3490–3495.

Matsubayashi Y, Ogawa M, Morita A, Sakagami Y (2002) An LRR receptor kinase involved in perception of a peptide plant hormone, phytosulfokinc. Science 296:1470–1472.

Meyres DER, Aucherlonie GJ, Webb RI, Wood B (2008) Uptake and localization of lead in the root system of *Brassica juncea*. Environ Pollut 153:323–332.

Miles CD, Brandle JR, Daniel DJ, Chu-Der O, Schnare PD, Uhlik DJ (1972) Inhibition of PS II in isolated chloroplasts by lead. Plant Physiol 49:820–825.

Minhas D, Grover A (1999) Transcript levels of genes encoding various glycolytic and fermentation enzymes change in response to abiotic stresses. Plant Sci 146:41–51.

Mishra S, Srivastava S, Tripathi RD, Kumar R, Seth CS, Gupta DK (2006) Lead detoxification by coontail (*Ceratophyllum demersum* L.) involves induction of

phytochelatins and antioxidant system in response to its accumulation. Chemosphere 65:1027–1039.

Mitani-Ueno N, Yamaji N, Zhao F-J, Ma JF (2011) The aromatic/arginine selectivity filter of NIP aquaporins plays a critical role in substrate selectivity for silicon, boron, and arsenic. J Exp Bot 62:4391–4398.

Mobin M, Khan NA (2007) Photosynthetic activity, pigment composition and antioxidative response of two mustard (*Brassica juncea*) cultivars differing in photosynthetic capacity subjected to cadmium stress. J Plant Physiol 164:601–610.

Mohanty N, Mohanty P (1998) Cation effects on primary processes of photosynthesis. In: Singh R, Sawhney SK (Eds) Advances in Frontier Areas of Plant Biochemistry, Delhi: Prentice Hall India, pp 1–18.

Møller IM, Sweetlove LJ (2010) ROS signaling-specificity is required. Trends Plant Sci 15:1–5.

Moons A (2005) Regulatory and functional interactions of plant growth regulators and plant glutathione S-transferases (GSTS). Plant Horm 72:155–202.

Moustafa E, Wong E (1976) Purification and properties of chalcone-flavanones isomerase from soya bean seed. Phytochemistry 6:625–632.

Murti CRK (1987) The cycling of arsenic, cadmium, lead and mercury in India. In: Hutchinson TC, Meema KM (Eds) Lead, mercury, cadmium and arsenic in the environment. John Wiley & Sons Ltd, pp 315–333.

Myśliwa-Kurdziel B, Strzałka K (2002) Influence of metals on biosynthesis of photosynthetic pigments. In: Prasad MNV, Strzałka K (Eds) Physiology and biochemistry of metal toxicity and tolerance in plants. Kluwer Academic Publisher pp 201–227.

Nahar S, Tajmir-Riahiha (1996) Complexation of heavy metal cations Hg, Cd, and Pb with proteins of PSII: evidence for metal–sulfur binding and protein conformational transition by FTIR spectroscopy. J Colloid Inter Sci 178:648–656.

Naik UC, Srivastava S, Thakur IS (2012) Isolation and characterization of *Bacillus cereus* IST105 from electroplating effluent for detoxification of hexavalent chromium. Environ Sci Pollut Res 19:3005–3014.

Nagajyoti PC, Lee KD, Sreekanth TVM (2010) Heavy metals, occurrence and toxicity for plants: a review. Environ Chem Lett 8:199–216.

Nagalakshmi N, Prasad MNV (2000) Responses of glutathione cycle enzymes and glutatione metabolism to copper stress in Scenedesmus bijugatus. Plant Sci 160:291–299.

Nagata T (2004) X-ray microanalysis of biological specimens by high voltage electron microscopy. Prog Histochem Cytochem 39:185–319.

Nakano Y, Asada K (1981) Hydrogen peroxide is scavenged by ascorbate-specific peroxidase in spinach chloroplasts. Plant Cell Physiol 22:867–880.

Nautiyal N, Sinha P (2012) Lead induced antioxidant defense system in pigeon pea and its impact on yield and quality of seeds. Acta Physiol Plant 34:977–983.

Németh G (1986) Induction of rooting. In: Bajaj YPS (Ed) Biotechnology in Agriculture and Forestry 1. Trees 1. Springer-Verlag, Berlin, pp 49−64.

Newton RP, Brenton AG, Smith CJ, Dudley E (2004) Plant proteome analysis by mass spectrometry: principles, problems, pitfalls and recent developments. Phytochemistry 65:1449–1485.

Nguyen AT, Donaldson RP (2005) Metal-catalyzed oxidation induces carbonylation of peroxisomal proteins and loss of enzymatic activities. Arch Biochem Biophysics 439:25–31.

Nocito FF, Pirovano L, Cocucci M, Sacchi GA (2002) Cadmium-induced sulfate uptake in maize roots. Plant Physiol 129:1872−1879.

Nyananyo BL (1992) Pollen morphology in the Portulacaceae (Centrospemu). Folia Geobotanica et Phytotaxonomica 27:387−400.

Nyananyo BL, Olowokudejo JD (1986) Taxonomic studies in the genus Talinum (Portulacaceae) in Nigeria. Willdenowia 16:455−463.

Nyffeler R, Eggli U (2010) Disintegrating Portulacaceae: A new familial classification of the suborder Portulacineae (Caryophyllales) based on molecular and morphological data. Taxon 59:227–240.

Ocampo G, Columbus JT (2010) Molecular phylogensis of suborder Cactineae (Caryophyllales), including insights in to photosynthetic diversification and historical biogeography. American J Bot 97:1827–1847.

Ocampo G, Columbus JT (2012) Molecular phylogenetic, historical biogeography, and chromosome number evolution of *Portulaca* (Portulacaceae). Mol Phylogen Evol 63:97–112.

Okanenko A, Taran N, Kosyk O (2003) Sulphoquinovosyl diacylglycerol and adaptation syndrome. Advance Res Plant Lipids Proc 361–364.

Oláh V, Lakatos G, Bertók C, Kanalas P, Szőllősi E, Kis J (2010) Sort-term chromium(VI) stress induces different photosynthetic responses in two duckweed species, *Lemna gibba* L. and *Lemna minor* L. Photosynthetica 48:513–520.

Pádua M, Aubert S, Casimiro A, Bligny R, Maryse A (2003) Block Effects of a sub-lethal copper exposure on non-green *Acer pseudoplatanus* cell lipids. Plant Physiol Biochem 41:471–477.

Palmer JL, Abeles RH (1979) The mechanism of action of S-adenosylhomocysteinase. J Biol Chem 254:1217–1226.

Panda BB, Panda KK (2002) Genotoxicity and mutagenicity of metals in plants. In: Prasad MNV, Strzalka K (Eds) Physiology and Biochemistry of metal toxicity and tolerance in plants. Kluwer Academic Publishers, Amsterdam, The Netherlands, pp 95–414.

Pandey J, Shubhashish K, Pandey R (2010) Heavy metal contamination of Ganga river at Varanasi in relation to atmospheric deposition. Tropical Ecology 51:365–373.

Panyaphu K, On TV, Sirisa-ard P, Srisa-nga P, ChansaKaow S, Nathakarnkitkul S (2011) Medicinal plants of the Mien (Yao) in Northern Thailand and their potential value in the primary healthcare of postpartum women. J Ethnopharma 135:226–237.

Parys E, Romanowska E, Siedlecka M, Poskuta JW (1998) The effect of lead on photosynthesis and respiration in detached leaves and in mesophyll protoplasts of *Pisum sativum*. Acta Physiol Plant 20:313–322.

Patnaik AR, Achary VMM, Panda BB (2011) Comet assay to assess DNA damage and genotoxic stress in plants. In: Roy BK, Chaudhary BR, Sinha RP (Eds) Plant

genome: biodiversity, conservation and manipulation, Narosa Publication, New Delhi, pp 17–29.

Patra M, Bhowmik N, Bandopadhyay B, Sharma A (2004) Comparison of mercury, lead and arsenic with respect to genotoxic effects on plant systems and the development of genetic tolerance. Environ Exp Bot 52:199–223.

Pearce DA, Sherman F (1999) Toxicity of copper, cobalt, and nickel salts is dependent on histidine metabolism in the yeast *Saccharomyces cerevisiae*. J Bacteriol 181:4774–4779.

Pena LB, Zawoznik MS, Tomaro ML, Gallego SM (2008) Heavy metals effects on proteolytic system in sunflower leaves. Chemosphere 72:741–746

Piechalak A, Tomaszewska B, Baralkiewicz D, Malecka A (2002) Accumulation and detoxification of lead ions in legumes. Phytochemistry 60:153–162.

Piotrowska A, Bajguz A, Godlewska-Zyłkiewicz B, Czerpak R, Kaminska M (2009) Jasmonic acid as modulator of lead toxicity in aquatic plant *Wolffia arrhiza* (Lemnaceae). Environ Exp Bot 66:507–513.

Posmyk MM, Kontek R, Janas KM (2009) Antioxidant enzymes activity and phenolic compounds content in red cabbage seedlings exposed to copper stress. Ecotoxicol Environ Saf 72:596–602.

Potters G, Horemans N, Jansen MAK (2010) The cellular redox state in plant stress biology- a charging concept. Plant Physiol Biochem 48:292–300.

Pourrut B, Perchet G, Silvestre J, Cecchi M, Guiresse M, Pinelli E (2008) Potential role of NADPH-oxidase in early steps of lead-induced oxidative burst in *Vicia faba* roots. J Plant Physiol 165:571–579.

Pourraut B, Shahid M, Dumat C, Winterton P, Pinelli E (2011a) Lead uptake, toxicity and detoxification in plants. Rev Environ Conta Toxicol 213:113–136.

Pourrut B, Jean S, Silvestre J, Pinelli E (2011b) Lead-induced DNA damage in Vicia faba root cells: Potential involvement of oxidative stress. Mutat Res 726:123–128.

Prasad MNV (1997) Trace metals. In: Prasad MNV (Ed), Plant ecophysiology, John Wiley & Sons Inc. New York, pp 207–249.

Prasad MNV, Sajwan KS, Naidu R (Eds) (2006) Trace elements in the environment: biochemistry, biotechnology and bioremediation. John Wiley & Sons Inc. New York, 726 pp.

Probst A, Liu H, Fanjul M, Liao B, Hollande E (2009) Response of *Vicia faba* L. To metal toxicity on mine tailing substrate: Geochemical and morphological changes in leaf and root. Environ Exp Bot 66:297−308.

Przymusiński Roman, Rucińska-Sobkowiak R, Ilska B, Gwóźdz EA (2007) Organospecific responses of lupin seedlings to lead localization of hydrogen peroxide and peroxidase activity. Acta Physiol Plant 29:411–416.

Qiao X, Shi G, Jia R, Chen L, Tian X, Xu J (2012) Physiological and biochemical responses induced by lead stress in *Spirodela polyrhiza*. Plant Growth Regul 67:217–225.

Qin G, Meng X, Wang Q, Tian S (2009) Oxidative damage of mitochondrial proteins contributes to fruit senescence: a redox proteomics analysis. J Proteome Res 8:2449–2462.

Qureshia M, Qadirb S, Zollaa L (2007) Proteomics-based dissection of stress-responsive pathways in plants. J Plant Physiol 164:1239–1260.

Rajkumar K, Sivakumar S, Senthilkumar P, Prabha D, Subbhuraam CV, Song YC (2009) Effects of selected heavy metals (Pb, Cu, Ni and Cd) in the aquatic medium on the restoration potential and accumulation in the stem cuttings of the terrestrial plant, *Talinum triangulare* Linn. Ecotoxicology 18:952–960.

Rajkumar M, Sandhya S, Prasad MNV, Freitas H (2012) Perspectives of plant-associated microbes in heavy metal phytoremediation. Biotechnol Advanc 30:1562–1574.

Raju M, Varakumar S, Lakshminarayana R, Krishnakantha TP, Baskaran V (2007) Carotenoid composition and vitamin A activity of medicinally important green leafy vegetables. Food Chemistry 101:1598−1605.

Rascio N, Navari-Izzo F (2011) Heavy metal hyperaccumulating plants: How and why do they do it? And what makes them so interesting? Plant Science 180:169–181.

Rashid A Camm EL, Ekramoddoullah KM (1994) Molecular mechanism of action of Pb^{2+} and Zn^{2+} on water oxidizing complex of Photosystem II. FEBS Lett 350:296–298.

Ravanel S, Block MA, Rippert P, Jabrin S, Curien G, Rébeillé F, Douce R (2004) Methionine metabolism in plants. J Biol Chem 279:22548–22557.

Raymond MJ, Smirnoff N (2002) Proline metabolism and transport in maize seedlings at low water potential. Annals Bot 89:813–823.

Ray P, Girard V, Gault M, Job C, Bonneu M, Mandrand-Berthelot M-A, Singh SS, Job D, Rodrigue A (2013) *Pseudomonas putida* KT2440 response to nickel or cobalt induced stress by quantitative proteomics. Metallomics 5:68–79.

Rausch T, Wachter A (2005) Sulfur metabolism: a versatile platform for launching defense operations. Treand Plant Sci 10:503–509.

Reddy AM, Kumar SG, Jyothsnakumari G, Thimmanaik S, Sudhakar C (2005) Lead induced changes in antioxidant metabolism of horsegram (*Macrotyloma uniflorum* (Lam.) Verdc.) and bengal gram (*Cicer arietinum* L.). Chemosphere 60:97–104.

Requejo R, Tena M (2005) Proteome analysis of maize roots reveals that oxidative stress is a main contributing factor to plant arsenic toxicity. Phytochemistry 66:1519–1528.

Reugsegger A, Schmutz D, Brunold C (1992) Effect of cadmium on γ-glutamylcysteine synthesis in maize seedlings. Plant Physiol 99:428–433.

Reznick AZ, Packer L (1994) Oxidative damage to proteins: spectrophotometric method for carbonyl assay. Meth Enzymol 233:357–363.

Rinalducci S, Murgiano L, Zolla L (2008) Redox proteomics: basic principles and future perspectives for the detection of protein oxidation in plants. J Exp Bot 59:3781–801.

Rise M, Cojocaru M, Gottlieb HE, Goldschmidt EE (1989) Accumulation of α-tocopherol in senescing organs as related to chlorophyll degradation. Plant Physiol 89:1028–1030.

Rodríguez-Celma J, Rellán-Álvarez R, Abadía A, Abadía J, López-Millán AF (2010) Changes induced by two levels of cadmium toxicity in the 2-DE protein profile of tomato roots. J Proteomics 73:1694–1706.

Rodríguez E, Azevedo R, Moreira H, Souto L, Santos C (2013) Pb^{2+} exposure induced microsatellite instability in *Pisum sativum* in a locus related with glutamine metabolism. Plant Phyiol Biochem 62:19–22.

Roh MS, Lee AK, Suh JK (2005) Production of high quality *Ardisia* plants by stem tip cuttings. Scientia Horticul 104:293−303.

Roldan-Puertas MC, Rodriguez-Serrano M, Corpas FJ, Gomez M, Del Rio LA, Sandalio LM (2004) Cadmium-induced subcellular accumulation of $O_2^{\bullet-}$ and H_2O_2 in pea leaves. Plant Cell Envion 27:1122–1134.

Romanowska E, Wasilewska W, Fristedt R, Vener AV, Zienkiewicz M (2012) Phosphorylation of PSII proteins in maize thylakoids in the presence of Pb ions. J Plant Physiol 169:345–352.

Rossato LV, Nicoloso FT, Farias JG, Cargnelluti D, Tabaldi LA, Antes FG, Dressler VL, Morsch VM, Schetinger MRC (2012) Effects of lead on the growth, lead accumulation and physiological responses of *Pluchea sagittalis*. Ecotoxicology 21:111–123.

Roth U, Roepenack-Lahaye E von, Clemens S (2006) Proteome changes in *Arabidopsis thaliana* roots upon exposure to Cd^{2+}. J Exp Bot 57:4003–4013.

Rucińska R, Sobkowiak R, Gwóźdź EA (2004) Genotoxicity of lead in lupin root cells as evaluated by the comet assay. Cellular Mole Biol Lett 9:519–528.

Rucińska-Sobkowiak Renata, Nowaczyk G, Krzesłowsk M, Rabęda I, Jurga S (2013) Water status and water diffusion transport in lupine roots exposed to lead. Environ Exp Bot 87:100–109.

Sanitá di Toppi L, Gremigni P, Pawlik Skowronska B, Prasad MNV, Cobbett CS (2003) Responses to heavy metals in plants-Molecular approach. In: Sanitá di Toppi L, Pawlik Skowronska B (Eds), Abiotic Stresses in Plants. Dordecht, Netherlands: Kluwer Academic, pp 33–156.

Samardakiewicz S, Wozny A (2000) The distribution of lead in duckweed (*Lemna minor* L.) root tip. Plant Soil 226:107–111.

Sarvanan RS, Rose JKC (2004) A critical evaluation of sample extraction techniques for enhanced proteomic analysis of recalcitrant plant tissues. Proteomics 4:2522–2532.

Sárvári É (2005) Effects of heavy metals on chlorophyll–protein complexes in higher plants: causes and consequences. In: Pessarakli M (Ed) Hand book of photosynthesis. CRC Press, Boca Raton, USA, pp 865–888.

Schreiber U, Klughammer C (2008) Nonphotochemical fluorescence quenching and quantum yields in PS I and PS II: Analysis of heat-induced limitations using Maxi-Imaging-PAM and Dual-PAM-100. PAM Application Notes 1:15–18.

Schützendübel A, Polle A (2002) Plant responses to abiotic stresses: heavy metal-induced oxidative stress and protection by mycorrhization. J Exp Bot 53:1351–1365.

Sedlak J, Lindsay RH (1968) Estimation of total, protein-bound, and non-protein sulfhydryl groups in tissue by Ellmans reagent. Anal Biochem 25:192–208.

Sekhar C, Kamala CT, Chary NS, Mukherjee AB (2007) Arsenic accumulation by *Talinum cuneifolium*- application for phytoremediation of arsenic contaminated soils of Patancheru, Hyderabad, India. Trace Metal Conta Environ 9:315–338.

Sengar RK, Gautam M, Sengar RK, Grag SK, Sengar K, Chaudhary R (2008) Lead stress effects on physio-biochemical activities of higher plants. Rev Environ Conta Toxicol 196:73–93.

Sengupta D, Kannan M, Reddy AR (2011) A root proteomics-based insight reveals dynamic regulation of root proteins under progressive drought stress and recovery in *Vigna radiata* (L.) Wilczek. Planta 233:1111–1127.

Seregin IV, Shpigun LK, Ivanov VB (2004) Distribution and toxic effects of cadmium and lead on maize roots. Russ J Plant Physiol 51:525–533.

Shahid M, Pinelli E, Dumat C (2012) Review of Pb availability and toxicity to plants in relation with metal speciation; role of synthetic and natural organic ligands. J Hazard Mater 219–220:1–12.

Shahid M, Pinelli E, Pourrut B, Silvestre J, Dumat C (2011) Lead-induced genotoxicity to *Vicia faba* L. roots in relation with metal cell uptake and initial speciation. Ecotoxicol Environ Saf 74:78–84.

Shakya K, Chettri MK, Sawidis T (2008) Impact of heavy metals (copper, zinc and lead) on the chlorophyll content of some mosses. Arch Environ Contam Toxicol 54:412–421.

Sharma P, Dubey RS (2005) Lead toxicity in plants. Braz J Plant Physiol 17:35–52.

Sharma RK, Agrawal M, Marshall F (2007) Heavy metal contamination of soil and vegetables in suburban areas of Varanasi, India. Ecotoxic Environ Saf 66:258–266.

Sharma RK, Agrawal M, Marshall F (2008) Atmospheric deposition of heavy metals (Cu, Zn, Cd and Pb) in Varanasi city, India. Environ Monit Assess 142:269–278.

Sharma SS, Dietz KJ (2006) The significance of amino acids and amino acids derived molecules in plant responses and adaptation to heavy metal stress. J Exp Bot 57:711–726.

Sharmila P, Saradhi PP (2002) Proline accumulation in heavy metal stressed plants: an adaptive strategy. In: Prasad MNV, Strzałka K (Eds) Physiology and biochemistry of metal toxicity and tolerance in plants. Kulwer Academic Publishers, Netherlands, pp 179–199.

Sharmin SA, Alam I, Kim K-H, Kim Y-G, Kim PJ, Bahk JD, Lee B-H (2012) Chromium-induced physiological and proteomic alterations in roots of *Miscanthus sinensis*. Plant Sci 187:113– 126.

Shaw BP, Sahu SK, Mishra RK (2004) Heavy metal induced oxidative damage in terrestrial plants. In: Prasad MNV (Ed) Heavy metal stress in plants- from biomolecules to ecosystems, Springer-Verlag, Heidelberg, Narosa, New Delhi, 2nd ed, pp 84–126.

Shaw BP, Prasad MNV, Jha VK, Sahu BB (2006) Detoxification/defense mechanisms in metal-exposed plants. In: Prasad MNV, Sajwan KS, Naidu R (Eds) Trace elements in the environment: biogeochemistry, biotechnology and bioremediation. CRC Press, Taylor and Francis Group, New York, U.S. pp 291–324.

Shen Y, Zhang Y, Chen J, Lin H, Zhao M, Peng H, Liu L, Yuan G, Zhang S, Zhang Z, Pan G (2013) Genome expression profile analysis reveals important transcripts in maize roots responding to the stress of heavy metal Pb. Physiol Planta 147:270–282.

Shevchenko A, Wilm A, Vorm O, Mann M (1996) Mass spectrometric sequencing of protein from silver-stained polyacrylamide gels. Anal Chem 68:850–858.

Shillito LM, Almond MJ, Nicholson J, Pantos M, Matthews W (2009) Rapid characterization of archaeological midden components using FT-IR spectroscopy, SEM-EDX and micro-XRD. Spectrochem. Acta Part A 73:133–139.

Shringarpure R, Grune T, Mehlhase J, Davies KJA (2003) Ubiquitin conjugation is not required for the degradation of oxidized proteins by proteasome. J Biol Chem 278:311–318.

Shu X, Yin LiY, Zhang QF, Wang WB (2012) Effect of Pb toxicity on leaf growth, antioxidant enzyme activities, and photosynthesis in cuttings and seedlings of *Jatropha curcas* L. Environ Sci Pollut Res. 19:893–902.

Siddiqui S (2012) Lead induced genotoxicity in *Vigna mungo* var. HD-94. J Saudi Soci Agricul Sci 11:107–112.

Siedlecka A, Baszyński T (1993) Inhibition of electron flow around photosystem I in chloroplasts of Cd treated maize plants is due to Cd-induced iron deficiency. Physiol Planta 87:199–202.

Siedlecka A, Tukendrof A, Skórzyńska-Polit E, Maksymiec W, Wjcik M, Baszyński T, Krupa Z (2001) Angiosperm (Asteraceae, Convolvulaceae, Fabaceae and Poaceae; other than Brassicaceae). In: Prasad MNV (Ed) Metals in the environment. Marcel Dekker, New York. Pp:171–217.

Singh HP, Kaur G, Batish DR, Kohli RK (2011) Lead (Pb)-inhibited radical emergence in *Brassica campestris* involves alterations in starch-metabolizing enzymes. Biol Trace Elem Res 144:1295–1301.

Singh R, Tripathi RD, Dwivedi S, Kumar A, Trivedi PK, Chakrabarty D (2010) Lead bioaccumulation potential of an aquatic macrophyte *Najas indica* are related to antioxidant system. Biores Tech 101:3025–3032.

Singha B, Das SK (2012) Removal of Pb(II) ions from aqueous solution and industrial effluent using natural biosorbents. Environ Sci Pollut Res 19:2212–2226.

Sinha P, Dube BK, Srivastava P, Chatterjee C (2006) Alteration in uptake and translocation of essential nutrients in cabbage by excess lead. Chemosphere 65:651–656.

Stasolla C, Katahira R, Thorpe TA, Ashihara H (2003) Purine and pyrimidine nucleotide metabolism in higher plants. J Plant Physiol 160:1271–1295.

Strasser BJ, Strasser RJ (1995) Measuring fast fluorescence transients to address environmental questions: the JIP-test. In: Mathis P (Ed) Photosynthesis: from light to biosphere. Dordrecht, Kluwer Academic Publishers, pp 977–980.

Strubińska J, Hanaka A (2012) Adventitious root system reduces lead uptake and oxidative stress in sunflower seedlings. Biol Planta 55:771–774.

Subrahmanyam D (2008) Effects of chromium toxicity on leaf photosynthetic characteristics and oxidative changes in wheat (*Triticum aestivum* L.). Photosynthetica 46:339–345.

Sudhakar R, Gowda N, Venu G (2001) Mitotic abnormalities induced by silk dyeing industry effluents in the cells of *Allium cepa*. Cytologia 66:235–239.

Sun Q, Ye ZH, Wang XR, Wong MH (2005) Increase of glutathione in mine population of *Sedum alfredii*: A Zn hyperaccumulator and Pb accumulator. Phytochemistry 66:2549–2556.

Sun S-Q, He M, Cao T, Yusuyin Y, Han W, Li J-L (2010) Antioxidative responses related to H_2O_2 depletion in *Hypnum plumaeforme* under the combined stress induced by Pb and Ni. Environ Monit Assess 163:303–312.

Sun R-L, Zhou Q-X, Sun F-H, Jin C-X (2007) Antioxidative defense and proline/phytochelatin accumulation in a newly discovered Cd-hyperaccumulator, *Solanum nigrum* L. Environ Exp Bot 60:468–476.

Sutherland CA, Milner EF (1990) Lead. In: Elvers B, Hawkins S, Schulz G, eds. Ullmann's encyclopedia of industrial chemistry. 5th edition. VCH Publishers, New York, pp 193–236.

Syshchikov DV (2009) State of antioxidant glutathione dependent system of maize plantlets at actions of Cd compounds. Herald Kharkiv Natl Agrar Univer 1:45–51.

Szabados S, Savouré AA (2010) Proline: a multifunctional amino acid. Trends Plant Sci 15:89–97.

Tang YT, Qiu RL, Zeng XW, Ying RR, Yu FM, Zhou XY (2009) Lead, zinc, cadmium hyperaccumulation and growth stimulation in *Arabis paniculata* Franch. Environ Exp Bot 66:126–134.

Tian S-k, Lu L, Yang X, Huang H, Brown P, Labavitch J, Liao H, He Z (2011) The impact of EDTA on lead distribution and speciation in the accumulator *Sedum alfredii* by synchrotron X-ray investigation. Environ Pollu 159:782–788.

Timperio AM, Egidi MG, Zolla L (2008) Proteomics applied on plant abiotic stresses: role of heat shock proteins (HSP). J Proteomics 71:391–411.

Titapiwatanakun B, Murphy AS (2009) Post-transcriptional regulation of auxin transport proteins: cellular trafficking, protein phosphorylation, protein maturation, ubiquitination, and membrane composition. J Exp Bot 60:1093–1107.

Torii K (2000) Receptor kinase activation and signal transduction in plants: an emerging picture. Curr Opin Plant Biol 3:362–367.

Tripathi RD, Srivastava S, Mishra S, Singh N, Tuli R, Gupta DK et al. (2007) Arsenic hazards: strategies for tolerance and remediation by plants. Trends Biotechnol 25:158–165.

Tuomainen M, Tervahauta A, Hassinen V, Schat H, Koistinen KM, Lehesranta S, Rantalainen Kimmo, Häyrinen J, Auriola S, Anttonen M, Kärenlampi S (2010) Proteomics of *Thlaspi caerulescens* accessions and an interaccession cross segregating for zinc accumulation. J Exp Bot 61:1075–1087.

Ukhun ME, Nwazota J, Nkwocha FO (1990) Levels of toxic minerai elements in selected foods marketed in Nigeria. Bull Environ Contam Toxicol 44:325−330.

Ukpong EI, Moses JO (2001) Nutrient requirements for the growth of waterleaf (*Talinum triangulare*) in Uyo metropolis, Nigeria. The Environmentalist 21:153−159.

Uwah EI, Ndahi NP, Ogugbuaja VO (2009) Study of the levels of some agricultural pollutants in soils and water leaf (*Talinum triangulare*) obtained in Maiduguri, Nigeria. J Applied Sci Environ Sanit 4:71–78.

Uzu G, Sobanska S, Aliouane Y, Pradere P, Dumat C (2009) Study of lead phytoavailability for atmospheric industrial micronic and sub-micronic particles in relation with lead speciation. Environ Pollut 157:1178–1185.

Vadas TM, Ahner BA (2009) Cysteine- and glutathione-mediated uptake of lead and cadmium into *Zea mays* and *Brassica napus* roots. Environ Pollut 157:2558–2563.

Vandeleur RK, Mayo G, Shelden MC, Gilliham M, Kaiser BN, Tyerman SD (2009) The role of plasma membrane intrinsic protein aquaporins in water transport through roots: diurnal and drought stress responses reveal different strategies between isohydric and anisohydric cultivars of grapevine. Plant Physiol 149:445–460.

Vassilev A Manolov P (1999) Chlorophyll fluorescence of barley (*Hordeum Vulgare* L.) seedlings grown in excess of Cd. Bulg J Plant Physiol 25:67–76.

Velikova V, Yordanov I, Edreva A (2000) Oxidative stress and some antioxidant systems in acid rain-treated bean plants. Plant Sci 151:59–66.

Verbruggen N, Hermans C, Schat H (2009) Molecular mechanisms of metal hyperaccumulation in plants. New Phytol 181:759–776.

Verma S, Dubey RS (2003) Lead toxicity induces lipid peroxidation and alters the activities of antioxidant enzymes in growing rice plants. Plant Sci 164:645–655.

Vernay P, Gauthier-Moussard C, Jean L, Bordas F, Faure O, Ledoigt G, Hitmi A (2008) Effect of chromium species on phytochemical and physiological parameters in *Datura innoxia*. Chemosphere 72:763–771.

Vesely T, Neuberg M, Trakal L, Szakova J, Tlustoa P (2012) Water Lettuce *Pistia stratiotes* L. response to lead toxicity. Water Air Soil Pollut 223:1847–1859.

Wallace IS, Choi W-G, Roberts DM (2006) The structure, function and regulation of the nodulin 26-like intrinsic protein family of plant aquaglyceroporins. Biochim Biophys Acta 1758:1165–1175.

Wang C, Gu X, Wang X, Guo H, Geng J, Yu H, Sun J (2012a) Stress response and potential biomarkers in spinach (*Spinacia oleracea* L.) seedlings exposed to soil lead. Ecotoxicol Environ Saf 74:41–47.

Wang C, Tian Y, Wang X, Geng J, Jiang J, Yu H, Wang C (2010) Lead-contaminated soil induced oxidative stress, defense response and its indicative biomarkers in roots of *Vicia faba* seedlings. Ecotoxicology 19:1130–1139.

Wang G, Su MY, Chen YH, Lin FF, Luo D, Gao SF (2006a) Transfer characteristics of cadmium and lead from soil to the edible parts of six vegetable species in southeastern China. Environ Poll 144:127–135.

Wang P, Zhang S, JieLu CW (2012b) Effects of Pb on the oxidative stress and antioxidant response in a Pb bioaccumulator plant *Vallisneria natans*. Ecotoxicol Environl Saf 78:28–34.

Wang W, Vinocur B, Shoseyov O, Altman A (2004) Role of plant heat-shock proteins and molecular chaperones in the abiotic stress response. Trends Plant Sci 9:244–252.

Wang W, Vignani R, Scali M, Cresti M (2006b) A universal and rapid protocol for protein extraction from recalcitrant plant tissues for proteomic analysis. Electrophoresis 27:2782–2786.

Wang Y, Qian Y, Hu H, Xu Y, Zhang H (2011) Comparative proteomic analysis of Cd-responsive proteins in wheat roots. Acta Physiol Plant 33:349–357.

Ware S, Pinion G (1990) Substrate adaptation in rock outcrop plants: Eastern United States *Talinum* (Portulacaceae). Bull Torrey Botan Club 117:284−290.

Wei ZL, Dong L, Tian ZH (2009) Fourier transform infrared spectometry study on early stage of cadmium stress in clover leaves. Pak J Bot 41:1743–1750.

Wierzbicka M (1994) Resumption of mitotic activity in *Allium cepa* root tips during treatment with lead salts. Environ Exp Bot 34:173–180.

Wierzbicka M (1998) Lead in the apoplast of *Allium cepa* L. root tips-ultrastructural studies. Plant Sci 133:105–119.

Wierzbicka M (1999) Comparison of lead tolerance in *Allium cepa* with other plant species. Environ Pollut 104:41–52.

Wigniewska J, Trejgell A, Tretyn A (2003) Plant signalling peptides. Acta Physiol Planta 25:105–122.

Wong D, Govindjee (1976) Effects of lead ions on photosystem I in isolated chloroplasts: studies on the reaction center P700. Photosynthetica 10:241–254.

Wozny A, Jerczynska E (1991) The effect of lead on early stages of *Phaseolus vulgaris* L. growth in vitro conditions. Biol Plantarum 33:33–39.

Wu L, Ge Q, Zhang J, Zhou J, Xu J (2012) Proteomic analysis of Cd-responsive proteins in *Solanum torvum*. Plant Mol Biol Rep. DOI 10.1007/s11105-012-0515-6.

Wu X-W, Ma H-W, Yang J, Wang F-J, Li Z-H (2012) Adsorption of Pb(II) from aqueous solution by a poly-elemental mesoporous adsorbent. App Surf Sci 258:5516–5521.

Xu C, Huang B (2008) Root proteomic responses to heat stress in two *Agrostis grass* species contrasting in heat stress. J Exp Bot 59:4183–4194.

Xu C, Sibicky T, Huang B (2010) Protein profile analysis of salt-responsive proteins in leaves and roots in two cultivars of creeping bentgrass differing in salinity tolerance. Plant Cell Rep 29:595–615.

Yalçın S, Sezer S, Apak R (2012) Characterization and lead(II), cadmium(II), nickel(II) biosorption of dried marine brown macro algae *Cystoseira barbata*. Environ Sci Pollut Res 19:3118–3125

Yan F, Yang W-K, Li X-Y, Lin T-T, Lun Y-N, Lin F, Lv S-W, Yan G-L, et al. (2008) A trifunctional enzyme with glutathione S-transferase, glutathione peroxidase and superoxide dismutase activity. Biochim Biophys Acta 1780:869–872.

Yan ZZ, Ke L, Tam NFY (2010) Lead stress in seedlings of *Avicennia marina*, a common mangrove species in South China, with and without cotyledons. Aquat Bot 92:112–118.

Yang Y, Zhang Y, Wei X, You J, Wang W, Lu J, Shi R (2011) Comparative antioxidative responses and proline metabolism in two wheat cultivars under short term lead stress. Ecotoxicol Environ Saf 74:733–740.

Yin X, Saha UK Ma LQ (2010) Effectiveness of best management practices in reducing Pb-bullet weathering in a shooting range in Florida, J Hazard Mater 179:895–900.

Yusuf A.A, Arowolo TA, Bamgbose O (2003) Cadmium, copper and nickel levels in vegetables from industrial and residential areas of Lagos City, Nigeria. Food Chemical Toxicol 41:375–378.

Yusuf M, Fariduddin Q, Varshney P, Ahmad A (2012) Salicylic acid minimizes nickel and/or salinity-induced toxicity in Indian mustard (*Brassica juncea*) through an improved antioxidant system. Environ Sci Pollut Res 19:8–18.

Yusuf MA, Kumar D, Rajwanshi R, Strasser RJ, Tsimilli-Michael M, Govindjee, Sarin NB (2010) Overexpression of γ-tocopherol methyl transferase gene in transgenic *Brassica juncea* plants alleviates abiotic stress: physiological and chlorophyll a fluorescence measurements. Biochem Biophy Acta 1797:1428–1438.

Youssef NB, Zarrouk M, Daoud D, Lemal F, Ouariti O, Ghorbal MH, Cherif A (1998) Membrane lipid changes in *Brassica napus* induced by $CdCl_2$. In: Sanchez J, Cerda-Olmedo E, Martinez-Force E (Eds). Advan Plant Lipid Res, pp 534–537.

Zhao C, Qiao M, Yu Y, Xia G, Xiang F (2010) The effect of the heterologous expression of *Phragmites australis* γ-glutamylcysteine synthetase on the Cd^{2+} accumulation of *Agrostis palustris*. Plant Cell Environ 33:877–887.

Zhang J, He Z, Tian H, Zhu G, Peng X (2007) Identification of aluminium-responsive genes in rice cultivars with different Al sensitivities. J Exp Bot 58:2269–2278.

Zhang J, Kirkham MB (1996) Enzymatic responses of the ascorbate-glutathione cycle to drought in sorghum and sunflower plants. Plant Sci 113:139–147.

Zhang J, Tian Shengke, Lu Lingli, Shohag MJI, Liao H, Yang X (2011) Lead tolerance and cellular distribution in *Elsholtzia splendens* using synchrotron radiation micro-X-ray fluorescence. J Hazard Mater 197:264–271.

Zhao FJ, Ago Y, Mitani N, Li RY, Su YH, Yamaji N et al. (2010) The role of the rice aquaporin *Lsi1* in arsenite efflux from roots. New Phytol 186:392–399.

Zhen WB, Ma QH (2009) Proline metabolism in response to salt stress in common reed (*Phragmites australis* (Cav.) Trin. ex Steud). Bot Mar 52:307–315.

Zheng L, Peer T, Seybold V, Lütz-Meindl U (2012) Pb-induced ultrastructural alterations and subcellular localization of Pb in two species of *Lespedeza* by TEM-coupled electron energy loss spectroscopy. Environ Exp Bot 77:196– 206.

Annexure:
List of publications, conferences abstract and reprints

List of publications

1. **Kumar Abhay,** Prasad MNV, Achary V.MM, Panda BB **(2012)** Elucidation of lead-induced oxidative stress in *Talinum triangulare* roots by analysis of antioxidant responses and DNA damage at cellular level. **Environmental Science and Pollution Research**. DOI:10.1007/s11356-012-1354-6.

2. Sytar O, **Kumar Abhay**, Latowski D, Kuczynska P, Strzałka K, Prasad MNV **(2012)** Heavy metals induced oxidative damage, defence reactions and detoxification mechanisms in plants. **Acta Physiologiae Plantarum**. DOI: 10.1007/s11738-012-1169-6**.**

3. Sytar O, Cai Z, Brestic M, **Kumar Abhay**, Prasad MNV, Taran N, Iryna S **(2012)** Foliar applied nickel on buckwheat (*Fagopyrum esculentum)* induced phenolic compounds as potential antioxidants. **Clean- Soil, Air, Water**. DOI: 10.1002/clen.201200512.

4. **Kumar Abhay**, Prasad MNV, Sytar O **(2012)** Lead toxicity, defense strategies and associated indicative biomarkers in *Talinum triangulare* grown hydroponically. **Chemosphere** 89:1056−1065.

5. **Kumar Abhay**, Prasad MNV **(2010)** Propagation of *Talinum cuneifolium* L. (Portulacaceae), an Ornamental Plant and Leafy Vegetable, by Stem Cuttings. **Floriculture and Ornamental Biotechnology** 4(SI 1):68−71.

Abstract published in seminar/conference/symposium

1. M.N.V. Prasad and **Abhay Kumar (2011)**. Heavy metal stress alleviation and adaptation mechanisms in plants- an ecophysiological perspective. In: International Conference on Plant Science in Post Genomic era. 17–19 February, 2011, Sambalpur, India, pp 44. (**Poster presented**)

2. **Abhay Kumar** and M.N.V. Prasad **(2011)**. *Talinum cuneifolium* (Ceylon spinach, Portulacaceae), an ideal plant for lead toxicity bioassays. 11th International conference on the Biogeochemistry of Trace Elements (ICOBTE-2011). 3-7 July-2011. Florence, Italy, pp S7–17. (**Poster presented**)

3. **Abhay Kumar** and M.N.V. Prasad **(2011)**. Lead toxicity and tolerance biomarkers in *Talinum cuneifolium* (Ceylon spinach, Portulacaceae). International Symposium on Environmental Risk Assessment. 17–19 October- 2011, Bharathiar University, Coimbatore, India, pp 99.

4. **Abhay Kumar** and M.N.V. Prasad **(2011)**. Indices of oxidative stress in lead (Pb) exposed *Talinum cuneifolium* (Ceylon spinach, Portulacaceae) - Relevance to phytoremediation. Acta Biochimica Polonica- IV Eurobiotech. 12–15 October, 2011. Krakow, Poland, P15.16, pp 104.

Elucidation of lead-induced oxidative stress in Talinum triangulare *roots by analysis of antioxidant responses and DNA damage at cellular level*

Abhay Kumar, M. N. V. Prasad, V. Mohan Murali Achary & Brahma B. Panda

Environmental Science and Pollution Research

ISSN 0944-1344

Environ Sci Pollut Res
DOI 10.1007/s11356-012-1354-6

Springer

Environ Sci Pollut Res
DOI 10.1007/s11356-012-1354-6

RESEARCH ARTICLE

Elucidation of lead-induced oxidative stress in *Talinum triangulare* roots by analysis of antioxidant responses and DNA damage at cellular level

Abhay Kumar · M. N. V. Prasad · V. Mohan Murali Achary · Brahma B. Panda

Received: 6 August 2012 / Accepted: 21 November 2012

Abstract Hydroponic experiments were performed with *Talinum triangulare* (Jacq.) Willd. focusing the root cellular biochemistry with special emphasis on DNA damage, structural, and elemental analyses in $Pb(NO_3)_2$ exposed with 0, 0.25, 0.5, 0.75, 1.0, and 1.25 mM for 7 days. Lead (Pb) increased reactive oxygen species production, lipid peroxidation, protein oxidation, cell death, and DNA damage and decreased the protein content in a dose-dependent manner. Likewise, a dose-dependent induction of antioxidative enzymes superoxide dismutase and catalase by Pb was evident. Ascorbate peroxidase on the other hand responded biphasically to Pb treatments by showing induction at low (0.25 and 0.50) and repression at high (0.75–1.25 mM) concentrations. The estimation of proline content also indicated a similar biphasic trend. Scanning electron microscope and energy-dispersive X-ray spectroscopy analysis showed that 1.25 mM Pb treatment resulted in ultrastructural modifications in roots and stem tissue that was marked by the change in the elemental profile. The findings pointed to the role of oxidative stress in the underlying Pb phytotoxicity and genotoxicity in *T. triangulare.*

Keywords Antioxidant response · Ceylon spinach · Comet assay · Pb stress · Plant bioassay · Tissue ultrastructure

Responsible editor: Elena Maestri

A. Kumar · M. N. V. Prasad (✉)
Department of Plant Sciences, University of Hyderabad, Hyderabad 500046, India
e-mail: prasad_mnv@yahoo.com

V. Mohan Murali Achary · B. B. Panda
Molecular Biology and Genomics Laboratory, Department of Botany, Berhampur University, Berhampur 760007, India

Introduction

Plants and microbes play important roles in detoxifying and stabilizing hazardous substances in the environment through the process of remediation (Kumar et al. 2012; Rajkumar et al. 2012). Lead (Pb) ranks second among the hazardous metals known to be toxic to human and non-human biota. Lead is a traditional metal with contemporary applications, which is responsible for increased Pb production and consumption worldwide. Lead is released into the environment from both natural and anthropogenic sources. Some of the sources of Pb pollution to the environment are from mining and smelting of Pb ores, automobile exhaust, sewage sludge, paints, batteries, armory, microelectronics, burning of fossils fuel in thermal and glass manufacturing plants, etc. (Anonymous 2007, 2011; Sengar et al. 2008; Shahid et al. 2012; Huang et al. 2012). Lead is also associated with insecticides, rubber, plastics, safety matches, food, alcoholic beverages, plasters, and medicines (Anonymous 2007). Lead is extremely persistent in the soil, air, water, and foodstuffs with no biological significance and has been a global concern (Anonymous 2007, 2011).

Lead can easily be absorbed, transformed, and accumulated in plants tissues where root is the primary site of accumulation (Kumar et al. 2012). Being a non-redox active metal, Pb can replace essential metals at enzyme active site causing cellular redox imbalance. In plants, excess Pb causes molecular damage either directly or indirectly through the formation of reactive oxygen species (ROS) such as hydrogen peroxide (H_2O_2) and superoxide radicals ($O^{\cdot}{}_2^-$) (Sharma and Dubey 2005; Reddy et al. 2005; Sengar et al. 2008; Singh et al. 2011; Pourraut et al. 2011; Kaur et al. 2012). The ROS attack of polyunsaturated fatty acid of membrane lipids causes lipid peroxidation, oxidative stress, and DNA damage and alter biochemical and molecular activities of cells (Sharma and Dubey 2005; Pourraut et al.

Published online: 21 December 2012

2011; Maldonado-Magaña et al. 2011; Kaur et al. 2012; Hu et al. 2012). Studies have shown that Pb phytotoxicity is mediated through oxidative stress (Hu et al. 2007; Gupta et al. 2009; Malecka et al. 2009; Lamhamdi et al. 2011). The relationship between Pb toxicity and genotoxicity has, however, not been established unequivocally (Shahid et al. 2011).

Plants counter free radicals overproduction by activating antioxidant defense system consisting of superoxide dismutase (SOD), catalase (CAT), peroxidases, together with other scavenging enzymes and low molecular weight antioxidants, such as glutathione, ascorbate, tocopherol, and proline (Sengar et al. 2008; Malecka et al. 2009; Kaur et al. 2012). Lead uptake, bioaccumulation, toxicity, and tolerance have been investigated in a number of terrestrial plants such as *Macrotyloma uniflorum* and *Cicer arietinum* (Reddy et al. 2005), *Brassica campestris* (Singh et al. 2011), *Triticum aestivum* (Lamhamdi et al. 2011; Kaur et al. 2012), *Potamogeton crispus* (Hu et al. 2007), *Zea mays* (Gupta et al. 2009), *Pisum sativum* (Malecka et al. 2009), and *Oryza sativa* (Li et al. 2012).

Talinum triangulare (Jacq.) Willd. (Ceylon spinach, Talinaceae) is a nutritious leafy vegetable plant. *Talinum* species are an important source of flavonoids, mineral constituents, and proteins in diet in Nigeria, America, India, and other parts of the world (Andarwulan et al. 2010). Moreover, the plant is known for its ornamental as well as antioxidative and medicinal values (Uwah et al. 2009; Kumar and Prasad 2010; Panyaphu et al. 2011). It can be easily propagated through stem cuttings that produce adventitious roots extensively in hydroponic medium (Kumar and Prasad 2010). Previous studies have reported that *T. triangulare* accumulate heavy metals (HMs) from contaminated media (Rajkumar et al. 2009; Kumar et al. 2012). Our earlier study investigated in leaf of *T. triangulare* has demonstrated that Pb induced oxidative stress that was marked by increase in ROS, malondialdehyde (MDA), carotenoid, anthocyanin, α-tocopherol, glutathione contents, and cell death and decrease in water potential, photosynthetic pigments, and nutrient elements (Kumar et al. 2012). The aims of the present study were (1) to investigate early symptoms of the Pb toxicity and relationship between Pb tolerance and antioxidant metabolism in roots in hydroponic condition and (2) to examine the Pb-induced DNA damage and changes in structural integrity and nutrient contents in *T. triangulare*.

Materials and methods

Plant description and treatment in hydroponic experiment

T. triangulare (Jacq.) Willd. used in the current experiments were collected from field gene bank maintained at the University of Hyderabad, India. *T. triangulare* was propagated through stem cuttings (5.0–7.0 mm diameter and 16–20 cm height) in conical flask containing 100 mL of modified Hoagland's nutrient media in plant growth chamber at 16/8 h (day/night) at 28±2 °C, which gives extensive adventitious roots, leaves, and vegetative propagules in about 3 weeks (Hoagland and Arnon 1950; Kumar and Prasad 2010). The nutrient media was replaced every 3–4 days. After 3 weeks of acclimatization, uniform stem cuttings with adventitious roots and leaves were selected and treated with $Pb(NO_3)_2$ at different Pb concentrations of 0 (control), 0.25, 0.5, 0.75, 1.0, and 1.25 mM for 7 days under the above conditions. Roots excised after 7 days of treatment were processed for analysis of various endpoints described as follows.

Estimation and visualization of H_2O_2 in root tissue

Fresh roots (0.5 g) were homogenized in ice bath with 5 mL of 0.1 % (*w*/*v*) trichloroacetic acid (TCA). The homogenate was centrifuged at 12,000×*g* for 15 min at 4 °C, and 0.5 mL of the supernatant was added to 0.5 mL of 10 mM potassium phosphate buffer (pH7.0) and 1 mL of 1 M potassium iodide. H_2O_2 concentration was estimated at 390 nm based on the absorbance of a standard curve and was expressed as nanomoles per gram FW Velikova et al. (2000).

In situ H_2O_2 visualization in control and Pb-treated roots was determined by 5 μM 2′,7′-dichlorodihydrofluorescein diacetate (H_2DCFDA) dye with using confocal microscope (Leica TCS SP2 AOBS Microscope, Germany) at 480 nm excitation and 520 nm emission wavelengths.

Estimation of cell death

Fresh roots (0.1 g) were stained with 0.25 % (*w*/*v*) aqueous solution of Evans blue for 15 min. After washing with Milli-Q water for 30 min, roots were excised and soaked with 3 mL of *N*,*N*-dimethylformamide for 1 h at room temperature. The absorbance of released Evans blue was measured at 600 nm (Baker and Mock 1994).

Estimation of lipid peroxidation

Lipid peroxidation in roots was determined as a function of malondialdehyde (MDA) content following the method of Heath and Packer (1968) with slight modifications. Roots (0.2 g) were homogenized in 3 mL 0.1 M Tris [tris (hydroxymethyl) amino methane] buffer containing 0.3 M sodium chloride and centrifuged at 10,000×*g* for 10 min. The supernatant (2 mL) was added to the reaction mixture containing 2 mL of 20 % TCA and 0.5 % 2-thiobarbituric acid (TBA) and was heated at 95 °C for 30 min. The product was further centrifuged at 10,000×*g* for 5 min, and the absorbance of the supernatant was measured at 532 nm.

The concentration of MDA was calculated using an extinction coefficient (ε=155 $mM^{-1}cm^{-1}$) and expressed in nanomoles per gram FW.

Estimation of lipoxygenase activity (LOX, E.C. 1.13.11.12)

Fresh root (0.5 g) was homogenized in 50 mM sodium phosphate buffer (pH7.0), 1 mM EDTA, 0.1 mM phenylmethanesulfonyl fluoride (PMSF), 2 % (*w*/*v*) polyvinylpolypyrrolidone (PVPP), 1 % (*v*/*v*) glycerol, and 0.1 % (*v*/*v*) Tween-20. The homogenate was centrifuged at 12,000×*g* for 20 min. The reaction was initiated by addition of 1 mM linoleic acid in 0.1 M sodium acetate buffer (pH5.6) to the supernatant. The increase in the activity of LOX was measured at 234 nm (ε=25 $mM^{-1}cm^{-1}$). One unit of activity was defined as the amount of enzyme catalyzing the synthesis of 1 μmol of hydroperoxide (HPOD) per minute (Ederli et al. 1997).

Estimation of antioxidative enzymes activities

Plant roots samples (1 g) were homogenized in 50 mM sodium phosphate buffer (pH7.8) for SOD enzyme, and (pH7.0) for CAT and ascorbate peroxidase (APX) enzymes activities, respectively, containing 2 % PVPP. Homogenates were centrifuged at 13,000×*g* for 20 min at 4 °C. For APX assay, additional 2 mM ascorbate was used in the homogenizing solution. The protein content in the supernatant was determined according to the method of Lowry et al. (1951) using a bovine serum albumin as a standard.

Superoxide dismutase (SOD, E.C. 1.15.1.1) activity was determined according to the method of Beauchamp and Fridovich (1971). Samples containing 50 μg of protein were mixed with 50 mM sodium phosphate buffer (pH7.8), 13 mM methionine, 75 μM nitroblue tetrazolium (NBT), 0.1 mM ethylenediaminetetraacetic acid (EDTA), and 2 μM of riboflavin (added at last). After mixing, samples were illuminated for 15 min using comptalux bulbs (40 W). The reaction mixture containing sample protein were kept in dark and served as blank, while the reaction mixture without sample protein that were kept under light served as positive control. The absorbance was taken at 560 nm. One unit of SOD activity is the amount of protein required to inhibit 50 % initial reduction of NBT under light.

Catalase (CAT, E.C. 1.11.1.6) activity was measured of consumption of H_2O_2 (ε=39.4 $mM^{-1}cm^{-1}$) according to the method of Aebi (1984). The reaction mixture contained 50 mM sodium phosphate buffer pH7.0, 10 mM H_2O_2, and 100 μg of protein in a final volume of 3 mL. The activity was determined by the oxidation of H_2O_2 at 240 nm.

Ascorbate peroxidase (APX, E.C. 1.11.1.11) was assayed by the method of Nakano and Asada (1981). The reaction mixture contained 50 mM sodium phosphate buffer (pH 7.0), 0.2 mM EDTA, 0.5 mM ascorbic acid, 250 mM H_2O_2, and 50 μg of protein. The activity was recorded as decrease in the absorbance at 290 nm, and the amount of ascorbate oxidized was calculated using ε=2.8 $mM^{-1}cm^{-1}$.

Estimation of protein oxidation

Equal amount of proteins were precipitated with equal volume of 20 % TCA. The tubes were centrifuged at 12,000×*g* for 10 min, and the pellet obtained was allowed to react with 500 μL of 10 mM 2,4-dinitrophenylhydrazine (DNPH) in 2 M HCl and incubated at room temperature for 1 h with regular vortexing. The samples were again precipitated with 500 μL of 20 % TCA, centrifuged at 12,000×*g* for 5 min. The resultant pellet was washed with ethanol:ethyl acetate (1:1). The precipitated protein was redissolved in 0.6 mL of 6 M guanidine-HCl. The optically clear solutions were obtained after two to three times repeated centrifugation at 6,000×*g* at 4 °C. Carbonyl concentration was calculated from the difference in absorbance recorded at 380 nm against a blank treated with 2 M HCl instead of DNPH (ε=22,000 $M^{-1}cm^{-1}$) and expressed in nanomoles of DNPH incorporated per milligram protein (Reznick and Packer 1994).

Estimation of proline content

Plant root (0.5 g) was homogenized in 5 mL of 3 % aqueous sulfosalicylic acid and the homogenate filtered through Whatman #2 filter paper. One milliliter of filtrate was reacted with 1 mL of freshly prepared acid ninhydrin reagent (0.625 g ninhydrin in 15 mL glacial acetic acid and 10 mL of 6 M phosphoric acid) and 1 mL glacial acetic acid. Reaction mixture was heated at 100 °C for 1 h and then kept in an ice bath to stop the reaction. The developed color was extracted with addition of 2 mL of toluene, and the toluene-chromophore absorbance was measured at 520 nm using toluene as a blank. Proline content was determined by using a standard curve (Bates et al. 1973).

Estimation of DNA damage by alkaline comet assay

For alkaline comet assay (Patnaik et al. 2011), rooted stem cuttings were taken out from treatment solutions and thoroughly washed with distilled water. Roots excised were placed in a 60-mm Petri dish and placed on ice. With the help of new razor blades, the roots were sliced in the medium containing 100 to 200 μL of chilled 0.4 M Tris-HCl buffer pH7.4, and the nuclei were collected into a microcentrifuge tube with the same buffer and kept at 4 °C. Before proceeding to the next step, nuclear suspension in 0.75 % low melting point agarose (LMP type VII, Sigma-Aldrich, USA) was prepared by mixing the above collected nuclei with equal volume (1:1) of 1.5 % LMP dissolved in

Tris-HCl buffer at 37 °C. Clean grease-free microscope slides pre-coated with 50 μL of 1 % normal melting point agarose (NMP type, I Sigma-Aldrich, USA) dissolved in distilled water were kept dry overnight at room temperature and labeled. Onto the above slides, 80 μL of the aforesaid nuclear suspension was layered at 37 °C with the aid of a cover slip (20×40 mm). After gelling of the agarose layer, the slides were kept over a chilled metal plate for 5 min; the cover slip from the top of the agarose layer containing the nuclei was gently removed. A second layer of 80 μL 75 % LMP agarose was spread over the nuclear layer, which was allowed to gel once again for 5 min. After removing of the cover slips, the slides with agarose-embedded nuclei were placed in a horizontal electrophoresis tank containing alkaline buffer (300 mM NaOH and 1 mM EDTA, ≥pH13) for 10 min that facilitated nuclear DNA unwinding, followed by electrophoresis at 0.75 Vcm^{-1} and 300 mA for 15 min in the same alkaline buffer at 4 °C. Slides were then washed in distilled water and neutralized with 0.4 M Tris buffer (pH7.4). After a 5-min wash in distilled water, nuclei were stained by spreading 200 μL ethidium bromide solution (2 μgmL^{-1}) over the gel on the slide. Analysis of comets was carried out employing an Olympus BX51 microscope with a fluorescence attachment (using the excitation filter 515–560 nm and barrier filter 590 nm) equipped with a Cohu camera and Kinetic Komet™ Imaging Software 5.5 (Andor™ Technology, www.andor.com). Two slides were prepared for each treatment. At least 50 comets were scored from each slide. The comet images were visualized and captured at ×100 magnification. Out of a number of parameters available in the software, comets were analyzed on the basis of the Olive tail moment (OTM)=Tail DNA%×Tail moment length (the distance between the intensity centroids of the head and the tail along the *x*-axis of the comet). This parameter allows us to detect variations in DNA distribution within the tail. Therefore, OTM is considered as an absolute parameter with a measurement unit of micrometer (Kumaravel et al. 2009). The entire process of comet assay was carried out in dim or yellow light.

Structural and elemental analysis

Structural analyses were done by environmental scanning electron microscope (ESEM, Philips XL-30) for root (tip) and stem transverse section (TS) of *T. triangulare* treated with 0, 0.25, and 1.25 mM Pb concentration. Elemental/chemical analyses were done with energy-dispersive X-ray spectroscopy (EDS, Oxford instruments) coupled with field emission scanning electron microscope (FESEM). Samples for ESEM and FESEM/EDS were prepared by primary fixation using 3 % glutaraldehyde in 0.05 M phosphate buffer for 90 min followed by secondary fixation in 2 % osmium tetroxide in 0.01 M sodium cacodylate buffer for 30 min followed by dehydration with a graded ethanol series, mounted on aluminum stubs, and coated with gold-palladium. The EDS analysis was carried out at an operating voltage of 20 kV and working distance of 8.5 mm. With the help of the INCA software, X-ray emission-based spectral peaks were analyzed. Electron-induced X-rays were detected by Si drift detector (Oxford Instruments) by measuring typical spectrum (contains characteristic peaks) intensities. A typical spectrum contains characteristic peaks for present elements, which are superimposed on a slowly varying background. This background contribution is carefully subtracted from the spectrum. Once these intensities have been determined, a comparison is then made with standards of known composition with the INCA software applications, which uses filtered least squares (FLS) technique for this filtering and fitting. The energy resolution of EDS detector is 70 to 130 eV (depending on the elements), which imposes a limit on the separation of peaks. When peaks overlap, it is still possible to interact individual peak area provided that the corresponding peak shapes are accurately known. The differences in analyzed elements energies are more than 130 eV. Thus, there were no overlapping of the peaks, and the elements were easily detected by the EDS.

Statistical analysis

All the experiments were in triplicate. The mean values± standard errors (SE) are reported in the figures. The statistical analysis was carried out by analysis of variance and Duncan's multiple range test using SIGMASTAT statistical software (version 11.0) that accounted statistical differences at $p \leq 0.05$ between each treatment, marked by different letters (Gomez and Gomez 1984).

Results

H_2O_2 estimation and visualization

Spectrophotometric estimation, together with histochemical visualization of H_2O_2 in the root tissue, clearly indicated that Pb significantly induces a dose-dependent H_2O_2 production (Fig. 1). Confocal results revealed that maximum fluorescence was observed at 1.25 mM Pb-treated root, which directly signify the maximum H_2O_2 production at this treatment, while no difference in autofluorescence was observed between control and 0.25 mM Pb-treated roots, which is corroborated with the H_2O_2 result observed spectrophotometrically. However, the significant ($p \leq 0.05$) increase in H_2O_2 production was reported at 0.5–1.25 mM Pb.

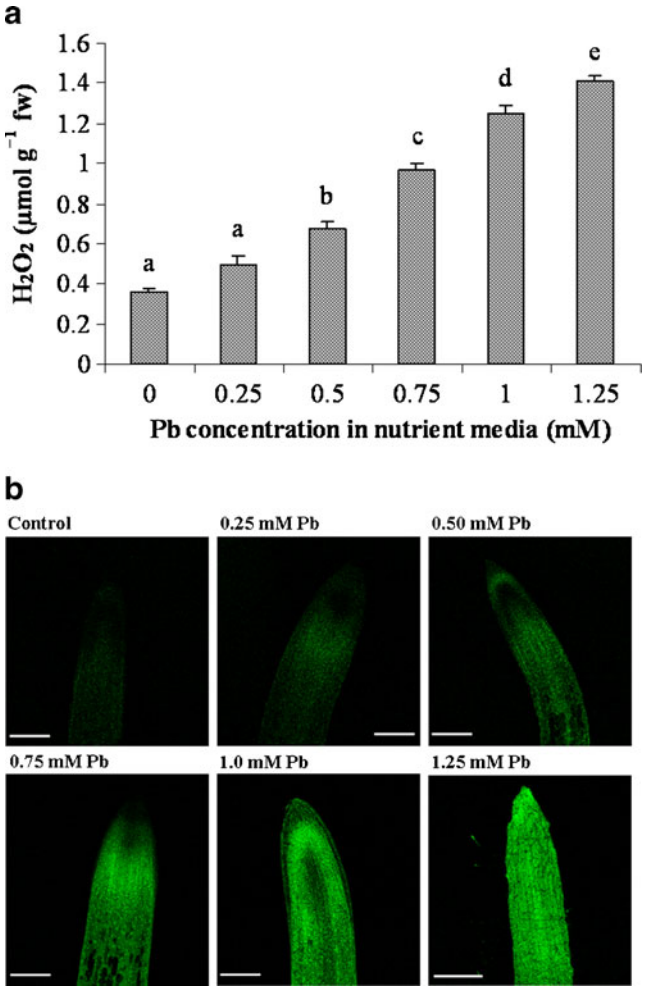

Fig. 1 H_2O_2 production in *Talinum triangulare* roots after 7 days of Pb treatment (**a**). The values represent mean±SE (n=3). *Different letters* indicate significant difference ($p \leq 0.05$) between each other. **b** Fluorescence micrograph of histochemical visualization of ROS (H_2O_2) in root tip of Pb-treated plant (*bar*=300 μm)

Lead-induced cell death, lipid peroxidation, LOX activity, and decrease protein turnover

Lead-induced oxidative damage in *T. triangulare* roots tissue was measured by Evans blue staining method (Fig. 2a) that showed a positive linear correlation (R^2=0.831) with dose-dependent H_2O_2 generation. Evans blue uptake by the root tissue was significantly ($p \leq 0.05$) increased by 125 % and 205 % at 1.0 and 1.25 mM Pb treatment, and no significant difference between treatments was observed below 0.75 mM Pb.

Lipid peroxidation in Pb-treated *T. triangulare* roots was measured by the estimation of MDA contents, a degradation product of membrane unsaturated fatty acid that reflected the extent of cell membrane damage in response to ROS. The increase in MDA contents presented a positive correlation (R^2=0.986; Fig. 2b), with the increasing Pb concentration in the treatment solutions. Lead induces significant ($p \leq 0.05$) lipid peroxidation at concentrations of 1.0 and 1.25 mM that accounted for 150.3 % and 180.3 % increases as compared to control, respectively. Lead enhanced the LOX enzyme activity in a concentration-dependent fashion (Fig. 2c). However, similar to MDA, the increase was significant ($p \leq 0.05$) at 0.75–1.25 mM. The increased LOX activities ranged between 9.5 % and 43.6 % in response to Pb treatment (0.25 to 1.25 mM), with respect to control. Experimental finding with the total protein content estimated at a range of concentrations of Pb in root tissue of *T. triangulare* indicated a concentration-dependent (R^2=0.89; Fig. 2d) decrease in the protein content. The decrease of the protein content was significant ($p \leq 0.05$) at 0.5 mM onwards.

Lead-induced changes in antioxidant enzymes activities

A linear increase in SOD activity was observed with increasing concentration of Pb treatment (R^2=0.983; Fig. 3a). However, the SOD activity remained unchanged up to 0.50 mM of Pb treatment. The highest SOD activities were observed at 0.75 (67.5 %), 1.0 (89.4 %), and 1.25 (105.3 %), which were significantly ($p \leq 0.05$) in comparison to control, respectively.

Similar to SOD, CAT activity presented a dose-dependent response in Pb-treated roots (Fig. 3b). The CAT activity in roots increased significantly at 0.25–1.25 mM of Pb compared to control. The highest CAT activity was observed at 1.0 mM of Pb, which increased 137.5 % in comparison to control. CAT activity was found to slightly decrease at 1.25 mM of Pb (127.3 %) in comparison to 1.0 mM of Pb.

Our results showed that 0.25 and 0.50 mM Pb slightly enhanced APX activity in comparison to control, which declined at further Pb concentrations in comparison to control (Fig. 3c). APX activity significantly ($p \leq 0.05$) decreased at only 1.0 and 1.25 mM of Pb in respect to control, respectively. The maximum increase and decrease in APX activities were observed at 0.50 mM (34 %) and at 1.25 mM (55.8 %), respectively.

Lead-induced protein oxidation and accumulation of proline

Protein oxidation is a measure of Pb-induced production of carbonyl contents. The accumulation of carbonyl contents was observed in Pb-treated roots (R^2=0.938; Fig. 4a). In comparison to control, the amount of carbonyls significantly increased ($p \leq 0.05$) to approximately 36 %, 38 %, and 42 % at 0.75, 1.0, and 1.25 mM Pb, respectively. Pb-induced protein oxidation showed a positive linear correlation (R^2= 0.960) with H_2O_2 contents.

Our experimental results showed that the free proline content was increased at 0.25–0.75 mM Pb, but decreased at 1.0–1.25 mM Pb when compared to control root, respectively (Fig. 4b). A moderate increase in free proline level

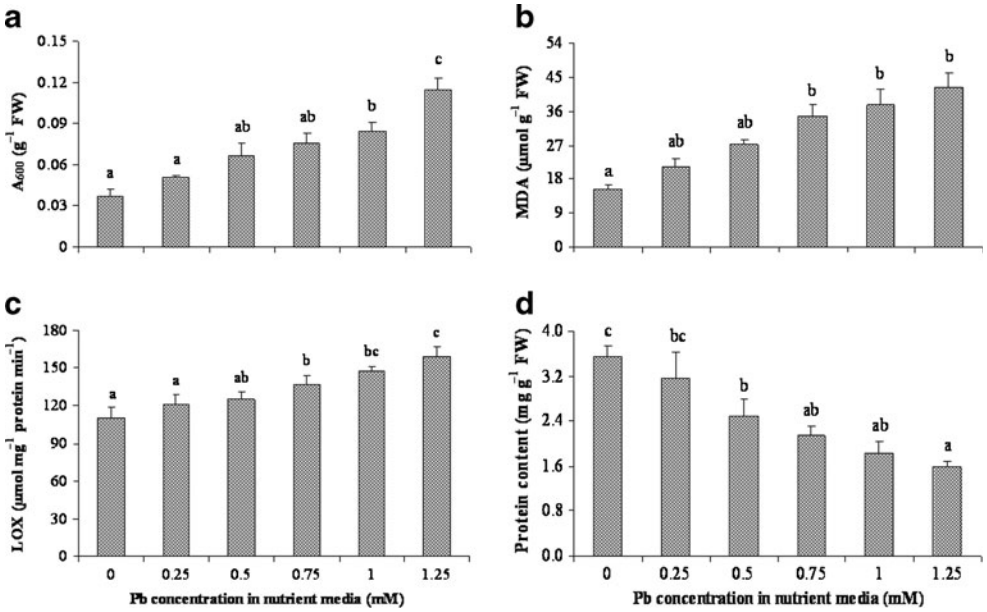

Fig. 2 Cell death measurements by Evans blue uptake (**a**), MDA contents (**b**), LOX activity (**c**), and total protein content (**d**) in *Talinum triangulare* roots after 7 days of Pb treatment. The values represent mean±SE (n=3). *Different letters* indicate significant difference ($p \leq 0.05$) between each other

was observed in the roots subjected to 0.25–0.75 mM of Pb over control root. The accumulation of proline increased as the stress prolonged and attained significant ($p \leq 0.05$) maximal levels at 0.25 mM of Pb (49.5 %) after 7 days experiment. There was a marginal decrease in the accumulated proline up to 0.75 mM of Pb treatment. However, the decrease in proline was as much as 39.2 %, even on continuing the treatment 1.25 mM of Pb.

Lead-induced DNA damage

Evidences from the OTM values (Fig. 5) comet assay revealed that the Pb at concentrations in the range 0.5–

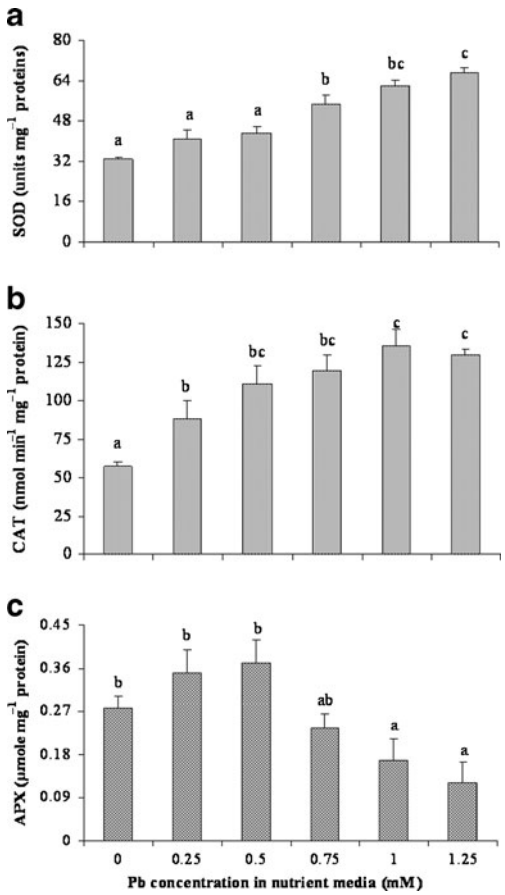

Fig. 3 Concentration-dependent responses in antioxidative enzymes SOD (**a**), CAT (**b**), and APX (**c**) activities in roots of *Talinum triangulare* after 7 days of Pb treatment. The values represent mean±SE (n=3). *Different letters* indicate significant difference ($p \leq 0.05$) between each other

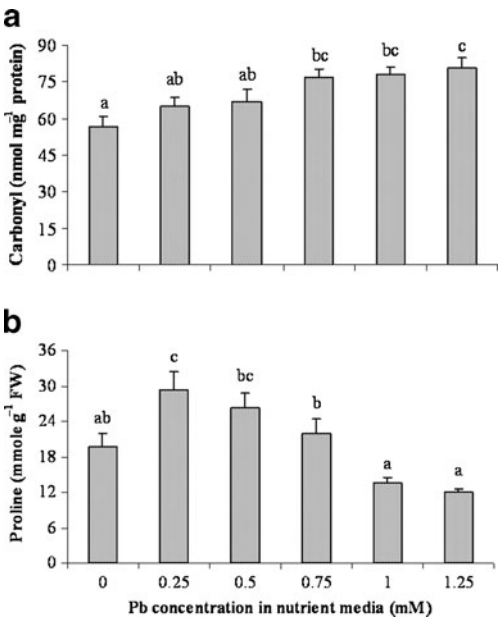

Fig. 4 Carbonyl content (**a**), protein oxidation, and accumulation of free proline (**b**) in root of *Talinum triangulare* after 7 days of Pb treatment. The values represent mean±SE (n=3). *Different letters* indicate significant difference ($p \leq 0.05$) between each other

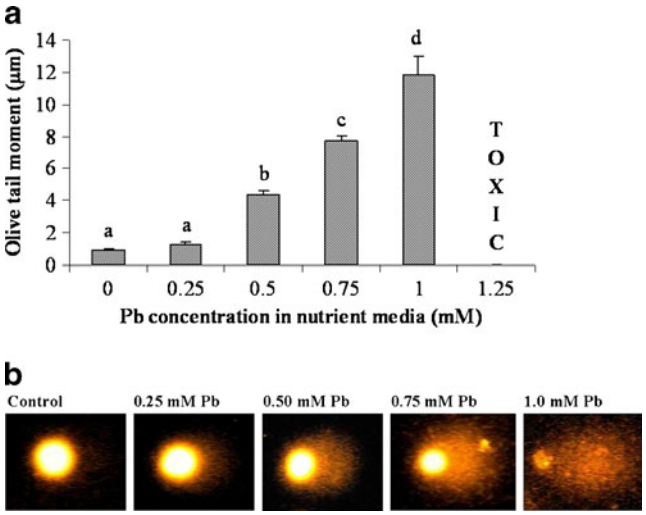

Fig. 5 Pb-induced DNA damage evaluated by comet assay on the basis of OTM. **a** Dose-dependent induction of DNA damage in root of *Talinum triangulare* after 7 days of Pb treatment. The values represent mean±SE (n=3). *Different letters* indicate significant difference ($p \leq 0.05$) between each other. **b** Comets in root cells of *T. triangulare* representing Pb-induced DNA damage

1.0 mM significantly ($p \leq 0.05$) induced DNA damage compared to the control in roots cells of *T. triangulare*. In our experimental conditions, Pb treatments at 0.25 mM induced very slight DNA damage, which was not significantly different from control. Pb treatment of 1.25 mM was observed as toxic and caused nuclear necrosis, and thus it was not possible to analyze the comet images at this concentration. After 7 days, DNA damage was significantly enhanced ($p \leq 0.05$) at doses of 0.50, 0.75, and 1.0 mM Pb treatment in comparison to control, respectively.

Lead-induced structural modification and elemental analysis

The scanning electron microscope (SEM) analysis revealed that 0.25 and 1.25 mM of Pb treatment altered the root anatomical surfaces (Fig. 6a–c), vascular tissues, and internal structure of the stem (Fig. 6d–f). SEM images of roots showed that Pb toxicity is able to rupture the root integrity, pore formation on surface, and modification of root tip. However, at 1.25 mM Pb, roots surface were highly porous in nature, and the pore size was larger in size than 0.25 mM Pb-treated root. SEM micrograph of stem showed that Pb caused disruption of vascular bundles especially xylem vessels, which reduces nutrient and water transport to the aerial part of the plant.

Results of EDS showed the atomic percentage and chemical characteristics of tissue. Microanalysis of root elements was performed at the root tip of the 0, 0.25, and 1.25 mM Pb-treated plant samples. X-ray microanalysis revealed the presence of Pb spectral peak in both Pb-treated roots (Fig. 6g–i), which support the presence of Pb in the sample. Semi-quantitative estimation of other elements such as oxygen (O), potassium (K), sodium (Na), calcium (Ca), magnesium (Mg), chlorine (Cl), silicon (Si), sulfur (S), and copper (Cu) was detected in control root tissues. (Table 1). Qualitative percentage composition analysis showed that only high spectral peak for O, K, and Pb were observed in 0.25 and 1.25 mM Pb-treated root in comparison to control root, respectively. Other elements were detected less or below detectable level in Pb-treated roots than in control root.

Discussion

In the present study, extracellular H_2O_2 production increased after 7 days of Pb treatment with respect to control. With confocal laser scanning microscope images, we could visualize that Pb significantly increased the H_2O_2 production in treated roots in comparison to control root. The dose-dependent increase in histochemically visualized cellular H_2O_2 generation was in good agreement with extracellular H_2O_2 generation in root tissue of *T. triangulare*. Our result is in good accordance with previous studies reporting higher H_2O_2 generation in *Wolffia arrhiza* (Piotrowska et al. 2009), *P. sativum* (Malecka et al. 2009), *T. aestivum* (Kaur et al. 2012), *O. sativa* (Li et al. 2012), and *Sedum alfredii* (Huang et al. 2012) upon Pb exposure. It has been reported that the disturbance in electron transport chain in the membrane is the major cause for ROS generation (Sharma and Dubey 2005; Pourraut et al. 2011). From our study, we can suggest that in vivo H_2O_2 analyses through histochemical visualization under Pb treatment was sensitive, fast, and reliable. Heavy metal stress in plant causes oxidative damage to membrane lipid and proteins through generation of ROS (Pena et al. 2008; Aravind et al. 2009; Huang et al. 2012). ROS play an important role as signal transduction that regulates plant defense responses to HMs stress (Aravind and Prasad 2003).

Earlier, we have reported that Pb taken up by *T. triangulare* is mostly accumulated in root, less in shoot, and least in leaf (below detection limit) (Kumar et al. 2012). The present results indicated that Pb accumulation leads to cell death in root tissue evaluated by Evans blue staining, a measure of disintegration of membrane integrity (Baker and Mock 1994). The measure of cell death showed a significant correlation with lipid peroxidation (R^2=0.855), LOX activity (R^2=0.874), as well as with H_2O_2 (R^2=0.831) generation in the root tissue of *T. triangulare* following exposure with Pb in the present study. Lipid peroxidation has been considered as the marker of oxidative stress. Pb-induced lipid peroxidation has been reported in a number of plants: *P. crispus* (Hu et al. 2007), *W. arrhiza* (Piotrowska et al. 2009), *Acacia farnesiana* (Maldonado-Magaña et al. 2011), *T.*

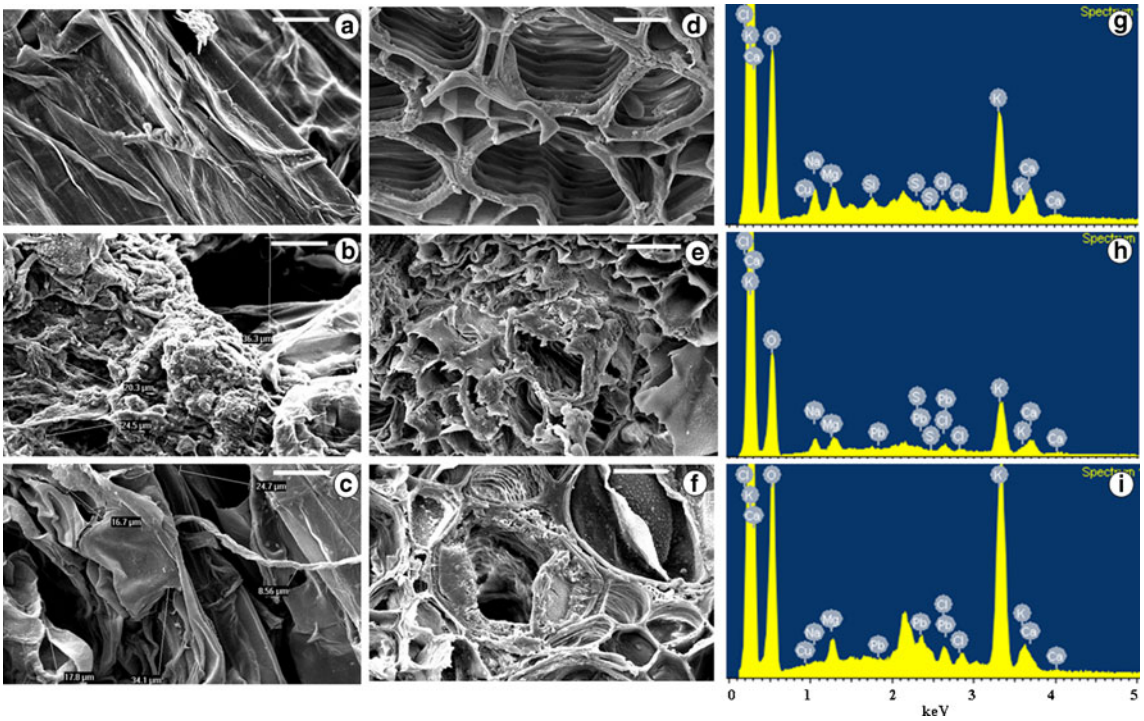

Fig. 6 Scanning electron micrographs showing the root surface of control (**a**), 0.25 mM Pb (**b**), and 1.25 mM Pb (**c**) and transverse sections of stem: control (**d**), 0.25 mM Pb (**e**), and 1.25 mM Pb-treated (**f**) plants for 7 days. Electron micrographs are at ×1,000 magnification, and *bar* represents 20 μm. **e**, **f** Damage of vascular bundle and clotted depositions along the cell walls of vascular bundles. EDS micrograph showed elemental atomic percentage in root of control (**g**), 0.25 mM Pb (**h**), and 1.25 mM Pb (**i**)

aestivum (Lamhamdi et al. 2011), *Salsola passerina*, *Chenopodium album* (Hu et al. 2012), and *S. alfredii* (Huang et al. 2012). Membrane lipid peroxidation is a very sensitive reaction caused by HMs stress and is initiated by ROS and/or by the enzyme LOX, which is the key enzyme that produces hydroperoxide and oxy-free radicals by catalyzing the peroxidation of unsaturated fatty acids of biomembranes (Aravind et al. 2009). Increased LOX activity in the present study showed good correlation with H_2O_2 generation (R^2=0.848) and lipid peroxidation (R^2=0.855). LOX-mediated lipid peroxides accumulation was reported in Pb-treated *S. alfredii* (Huang et al. 2012). It is possible that the Pb induces the LOX activity, which through production of hydroperoxide derivative attacks the cell membrane and causes oxidative stress in *T. triangulare* root cells.

Table 1 Analysis of atomic percentage of elements by energy dispersive spectroscopy (EDS) in roots of *Talinum triangulare* treated with 0 (control), 0.25, and 1.25 mM of Pb for 7 days

	Atomic percentage of elements in roots of *T. triangulare*		
Elements	Control	0.25 mM Pb	1.25 mM Pb
O	82.88	84.50	84.69
K	7.33	6.91	11.18
Na	3.74	3.50	0.55
Ca	2.08	1.95	0.67
Mg	1.83	1.82	1.50
Cl	0.91	0.83	0.78
Si	0.72	ND	ND
S	0.23	0.20	ND
Cu	0.28	ND	0.22
Pb	ND	0.29	0.41

ND not detected

The dose-dependent decline in protein content in Pb-treated roots observed in the present study could be due to inhibition of protein synthesis and/or protein oxidation. Lead treatment induces a substantial increase in the formation of oxidative product of proteins measured as protein carbonyls content, which was reflected as a decrease in the total protein content. Carbonyls containing oxidative products are formed as a result of hydroxyl radical ($^{\bullet}OH$) attack on susceptible amino acids or peptide side chain of proteins (Aravind and Prasad 2003; Pena et al. 2008). A variety of proteins function as scavengers of ROS, including SOD, CAT, and APX measured here that represent biomarkers of antioxidative response to Pb stress (Reddy et al. 2005; Wang et al. 2011; Huang et al. 2012). In contrast to protein concentration, SOD and CAT activities were gradually increased and were negatively correlated (R^2=0.569 and R^2=

0.479, respectively) with the total protein contents. SOD is considered as the first line of defense to scavenge ROS radicals generated by various stresses (Reddy et al. 2005; Hu et al. 2007). SOD is the key enzyme in plant cells that dismutates superoxide radical ($O_2^{\bullet-}$) to form H_2O_2 and O_2. Increase in SOD activity showed good correlation with Pb-induced membrane damage (R^2=0.851) and increased ROS (R^2=0.96) production, respectively. CAT and APX are the two important H_2O_2 scavenging enzymes. CAT detoxifies H_2O_2 directly, whereas APX, a component of the ascorbate–glutathione cycle, detoxifies H_2O_2 in presence of ascorbate (Sharma and Dubey 2005). Increase in CAT activity could possibly be due to the result of both a direct effect of Pb and an indirect effect mediated via an increase in H_2O_2 level through SOD. Similar to CAT, the increased APX activity may catalyze the oxidation of excess H_2O_2 caused by Pb and thus may play a detoxifying role. However, APX activity initiated to decline as the concentration of Pb rose to 0.75 mM, suggesting that the antioxidative potential of APX had reached maximum level to maintain the stability of the antioxidative system (Sharma and Dubey 2005; Pourraut et al. 2011). It is observed that except APX, the tendencies of LOX, SOD, and CAT activities showed positive correlation with the concentration of Pb in treatment solution.

Proline is a multifunctional amino acid, which is reported to accumulate in plant cells in response to various stresses including HMs stress (Szabados and Savouré 2010). It is suggested that accumulation of compatible amino acids like proline seems to be one of the means by which plant cells combat non-enzymatically against Pb-generated free radicals (Sharmila and Saradhi 2002). Proline followed the similar trend as APX activity, which was also enhanced at 0.25–0.75 mM Pb. Proline contents showed an inverted U-shaped dose–response curve, suggesting the hormetic response against increasing Pb concentrations. However, at 1.0 and 1.25 mM Pb, both APX activity and proline content were less than control values, respectively. Result of carbonyl contents showed that Pb at 0.75, 1.0, and 1.25 mM caused the significantly high rate of protein carbonylation that might be resulted in dysfunction in cellular proteins or enzymes (Aravind and Prasad 2003). It is possible that Pb at higher concentrations have interfered in the proline (monocarboxylic acid) biosynthesis enzymes or may be due to increased proline catabolism at those Pb concentrations (Sharmila and Saradhi 2002), but it needs further studies.

DNA damage in control and Pb-treated roots was estimated using the alkaline comet assay, which is a quick and sensitive fluorescent method that allows measurement of DNA strand damage in individual cells (Patnaik et al. 2011). Visual examinations gave a fairly good indication of DNA damage, which showed an individual isolated nucleus comprising a head and a tail. The head corresponds to the DNA amounts that still remain in the nuclear matrix region, whereas the tail reveals the DNA fragments migrating from the nuclei (Kumaravel et al. 2009). Alkaline comet assay detects DNA damage as single-stranded and/or double-stranded DNA breaks at the level of eukaryotic genome. Ability of Pb to cause DNA damage in root cells of *Lupinus luteus* was first demonstrated by Rucińska et al. (2004). Subsequently, comet assay using *Nicotiana tabacum* and *Solanum tuberosum* plants was successfully applied to monitor genotoxicity of soils heavily contaminated with cadmium (Cd), Cu, and Pb (Gichner et al. 2006). In the present study, the Pb treatment significantly increased the frequency of DNA damage at 0.50–1.0 mM (Fig. 5) that followed a dose–response (Shahid et al. 2011), which perhaps was mediated through the generation of ROS. The potential of genotoxicity was reported in root cells of *Vicia faba* upon Pb exposure (Shahid et al. 2011).

Structural modification in roots and stem of *T. triangulare* plants due to uptake and accumulation of Pb was investigated by using SEM. In our experiment, we have noticed that given Pb treatment resulted in gradual changes in root morphology and stem internal structure, leading to a deformed structural organization compared to respective control. Pb treatment developed longitudinal ruptures in root, which resulted in formation of pores. Rupture in root's rhizodermis and outer cortex has been reported in cowpea (*Vigna unguiculata*) exposed to Al, Cu, and lanthanum (La) (Kopittke et al. 2008). Certainly, the rupture on the Pb-treated roots appears to be more or less similar to those formed in Al-, Cu-, and La-treated cowpea roots (Kopittke et al. 2008). Further analysis of stem TS revealed that most of the Pb was accumulated within the xylem vessels (Fig. 6e, f). The increased number of vacuoles and the loss of cell shape and decrease in intercellular spaces have been also observed in the Pb-treated plant over the control plant, which may inhibit the translocation or uptake of nutrient elements, Pb, and water from roots to stems and aerial part of the plant. This is confirmed in our previous study by the significant decrease in relative water content and atomic percentage of nutrient elements in leaves of *T. triangulare* (Kumar et al. 2012). However, 1.25 mM Pb concentration resulted in higher amount of morphological and structural modification in roots and stems in comparison to control and 0.25 mM Pb-treated plants, respectively.

The EDS analysis of intercellular elements distribution in the *T. triangulare* root revealed that Pb amount was higher in the 1.25 mM Pb-treated group compared to the 0.25 mM Pb. Similarly, the atomic percentage of O and K were also found to increase in 1.25 mM Pb-treated sample (Table 1). In contrast to the elements described above, the atomic percentage of other elements in Pb-treated root tissues declined, which suggested the avoidance of the elemental uptake. It was noted that in *Brachiaria decumbens* (signal grass), *Chloris gayana* (Rhodes grass) (Kopittke et al.

2007), and *Spirodela polyrhiza* (Qiao et al. 2012), toxic levels of Pb caused reductions in most of the nutrient concentrations in shoot tissue. A similar result was observed for Na, Ca, Mg, Cl, Si, S, and Cu atomic percentage in the present study. The study showed that Pb treatment had negative effects on the nutrient elements in the *T. triangulare* root. Atomic percentage of Si and S analyzed by EDS were below detection limit in both 0.25 and 1.25 mM Pb-treated roots. Metal transporters belonging to the CaCA (Ca-calmodulin) superfamily have been identified as being able to transport H^+, Ca^{2+}, Na^+, and K^+ (Manara 2012). The integral component of Ca^{2+} cycling systems involves the efflux of Ca^{2+} across membranes against a concentration gradient, which further is achieved by using a counter electrochemical gradient of other ions such as H^+, Na^+, or K^+ (Emery et al. 2012). The Na or K/Ca ratio is crucial for water balance in plants. Competition interference with such transporters may form the basis of the negative interactions between nutrient elements and Pb in plants. Furthermore, essential metals Na, Mg, Cu, and Ca act as catalyst for many of the enzymatic processes that are necessary for plant growth, development, and metabolic processes (Sharma and Dubey 2005). Thus, we may postulate that decreases in the nutrients atomic percentage in the present study were more effective in the direct or indirect role of altered plant growth and metabolic characteristics.

Conclusions

Considering our results, we can conclude that accumulated Pb in the root tissue causes oxidative stress and genotoxicity, which is manifested by increased ROS production, cell death, and increased MDA content and increased LOX activity in comparison to control. *T. triangulare* showed good tolerance mechanism against Pb toxicity through the increased activity of SOD, CAT, and APX and accumulation of free proline in Pb-treated roots. The increase in Pb treatment caused reduction in total protein contents, which may be possible due to increased protein oxidation. Result of genotoxicity concluded that the comet assay is an efficient bioassay technique that demonstrates the Pb-induced DNA damage and cell death in *T. triangulare* roots. SEM analyses revealed that Pb treatment developed ruptures in root surface, which resulted in formation of pores on root, Pb accumulation within the xylem vessels, and the loss of the cell integrity in stem. The atomic percentage of elements in Pb-treated root tissues declined, supporting the idea of an avoidance mechanism. In conclusion, hydroponically cultivated adventitious roots of *T. triangulare* were useful for rhizofiltration. Further research on the molecular mechanism(s) of Pb detoxification in plant is required to improve our understandings.

Acknowledgements A.K. gratefully acknowledges the University of Hyderabad Research Scholarship through the University Grant Commission, New Delhi. The authors express their gratitude to Mr. S. Pavan Kumar and Ms. Nalini of the Central Instrument Laboratory, UoH for ESEM and confocal studies, respectively, and M. Laxminarayan for helping with the FESEM/EDS study. M.N.V.P. gratefully acknowledge the award of Pitamber Pant National Environment Fellowship by the Ministry of Environment and Forests, GOI, New Delhi (MoEF Ref. No. 17/3/2010-RE Dt 29-2-2012).

References

Aebi H (1984) Catalase in vitro. Meth Enzymol 105:121–126

Andarwulan N, Batari R, Sandrasari DA, Bolling B, Wijaya H (2010) Flavonoid content and antioxidant activity of vegetables from Indonesia. Food Chem 121:1231–1235

Anonymous (2007) Toxicological profile for lead. US Department of Health and Human Services, Public Health Service, Agency for Toxic Substances and Disease Registry (ATSDR), Atlanta

Anonymous (2011) Hazardous metals and minerals pollution in India: sources toxicity and management. A position Paper. Indian National Science Academy (INSA), New Delhi, pp 1–24

Aravind P, Prasad MNV (2003) Zinc alleviates cadmium-induced oxidative stress in *Ceratophyllum demersum* L.: a free floating freshwater macrophyte. Plant Physiol Biochem 41:391–397

Aravind P, Prasad MNV, Malec P, Waloszek A, Strzałka K (2009) Zinc protects *Ceratophyllum demersum* L. (free-floating hydrophyte) against reactive oxygen species induced by cadmium. J Trace Ele Med Biol 23:50–60

Baker CJ, Mock NM (1994) An improved method for monitoring cell death in cell suspension and leaf disc assays using Evans blue. Plant Cell Tissue Org Cult 39:7–12

Bates LE, Waldren RP, Teare ID (1973) Rapid determination of free proline for water stress studies. Plant Soil 39:205–207

Beauchamp C, Fridovich I (1971) Superoxide dismutase: improved assays and an assay applicable to acrylamide gels. Anal Biochem 44:276–287

Ederli L, Pasqualini S, Batini P, Antonielli M (1997) Photoinhibition and oxidative stress: effects on xanthophyll cycle, scavenger enzymes and abscisic acid content in tobacco plants. J Plant Physiol 151:422–428

Emery L, Whelan S, Hirschi KD, Pittman JK (2012) Phylogenetic analysis of Ca^{2+}/cation antiporter genes and insights into their evolution in plants. Front Plant Sci. doi:10.3389/fpls.2012.00001

Gichner T, Patkova Z, Szakova J, Demnerova K (2006) Toxicity and DNA damage in tobacco and potato plants growing on soil polluted with heavy metals. Ecotoxicol Environ Saf 65:420–426

Gomez KA, Gomez AA (1984) Statistical procedures for agricultural research, 2nd edn. Wiley, New York, Paperback, pp 680

Gupta DK, Nicoloso FT, Schetinger MR, Rossato LV, Pereira LB, Castro GY, Srivastava S, Tripathi RD (2009) Antioxidant defense mechanism in hydroponically grown *Zea mays* seedlings under moderate lead stress. J Hazard Mater 172:479–484

Heath RL, Packer L (1968) Peroxidation in isolated chloroplasts 1. Kinetics and stoichiometry of fatty acid peroxidation. Arch Biochem Biophys 125:189–198

Hoagland DR, Arnon DI (1950) The water-culture for growing plants without soil. Calif Agric Exp Sta Circ 347:1–32

Huang H, Gupta DK, Tian S, Yang X, Li T (2012) Lead tolerance and physiological adaptation mechanism in roots of accumulating and non-accumulating ecotypes of *Sedum alfredii*. Environ Sci Pollut Res 19:1640–1651

Hu JZ, Shi GX, Xu QS, Wang X, Yuan QH, Du KH (2007) Effects of Pb^{2+} on the active oxygen-scavenging enzyme activities and ultrastructure in *Potamogeton crispus* leaves. Russ J Plant Physiol 54:414–419

Hu R, Sun K, Su X, Pan Y, Zhang Y, Wang X (2012) Physiological responses and tolerance mechanisms to Pb in two xerophils: *Salsola passerina* Bunge and *Chenopodium album* L. J Hazard Mater 205–206:131–138

Kaur G, Singh HP, Batish DR, Kohli RK (2012) A time course assessment of changes in reactive oxygen species generation and antioxidant defense in hydroponically grown wheat in response to lead ions (Pb^{2+}). Protoplasma 249:1091–1100

Kopittke PM, Blamey FPC, Menzies NW (2008) Toxicities of soluble Al, Cu, and La include ruptures to rhizodermal and root cortical cells of cowpea. Plant Soil 303:217–227

Kopittke PM, Asher CJ, Blamey FPC, Menzies NW (2007) Toxic effects of Pb^{2+} on the growth and mineral nutrition of signal grass (*Brachiaria decumbens*) and Rhodes grass (*Chloris gayana*). Plant Soil 300:127–136

Kumar A, Prasad MNV (2010) Propagation of *Talinum cuneifolium* L. (Portulacaceae), an ornamental plant and leafy vegetable, by stem cuttings. Floricult Ornament Biotech 4(SI-1):68–71

Kumar A, Prasad MNV, Sytar O (2012) Lead toxicity, defense strategies and associated indicative biomarkers in *Talinum triangulare* grown hydroponically. Chemosphere 89:1056–1065

Kumaravel TS, Vilhar B, Faux SP, Jha AN (2009) Comet assay measurements: a perspective. Cell Biol Toxicol 25:53–64

Lamhamdi M, Bakrim A, Aarab A, Lafont R, Sayah F (2011) Lead phytotoxicity on wheat (*Triticum aestivum* L.) seed germination and seedlings growth. C R Biol 334:118–126

Li X, Bu N, Li Y, Ma L, Xin S, Zhang L (2012) Growth, photosynthesis and antioxidant responses of endophyte infected and non-infected rice under lead stress conditions. J Hazard Mater 213:55–61

Lowry OH, Rosebrough NJ, Farr AL, Randall RJ (1951) Protein measurement with the Folin-phenol reagent. J Biol Chem 193:265–275

Maldonado-Magaña A, Favela-Torres E, Rivera-Cabrera F, Volke-Sepulveda TL (2011) Lead bioaccumulation in *Acacia farnesiana* and its effect on lipid peroxidation and glutathione production. Plant Soil 339:377–389

Malecka A, Piechalak A, Tomaszewska B (2009) Reactive oxygen species production and antioxidative defense system in pea root tissues treated with lead ions: the whole roots level. Acta Physiol Plant 31:1053–1063

Manara A (2012) Plant responses to heavy metal toxicity. In: Furini A (ed) Plants and heavy metals, Springer briefs in biometals. Springer, New York, pp 27–53

Nakano Y, Asada K (1981) Hydrogen peroxide is scavenged by ascorbate-specific peroxidase in spinach chloroplasts. Plant Cell Physiol 22:867–880

Panyaphu K, On TV, Sirisa-ard P, Srisa-nga P, ChansaKaow S, Nathakarnkitkul S (2011) Medicinal plants of the Mien (Yao) in Northern Thailand and their potential value in the primary healthcare of postpartum women. J Ethnopharma 135:226–237

Patnaik AR, Achary VMM, Panda BB (2011) Comet assay to assess DNA damage and genotoxic stress in plants. In: Roy BK, Chaudhary BR, Sinha RP (eds) Plant genome: biodiversity, conservation and manipulation. Narosa, New Delhi, pp 17–29

Pena LB, Zawoznik MS, Tomaro ML, Gallego SM (2008) Heavy metals effects on proteolytic system in sunflower leaves. Chemosphere 72:741–746

Piotrowska A, Bajguz A, Godlewska-Zyłkiewicz B, Czerpak R, Kaminska M (2009) Jasmonic acid as modulator of lead toxicity in aquatic plant *Wolffia arrhiza* (Lemnaceae). Environ Exp Bot 66:507–513

Pourraut B, Shahid M, Dumat C, Winterton P, Pinelli E (2011) Lead uptake, toxicity and detoxification in plants. Rev Environ Conta Toxicol 213:113–136

Qiao X, Shi G, Jia R, Chen L, Tian X, Xu J (2012) Physiological and biochemical responses induced by lead stress in *Spirodela polyrhiza*. Plant Growth Regul 67:217–225

Rajkumar K, Sivakumar S, Senthilkumar P, Prabha D, Subbhuraam CV, Song YC (2009) Effects of selected heavy metals (Pb, Cu, Ni and Cd) in the aquatic medium on the restoration potential and accumulation in the stem cuttings of the terrestrial plant, *Talinum triangulare* Linn. Ecotoxicology 18:952–960

Rajkumar M, Sandhya S, Prasad MNV, Freitas H (2012) Perspectives of plant-associated microbes in heavy metal phytoremediation. Biotechnol Advanc 30:1562–1574

Reddy AM, Kumar SG, Jyothsnakumari G, Thimmanaik S, Sudhakar C (2005) Lead induced changes in antioxidant metabolism of horsegram (*Macrotyloma uniflorum* (Lam.) Verdc.) and bengalgram (*Cicer arietinum* L.). Chemosphere 60:97–104

Reznick AZ, Packer L (1994) Oxidative damage to proteins: spectrophotometric method for carbonyl assay. Meth Enzymol 233:357–363

Rucińska R, Sobkowiak R, Gwóźdź EA (2004) Genotoxicity of lead in lupin root cells as evaluated by the comet assay. Cellular Mole Biol Lett 9:519–528

Sengar RK, Gautam M, Sengar RK, Grag SK, Sengar K, Chaudhary R (2008) Lead stress effects on physio-biochemical activities of higher plants. Rev Environ Conta Toxicol 196:73–93

Shahid M, Pinelli E, Dumat C (2012) Review of Pb availability and toxicity to plants in relation with metal speciation; role of synthetic and natural organic ligands. J Hazard Mater 219–220:1–12

Shahid M, Pinelli E, Pourrut B, Silvestre J, Dumat C (2011) Lead-induced genotoxicity to *Vicia faba* L. roots in relation with metal cell uptake and initial speciation. Ecotoxicol Environ Saf 74:78–84

Sharma P, Dubey RS (2005) Lead toxicity in plants. Braz J Plant Physiol 17:35–52

Sharmila P, Saradhi PP (2002) Proline accumulation in heavy metal stressed plants: an adaptive strategy. In: Prasad MNV, Strzałka K (eds) Physiology and biochemistry of metal toxicity and tolerance in plants. Kulwer Academic, Netherlands, pp 179–199

Singh HP, Kaur G, Batish DR, Kohli RK (2011) Lead (Pb)-inhibited radical emergence in *Brassica campestris* involves alterations in starch-metabolizing enzymes. Biol Trace Elem Res 144:1295–1301

Szabados S, Savouré AA (2010) Proline: a multifunctional amino acid. Trends Plant Sci 15:89–97

Uwah EI, Ndahi NP, Ogugbuaja VO (2009) Study of the levels of some agricultural pollutants in soils and water leaf (*Talinum triangulare*) obtained in Maiduguri, Nigeria. J Appl Sci Environ Sanit 4 (2):71–78

Velikova V, Yordanov I, Edreva A (2000) Oxidative stress and some antioxidant systems in acid rain-treated bean plants. Plant Sci 151:59–66

Wang C, Gu X, Wang X, Guo H, Geng J, Yu H, Sun J (2011) Stress response and potential biomarkers in spinach (*Spinacia oleracea* L.) seedlings exposed to soil lead. Ecotoxicol Environ Saf 74:41–47

Heavy metal-induced oxidative damage, defense reactions, and detoxification mechanisms in plants

Oksana Sytar, Abhay Kumar, Dariusz Latowski, Paulina Kuczynska, Kazimierz Strzałka & M. N. V. Prasad

Acta Physiologiae Plantarum

ISSN 0137-5881

Acta Physiol Plant
DOI 10.1007/s11738-012-1169-6

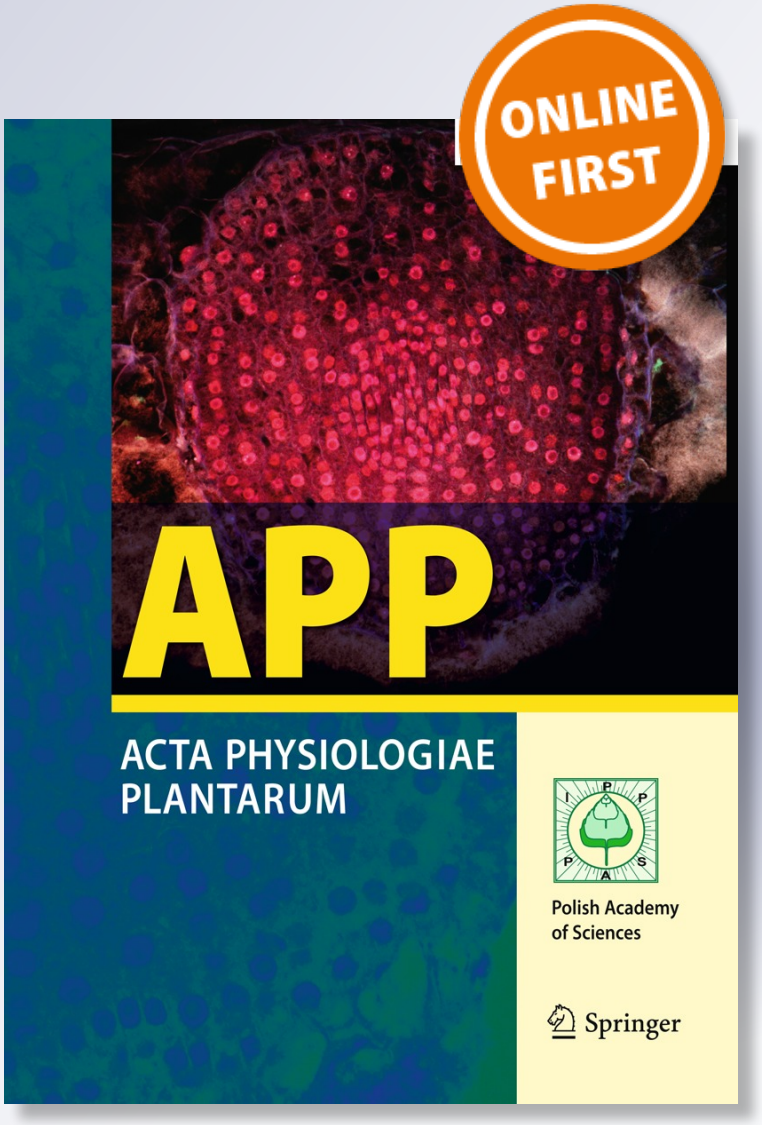

Springer

Acta Physiol Plant
DOI 10.1007/s11738-012-1169-6

REVIEW

Heavy metal-induced oxidative damage, defense reactions, and detoxification mechanisms in plants

Oksana Sytar · Abhay Kumar · Dariusz Latowski · Paulina Kuczynska · Kazimierz Strzałka · M. N. V. Prasad

Received: 25 June 2012 / Revised: 12 November 2012 / Accepted: 22 November 2012

Abstract Heavy metal (HMs) contamination is widespread globally due to anthropogenic, technogenic, and geogenic activities. The HMs exposure could lead to multiple toxic effects in plants by inducing reactive oxygen species (ROS), which inhibit most cellular processes at various levels of metabolism. ROS being highly unstable could play dual role (1) damaging cellular components and (2) act as an important secondary messenger for inducing plant defense system. Cells are equipped with enzymatic and non-enzymatic defense mechanisms to counteract this damage. Some are constitutive and others that are activated only when a stress-specific signal is perceived. Enzymatic scavengers of ROS include superoxide dismutase, catalase, glutathione reductase, and peroxidase, while non-enzymatic antioxidants are glutathione, ascorbic acid, α-tocopherol, flavonoids, anthocyanins, carotenoids, and organic acids. The intracellular and extracellular chelation mechanisms of HMs are associated with organic acids such as citric, malic and oxalic acid, etc. The important mechanism of detoxification includes metal complexation with glutathione, amino acids, synthesis of phytochelatins and sequestration into the vacuoles. Excessive stresses induce a cascade, MAPK (mitogen-activated protein kinase) pathway and synthesis of metal-detoxifying ligands. Metal detoxification through MAPK cascade and synthesis of metal-detoxifying ligands will be of considerable interest in the field of plant biotechnology. Further, the photoprotective roles of pigments of xanthophylls cycle under HMs stress were also discussed.

Keywords Antioxidants · Flavonoids · Heavy metals · MAPK pathway · Oxidative stress · Phenolic compounds · Phytochelatins

Abbreviations

AE	Accumulating ecotype
APX	Ascorbate peroxidases
AsA	Ascorbic acid
CAT	Catalase
Cys	Cysteine
DHA	Dehydroascorbate
ETC	Electron transport chain
Glu	Glutamine
Gly	Glycine
GR	Glutathione reductase
GSH	Glutathione (reduced)
GSSG	Glutathione (oxidized)
GST	Glutathione-*S*-transferase
HMs	Heavy metals
H_2O_2	Hydrogen peroxide
LOX	Lipoxygenase
LP	Lipid peroxidation
MAPK	Mitogen-activated protein kinase
MAPKK	MAPK kinase

Communicated by A. K. Kononowicz.

O. Sytar · A. Kumar · M. N. V. Prasad (✉)
Department of Plant Sciences, University of Hyderabad, Hyderabad 500046, India
e-mail: prasad_mnv@yahoo.com

O. Sytar
Department of Plant Physiology and Ecology, Kyiv National University of Taras Shevchenko, Volodymyrskya str. 64, Kyiv 01033, Ukraine

D. Latowski · P. Kuczynska · K. Strzałka
Departament of Plant Physiology and Biochemistry, Faculty of Biochemistry, Biophysics and Biotechnology, Jagiellonian University, Gronostajowa str. 7, 30-387 Krakow, Poland

Published online: 13 December 2012

MAPKKK	MAPK kinase kinase
MDA	Malondialdehyde
MDHA	Monodehydroascorbate
NAD^+	Nicotinamide adenine dinucleotide (oxidized)
NADH	Reduced NAD
$NADP^+$	Nicotinamide adenine dinucleotide phosphate (oxidized)
NADPH	Reduced NADP
NAE	Non-accumulating ecotype
$O_2^{\bullet-}$	Superoxide radical
PCs	Phytochelatins
PCS	Phytochelatins synthase
POD	Peroxidases
PSII	Photosystem II
PSI	Photosystem I
PUFA	Poly unsaturated fatty acids
ROS	Reactive oxygen species
SOD	Superoxide dismutase
SQDG	Sulfoquinovosyldiacyglycerol

Introduction

Environmental pollution by heavy metals (HMs) such as cadmium (Cd), lead (Pb), nickel (Ni), mercury (Hg), copper (Cu), zinc (Zn), calcium (Ca), magnesium (Mg), manganese (Mn), cobalt (Co) and metalloids, i.e. arsenic (As) poses threat to all forms of life. Toxic metals are bioavailable to plants through their uptake from soil and water. Many previous studies have revealed the phytotoxic effects of elevated concentrations of HMs on growth, water potential, physiological, biochemical and molecular processes of plants (Malec et al. 2008, 2009; Maleva et al. 2009; Wan et al. 2011; Gangwar et al. 2011; Yusuf et al. 2012; Kumar et al. 2012). Despite the toxicity of these HMs, several plants growing in metals polluted soil are able to exclude, accumulate or hyperaccumulate HMs and acquire a wide range of adaptive strategies (Sharma and Dietz 2006; Anjum et al. 2012; Ahmad and Prasad 2012). However, sensitive plants develop visible symptom of phytotoxicity due to metal exposure. Some of well-established HMs phytotoxic manifestations include generation of reactive oxygen species (ROS) and reactive nitrogen species (NO) as well as replacement of enzyme cofactors and transcription factors, inhibitions of antioxidative enzymes, cellular redox imbalance, ionic transport imbalance, DNA damage and protein oxidation (Aravind et al. 2009; Ann et al. 2011; Gangwar et al. 2011; Huang et al. 2012). HMs stress caused reduction of molecular oxygen and produced intermediate products such as superoxide radicals ($O_2^{\bullet-}$), hydroxyl radicals ($OH^{\bullet-}$) and hydrogen peroxide (H_2O_2), which are more toxic and reactive than O_2. These active molecules are involved in the free radical chain reaction of membrane lipids and proteins, thus causing oxidative decomposition of them (Fig. 1) (Kanoun-Boulé et al. 2009; Ann et al. 2011).

In the past, for many years ROS were considered as dangerous molecules which must be maintained at low level in cells. However, recently this point of view has been changed. It has been shown that ROS can also play an important role in plant defense against oxidative explosion and can serve as markers of the certain stages of development, such as formation of tracheids and the cross-link in cell walls, lignifications, and programmed cell death and also serve as signaling/alarm molecules in regulation of gene expression process (Schützendübel and Polle 2002). Due to diverse functions of the active oxygen species, cells must strictly control the level of ROS. This controlling systems is composed of antioxidants including enzymes such as superoxide dismutase (SOD, E.C. 1.15.1.1), catalase (CAT, E.C. 1.11.1.6), glutathione reductase (GR, E.C. 1.6.4.2), peroxidase (POD, E.C. 1.11.1.7), ascorbate peroxidase (APX, E.C. 1.11.1.11) and guaiacol peroxidases (GPX, E.C. 1.11.1.7) and non-enzymatic antioxidants such as ascorbic acid (AsA), glutathione (GSH) and tocopherol to suppress the ROS (Munne-Bosch 2005; Kanoun-Boulé et al. 2009; Maleva et al. 2009; Shu et al. 2012; Kumar et al. 2012). These non-enzymatic antioxidants are intermediates of ascorbate–glutathione cycle (AGC) which plays a major role in H_2O_2 scavenging pathway operating in the chloroplasts as well as the cytosol. Operations of the AGC not only maintain the reduced active forms of AsA and GSH on an appropriate level, thereby adjusting the cellular redox potential but also participate in ROS detoxification (Munne-Bosch 2005; Potters et al. 2010).

Photoxidative damage and photoprotective role of plant under HMs stress

Photosynthesis is one of the most studied biological processes under various stress conditions. Different plants and parts exhibit diverse pattern of HMs accumulation which would influence biosynthesis of photosynthetic pigments (reduction of photosynthetic pigments such as chlorophylls and carotenoids contents) (Mobin and Khan 2007; Shakya et al. 2008; Vesely et al. 2011). Accumulated HMs in plants may interact with the photosynthetic machinery and resulted in a wide variety of toxic effects, including photo-oxidative damage. In particular, they alter the chloroplast membrane functions and component of the photosynthetic electron transport chain (ETC), thus impairing the light phase of photosynthesis (Myśliwa-Kurdziel and Strzałka 2002; Malec et al. 2008; Ventrella et al. 2011).

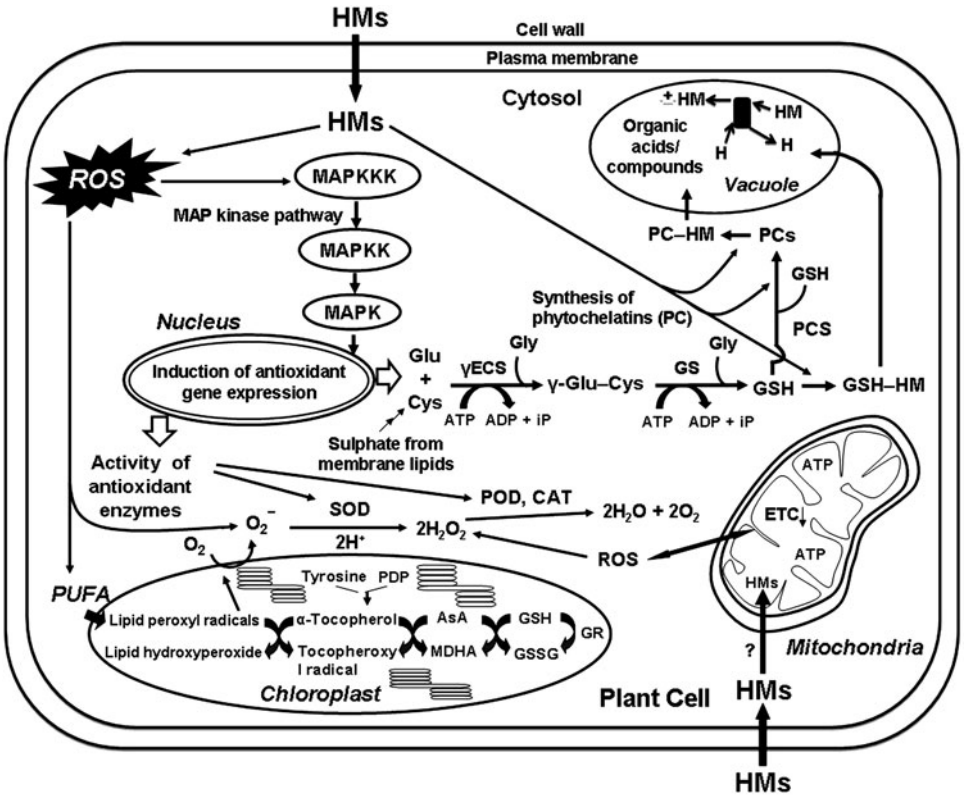

Fig. 1 Heavy metal induced oxidative stress, tolerance and detoxification mechanisms in plant cell. *ADP* adenosine dinucleotide phosphate, *AsA* ascorbic acid, *ATP* adenosine triphosphate phosphate, *CAT* catalase, *Cys* cysteine, *γ-ECS* γ-glutamylcysteine synthetase, *ETC*↓ electron transport chain damage, *Glu* glutamine, *Gly* glycine, *GR* glutathione reductase, *GS* glutathione synthetase, *GSH* glutathione (reduced), *GSSG* glutathione (oxidized), *H* hydrogen molecule, *HMs* heavy metals, H_2O_2 hydrogen peroxide, *MAPK* mitogen-activated protein kinase, *MAPKK* MAPK kinase, *MAPKKK* MAPK kinase kinase, *MDHA* monodehydroascorbate, *iP* inorganic phosphate, O_2 oxygen molecule, $O_2^{\bullet-}$ superoxide radicals, *PCs* phytochelatins, *PCS* phytochelatins, *PDP* phytol diphosphate, *POD* peroxidases, *PUFA* polyunsaturated fatty acids, *ROS* reactive oxygen species, *SOD* superoxide dismutase, *SQDG* sulfoquinovosyldiacylglycerol

Chloroplasts, thylakoid membranes, photosystem (PS) II and I from higher plants could provide a great opportunity to build a system for HMs toxicity bioassays. Photosynthetic inhibition during HMs stress is one of the primary actions in plants because they invariably affect the photosynthetic apparatus and its functions, either directly or indirectly by inhibiting both light and dark reactions of photosynthesis. It is known that HM decrease photosynthetic rate, stomatal conductivity, transpiration rate, plant growth and agricultural productivity (Myśliwa-Kurdziel and Strzałka 2002; Malec et al. 2008; Shakya et al. 2008; Wan et al. 2011; Yusuf et al. 2012). The negative effect of HMs ions on growth, leaf enzyme activities, photosynthesis together with activities of both PSII and PSI was found to be dose dependent (Babu et al. 2010). This effect was further increased with an increase in duration of exposure (Chugh and Sawhney 1999). HMs ions affect the electron transport system at multiple sites and alter the energy transfer from one level to another level. Impact of HMs ions on the electron transport system in plant have been analyzed in isolated chloroplast (Khan et al. 2007), which indicates that PSII is more susceptible to HMs compared with PSI. But these metals can inhibit the PSI activity at much higher concentrations (Ivanov et al. 2006; Hörcik et al. 2007). HMs affect chlorophylls as well as the carotenoids in plants (Ghnaya et al. 2009) because toxic effect of HMs appears to be related to production of ROS which induces synthesis of low-molecular-weight compounds such as carotenoids (Kumar et al. 2012). Carotenoids play an important role in the prevention of several degenerative stresses in plants owing to their antioxidant function. Carotenoids play photoprotective role as quenchers of the high ROS levels that can initiate a cascade of function as chain-breaking antioxidants (Young and Frank 1996).

Plants have developed several mechanisms to avoid photodamage and one of the most important photoprotective mechanisms is the release of excessive excitation energy (Janik et al. 2008; Latowski et al. 2011). This process of dissipation energy in PSII depends on the

zeaxanthin (Zx), antheraxanthin (Ax) and the de-epoxidized components of xanthophyll cycle (Tóth et al. 2007; Latowski et al. 2011). The role of xanthophyll cycle under HMs impact is confirmed by number of reports. A decrease in xantophyll level was observed in *Pinus sylvestris* growing in area contaminated with Al, Pb and Cu (Matysiak 2001). It has also been observed that in Cd-stressed leaves of *Secale cereale* reduction of the second step of violaxanthin de-epoxidation leads to Ax accumulation and increase in the *cis*-isomers fraction in violaxanthin (Janik et al. 2008). The Cd inhibition of Zx epoxidase was also reported both in violaxanthin and diadinoxanthin cycles (Bertrand et al. 2001; Latowski et al. 2005). It was shown that this inhibition was reversed by Zn, what was accepted as evidence that mechanism of Cd inhibition was based on interaction of Cd with cysteine residues of enzyme (Latowski et al. 2005). On the other hand, the large increase in the amount of all xanthophyll cycle pigments was observed as an antioxidative response for Cd-treated duckweed plants (Appenroth et al. 1996). It shows that xanthophylls in plants play an important role in quenching of free radical-induced reactions and can also prevent generation of free radicals, thereby limiting free radical/oxidative damage. Plant adaptation and survival during HMs stress depends on the ability to resist the oxidative damage and antioxidant systems activity.

Lipid peroxidation and enzymatic system during HMs stress

Plasma membranes are considered a primary target for metal toxicity in both leaves and roots. Membrane damage was deduced from the analysis of TBA (thiobarbituric acid) active products level, after reaction using TBA assay. This is one of the basic methods of research process to determine lipid peroxidation (LP) in the biological systems (Fig. 2). Various results testified that under action of HMs, plants often activate processes of LP (Dazy et al. 2009; Iqbal et al. 2010; Ann et al. 2011; Yusuf et al. 2012; Kumar et al. 2012).

Measurement of the level of thiobarbituric acid reactive substances (TBARS) in tissues is widely used as an index of LP also. Malondialdehyde (MDA) is thiobarbituric acid reactive substances. LP is a biochemical marker for the free radical-mediated injury by production of ROS. The investigations with increasing Pb concentration showed the Pb-induced lipid peroxides and oxidative stress in rice (Verma and Dubey 2003) and *Talinum triangulare* leaves (Kumar et al. 2012). The accumulation of Cd and Cu in the plant tissues enhanced LP (Khan et al. 2007; Ghnaya et al. 2009; Ann et al. 2011). Increase in MDA content in Hg- and Cd-treated *Phaseolus aureus* leaves was observed, but in case of Hg the change was more significant. It is probably because of the direct effect of Hg on the photosynthetic electron transport (PET) causing generation of singlet oxygen; in contrast, Cd does not affect PET directly (Shaw 1995). Stimulation process of LP might be activated by lipoxigenase (LOX) with the formation of hydroperoxide because the early stress reactions occur at the membranes level (Huang et al. 2012). The object of the LP on the membranes level can be unsaturated fatty acids. The process of LP is connected with activity of main antioxidant enzymes. The change of enzyme activity determines intensity and function of cells and organism as a whole and also their viability in the environment conditions. The results of experiment with clones of *Salix viminalis* with different resistance to Cd, Cu, and Zn showed that SOD activity was higher in untreated resistant clones compared with the sensitive ones (Fig. 3) (Landberg and Greger 2002). Yusuf et al. (2012) showed that Ni treatment (100 mg kg^{-1}) caused increased level of LP in *B. juncea*, which further decreased after external supplementation of sulfosalicylic acid, a known antioxidant (Table 1).

The study with HMs salts, cobalt chloride ($CoCl_2$) and cadmium chloride ($CdCl_2$), influenced glyoxylate cycle enzymes and mitochondrial succinate dehydrogenase activities in germinating soybean seeds. $CoCl_2$ increased isocitrate lyase activity on the third day and $CdCl_2$ suppressed isocitrate lyase activity on the very first day. Cobalt chloride and $CdCl_2$ suppressed succinate dehydrogenase activity on fifth day might have caused oxidative stress (Bezdudna 2009). Perhaps increase in isocitrate lyase activity in the presence of Co was due to the fact that Co ions in physiological concentrations are the promoters of metabolic processes and contribute to more intensive mobilization of reserve compounds. Inhibitory effects on succinate dehydrogenase by HMs have been demonstrated (Seregin and Ivanov 2001). The effect of Pb on growth and activities of antioxidant enzymes in leaf of accumulating ecotype (AE) and non-accumulating ecotype (NAE) of *Sedum alfredii* have showed that accumulating ecotype was more tolerant to excessive Pb levels in growth medium (Liu et al. 2008). Under such conditions the activities of SOD and CAT were elevated in leaves of AE. However, in NAE, only SOD activity was increased while CAT activity was declined after Pb treatment comparing with the control plants. With increase in Pb level, MDA content increased significantly in both ecotypes of *S. alfredii*, indicating that Pb toxicity leads to LP and membrane damage, but MDA content in leaves of NAE was higher than in AE plants (Liu et al. 2008; Huang et al. 2012). Pb treatment caused increased generation of ROS in root cells in both ecotypes. Furthermore, ROS caused increased enzyme activities of SOD, CAT, APX, POD and LOX. The response of AE root cells manifested in higher activities for SOD, POD, LOX and AsA than NAE root cells (Huang et al. 2012).

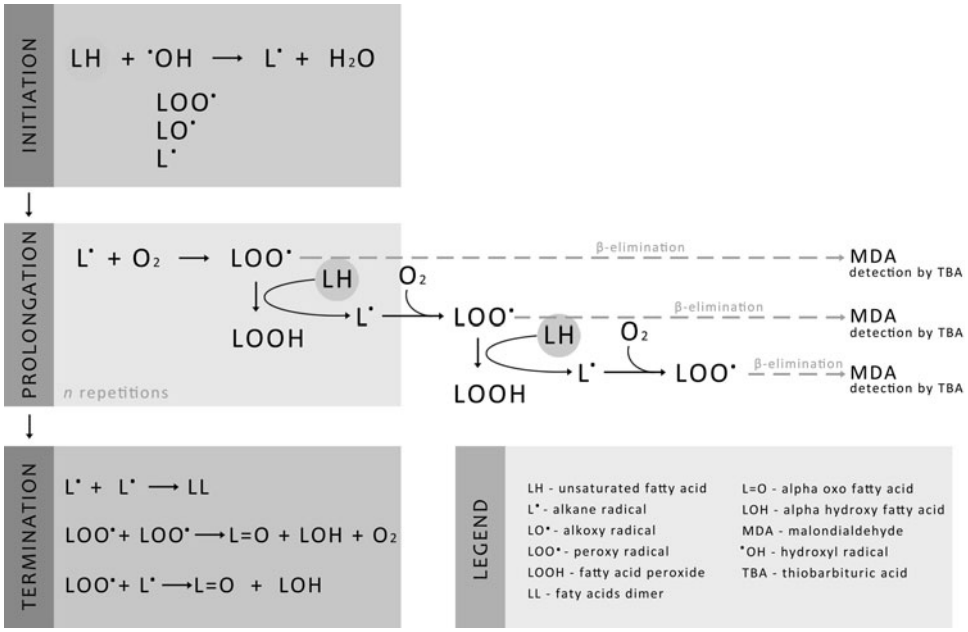

Fig. 2 Non-enzymatic lipid peroxidation. In the first stage some radicals detach hydrogen from unsaturated fatty acids. The product, alkane radical, may react with molecular oxygen and forms peroxyl radical which can detach hydrogen from next unsaturated fatty acid. This reaction can go many times up to termination, last stage of lipids peroxidation where radicals react with each other and form damaged lipids. Products of lipids peroxidation after β-elimination usually form malondialdehyde detected by thiobarbituric acid

Studies of Pb with *Potamogeton crispus* (freshwater plant) showed that the high peroxidases activities and MDA content were observed with an increase in Pb concentration, whereas SOD and CAT activities first decreased and then increased. Simultaneously, high concentrations of Pb aggravated ultrastructural damage to leaf cells including disruption of chloroplasts, mitochondrial cristae, nuclear membrane and nucleoli and disappearance of chloroplast envelopes, vacuolation of mitochondria and condensation of chromatin. Changes in antioxidative enzymes activities and damage to fine structure are the results of Pb-induced ROS accumulation (Hu et al. 2007). Concomitant changes in CAT, POD and SOD activities are responsible for removal and destruction of ROS, and hence referred as antioxidative enzymes; however, they have got important bearings on the oxidative damage of membranes in organisms under oxidative stress conditions (Ghnaya et al. 2009).

Metals such as Ca, Mg, Cu, Zn and Mn are essential for plant growing. However, little is known about the effects of all these metals as oxidative stress factors in plants. The responses of antioxidative enzymes such as SOD, CAT, AsAdep POD and guaiacol-dependent peroxidase (Gua-dep POD) activities and also LP levels can serve as indicators of oxidative damage induced by Ca, Mg, Cu, Zn and Mn. Experiment with *Mentha pulegium* grown in the excess and absence of Cu^{2+}, Zn^{2+} and Mn^{2+} as micronutrients showed that under excess Cu significantly increased all antioxidant enzymes such as SOD, CAT AsA-dep POD and Gua-dep POD, evidence of Haber–Weiss reaction (Fig. 4), which leads to maximum increases of LP levels (Candan and Tarhan 2003). Inhibition of SOD, CAT and AsA-dep POD activities under excess Zn^{2+} condition caused higher LP levels than the Mn stress condition. Excess Mn^{2+} enhances the activity of SOD and CAT enzymes, whereas they decreased in the absence of Mn^{2+}. Activities of AsA-dep and Gua-dep POD were inversely related to SOD and CAT activities. Increases of CAT activities together with SOD caused lower LP levels in *M. pulegium* under Mn^{2+} toxicity than Cu^{2+} and Zn^{2+} and provide a partial protection against oxidative damage. Candan and Tarhan (2003) also reported the potential of Mn, Zn and Cu to cause oxidative damage in the following order Mn < Zn < Cu.

Extended research on HMs influence on enzymes activity resulted in numerous reports on changes in in vivo and in vitro activities. For instance, the expression of genes of cytosolic Cu, Zn-SOD slightly decreased, while the Mn-SOD increased in the presence of excess Cd ions (Ann et al. 2011). Cd (15 μM) treatment at the germination stage in *Solanum nigrum* showed that activities of SOD and APX were increased and CAT was decreased after 45 days of treatment (Fidalgo et al. 2011). It has also been reported that activities of SOD, CAT, APX, and DHAR increased upon Cd treatment in two varieties of rice (Iqbal et al. 2010). Observations revealed an increase in the activity of

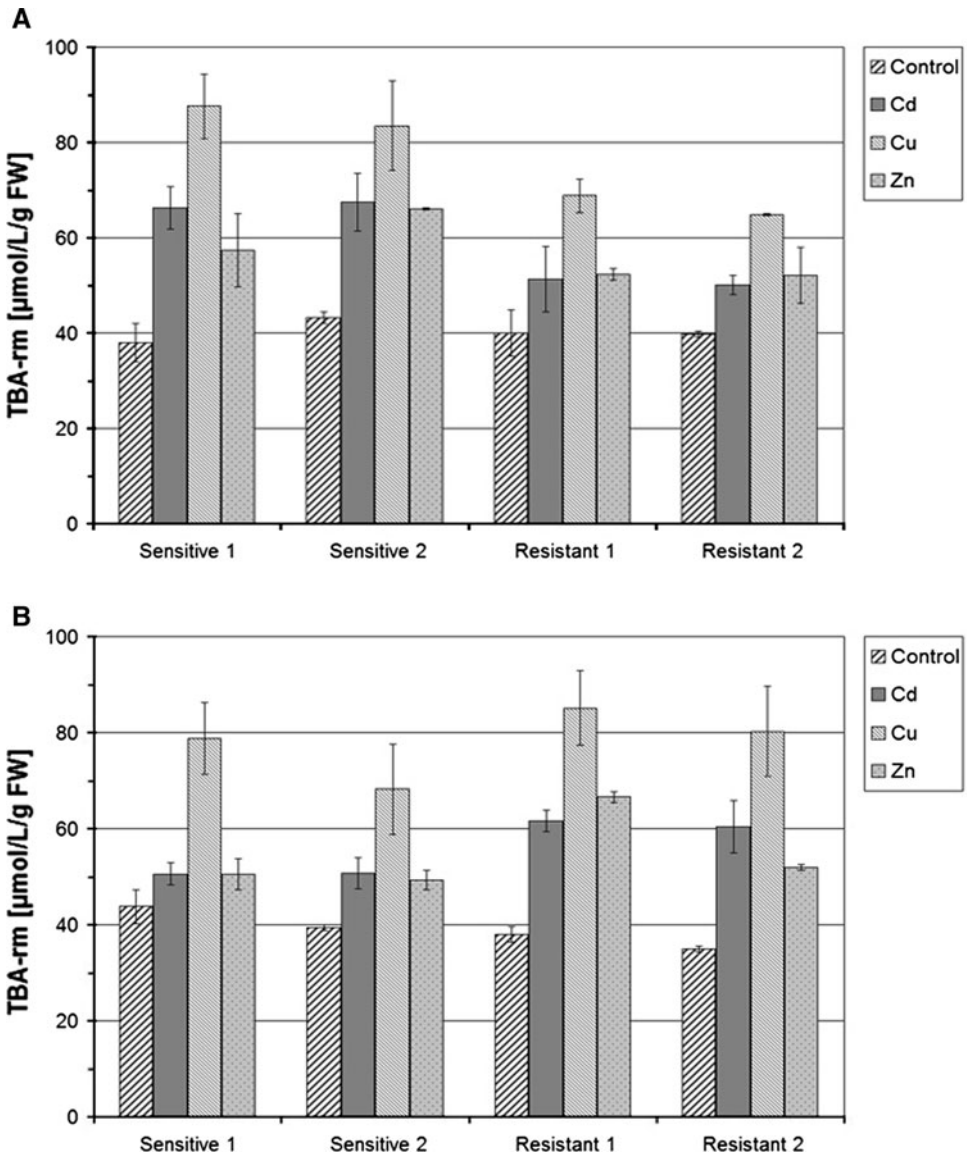

Fig. 3 The concentration of TBA-rm in shoots (**a**) and roots (**b**) in two sensitive and two resistant (to Cd, Cu and Zn) clones of *Salix viminalis*. The concentration was measured relative to plant fresh weight. Cuttings were treated with 7 µmol/L $CdCl_2$, 3 µmol/L $CuCl_2$, 70 µmol/L $ZnCl_2$ for 20 days. Lipid peroxidation by metals was measured according to Landberg and Greger (2002)

SOD, CAT, POD and APX coinciding with the time of cultivation. Pb-dependent increase in activities of SOD, CAT, APX, GST and POD from wheat seedling extracts was observed at 0.15, 0.30, 1.5 and 3.0 mM of Pb concentration (Lamhamdi et al. 2011). It was reported that in potato tuber parenchyma tissue the APX activity decreased during the first hour of Cd treatment from a cultivar more tolerant to Cd. This cultivar showed constitutively higher CAT activity, and CAT synthesis was induced faster by Cd ions in parenchyma than in other more susceptible tissues (Stroinski and Kozlowska 1997). The other studies revealed that cooperative action of CAT, POD and APX is required for protection against the toxic effects of reduced oxygen species.

HMs (Cd, Cu, Pb, Zn at 0.1, 1, 10, 100 and 1,000 µM concentrations) exposure disturbed the cellular redox status in *Fontinalis antipyretica*. These HMs induced significant changes in SOD and CAT activities and increased LP level. Moreover, the SOD activity and MDA level often presented clear linear relationships with a wide range of HMs concentrations. This suggested that these enzymes could be used as environmental biomarkers of HMs pollutions (Dazy et al. 2009). The activity of antioxidant enzymes depends on exposure dose of HM. Ni ions, at

Table 1 Summary of the responses of ROS, MDA, antioxidative enzymes and glutathione (GSH) levels in different plants exposed to various toxic heavy metals (HMs) and metalloid

Plant species	HMs	Concentrations	Antioxidant systems								References
			ROS	MDA	SOD	CAT	POX	APX	GR	GSH	
Talinum triangulare	Pb	0.25–1.25 mM	↑	↑						↑↓	Kumar et al. (2012)
Brassica juncea	Ni	100 mg kg^{-1}	↑	↑	↑	↑	↑				Yusuf et al. (2012)
Sedum alfredii	Pb	10–200 μM	↑	↑	↑	↑	↑	↑		↑	Huang et al. (2012)
Pisum sativum	Cr	50–250 μM			↑	↓		↑	↓	↓	Gangwar et al. (2011)
Oryza sativa	Pb	50–200 μM	↑	↑↓	↓	↑	↑↓	↓	↑	↑	Panda et al. (2011)
Arabidopsis thaliana	Cd, Cu	Cd–10 μM; Cu–5 μM	↑	↑	↑	↑(Cd) ↓(Cu)		↑(Cd) ↓(Cu)	↑(Cd) ↓(Cu)	↑	Ann et al. (2011)
Solanum nigrum	Cd	15 μM		↑	↑	↑		↑			Fidalgo et al. (2011)
Triticum aestivum	Pb	0.15–3 mM	↑	↑	↑	↑	↑	↑			Lamhamdi et al. (2011)
Brassica juncea	Cd	25–50 μmol L^{-1}	↑	↑	↑	↑		↑	↑	↑	Iqbal et al. (2010)
Fontinalis antipyretica	Cd, Zn, Cu, Pb	0.1–1,000 μM		↑	↑	↑		↑(Cd, Zn, Cu); ↓(Pb)	↓		Dazy et al. (2009)
Lemna minor	Cu	25–100 μM		↑	↑	↓					Kanoun-Boulé et al. (2009)
Elodea canadensis	Ni	10–50 μM		↑	↑	↓			↑		Maleva et al. (2009)
Ceratophyllum demersum	Cd	1–10 μM							↓	↑	Mishra et al. (2009)
Wolffia arrhiza	Pb	1–1,000 mM		↑		↑				↑	Piotrowska et al. (2009)
Medicago sativa	Hg	10 μM		↑	↑		↑	↓	↓	↓	Zhou et al. (2009)
Brassica oleracea	Cu	2.5 mM		↑	↑	↓	↑	↑	↓		Posmyk et al. (2009)
Arachis hypogaea	Cd	25–100 μM			↑	↑	↑	↑	↑		Dinakar et al. (2008)
Sedum alfredii	Pb	0.02–0.2 mM		↑	↑	↓					Liu et al. (2008)
Elsholtzia haichowensis	Cu	10–300 μM	↑	↑	↑	↑	↑	↑			Zhang et al. (2008)
Ceratophyllum demersum	As	10–250 μM	↑	↑	↑			↓	↓	↑	Mishra et al. (2008)
Brassica juncea	Cd	25–100 mg kg^{-1}	↑	↑	↑	↑		↑	↓↑		Mobin and Khan (2007)
Potamogeton crispus	Pb	5–20 mg L^{-1}		↑	↓	↓	↑				Hu et al. (2007)
Triticum aestivum	Cd	100 mg kg^{-1}	↑	↑	↑	↑		↑	↑		Khan et al. (2007)
Arabidopsis thaliana	Cd, Cu	100 μM	↑	↑	↑(Cd); ↓(Cu)	↑(Cd); ↓(Cu)		↑			Maksymiec and Krupa (2006)

Table 1 continued

Plant species	HMs	Concentrations	Antioxidant systems								References
			ROS	MDA	SOD	CAT	POX	APX	GR	GSH	
Macrotyloma uniflorum, Cicer arietinum	Pb	1–4 mM		↑	↑	↑	↑		↑	↑	Reddy et al. (2005)
Oryza sativa	Pb	500–1,000 μM		↑	↑	↓	↑	↓	↑		Verma and Dubey (2003)
Vicia faba	Cd	2–2,000 μM			↑	↓	↑		↑		Cordova et al. (2003)
Mentha pulegium	Ca, Mg, Cu, Zn, Mn	Ca, Mg 2–4 mM; Cu, Zn, Mn 1 μM		↑	↑						Candan and Tarhan (2003)

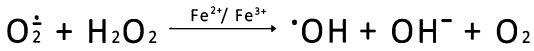

Fig. 4 Haber–Weiss reaction catalyzed by iron

concentrations up to 10 μM could induce sub-lethal oxidative stress in *Elodea canadensis* leaves. The appearance of several new polypeptides with apparent molecular weights below 20 kDa was found by SDS-PAGE in Ni treated *E. canadensis* leaves (Maleva et al. 2009). Wang et al. (2004) reported that Cu treatment causes increases in activities of POD, APX, SOD and decrease in activity of CAT in *B. junicea* seedlings.

Connections between enzymatic system and other antioxidants during HMs stress

The HMs effect on living organisms depends on their chemical and physical properties. It is possible to select three different molecular mechanisms of HMs toxicity: (a) ROS production via the auto-oxidation or via Fenton reaction, (b) blocking of essential functional groups in biomolecules and (c) substitution of necessary metal ions from biomolecules (Schützendübel and Polle 2002). The cellular redox state maintains normal cell homeostasis and is a key determinant of metal phytotoxicity. HMs ions are well-known causing agent for altering cellular redox balance. Influence of HMs on the cellular redox balance is connected with development of oxidative stress and damage in plants. In these conditions the ability of plants to resist oxidative stress while using antioxidant systems is limited. Many studies showed that ample amount of HMs leads to reduction of redox active enzymes activities. The cellular redox state is made of the individual redox active molecules in cells and for each of them redox state can be defined as the ratio between reduced and oxidized molecules within a pool (Potters et al. 2010; Huang et al. 2012). Components of cellular redox state are ascorbate (ASC), glutathione (GSH or GSSG) and pyridine nucleotides nicotinamide adenine dinucleotide (NAD^+) and nicotinamide adenine dinucleotide phosphate ($NADP^+$) (Ann et al. 2011). The literature data testify that exposure of plants to high concentrations of redox active metals, such as Cd and Cu results in an oxidative damage (Ann et al. 2011). The investigation with short-term exposition of Cd^{2+} and Cu^{2+} induces accumulation of $O_2^{\bullet-}$ and H_2O_2 in *Arabidopsis thaliana*. Furthermore, only excess Cd induces the SOD activity. But theses responses were decreased in the presence of imidazole and propyl gallate, inhibitors of NADPH (reduced $NADP^+$) oxidase and jasmonate synthesis pathway. The authors suggest that Cd and Cu-induced accumulation of $O_2^{\bullet-}$ and H_2O_2 was mostly connected with the activity of NADPH oxidase, induction of jasmonate signaling pathways and partially due to increased SOD activity (Maksymiec and Krupa 2006).

Glutathione is widely distributed redox active molecule in living cells and the tripeptide GSH (γ-Glu-Cys-Gly) is playing a key role in scavenging ROS and protecting membrane to damage by these ROS. The oxidized form of glutathione (GSSG) is readily converted to reduced form (GSH) by the enzyme glutathione reductase (GR). GR also plays a key role in the antioxidant defense processes, by reducing GSSG, thus allowing a high GSH/GSSG ratio to be maintained. Study on maize plantlets after 6 days action of low Cd concentration showed to increase in GR and glutathione peroxidase (GP) activity (Syshchikov 2009). This is well explained by the response of sugarcane treated with Cd. The analysis of leaves and roots of sugarcane plant has consistently shown that GR activity increases in response to Cd exposure to detoxify H_2O_2 or to produce glutathione for the synthesis of phytochelatins, whereas CAT activity has been shown to exhibit considerable variability (Fornazier et al. 2002).

The results with decrease GR activity were observed in research with Cd action on plants *Vicia faba*. The negative correlation of antioxidative enzyme activity to concentration of Cd was showed (Cordova et al. 2003). GR is a member of flavoenzyme family which catalyzes the NADPH-dependent reduction of glutathione disulphide (GSSG) to glutathione (GSH). This reaction maintains a proper GSH/GSSG ratio in cells. For example, in rice seedlings Pb toxicity causes an increase in GSH/GSSG ratio and the total glutathione pool. On the other hand, decrease in GSH/GSSG ratio was observed in Pb-treated *Talinum triangulare* leaf (Kumar et al. 2012). The authors suggested that this is evidently due to induction in GSH biosynthesis and rapid reduction of GSSG by the enzyme GR after Pb treatment. Verma and Dubey (2003) reported that GR activity increased which suggests possible involvement of GR in regenerating GSH from GSSG under Pb ions action. The increase in activity of GR after Cd treatment was reported in leaves of *Ceratophyllum demersum* (Mishra et al. 2009) and *B. juncea* (Iqbal et al. 2010).

High concentrations of HMs induce activity of $NADP^+$-reducing enzymes. The $NADP^+$ dependent antioxidant enzymes phosphoenolpyruvate carboxylase, NADP-malic enzyme (NADP-ME), and pyruvate, phosphate dikinase participate in the process of concentrating CO_2 in C4 photosynthesis. Non-photosynthetic counterparts of these enzymes, which are present in all plants, play important roles in the maintenance and replenishment of Krebs cycle intermediates, thereby contributing to the biosynthesis of amino acids and other compounds and providing NADPH for biosynthesis and the antioxidant system. Enhanced activities of PEPC and/or NADP-ME and/or PPDK were found in plants under various types of abiotic stress, such as presence of HMs in the soil (Doubnerová and Ryšlavá 2011).

The electron spin resonance spectra indicated a drastic increase in hydroxyl radicals ($OH^{\bullet -}$) in the free-floating hydrophyte *C. demersum* after 10 μmol L^{-1} Cd treatments, which was closely correlated with the enhanced formation of H_2O_2 and generation of $O_2^{\bullet -}$ triggered by the NADPH oxidation (Kawano et al. 2001). The supplementation with Zn (10–200 μmol L^{-1}) to 10 μmol L^{-1} Cd treatments significantly decreased the production of free radicals, especially by eliminating precursors of $OH^{\bullet -}$ through inhibition of NADPH oxidation. Cd-induced ROS production which substantially increased the oxidative products of proteins measured as carbonyls was effectively inhibited by Zn supplementation (Aravind et al. 2009).

A different mechanism of metal tolerance has been reported in *Lemna minor* and *Spirodela polyrrhiza* from the uranium-polluted area. Tolerance was based on the existence of protective mechanism limiting the metal uptake rather than enhancement of the antioxidative metabolism. Rather the electric conductivity (EC) and MDA content were increased after Cu exposure, direct symptoms of oxidative stress. Significant increase of EC was observed in *L. minor* from a non-contaminated pond for all Cu concentrations while the increase of EC in *L. minor* and *S. polyrrhiza* (from the uranium-polluted area) became significant only after 50 μM Cu treatment. However, MDA content significantly increased at all treated plants. It was also reported that the protein content and CAT activity declined with an increasing Cu concentration. In contrast, a significant effect of Cu on CAT activity was observed only in uranium-polluted area. Further, SOD activity increased with increasing concentrations of Cu, in a very similar trend between the three duckweed populations (Kanoun-Boulé et al. 2009).

Role of phenols and flavonoids under HMs stress

Parallel to enzymatic system plant cells posses a non-enzymatic antioxidative defense system against ROS, which included phenols and flavonoids. Synthesis of isoflavonoids is an effective strategy against ROS. Phenolic compounds which could be also substrates for different peroxidases were the first line of defense against Cu stress in experiment with red cabbage (Posmyk et al. 2009). The analysis of antioxidant enzyme activities suggested that peroxidases were the most active enzymes in Cu-exposed red cabbage seedlings. Plant phenolic compounds such as flavonoids and lignin precursors have been recognized largely as beneficial antioxidants which can scavenge harmful active oxygen species. Phytophenolics can act as antioxidants by donating electrons to guaiacol type peroxidases (GuPXs) for detoxification of H_2O_2 produced under stress conditions (Sakihama et al. 2002). The electron spin resonance signals of phenoxyl radicals are eliminated by monodehydroascorbate (MDHA) reductase, suggesting that phenoxyl radicals, like the ascorbate radical, are enzymatically recycled to parent phenolics. Thus, phenolics in plant cells can form an antioxidant system equivalent to that of ascorbate. In contrast to their antioxidant activity, phytophenolics also have the potential to act as pro-oxidants under certain conditions. Zn, Ca, Mg and Cd have been found to stimulate phenoxyl radical-induced lipid peroxidation (Sakihama et al. 2002). It was shown in experiment with *Raphanus sativus* that phenolic acids as well as the total and reduced ascorbate content increased with the intensification of Cu treatment. In parallel with increase membrane damage and lipid peroxidation, process of glutathione oxidation was also stimulated under elevated Cu concentration; indicating an acceleration of oxidative processes. Accumulations of phenolic compounds were

also observed in roots of maize (Shemet and Fedenko 2005) and scot pine (Schützendübel et al. 2001) under Cd treatment. The possible reason for the induction of phenolic metabolism may be the increase of phenylalanine ammonia lyase activity, which is observed under stress conditions (Schützendübel et al. 2001). In maize roots it was due to the increase in content of cyanidin-3-glucoside with its chromophore group modified by binding to Cd ions (Shemet and Fedenko 2005). The phenolic metabolism in tea (*Camellia sinensis* L.) callus culture showed Cd-depended response. The content of phenolic compounds, including flavones, in the leaf calli decreased, while in the stem and root calli it increased (at the Cd concentration of 6.3×10^{-5} M) or was close to a control one (at the Cd concentration of 10.6×10^{-5} M). The lignin content in root and stem calli increased, but it did not change in the leaf calli (Zagoskina et al. 2007).

Flavonoids are considered as large family of plant secondary metabolites and are well known antioxidants. Antioxidants such as anthocyanins (in vacuole) and tocopherol (membrane associated) are major components found in the plants and protect them against oxidative stresses (Araceli et al. 2009; Hernandez et al. 2009). It is well known that the compounds which are easy to oxidize are often the best antioxidants. Flavonoids have ability to capture free radical ions by donation of phenolic hydrogen atoms and showed antioxidant activity may protect plant cells from adverse effects of abiotic stresses (Hernandez et al. 2009). In particular, anthocyanins have shown a higher antioxidant activity than vitamins C and E (Araceli et al. 2009). It is reported that in maize seedlings cyanidin is localized at external parts of root's parenchyma. Therefore, this localization probably has adaptive role as barrier in adaptation to Cd stress. This might be as result of either antioxidative ability of anthocyanins and flavonoids, which increases upon HMs action, or accumulation of anthocyanin which coincides with the highest content of Cd in root tissues (Yamasaki et al. 1997). α-Tocopherol is chemically the most active form of vitamin E and is capable of scavenging free oxygen radicals and lipid peroxides. The tocopherol biosynthesis mainly takes place in plastids of higher plants from two precursors derived from metabolic pathways such as homogentisic acid and phytyl diphosphate. The former is an intermediate of degradation of aromatic amino acids and latter one arises from methylerythritol phosphate pathway (Lushchak and Semchuk 2012). α-Tocopherol may be involved in the protection of the plant tissues against oxidative stress and can physically quench O_2 in chloroplast. It has been estimated that before being degraded, one molecule of α-tocopherol can deactivate up to 220 O_2 molecules by resonance energy transfer. In addition, the α-tocopherol can chemically scavenge O_2 and lipid peroxyl radicals (Munne-Bosch 2005). α-Tocopherol levels can change significantly during the environmental stress conditions. It has been reported that abiotic stress factors, in particular HMs, might alter the different form of α-tocopherol levels in plant tissues (Collin et al. 2008; Yusuf et al. 2010; Lushchak and Semchuk 2012; Kumar et al. 2012). *A. thaliana* treated with 75 μM Cd and 75 μM Cu showed increase in α-tocopherol content in comparison with control. The increased concentration of α-tocopherol in Cd- or Cu-treated *Arabidopsis* leaves was associated with the up-regulation of a number of genes related to tocopherol biosynthesis (Collin et al. 2008). Experiment with wild-type and transgenic *B. juncea* plants of over expressing the γ-TMT gene showed Cd-induced increased accumulation of α-tocopherol in both plants compared with control (Yusuf et al. 2010). An increase in tocopherol content in the shoots was associated with the enhancement of LP in wheat exposed to Ni (Gajewska and Skłodowska 2007). This antioxidant is able to scavenge of lipid peroxides, and thus its increased concentration might result in the reduction of oxidative injuries of cell membranes.

Role of ROS in signaling cascades under HMs stress

Excessive amounts of HMs trigger a wide range of cellular responses including changes in gene expression and synthesis of metal-detoxifying peptides. Mitogen-activated protein kinase (MAPK) cascades are signaling modules which transfer information from sensors to cellular responses and represent an evolutionary conserved signaling mechanism in eukaryotes (MAPK Group 2002). It has been reported that MAPK cascades are likely to be one of the converging points in the defense-signalling network under both biotic and abiotic stress in plants (Nakagami et al. 2005). Basically, MAPK cascades engage the stimulus-triggered activation of MAPK kinase kinase (MAPKKK) which phosphorylates a MAPK kinase (MAPKK). MAPKK further phosphorylates a MAPK. It has been reported that plants have an unusually large number of MAPK components, such as more than 20 MAPKs, 10 MAPKKs and 60 MAPKKKs (MAPK Group 2002). Plants respond to HMs stress by induction of several distinct MAPK pathways under elevated levels of Cu and Cd. Exposure of *Medicago sativa* L. plants to excess Cu or Cd ions activated four distinct MAPKs: SIMK (salt stress-induced MAPK), MMK2 (*Medicago* MAPKK), MMK3 (*Medicago* MAPKKK) and SAMK (stress-activated MAPK). Comparison of the kinetics of MAPK activation revealed that SIMK, MMK2, MMK3 and SAMK are very rapidly activated by Cu ions, while Cd ions induced delayed MAPK activation (Jonak et al. 2004).

Plants exposed to HMs, synthesize a set of diverse metabolites that include specific amino acids, such as

proline and histidine, peptides such as glutathione, phytochelatins (PCs) and the amines (Sharma and Dietz 2006). These molecules have three major functions, namely metal binding, antioxidant defense and signaling. Some amino acids, particularly proline (Pro) and histidine (His), also play roles in the chelation of metal ions both within plant cells and in the xylem sap (Rai 2002; Sharma and Dietz 2006). Pro executes the significant beneficial functions under metal stress. Many plants have been reported to accumulate Pro when exposed to HMs (Talanova et al. 2000; Yusuf et al. 2012). His, glutathione and PCs play a role in metal binding while polyamines function as signaling molecules and antioxidants. Their accumulation is considered as active plant response. Therefore, content changes of these metabolites bear functional significance in the metal stress tolerance (Sharma and Dietz 2006). Exposure of hyperaccumulator *Alyssum lesbiacum* to Ni is known to result in a dose-dependant increase in xylem sap concentrations of both Ni and the chelators free His. It has been reported that an enhanced release of Ni into the xylem is associated with concurrent release of His from an increased root-free His pool. Particularly in *B. juncea* roots, Ni uptake is independent of simultaneous uptake of His (Kerkeb and Krämer 2003). Siripornadulsil et al. (2002) have demonstrated that increased Pro levels provide enhanced protection against Cd in microalgae. It is interesting to note that Pro reduces Cd stress not by sequestering Cd, but by reducing Cd-induced free radical damage and maintaining a stringent reducing environment (higher GSH levels) within the cell (Siripornadulsil et al. 2002).

Role of sulfur metabolism and metal binding phytochelatins in HMs detoxification

Production of ROS and damage of plant cells as a result of oxidative stress are characteristic of the action of HMs such as Cd and Zn. Plants exposition on HMs solutions cause the reactions of the antioxidant systems which depend on plant type, tissues which are explored, metals which are used in an experiment and intensity of stresses. In most cases, HMs cause decline of level of glutathione in plant tissues. Such reaction is usually observed after actions of Cd and predefined the growing consumption of glutathione, which is used for the synthesis of PCs (Anjum et al. 2012; Zhao et al. 2010; Cobbett 2000). The PCs consist of repeating units of γ-glutamylcysteine followed by a single C-terminal glycine, with the number of repeating units ranging from 2 to 11 (Anjum et al. 2012; Cobbett 2000). PCs are synthesized enzymatically by PC synthase (PCS) by the transfer of γ-Glu-Cys moieties to glutathione (GSH) (Thangavel et al. 2007; Zhao et al. 2010). PCS was purified from a variety of plant species and was found to be produced constitutively in the absence of metal induction (Grill et al. 1986). PCs have important role in detoxification of HMs and also metalloids, in particular arsenate. Arsenate and arsenite are easily absorbed by plants and induces the biosynthesis of PCs in vivo and in vitro. Arsenate and arsenite induced PCs were observed in the cellular cultures of *Rauvolfia serpentine* and *Silene vulgaris* and in germinating seeds of *A. thaliana* (Schmoger et al. 2000). At the same time, in literature there is information that expression of iron (Fe) and Cu chelators, for example, metallothioneins (MTs) and PCs protects plants from metal-induced oxidative damages (Schützendübel et al. 2001; Schützendübel and Polle 2002). They are effective in binding metal ions by formation of stable metal–PC complexes, thereby reducing the intracellular concentration of free metal ions (Cobbett 2000). Significant increases were observed in the levels of various thiols including PCs, the activities of enzymes of thiolic metabolism as well as arsenate reductase in the *C. demersum* under As toxicity (Mishra et al. 2008).

Sulfur metabolism tightly regulates biosynthesis of PCs in plants through the regulation of GSH and helps metal sequestration (Thangavel et al. 2007). Sulfur is incorporated into organic molecules in plants and is located in thiol (–SH) groups in proteins (cys-residues) or non-protein thiols. Cd exposure to *Egeria densa* (water weed) resulted in both a formation of thiol-enriched Cd complexing peptides and a synthesis of low-molecular-weight metal chelators. Two Cd-binding fractions, a thiol-enriched fraction and a non-thiol fraction with a lower molecular weight were identified in extracts by gel filtration. The main fraction of thiol-containing polypeptide, purified by gel filtration and anion-exchange chromatography had a molecular weight of 10 kDa. This peptide was characterized by a broad absorption band specific to mercaptide bonds and Cd-sensitive fluorescence emission of aromatic amino acid residues (Malec et al. 2009).

Sulfonic acids, which contain S as SO_3^{3-} and are found in glucose-6-sulfonate, cysteic acid and sulfolipids (Pilon-Smits and Pilon 2000) are also playing a role in detoxification of HMs. Sulfoquinovosyldiacyglycerol (SQDG), deacylation product of sulpholipid, is a the predominant sulfur-containing lipid present in plants. This sulfolipid is present in plastid membranes and likely is involved in chloroplast functioning. The route of biosynthesis and physiological function of sulfoquinovosyl diacylglycerol is still under investigation. Recent studies have provided the evidence showing that the sulfite is the likely sulfur precursor for the formation of the sulfoquinovose group of this lipid (Harwood and Okanenko 2003). Cd-induced a decrease in SQDG contents in *B. napus* leaves, which was accompanied by a sharp increase in extra-chloroplastic lipids (Youssef et al. 1998). It is reported that Pb treatment at various concentrations decreased SQDG in leaves of *T. triangulare* (Kumar et al. 2012) and in leaves and roots of wheat (Okanenko et al., 2003). It is possible due to the competitive usage of sulfur for sulfur-containing Cys-rich

peptides (PCs/MTs), protein synthesis and essential metabolites rather than for SQDG synthesis (Sato et al. 2000).

PC synthesis is induced by a variety of HMs (Schützendübel and Polle 2002; Shaw et al. 2005; Mishra et al. 2008, 2009; Ahmad and Prasad 2012). The significant increase in the activities of cysteine synthase, glutathione-*S*-transferase (GST), GR and PCS were noticed in response to Cd (Mishra et al. 2009). PCs link HMs, the complexes formed with them are then transported to tonoplast which transfers to the vacuole, where they get stored and detoxified from cells. An ABC-transporter, Hmt1, accepting low-molecular-weight PC-HM complexes as substrate, has been identified in *Schizosaccharomyces pombe* (Ortiz et al. 1995), and an MgATP-dependent transport activity for PC_3 and PC_3-Cd complexes has also been demonstrated in plants (Salt and Rauser 1995). This mechanism is characteristic of many types of plants.

The PCS genes in wheat (Clemens et al. 1999) and in *Arabidopsis* (Lee and Korban 2002) are regulated at the transcriptional level. However, transcriptional regulation of *AtPCS1* in *Arabidopsis* is observed only during early developmental stages, and it disappears as plants grow older (Lee and Korban 2002). Molecular characterization of PCS gene expression in transgenic *Arabidopsis* has revealed its presence in leaves, roots, cotyledons and stems, but not in root-tips or root hairs throughout all stages of plant development (Lee et al. 2002). In an attempt to understand the structural/functional organization of PCS, Rutolo et al. (2004) conducted a limited proteolyses analysis of the *Arabidobsis At*PCS1 enzyme followed by functional characterization of the resulting polypeptide fragments. Their results suggested that *At*PCS1 is composed of a protease-resistant, presumably highly structured, N-terminal domain and flanked by an intrinsically unstable C-terminal region. Sachiko et al. (2009) carried out point mutations into the PCS by replacing Cys358, Cys359, Cys363 and Cys366 residues with Ala and noted lower PCs synthesis ability of mutant than the wild-type enzyme (Sachiko et al. 2009). Furthermore, mutant PCS experienced more damage than wild-type under oxidative conditions which suggests the importance of Cys-rich region of PCS for antioxidant activity. Zhang et al. (2010) studied the relationship between PCs synthesis and Cd accumulation in Cd-hyperaccumulator *S. alfredii* and suggested that PCs do not detoxify Cd in roots but might act as the major intracellular Cd detoxification mechanism in shoots like in non-resistant plants (Zhang et al. 2010).

Conclusions and perspectives

The published literatures provide convincing evidence, as presented above, suggesting the crucial roles of enzymatic and non-enzymatic antioxidants in different plants under HMs stress. Non-enzymatic antioxidants include redox active molecules, phenols and flavonoids. There is a lack of reports on extensive molecular aspects of HMs influence on the redox state of such compounds as such as glutathione, ascorbate, pyridine nucleotides NAD(P)H and their redox couple GSH/GSSG, AsA/MDHA and NAD(P)H/$NAD(P)^+$ in plants. Much progress has been done on different aspects of PCs and glutathione metabolisms and its related enzymes, taking into consideration their significance in HMs uptake, distribution and detoxification mechanisms in plants. But a number of questions such as the regulation of thiols in SQDG metabolism and molecular metabolic characterization of sulfur, phenolics and flavonoids in economically important plant species growing under the influence of various HMs are yet to be answered. Further attention should be paid to the possible involvement of fast and transient activation of signaling component, MAPK, and other redox active systems in plants with HMs accumulation ability and sensitivity should be thoroughly investigated.

Author contribution The work presented here is accomplished with contributions from all authors. Oksana Sytar and Abhay Kumar contributed equally to this manuscript viz., literature survey, preparation of the draft manuscript and bear the basic responsibility. Dariusz Latowski, Paulina Kuczyńska and Kazimierz Strzałka provided key inputs on oxidative damage, defense reactions and detoxification mechanisms and also contributed three figures (Figs. 2, 3, 4). The idea to prepare a review on this subject-specific topic was moved by M.N.V. Prasad who provided basic information and outlines. M.N.V. Prasad and Kazimierz Strzałka together structured it critically and brought it to this present format.

Acknowledgments O.S. gratefully acknowledges the award of 3-month research training scholarship by the Centre for International Co-operation in Science (CICS) (Formerly CCSTDS) Chennai, India, which was hosted by MNVP. A.K. gratefully acknowledges University of Hyderabad Research Scholarship through the University Grant Commission, New Delhi. M.N.V.P. gratefully acknowledge the award of Pitamber Pant National Environment Fellowship by the Ministry of Environment and Forests, GOI, New Delhi (MoEF Ref. No. 17/3/2010-RE Dt 29-2-2012).

Conflict of interest The authors declare that they have no conflict of interest.

References

Ahmad P, Prasad MNV (2012) (eds) Abiotic stress responses in plants: Metabolism, productivity and sustainability. Springer, New York. ISBN 978-1-4614-0633-4

Anjum NA, Ahmad I, Mohmood I, Pacheco M, Duarte AC, Pereira E, Umar S, Ahmad A, Khan NA, Iqbal M, Prasad MNV (2012)

Modulation of glutathione and its related enzymes in plants' responses to toxic metals and metalloids- a review. Environ Exp Bot 75:307–324

Ann C, Karen S, Jos R, Kelly O, Els K, Tony R, Nele H, Nathalie V, Suzy VS, Frank VB, Yves G, Jan C, Jaco V (2011) The cellular redox state as a modulator in cadmium and copper responses in *Arabidopsis thaliana* seedlings. J Plant Physiol 168:309–316

Appenroth KJ, Teller S, Horn M (1996) Photophysiology of turion formation and germination in *Spirodela polyrhiza*. Biol Plant 38:95–106

Araceli CO, Ma de Lourdes PH, Ma Elena PH, Rodríguez JA, Carlos Andrés GV (2009) Chemical studies of anthocyanins. Rev Food Chem 13:859–871

Aravind P, Prasad MNV, Malec P, Waloszek A, Strzalka K (2009) Zinc protects *Ceratophyllum demersum* L. (free floating hydrophyte) against reactive oxygen species induced by cadmium. J Trace Elem Med Biol 23:50–60

Babu NG, Sarma PA, Attitalla IH, Murthy SDS (2010) Effect of selected heavy metal ions on the photosynthetic electron transport and energy transfer in the thylakoid membrane of the cyanobacterium, *Spirulina platensis*. Acad J Plant Sci 3:46–49

Bertrand M, Schoefs B, Siffel P, Rohacek K, Molnar I (2001) Cadmium inhibits epoxidation of diatoxanthin to diadinoxanthin in the xanthophyll cycle of marine diatom *Phaeodactylum tricornutum*. FEBS Lett 508:153–156

Bezdudna EF (2009) Influence of heavy metal salts on activity of glyoxylate cycle enzymes and mitochondrial succinate dehydrogenase in germinating soybean seeds. Physiol Biochem Cultiv Plants 41:176–182

Candan N, Tarhan L (2003) The correlation between antioxidant enzyme activities and lipid peroxidation levels in *Mentha pulegium* organs grown in Ca^{2+}, Mg^{2+}, Cu^{2+}, Zn^{2+} and Mn^{2+} stress conditions. Plant Sci 165:769–776

Chugh LK, Sawhney SK (1999) Photosynthetic activity of *Pisum sativum* seedling grown in presence of cadmium. Plant Physiol Biochem 37:297–303

Clemens S, Kim EJ, Neumann D, Schroeder JI (1999) Tolerance to toxic metals by a gene family of phytochelatin synthases from plants and yeast. EMBO J 18:3325–3333

Cobbett CS (2000) Phytochelatin biosynthesis and function in heavy-metal detoxification. Curr Opin Plant Biol 3:211–216

Collin VC, Eymery F, Genty B, Rey P, Havaux M (2008) Vitamin E is essential for the tolerance of *Arabidopsis thaliana* to metal-induced oxidative stress. Plant Cell Environ 31:244–257

Cordova REV, Valgas C, Souza-Sierra MM (2003) Biomass growth, micronucleus induction, and antioxidant stress enzyme responses in *Vicia faba* exposed to cadmium in solution. Environ Toxicol Chem 22:645–649

Dazy M, Masfaraud JF, Ferard JF (2009) Induction of oxidative stress biomarkers associated with heavy metal stress in *Fontinalis antipyretica* Hedw. Chemosphere 75:297–302

Dinakar N, Nagajyothi PC, Suresh S, Udaykiran Y, Damodharam T (2008) Phytotoxicity of cadmium on protein, proline and antioxidant enzyme activities in growing *Arachis hypogaea* L. seedling. J Environ Sci 20:199–206

Doubnerová V, Ryšlavá H (2011) What can enzymes of C4 photosynthesis do for C3 plants under stress? Plant Sci 180:575–583

Fidalgo F, Freitas R, Ferreira R, Pessoa AM, Teixeira J (2011) *Solanum nigrum* L. antioxidant defense system isozymes are regulated transcriptionally and post-translationally in Cd-induced stress. Environ Exp Bot 72:312–319

Fornazier RF, Ferreira RR, Vitória AP, Molina SMG, Lea PJ, Azevedo RA (2002) Effects of cadmium on antioxidant enzyme activities in sugar cane. Biol Planta 45:91–97

Gajewska E, Skłodowska M (2007) Relations between tocopherol, chlorophyll and lipid peroxides contents in shoots of Ni-treated wheat. J Plant Physiol 164:364–366

Gangwar S, Singh VP, Srivastava PK, Maurya JN (2011) Modification of chromium (VI) phytotoxicity by exogenous gibberellic acid application in *Pisum sativum* (L.) seedlings. Acta Physiol Plant 33:1385–1397

Ghnaya AB, Charles G, Hourmant A, Hamida JB, Branchard M (2009) Physiological behavior of four rapeseed cultivar (*Brassica napus* L.) submitted to metal stress. C R Biol 332:363–370

Grill E, Loffler S, Winnacker EL, Zenk MH (1986) Phytochelatins, the heavy-metal-binding peptides of plants, are synthesized from glutathione by a specific γ-glutamylcysteine dipeptidyl transpeptidase (phytochelatins synthase). Proc Natl Acad Sci USA 86:6838–6842

Harwood JL, Okanenko AA (2003) Sulphoquinovosyldiacylglycerol (SQDG)- the sulpholipid of higher plants. In: Abrol YP, Ahmad A (eds) Sulphur in plants. Kluwer Acad Publishers, Dordrecht, pp 189–219

Hernandez I, Alegre L, Breusegem FV, Munne-Bosch S (2009) How relevant are flavonoids as antioxidants in plants? Trends Plant Sci 14:125–132

Hörcik ZT, Kovács L, Láposi R, Mészáros L, Lakatos G, Garab G (2007) Effects of chromium on photosystem II in the unicellular green alga, *Chlorella pyrenoidosa*. Photosynthetica 45:65–69

Hu JZ, Shi GX, Xu QS, Wang X, Yuan QH, Du KH (2007) Effects of Pb^{2+} on the active oxygen-scavenging enzyme activities and ultrastructure in *Potamogeton crispus* leaves. Russ J Plant Physiol 54:414–419

Huang H, Gupta DK, Tian S, Yang X, Li T (2012) Lead tolerance and physiological adaptation mechanism in roots of accumulating and non-accumulating ecotypes of *Sedum alfredii*. Environ Sci Pollut Res 19:1640–1651

Iqbal N, Masood A, Nazar R, Syeed S, Khan NA (2010) Photosynthesis, growth and antioxidant metabolism in mustard (*Brassica juncea* L.) cultivars differing in Cd tolerance. Agri Sci China 9:519–527

Ivanov AG, Krol M, Sveshnikov D, Selstam E, Sandström S, Koochek M, Park YI, Vasilév S, Bruce D, Oquist G, Huner NP (2006) Iron deficiency in cyanobacteria causes monomerization of photosystem I trimers and reduces the capacity for state transitions and the effective absorption cross section of photosystem I in vivo. Plant Physiol 141:1436–1445

Janik E, Grudziński W, Gruszecki WI, Krupa Z (2008) The xanthophyll cycle pigments in *Secale cereale* leaves under combined Cd and high light stress conditions. J Photochem Photobiol B 90:47–52

Jonak C, Nakagami H, Hirt H (2004) Heavy metal stress. Activation of distinct mitogen-activated protein kinase pathways by copper and cadmium. Plant Physiol 136:3276–3283

Kanoun-Boulé M, Vicente JAF, Nabais C, Prasad MNV, Freitas H (2009) Ecophysiological tolerance of duckweeds exposed to copper. Aquat Toxicol 91:1–9

Kawano T, Kawano N, Muto S, Lapeyrie F (2001) Cation-induced superoxide generation in tobacco cell suspension culture is dependent on ion valence. Plant Cell Environ 24:1235–1241

Kerkeb L, Krämer U (2003) The role of free histidine in xylem loading of nickel in *Alyssum lesbiacum* and *Brassica juncea*. Plant Physiol 131:716–724

Khan NA, Singh S, Nazar R (2007) Activities of antioxidative enzymes, sulphur assimilation, photosynthetic activity and growth of wheat (*Triticum aestivum*) cultivars differing in yield potential under cadmium stress. J Agro Crop Sci 193:435–444

Kumar A, Prasad MNV, Sytar O (2012) Lead toxicity, defense strategies and associated indicative biomarkers in *Talinum triangulare* grown hydroponically. Chemosphere 89:1056–1165

Lamhamdi M, Bakrim A, Aarab A, Lafont R, Sayah F (2011) Lead phytotoxicity on wheat (*Triticum aestivum* L.) seed germination and seedlings growth. C R Biol 334:118–126

Landberg T, Greger M (2002) Differences in oxidative stress in heavy metal resistant and sensitive clones of *Salix viminalis*. J Plant Physiol 159:69–75

Latowski D, Kruk J, Strzałka K (2005) Inhibition of zeaxanthin epoxidase activity by cadmium ions in higher plants. J Inorg Biochem 99:2081–2087

Latowski D, Kuczyńska P, Strzałka K (2011) Xanthophyll cycle-a mechanism protecting plants against oxidative stress. Redox Rep 16:78–90

Lee S, Korban SS (2002) Transcriptional regulation of *Arabidopsis thaliana* phytochelatin synthase (*AtPCS1*) by Cd during early stages of plant development. Planta 215:689–693

Lee S, Moon JS, Domier LL, Korban SS (2002) Molecular characterization of phytochelatin synthase expression in transgenic *Arabidopsis*. Plant Physiol Biochem 40:727–733

Liu D, Li TQ, Yang XE, Islam E, Jin XF, Mahmood Q (2008) Effect of Pb on leaf antioxidant enzyme activities and ultrastructure of the two ecotypes of *Sedum alfredii* Hance. Russ J Plant Physiol 55:68–76

Lushchak VI, Semchuk NM (2012) Tocopherol biosynthesis: chemistry, regulation and effects of environmental factors. Acta Physiol Plant. doi:10.1007/s11738-012-0988-9

Maksymiec W, Krupa Z (2006) The effects of short-term exposition to Cd, excess Cu ions and jasmonate on oxidative stress appearing in *Arabidopsis thaliana*. Environ Exp Bot 57:187–194

Malec P, Waloszek KA, Prasad MNV, Strzałka K (2008) Zinc reversal of Cd-induced energy transfer changes in photosystem II of *Ceratophyllum demersum* L. as observed by whole-leaf 77K fluorescence. Plant Stress 2:121–126

Malec P, Maleva MG, Prasad MNV, Strzałka K (2009) Identification and characterization of Cd-induced peptides in *Egeria densa* (water weed): putative role in Cd detoxification. Aquat Toxicol 95:213–221

Maleva MG, Nekrasova GF, Malec P, Prasad MNV, Strzałka K (2009) Ecophysiological tolerance of *Elodea canadensis* to nickel exposure. Chemosphere 77:393–398

MAPK Group (2002) Mitogen-activated protein kinase cascades in plants: a new nomenclature. Trends Plant Sci 7:301–308

Matysiak R (2001) Content of carotenoid in needles of *Pinus sylvestris* L. growing in polluted area. Dendrobiology 46:39–42

Mishra S, Srivastava S, Tripathi RD, Trivedi PK (2008) Thiol metabolism and antioxidant systems complement each other during arsenate detoxification in *Ceratophyllum demersum* L. Aquat Toxicol 86:205–215

Mishra S, Tripathi RD, Srivastava S, Dwivedi S, Trivedi PK, Dhankher OP, Khare A (2009) Thiol metabolism play significant role during Cd detoxification by *Ceratophyllum demersum* L. Biores Tech 100:2155–2161

Mobin M, Khan NA (2007) Photosynthetic activity, pigment composition and antioxidative response of two mustard (*Brassica juncea*) cultivars differing in photosynthetic capacity subjected to cadmium stress. J Plant Physiol 164:601–610

Munne-Bosch S (2005) The role of ά-tocopherol in plant stress tolerance. J Plant Physiol 162:743–748

Myśliwa-Kurdziel B, Strzałka K (2002) Influence of metals on biosynthesis of photosynthetic pigments. In: Prasad MNV, Strzałka K (eds) Physiology and biochemistry of metal toxicity and tolerance in plants. Kulwer Academic Publishers, The Netherlands, pp 201–227

Nakagami H, Pitzschke A, Hirt H (2005) Emerging MAP kinase pathways in plant stress signalling. Trends Plant Sci 10:339–346

Okanenko A, Taran N, Kosyk O (2003) Sulphoquinovosyl-diacylglycerol and adaptation syndrome. In: Murata N, Yamada M, Nishida I, Sekiya J, Hajime W (eds) Advanced research on plant lipids. Proceedings of the 15th international symposium on plant lipids. Kluwer Academic Publishers, Dordrecht, pp 361–364

Ortiz DF, Ruscitti T, MacCue KF, Ow DW (1995) Transport of metal-binding peptides by HMT1, a fission yeast ABC-type vacuolar membrane protein. J Biol Chem 270:4721–4728

Panda P, Nath S, Chanu TT, Sharma GD, Panda SK (2011) Cadmium stress-induced oxidative stress and role of nitric oxide in rice (*Oryza sativa* L.). Acta Physiol Plant 33:1737–1747

Pilon-Smits EAH, Pilon M (2000) Sulfur metabolism in plastids. In: Wise RR, Hoober JK (ed). The structure and function of palstis. Springer, USA, pp 387–402

Piotrowska A, Bajguz A, Godlewska-Zyłkiewicz B, Czerpak R, Kaminska M (2009) Jasmonic acid as modulator of lead toxicity in aquatic plant *Wolffia arrhiza* (Lemnaceae). Environ Exp Bot 66:507–513

Posmyk MM, Kontek R, Janas KM (2009) Antioxidant enzymes activity and phenolic compounds content in red cabbage seedlings exposed to copper stress. Ecotoxicol Environ Saf 72:596–602

Potters G, Horemans N, Jansen MAK (2010) The cellular redox state in plant stress biology-a charging concept. Plant Physiol Biochem 48:292–300

Rai VK (2002) Role of amino acids in plant responses to stress. Biol Plant 45:481–487

Reddy AM, Kumar SG, Jyonthsnakumari G, Thimmanaik S, Sudhakar C (2005) Lead induced changes in antioxidant metabolism of horse gram (*Macrotyloma uniflorum* (Lam.)Verdc.) and bengal gram (*Cicer arietinum* L.). Chemosphere 60:97–104

Rutolo R, Peracchi A, Bolchi A, Infusini G, Amoresano A, Ottonello S (2004) Domain organization of phytochelatin synthase: functional properties of truncated enzyme species identified by limited proteolysis. J Biol Chem 279:14686–14693

Sachiko M, Mundelanji V, Takafumi K, Shingo N, Kentaro S, Naoki T (2009) Role of C-terminal Cys-rich region of phytochelatin synthase in tolerance to cadmium ion toxicity. J Plant Biochem Biotechnol 18:175–180

Sakihama Y, Cohen MF, Grace SC, Yamasaki H (2002) Plant phenolic antioxidant and pro-oxidant activities: phenolics-induced oxidative damage mediated by metals in plants. Toxicology 177:67–80

Salt DE, Rauser WE (1995) Mg-ATP-dependent transport of phytochelatins across the tonoplast of oat roots. Plant Physiol 107:1293–1301

Sato N, Hagio M, Wada H, Tsuzuki M (2000) Environmental effects on acidic lipids of thylakoid membranes. Biochem Soc Trans 28:912–914

Schmoger MEV, Oven M, Grill E (2000) Detoxification of arsenic by phytochelatins in plants. Plant Physiol 122:793–802

Schützendübel A, Polle A (2002) Plant responses to abiotic stresses: heavy metal-induced oxidative stress and protection by mycorrhization. J Exp Bot 53:1351–1365

Schützendübel A, Schwanz P, Teichmann T, Gross K, Langelfeld-Heyser L, Godbold DL, Polle A (2001) Cd-induced changes in antioxidative systems, hydrogen peroxide content, and differentiation in *Scots pine* roots. Plant Physiol 127:887–898

Seregin IV, Ivanov VB (2001) Physiological aspects of cadmium and lead toxic effects on higher plants. Russ J Plant Physiol 48:523–544

Shakya K, Chettri MK, Sawidis T (2008) Impact of heavy metals (copper, zinc and lead) on the chlorophyll content of some mosses. Arch Environ Contam Toxicol 54:412–421

Sharma S, Dietz KJ (2006) The significance of amino acids and amino acid-derived molecules in plant responses and adaptation to heavy metal stress. J Exp Bot 57:711–726

Shaw BP (1995) Effects of mercury and cadmium on the activities of antioxidative enzymes in the seedlings of *Phaseolus aureus*. Biol Plant 37:587–596

Shaw BP, Prasad MNV, Jha VK, Sahu BB (2005) Heavy elements in the environment. In: Prasad MNV, Sajwan KS, Naidu R (eds) Biogeochemistry, biotechnology and bioremediation, CRC Press, Boca Raton, pp 271–289

Shemet SA, Fedenko VS (2005) Accumulation of phenolic compounds in maize seedlings under toxic Cd influence. Physiol Biochem Cultiv Plants 37:505–512

Shu X, Yin L, Zhang Q, Wang W (2012) Effect of Pb toxicity on leaf growth, antioxidant enzyme activities, and photosynthesis in cuttings and seedlings of *Jatropha curcas* L. Environ Sci Pollut Res 19:893–902

Siripornadulsil S, Traina S, Verna DPS, Sayre RT (2002) Molecular mechanisms of proline-mediated tolerance to toxic heavy metals in transgenic microalgae. Plant Cell 14:2837–2847

Stroinski A, Kozlowska M (1997) Cadmium-induced oxidative stress in potato tuber. Acta Soc Bot Pol 66:189–195

Syshchikov DV (2009) State of antioxidant glutathione dependent system of maize plantlets at actions of Cd compounds. Herald Kharkiv Natl Agrar Univ 1:45–51

Talanova VV, Titov AF, Boeva NP (2000) Effect of increasing concentration of lead and cadmium on cucumber seedlings. Biol Planta 43:441–444

Thangavel P, Long S, Minocha R (2007) Changes in phytochelatins and their biosynthetic intermediates in red spruce (*Picea rubens* Sarg.) cell suspension culture under cadmium and zinc stress. Plant Cell Tissue Org Cult 88:201–216

Tóth SZ, Schansker G, Garab G, Strasser RJ (2007) Photosynthetic electron transport activity in heat-treated barley leaves: the role of internal alternative electron donors to photosystem II. Biochim Biophys Acta 1767:295–305

Ventrella A, Catucci L, Piletska E, Piletsky S, Agostiano A (2011) Interactions between heavy metals and photosynthetic materials studied by optical techniques. Bioelectrochemistry 77:19–25

Verma S, Dubey RS (2003) Lead toxicity induces lipid peroxidation and alters the activities of antioxidant enzymes in growing rice plants. Plant Sci 164:645–655

Vesely T, Neuberg M, Trakal L, Szakova J, Tlustoa P (2011) Water lettuce *Pistia stratiotes* L. response to lead toxicity. Water Air Soil Pollut 223:1847–1859

Wan G, Najeeb U, Jilani G, Naeem MS, Zhou W (2011) Calcium invigorates the cadmium-stressed *Brassica napus* L. plants by strengthening their photosynthetic system. Environ Sci Pollut Res 18:1478–1486

Wang SH, Yang ZM, Yang H, Lu B, Li SQ, Lu YP (2004) Copper-induced stress and antioxidative responses in roots of *Brassica junicea* L. Bot Bull Acad Sin 45:203–212

Yamasaki H, Sakihama Y, Ikehara N (1997) Flavonoid-peroxidase reaction as a detoxification mechanism of plant cells against H_2O_2. Plant Pysiol 115:1405–1412

Young AJ, Frank HA (1996) Energy transfer reactions involving carotenoids: quenching of chlorophyll fluorescence. J Photochem Photobiol B 36:3–15

Youssef NB, Zarrouk M, Daoud D, Lemal F, Ouariti O, Ghorbal MH, Cherif A (1998) Membrane lipid changes in *Brassica napus* induced by Cd chloride. In: Sanches J, Cerda-Olimero E, Martinez-Force E (eds) Advances in plant lipid research. Universidad de Sevilla, Spain, pp 534–537

Yusuf MA, Kumar D, Rajwanshi R, Strasser RJ, Tsimilli-Michael M, Govindjee Sarin NB (2010) Overexpression of γ-tocopherol methyl transferase gene in transgenic *Brassica juncea* plants alleviates abiotic stress: physiological and chlorophyll *a* fluorescence measurements. Biochem Biophy Acta 1797:1428–1438

Yusuf M, Fariduddin Q, Varshney P, Ahmad A (2012) Salicylic acid minimizes nickel and/or salinity-induced toxicity in Indian mustard (*Brassica juncea*) through an improved antioxidant system. Environ Sci Pollut Res 19:8–18

Zagoskina NV, Goncharuk EA, Alyavina AK (2007) Effect of cadmium on the phenolic compounds formation in the callus cultures derived from various organs of the tea plant. Russ J Plant Physiol 54:237–243

Zhang H, Xia Y, Wang G, Shen Z (2008) Excess copper induces accumulation of hydrogen peroxide and increases lipid peroxidation and total thiol activity of copper-zinc superoxide dismutase in roots of *Elsholtzia haichowensis*. Planta 227:465–475

Zhang ZC, Chen BX, Qiu BS (2010) Phytochelatin synthesis plays a similar role in shoots of the cadmium hyperaccumulator *Sedum alfredii* as in non-resistant plants. Plant Cell Environ 33:1248–1255

Zhao C, Qiao M, Yu Y, Xia G, Xiang F (2010) The effect of the heterologous expression of *Phragmites australis* γ-glutamylcysteine synthetase on the Cd^{2+} accumulation of *Agrostis palustris*. Plant Cell Environ 33:877–887

Zhou ZS, Guo K, Elbaz AA, Yang ZM (2009) Salicylic acid alleviates mercury toxicity by preventing oxidative stress in roots of *Medicago sativa*. Environ Exp Bot 65:27–34

DOI: 10.1002/clen.201200512

Research Article: The results indicate that common buckwheat shows Ni hyperaccumulation. It is suggested that Ni act on lipid peroxidation process and induced changes in phenolic acids compositions. The mentioned biochemical changes in buckwheat play an important role as non-enzymatic antioxidative systems.

Foliar Applied Nickel on Buckwheat (*Fagopyrum Esculentum*) Induced Phenolic Compounds as Potential Antioxidants

O. Sytar*, Z. Cai, M. Brestic, A. Kumar, M. N. V. Prasad, N. Taran, S. Iryna

Clean – Soil, Air, Water **2013**, 00 (00), 0000–0000

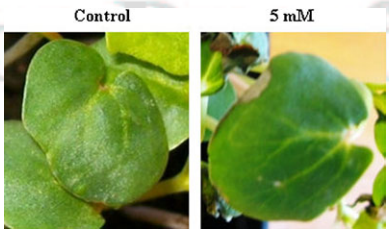

CLEAN
Soil Air Water

Oksana Sytar[1,2]
Zhenzhen Cai[3]
Marian Brestic[2]
Abhay Kumar[4]
M. N. V. Prasad[4]
Nataliya Taran[1]
Smetanska Iryna[3,5]

[1]Department of Plant Physiology and Ecology, Taras Shevchenko National University of Kyiv, Faculty of Biology, Kyiv, Ukraine
[2]Department of Plant Physiology, Slovak University of Agriculture in Nitra, Nitra, Slovakia
[3]Department of Methods of Food Biotechnology, Berlin University of Technology, Institute of Food Technology and Food Chemistry, Berlin, Germany
[4]Department of Plant Sciences, University of Hyderabad, Hyderabad, India
[5]Agricultural Faculty, Department of Plant Food Processing, University of Applied Science Weihenstephan-Triesdorf, Weidenbach, Germany

Research Article

Foliar Applied Nickel on Buckwheat (*Fagopyrum Esculentum*) Induced Phenolic Compounds as Potential Antioxidants

In this study, *Fagopyrum esculentum* (common buckwheat) sprayed with nickel (Ni) (0, 0.5, 1.0, 3.0, and 5.0 mM) for different duration has been investigated for Ni accumulation, malondialdehyde (MDA), total phenolics, and phenolic acids[Q1]. Ni accumulation significantly increased in dose-dependent manner. Plants exposed for 72 h, showed visible damages as chlorosis and irreversible necrosis. The MDA and total phenolic contents increased at 24 h of Ni treatments. HPLC data revealed that phenolic acids are in good correlation with concentration and durations of treatments. After 24 and 48 h the contents of chlorogenic, *p*-hydroxybenzoic, hesperetic, *p*-anisic, and caffeic acids increased in Ni treated leaves. On the other hand, *p*-hydroxybenzoic, hesperetic, *p*-anisic, *p*-coumaric, caffeic acids contents decreased after 72 h of Ni exposure. Vanillic and cinnamic acid followed same pattern and increased significantly at 3.0 and 5.0 mM after 48 h of Ni exposure. It may suggest that buckwheat can be possible hyperaccumulators of Ni, because of high Ni accumulation in tissues through foliar treatment. Furthermore, the analyzed phenolic acids have potential role as antioxidants, which provide tolerance to buckwheat against Ni treatment.

Keywords: Cellular protection; Heavy Metal; Hyperaccumulation; Malondialdehyde

Received: September 25, 2012; *revised:* October 30, 2012; *accepted:* November 5, 2012

DOI: 10.1002/clen.201200512

1 Introduction

The increasing levels of heavy metals (HMs) in the environment, their bioavailability to plants and entry into the food chain are of major health concerns [1]. Although nickel (Ni) is one of the essential micronutrients, its excess exposure to plants can be toxic. Ni is considered as a risk element due to its high worldwide bioavailability [2–4]. Ni is emitted to the atmosphere from volcanoes, windblown dusts, by combustion of fossil fuels, automobile exhausts and other technogenic activities of human being [5–7]. Elevated Ni concentrations are measured in the soil, water, and air along the highways. However, 20% of the total Ni presents in the atmosphere is associated with traffic pollutions [8], which is of a global concern for health risks.

Plant responds differently external concentrations of trace elements. The effect of metalliferous substances on the surface of leaves is an important aspect of scientific investigation where the process of assimilation, dissimilation, and transpiration takes place. Air contamination by Ni causes morphological, physiological, and biochemical changes in plants [9] as well as compete with other cations such as Ca^{2+}, Fe^{2+}, and Zn^{2+} in the cells and caused ionic imbalances [10]. Enzyme, glutathione, and phenolics activities might play a central role in cellular protection against the Ni induced oxidative stress. Proline contents proportionally increased with the elevated Ni concentrations [11–13]. The toxic level of Ni in endoderm and parenchyma cells blocks cell division and results in the prevention of root branching [14]. Studies have reported a good correlation between the content of Ni in soil and plant leaves [15, 16]. Ni concentrations in leaves of different plant species growing in urban and sub-urban situation show a wide range of variation. The toxic concentrations of Ni have been recorded as 16.2 $\mu g\,g^{-1}$ in *Quercus petraea* in the national park of *Fruška gora* in Serbia and as 15.4 $\mu g\,g^{-1}$ in *Tilia tomentosa*. In Avala mountain (Serbia) Ni concentrations in *Quercus petraea* ranged from 2.9 to 7.0 $\mu g\,g^{-1}$ [5].

Phytoremediation is gaining global significance for remediation of contaminants. Metal hyper-accumulating plants can accumulate exceptionally high amounts of metals (thousands of ppm) in their tissues. Hyperaccumulators are defined as species capable of accumulating metals at unusually higher levels. In case of Ni this value is about 10 000 ppm. So far, approximately 400 plant species spread across 45 families have been reported as HMs hyperaccumulator [17–19]. *Fagopyrum esculentum* (Moench) (common buckwheat, *Polygonaceae*) is a crop plant and it has reported that common buckwheat can naturally accumulated up to 4.20 $\mu g\,g^{-1}$ of Pb in its shoot [20]. This relevant finding qualifies this species as an excellent candidate for remediating Pb-contaminated soils [21]. Plants possess a range of potential cellular mechanisms that may be involved in the detoxification and tolerance of HMs stress [22]. Buckwheat, e.g.,

Correspondence: Dr. O. Sytar, Department of Plant Physiology, Slovak University of Agriculture in Nitra, Tr. A. Hlinku 2, 949 76 Nitra, Slovakia
E-mail: s-pi-r@hotmail.com

Abbreviations: HM, heavy metal; **MDA**, malondialdehyde; **ROS**, reactive oxygen species

Dr. Z. Cai contributed equally to this article.

Additional correspondence: Professor M. Brestic,
E-mail: marian.brestic@gmail.com

secrets oxalic acid from the roots in response to Al stresses, and accumulates non-toxic Al-oxalate in the leaves [19].

Literature data survey showed that there are no reports about adaptations of buckwheat plants sprayed with foliar Ni. Salim et al. [21] reported that foliar treatment analysis with Pb, Cd, and Cu showed higher percentage of accumulation in aerial part of plants in comparison to root treatment analysis. Therefore, we aimed to analyze the effect of foliar treatment of different Ni concentrations on visible symptoms and biochemical parameters with special emphasis on the role of phenolic compounds and consequent oxidative responses.

2 Materials and methods

2.1 Plant treatment

Seeds were germinated in the pots in the greenhouse for 14 days in 16/8 h photoperiod at 23°C at roughly 65% humidity. The experiments were achieved in pots with 1 L capacity and diameter of pot was 14 cm. The four plants were growth in one pot. The soil cambic chernozem without any nickel content was used in pot experiments. After 14 days of planting, Ni was applied as foliar spray at concentrations of 0.5, 1.0, 3.0, and 5.0 mM in the form of $Ni(NO_3)_2$. Plants treated with distilled water were referred as control. Young seedlings were used in the study, because they can demonstrate a stronger reaction to Ni stress. Leaves were separated from treated plants after 24, 48, and 72 h of exposure and washed with double distilled water (DDW) and were used for the study of various parameters. All experiments were set up in triplicate and each replicate contained for plants in pots (six pots for one experiment). Leaves were taken from each plant in each of the three experiments for increase biological replication. Each extract from one biological replicate was measured three times (analytical replication).

2.2 Quantification of Ni accumulation in plants leaves

The leaves of Ni treated plants were separated, washed with DDW, and oven dried at 80°C until complete dry. Dried plant (1.0 g) material was digested with 4 mL $HNO_3/HClO_4$ (3:1). The digested material was dissolved in the 10 mL of 0.1 N HNO_3. This solution was analyzed for Ni content using atomic absorption spectrophotometer (240FS AA Fast Sequential AAS, Varian).

2.3 Lipid peroxidation assay (LP)

LP in leaves was determined by estimation of malondialdehyde (MDA) content following Heath and Packer [23] with slight modifications. Plant material (0.2 g of leaves) was homogenized in 3 mL 0.1 M Tris buffer containing 0.3 M NaCl. 2 mL of 20% trichloroacetic acid (TCA) containing 0.5% 2-thiobarbituric acid (2-TBA) and 2 mL 20% TCA were mixed. The mixture was heated at 95°C for 30 min and then homogenate was centrifuged at $10\,000 \times g$ for 5 min. Absorbance of the supernatant was taken at 532 and 632 nm. The concentration of MDA was calculated using an extinction coefficient ($\varepsilon = 155\ mM^{-1}\ cm^{-1}$) and expressed in nmol g^{-1} FW.

2.4 Determination of total phenolics

Total phenolics were determined by using Folin-Ciocalteu reagent [24]. Twenty milligrams powdered samples (freeze-dried) were extracted for 10 min with 500 μL of 70% methanol at 70°C. The mixtures were centrifuged at $3500 \times g$ for 10 min and the supernatants were collected in separate tubes. The pellets were re-extracted under identical conditions. Supernatants were combined and used for total phenolics assay and for HPLC analysis. For total phenolics assay 20 μL of extract was dissolved into 2 mL of distilled water. Two hundred microliters of dissolved extract were mixed with 1 mL of Folin-Ciocalteu reagent (previously diluted tenfold with distilled water) and kept at 25°C for 3–8 min; 0.8 mL of sodium bicarbonate (75 g L^{-1}) solution were added to the mixture. After 60 min at 25°C, absorbance was measured at 765 nm. The results were expressed as gallic acid equivalents.

2.5 Analysis of hydroxycinnamic acid derivatives

The leaves were harvested and frozen in liquid nitrogen for the preventing of phenolic compound volatilization. Afterwards the samples were lyophilized. Further, finishing the freeze-drying process the material was grounded by flint mill ($20\,000 \times g$, 2 min). A total of 20 mg grounded samples from leaves suspension were extracted for 15 min using 750 μL 70% methanol (v/v, pH 4.0, phosphoric acid) in ultrasonic water bath on ice. Samples were centrifuged for 5 min at $6000 \times g$. The supernatants were collected and the pellets were re-extracted twice more with 500 μL 70% methanol. Coumaric acid or cinnamic acid (40 μL of 3 mM solution) was added as internal standard to the first extraction. The combined supernatants from each sample were reduced to near dryness in a centrifugation evaporator (Speed Vac, SC 110) at 25°C. Samples were added up up to 1 mL with 40% acetonitrile. The samples were filtrated using 0.22-μm filters, and then analyzed with HPLC. The chromatography was performed using a Dionex Summit P680A HPLC system with an ASI-100 auto sampler and a PDA-100 photodiode array detector.

Extracts (10 μL) were analyzed at a flow rate of 0.4 mL min^{-1} and a column temperature of 35 °C. A 30-min gradient program was used with 1% v/v phosphoric acid in ultrapure water (eluent A) and of 40% v/v acetonitrile in ultrapure water (eluent B) as follows: 0–1 min: 0.5% B, 1–10 min: 0–40% B, 10–12 min: 40% B, 12–18 min: 40–80% B, 18–20 min: 80% B, 20–24 min: 80–99% B, 24–30 min: 99–100% B. The gradient program was followed by a 4-min period to return to 0.5% B and a 5-min equilibration period resulting in a total duration of 39 min. The eluent was monitored at 290, 330, and 254 nm. Phenolic acid quantity was calculated from HPLC peak areas at 290 nm against the internal standard.

2.6 Statistical analysis

The experiment was repeated at least three times. The mean values ± standard deviations (SD) are reported in the figures. Significant differences ($p \leq 0.05$) between control and Ni treatments were quantified using analysis of variance (ANOVA – Duncan's multiple tests, SIGMASTAT, version-11.0). Different letters indicating significant ($p \leq 0.05$) difference between each treatment at a individual treatment duration.

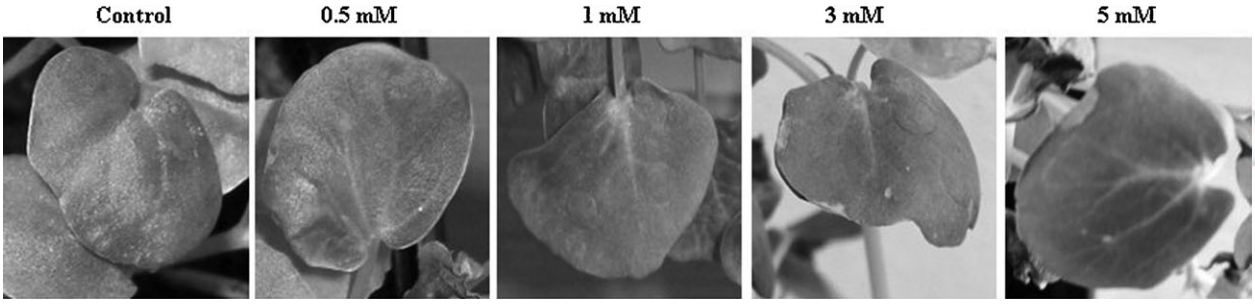

Figure 1. Visual symptoms observation, chlorosis, in buckwheat leaves at 72 h under different concentrations of Ni treatment.

3 Results and analysis

3.1 Visible symptoms

Our study showed that under foliar Ni treatment chronic chlorotic mottling of young leaves can be visible at only 72 h of exposure under Ni excess (Fig. 1). In all treated plants with different concentrations of Ni, especially 3.0 and 5.0 mM, the visible damages of leaves has observed in the form of chlorosis and irreversible necrosis, appear on leaf edges.

3.2 Ni concentrations in plant leaves

F. esculentum was found to be sensitive to Ni foliar effect. The Ni accumulation in plant leaves showed significantly ($p \leq 0.05$) dose-dependent increasing compared to control (Fig. 2A). But interestingly in our experimental conditions, exposure periods were not significantly affected on Ni accumulation levels in buckwheat leaves. The Ni accumulation was increased to ca. 4.3-fold at 5.0 mM in comparison to 0.5 mM Ni treated leaves at all treatment durations.

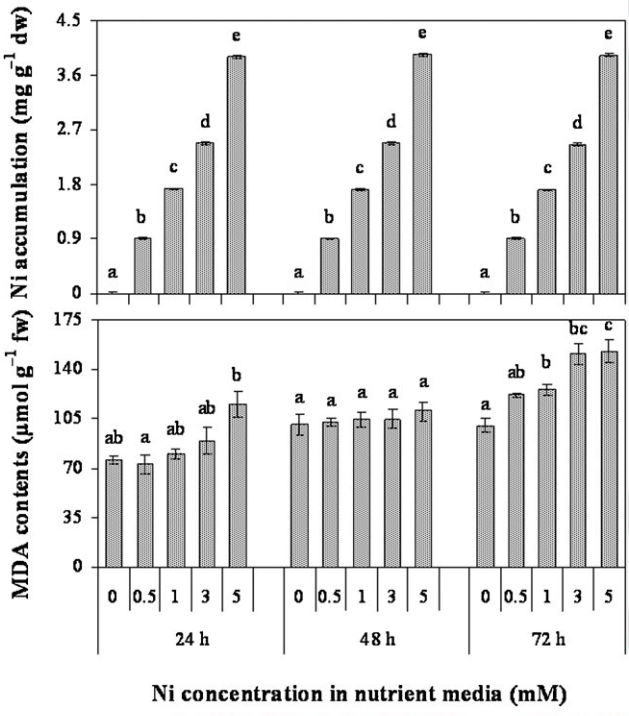

Figure 2. Ni accumulation (A) and MDA content (B), marker of lipid peroxidation, in buckwheat leaves treated with different Ni concentration for 24, 48, and 72 h. All the values are mean of triplicates ± SD. Different letters indicating significant ($p \leq 0.05$) difference between each treatment at a individual treatment duration.

3.3 Lipid peroxidation

Lipid peroxidation is a biochemical marker for the free radical mediated injury. Ni-induced lipid peroxidation in leaves of buckwheat was measured by the concentration of MDA produced, a degradation product of membrane unsaturated fatty acid, that reflects the extent of cell membrane damage in response to reactive oxygen species (ROS) production. At 24 h of exposure under different Ni concentrations have been showed dose-depended increasing of MDA content which can evidence about Ni-induced toxicity. Ni exposure with 5 mM concentration the level of MDA content has been increased (Fig. 2B) on 34% compared to control at 24 h. The MDA content in buckwheat were increased insignificantly at 48 h and significantly ($p \leq 0.05$) at 72 h in all Ni treated plant in comparison to control, respectively.

3.4 Total phenolics content

In all experimental variants, different Ni treatments at 24 and 48 h significantly ($p \leq 0.05$) increased the total phenolic contents (Fig. 3). Ni treatment of 0.5, 1.0, 3.0, and 5.0 mM for 24 h were significantly

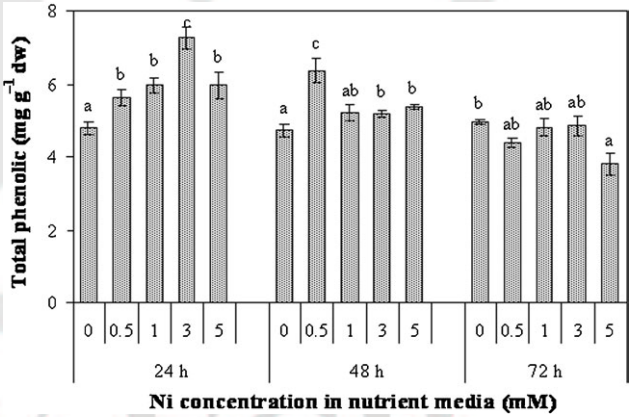

Figure 3. Total phenolics content in buckwheat leaves treated with different Ni concentration for 24, 48, and 72 h. All the values are mean of triplicates ± SD. Different letters indicating significant ($p \leq 0.05$) difference between each treatment at a individual treatment duration.

CLEAN Soil Air Water

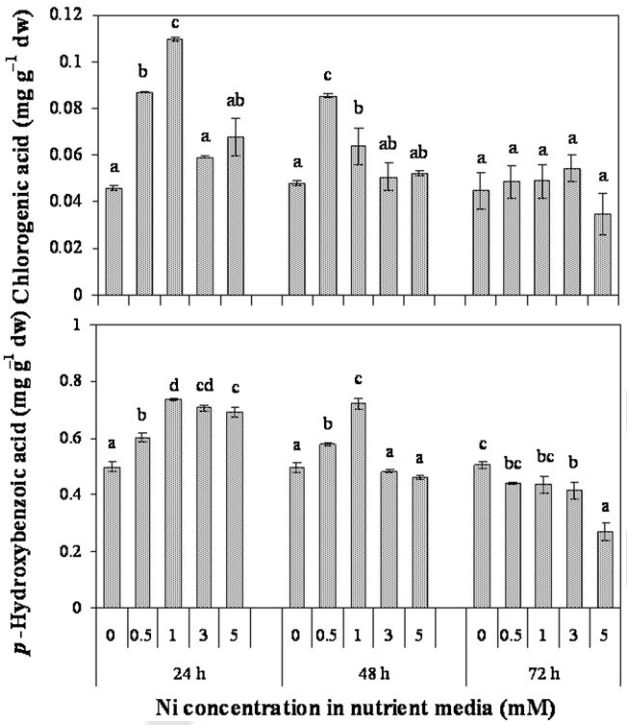

Figure 4. Chlorogenic acid (A) and *p*-hydroxybenzoic acid (B) contents in buckwheat leaves treated with different Ni concentration for 24, 48, and 72 h. All the values are mean of triplicates ± SD. Different letters indicating significant ($p \leq 0.05$) difference between each treatment at a individual treatment duration.

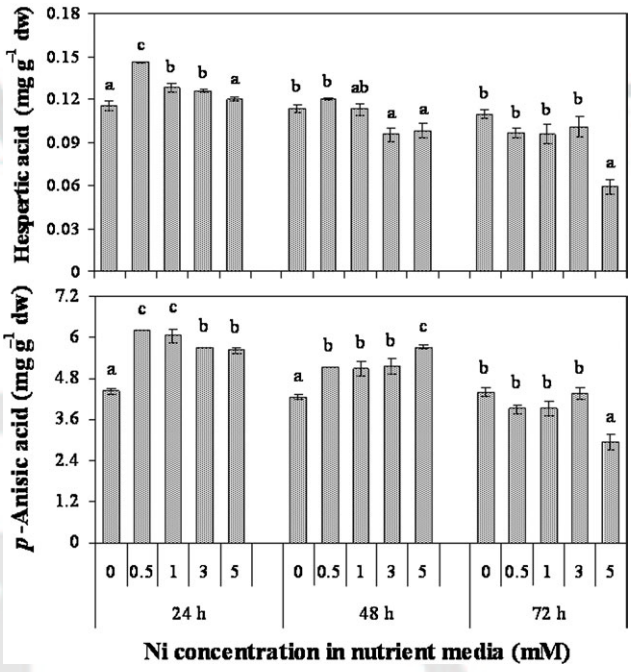

Figure 5. Hespertic acid (A) and *p*-coumeric acid (B) contents in buckwheat leaves treated with different Ni concentration for 24, 48, and 72 h. All the values are mean of triplicates ± SD. Different letters indicating significant ($p \leq 0.05$) difference between each treatment at a individual treatment duration.

increased the phenolic contents by ca. 17, 24, 51, and 24% over control, respectively. At 48 h, total phenolics content at 0.5, Ni exposure was significantly ($p \leq 0.05$) increased by ca. 35, 10, 10, and 14% in compared to control, respectively. At 72 h of exposure in all experimental variants total phenolic contents were almost at control level.

3.5 Phenolic acids composition and content

In buckwheat, we analyzed the few phenolic acids viz. chlorogenic acid (Fig. 4A), *p*-hydroxybenzoic acid (Fig. 4B), hesperetic acid (Fig. 5A), *p*-anisic acid (Fig. 5B), *p*-coumaric acid (Fig. 6A), caffeic acid (Fig. 6B), cinnamic acid (Fig. 7A), and vanillic acid (Fig. 7B). The quantity of analyzed phenolic acids has been different during Ni exposure and depended from Ni concentrations. In Ni treated seedlings, high content of *p*-hydroxybenzoic, hesperetic, and *p*-anisic acids has been observed over control. At 24-h exposure of 0.5, 1.0, 3.0, and 5.0 mM Ni concentrations significantly ($p \leq 0.05$) induced the chlorogenic acid contents with 90.8, 140.6, 30, and 48% over control leaf, respectively (Fig. 4A). Buckwheat seedlings treated with 0.5 mM Ni at 48 h increased the chlorogenic acid content by 77.7% as compared to control. But at 48 h of exposure, chlorogenic acid content back to control level in variants after foliar treatment with solution 3.0 and 5.0 mM concentration of Ni. Than at 72 h of exposure in all experimental variants under effect of differ Ni concentrations (0.5–5.0 mM) content of chlorogenic acid back to control level.

Results of our study showed that at 24 h of Ni exposure in all treated plants the *p*-hydroxybenzoic acid contents were higher than

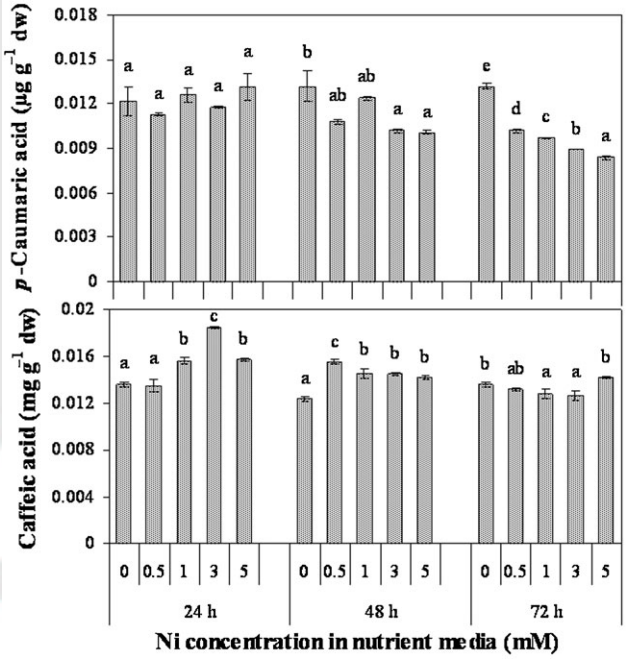

Figure 6. *p*-Anisic acid (A) and Cinnamic acid (B) contents in buckwheat leaves treated with different Ni concentration for 24, 48, and 72 h. All the values are mean of triplicates ± SD. Different letters indicating significant ($p \leq 0.05$) difference between each treatment at a individual treatment duration.

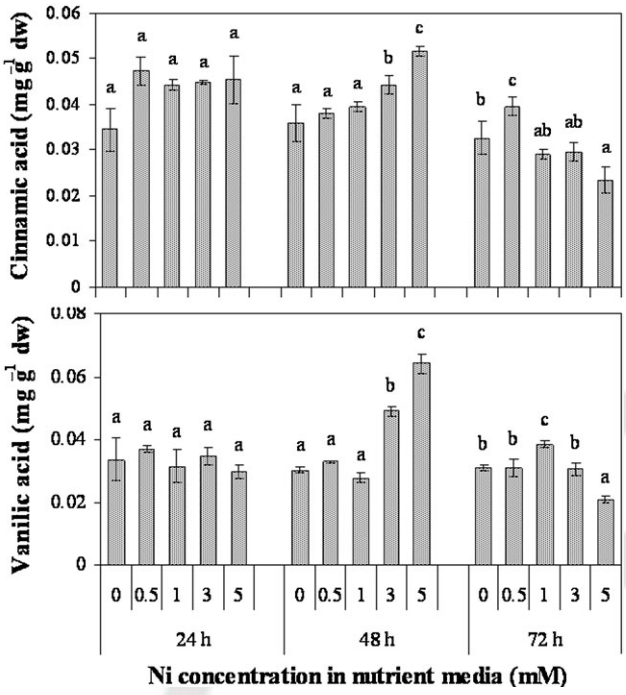

Figure 7. Vanillic acid (A) and caffeic acid (B) contents in buckwheat leaves treated with different Ni concentration for 24, 48, and 72 h. All the values are mean of triplicates ± SD. Different letters indicating significant ($p \leq 0.05$) difference between each treatment at an individual treatment duration.

control (Fig. 4B). Significant ($p \leq 0.05$) increase in *p*-hydroxybenzoic acid was observed at 0.5 (20.7%), 1.0 (47.6%), and 3.0 (41.3%) and 5.0 (38.3%) in comparison to control. On the other hand, at 48 h of exposure, *p*-hydroxybenzoic acid increase was 0.5 (16.7%) and 1.0 (45.4%) mM Ni in comparison to control, respectively. Ni treatment at (3.0 and 5.0 mM) the content of *p*-hydroxybenzoic acid was almost equivalent to control. However, at 72-h exposure *p*-hydroxybenzoic acid was on par with control level at 0.5 and 1 mM Ni, but decreased by ca. 21 and 87% at 3.0 and 5.0 mM Ni in comparison to control, respectively.

HPLC results revealed that hesperetic acid, one of the hesperetin metabolites, contents were increased only at 24 h in Ni treated plants but the at 48 and 72 h it was gradually decreased as the external supplementation of Ni increased (Fig. 5A). The highest increase (26.2%) in hesperetic acid content was observed at 0.5 mM Ni in comparison to control, which gradually declined to further concentrations and maintain an increased value of 4.3% at 5.0 mM Ni at 24 h, respectively. The visible changes in hesperetic acid among treatment period have been shown under excess of Ni with concentration 5.0 mM. At 48 and 72 h of 5.0 mM Ni, hesperetic acid content was significantly decreased by 15.6 and 85.7% in comparison to control, respectively.

The content of analyzed *p*-anisic acid in the experimental variants of buckwheat seedlings have shown the same pattern of hesperetic acid but at 48 h the *p*-anisic acid content were increased after treatment with different Ni concentrations (Fig. 5B). At 24 h of Ni exposure at 0.5, 1.0, 3.0, and 5.0 mM Ni *p*-anisic acid contents were significantly ($p \leq 0.05$) increased compared to control by 40.7, 36.7, 28.9, and 27.2%, respectively. But in contrast to hesperetic acid the *p*-anisic acid contents were increased and ranged from 20 to 34% at 0.5–5.0 mM Ni at 48 h of treatment. At 72 h, the content of *p*-anisic acid levels declined to control level, except for 5.0 mM Ni, where it is significantly decreased by 49.9% in comparison to control. The changes in content of *p*-anisic acid under Ni excess make evidence about participation of this phenolic acid in defense reactions against development of oxidative stress caused by Ni treatments. *p*-Coumaric acid (Fig. 6A), caffeic acids, (Fig. 6B) cinnamic acid (Fig. 7A), and vanillic acid (Fig. 7B) are representative of cinnamic acid derivatives and were identified in control and Ni treated buckwheat leaves. The *p*-coumaric acid declined in Ni treated buckwheat leaves at all treatment durations, but significantly decreased at only 48 and 72 h (Fig. 6A). *p*-Coumaric acid gradually increased as the function of external Ni treatment, which ranged between 22.2 to 33.3% at 48 h and 29.4 to 57.4% at 0.5–5.0 mM Ni at 72 h in respect to control, respectively.

Similar to *p*-anisic acid, caffeic acid contents were also increased at initial concentration and decreased at further concentration at 24 h Ni treatments (Fig. 6B). While at 48 h of Ni exposure caffeic acid contents were significantly ($p \leq 0.05$) higher than the control level but it is decreasing from 25 to 14.5% when the concentration increased by 0.5–5.0 mM Ni. Ni exposures for 72 h decreased the caffeic acid contents and bring it to on control level.

Cinnamic acid is a precursor in biosynthetic pathway of salicylic acid signaling molecule [25]. An increase in cinnamic acid content was observed at 24 and 48 h of Ni exposure, but the increased level was not significantly different with control values (Fig. 7A). The significant increase in cinnamic acid was observed at only 5.0 mM at 48 h and and at 0.5 mM Ni at 72 h.

4 Discussions and conclusions

4.1 Discussions

Our results were suggested that 72 h of different Ni treatment caused leaf damage, interveinal chlorosis and spotting necrosis. Similar responses have reported in tomato leaves after foliar Ni treatments [26]. High Ni concentrations have toxic effect. Significant changes in chlorophyll and antioxidative systems were observed after 72 h after Ni treatment, which was correlated with the accumulated Ni into the leaves [27]. Visible symptoms, chlorosis, and necrosis, of Ni toxicity were, also reported in leaves of wheat [28] and cabbage [29] on the third day of Ni treatment. Exposure of 500 μM Ni to cabbage in sand culture led to increased accumulation of the metals, induction of visible symptoms of metal toxicity and inhibition of plant growth [29]. Despite all this physiological changes, all plants survived, which could suggest there is a complex interference of Ni with plant metabolism.

Obtained results represented that the Ni accumulation in the tissues increased as the exogenous Ni concentration increased. But interestingly, the Ni accumulation were concentration dependent, the treatment duration has no significant effect on Ni accumulation. The efficiency of metal uptake by plants depends on several processes for aerial metal uptake by leaves and its translocation to the different tissues. Results of Ni accumulation showed that buckwheat were accumulated considerable higher percentage of Ni in its tissues. Usually, the amount of metal accumulation in plants increased with the increasing external metal concentrations [21] what we also observed in our experiment. Previous studies reported that *Brassica juncea*, hyperaccumulator of various metal ions [30], was accumulated 0.135 mg g^{-1} dw Ni at a given concentration of 100 mg L^{-1} [31]. The accumulation level of Ni in different species

may vary. The plant having potential to accumulate more than 1 mg g^{-1} dw of Ni are considered as hyperaccumulator for Ni [32]. Salim et al. [21] has been showed that amount of taken HMs were comparatively higher in foliar-treated plants than in root-treated plants. Our experimental results showed that 1.0, 3.0, and 5.0 mM Ni treated buckwheat was accumulated considerable higher than 1 mg g^{-1} of Ni in its leaves, which is supporting that buckwheat plants can be a possible hyperaccumulators of Ni.

Continuous gradual increase of ROS, such as superoxide radical ($O_2^{\cdot-}$) and hydrogen peroxide (H_2O_2), formation in leaf tissues with increase of Ni concentration induced accumulation of MDA [28, 33]. Our results showed that the increase in the MDA represents the Ni-induced oxidative stress resulting in peroxidation of membrane's lipids composition. Excess of Ni promoted ROS burst which resulted in to lipid peroxidation and increased production of MDA [34]. Maximum MDA concentration was observed at 5 mM Ni at 72 h, when total phenolic and phenolic acids contents were significantly declined. On the other hand, at 0.25 mM Ni at 24 h MDA content was declined which were in good correlation with total phenolic and some phenolic acids contents, suggested that level of lipid peroxidation is in positive relation with antioxidative systems. It has been reported that high concentration of Ni can result in increased ROS and lipid peroxidation level in *Salix acmophylla* [35], wheat [27, 28, 33] *Vigna mungo* [36], and *Alyssum markgrafii* [34].

During HMs stress phenolic compounds are act as metal chelators and as well as scavenger of ROS molecules. Phenolics, especially flavonoids and phenylopropanoids, are oxidized by peroxidase and act in H_2O_2 scavenging through phenolic/ascorbate/peroxidase system. Their antioxidant action resides mainly in their chemical structure [37]. It can suggest that phenolic contents have potential role as antioxidants in buckwheat, which represent dynamics development of adaptive reactions under Ni stress. We observed that at 24 h of exposure under Ni stress MDA content has been dose-dependent increased. But the 5 mM Ni concentration had negative effect on buckwheat leaves. Sgherri et al. [38] has showed than in *Raphanus sativus* plants grown under copper (Cu) concentration showed the increased phenolic acids as well as reduced ascorbate contents. The increasing of phenolic compound contents has been observed in wheat in response to Ni toxicity [39] and in maize in response to Al [40]. *Phyllantus tenellus* leaves contained more phenolics than control plants after being sprayed with Cu sulfate [39]. Higher accumulation of soluble phenolics was also measured in leaves of the Cd-accumulating *Crotalaria juncea* [41]. Cd at 3, 60, and 120 μM also caused increase of soluble phenolics and PAL activity in chamomile roots, but with lower intensity compared to Cu effects [42]. Thus it seems that the responses of phenolic metabolism are metal-specific and may reflect the different physical properties of metals.

Phenolic acids were known to play a role in the induction of abiotic stress resistance [43]. Phenolics, particularly polyphenols as opposed to monophenols, function as antioxidants to support the primary ascorbate-dependent detoxification system as a backup defense mechanism of vascular plants [44, 45]. Plant-derived flavonoids and phenolic acids showed inhibitory effects on MDA content [46]. Therefore, we supposed that detailed HPLC analysis of phenolic acids under Ni stress would be useful for getting new knowledge about role of phenolic acids in Ni resistance.

Chlorogenic acid is an extremely widespread plant metabolite that appears to provide protection against certain forms of stress [47]. For example, chlorogenic acid is an important antioxidant in plants, which can protects against lipid peroxidation [48]. In comparison to *Ramonda serbica* [38] and *Raphanus sativus* [49], buckwheat showed higher percentage of chlorogenic acid in its leaves. Ni treatment for 24 and 48 h increased the chlorogenic acid content, but interestingly at 72 h of treatment duration it decreased to control level. Accumulation of chlorogenic acid in chamomile roots was at 24 h of Cu exposure also and in relation to concentration of metals. Kováčik et al. have suggested about involvement of chlorogenic acid in antioxidative protection in Cu treated *Scenedesmus quadricauda* [50]. The spin-stabilizing metals, such as Ni, able produce effects similar to Al, Zn, Cd, Mg, and Ca, all of which have been reported to have the spin-stabilizing effects, stimulate lipid peroxidation induced by the oxidized form of chlorogenic acid [51]. On the other hand, the oxidized form of chlorogenic acid enhances lipid peroxidation resulted in to oxidative stress [51]. Phenolic compounds have been described as electron-donating agents [37], and therefore we suppose that chlorogenic acid can act as antioxidants too. Moreover, it has also been suggested that phenolics may act as biomarkers of metal exposure [52].

Literature data shows that *p*-hydroxybenzoic acid increases the impermeability of cell walls, leading to increase in the resistance against biotic stress [43]. Biotic and abiotic stress factor can induce development of oxidative reactions in plant and unspecific response against stress has similar way in both cases. In our experimental condition, the increasing content of *p*-hydroxybenzoic acid in all concentration at 24 h and 0.5 and 1.0 mM Ni at 48 h have showed its important role as the anti-oxidative metabolites against Ni-toxicity. The biosynthesis of salicylic acid is catalyzed by benzoic acid 2-hydroxylase and connected with *p*-hydroxybenzoic acid, which also support its relation with other strong antioxidant [53]. It has been reported that exogenous supplementation of *p*-hydroxybenzoic acid was provided tolerance against drought stress in wheat plants [54]. On the other hand, *p*-hydroxybenzoic acid was the only phenolic compound examined that failed to induce chilling tolerance in young maize plants [43]. Therefore, it can be deduced that increased *p*-hydroxybenzoic acid could considered as evidence about development of tolerance response to excess Ni in buckwheat plants.

HPLC results revealed that hesperetic acid (3-hydroxy-4-methoxycinnamic acid, Fig. 2B), one of the hesperetin metabolites, and *p*-anisic acid contents were increased only at 24 h in Ni treated plants but at 48 and 72 h it was gradually decreased as the external supplementation of Ni increased. Especially high stimulation has been observed under 5.0 mM Ni concentrations. It can suggest that stressful effect of 5.0 mM Ni on development of oxidative process in buckwheat seedlings. It was reported that, hesperitin, taxifolin, and naringenin exhibited appreciable antioxidant activities (61–84%) and plays a protective role against dimethylbenz(*a*)anthracene (DMBA)-induced oxidative stress [55]. Hsin-Ling et al. [56] reported that hesperetin metabolites showed higher antioxidant activity against various oxidative systems, including superoxide anion scavenger, reducing power and metal chelating effects, than that of hesperetin [57]. The changes in content of *p*-anisic acid under excess Ni provide evidence about the active role in defense reactions against Ni treatments.

The changes content of *p*-coumaric acid content related to phenolic acids accumulation in metal-treated plants are scarce. For example, Tolra et al. [58] detected ferulic and *p*-coumaric acid in Al-treated *Rumex acetosela*, but did not observe any significant changes in them, indicating that they are not involved in Al detoxification mechanisms. In our experiment, the content of *p*-coumaric acid showed dose-dependent reduction at 48 and 72 h at all

experimental treatments. We suppose that decreasing of *p*-coumaric acid content is connected with its polymerization, which leads to the formation of lignin. This is a usual process in plants, whereas enhanced lignifications in both biotic and abiotic stress conditions can serve as a barrier limiting metal/pathogen entry into tissue [59, 60]. In addition to lignin, suberin deposition may also retain metals in the plant tissue and restrict apoplastic passage between cells [61].

Similar to *p*-anisic acid, caffeic acid contents were also increased at initial concentration and decreased at subsequent concentration at 24-h Ni treatments, which further reduced and came up to the control level at the 48 and 72 h of Ni exposure. *p*-Hydroxybenzoic acid and *p*-anisic acid are benzoic acid derivatives increased at 24 h of exposure can provide evidence of their role in Ni detoxification. Especially the content of *p*-anisic acid was high in buckwheat seedlings as compared to the content of other phenolic acids. Furthermore, phenolic structures can function as metal chelators [62] and phenolics can participate in ROS scavenging through peroxidases [38].

Cinnamic acid is a precursor in biosynthetic pathway of salicylic acid signaling molecule [25] and significant increase in cinnamic acid contents were observed at only 5.0 mM at 48 h and at 0.5 mM Ni at 72 h. The tendency to increase cinnamic acid content has also been observed in all treatment concentrations at 24 h. The values of cinnamic acid might be associated with salicylic acid metabolisms, which play a defense response against Ni stress. Salicylic acid was found to enhance the activities of antioxidant enzymes, CAT, peroxidase, and superoxide dismutase [63]. It has been reported that cinnamic acid derivatives were increase in the Cd treated *Erica andevalensis* [57]. Furthermore in our experimental conditions, their quantities were less than other analyzed phenolic acids, but changes in their contents have evidence about their role in adaptive reactions in photosynthetic tissues under Ni treatments. Phenolic metabolites have antioxidative properties due to the availability of hydroxyl (OH^-) groups in the molecule. Hydroxylated cinnamates are more effective than their benzoate counterparts [64].

In addition to the antioxidative properties of simple phenolics, polymerization of *p*-coumaric, ferulic, and sinapic acids and their respective alcohols are involved in lignin biosynthesis. The antioxidant and anti-radical activity of phenolic acids correlated positively with the number of $OH^{\cdot ü}$ groups bound to the aromatic ring. The strong antioxidative potential, scavenging of H_2O_2 and $DPPH^{\cdot}$ radical activity was exhibited phenolic acids with three $OH^{\cdot ü}$ groups bonded to the aromatic ring in an ortho-position in relation to each other. Phenolic acids with two $OH^{\cdot ü}$ groups bonded to aromatic ring in the ortho-position, such as caffeic acids, showed strong antioxidant and anti-radical activity [65]. It is possible to say that under Ni excess mostly phenolics acids with higher number of $OH^{\cdot ü}$ groups bonded to the aromatic ring (two and more) showed significant changes at 24 and 48 h of Ni exposure. From identified phenolic acids in buckwheat seedlings chlorogenic acid is a compound with more than two $OH^{\cdot ü}$ groups bonded to the aromatic ring. *p*-Hydroxybenzoic, hesperetic, coumaric, vanillic, and caffeic acids are compounds with two $OH^{\cdot ü}$ groups bonded to the aromatic ring. *p*-Anisic acid is a benzoic acid, the simplest aromatic carboxylic acid containing carboxyl group bonded directly to benzene ring.

4.2 Conclusions

Common buckwheat is the first known Pb hyperaccumulator species with high biomass productivity and we observed the same response against Ni treatment. Our results suggest that foliar treatment with different high concentrations of Ni act on lipid peroxidation process and induced changes in phenolic acids compositions. These biochemical changes in buckwheat played an important role as non-enzymatic antioxidative systems, which made buckwheat as a potential hyperaccumulator of toxic metals like Ni.

Acknowledgments

This work was financially supported by the National Scholarship Programme of Slovak Republic (SAIA). The authors are grateful to Mrs. Jana Ferencova, Ms. Andrea Valigurova, and Mrs. Elena Hunkova for their excellent technical assistance.

The authors have declared no conflict of interest.

References

[1] J. Ruqaya, A. Altaf, I. Muhammad, Phytoremediation of Heavy Metals: Physiological and Molecular Mechanisms, *Bot. Rev.* **2009**, *75 (4)*, 339–364.

[2] M. Florek, B. Maňkovská, J. Oszlányi, M. V. Frontasyeva, E. Ermakova, S. S. Pavlov, The Slovak Heavy Metals Survey by Means the Bryophyte Technique, *Ecológia* **2007**, *26 (1)*, 99–114.

[3] M. Peris, L. Recatalá, C. Micó, R. Sánchez, J. Sanchez, Increasing the Knowledge of Heavy Metal Contents and Sources in Agricultural Soils of the European Mediterranean Region, *Water Air Soil Pollut.* **2007**, *192*, 25–37.

[4] H. M. Zakir, N. Shikazono, Environmental Mobility and Geochemical Partitioning of Fe, Mn, Co, Ni and Mo in Sediments of an Urban River, *J. Environ. Chem. Ecotoxicol.* **2011**, *3 (5)*, 116–126.

[5] D. Stanković, M. Knežević, B. Krstić, M. Šijačić-Nikolić, D. Vilotić, Nickel Content in Plants and Soil in the Area of the Protected Natural Resource ''Avala'' – Belgrade, *Bull. Fac. For.* **2011**, *103*, 131–146.

[6] B. Krstić, D. Stanković, R. Igić, N. Nikolić, The Potential of Different Plant Species for Nickel Accumulation, *Biotechnol. Biotechnol. Equip.* **2007**, *21 (4)*, 431–436.

[7] S. Stegen, F. Queirolo, C. Carrasco, Concentrations of Ni and Co in Crop Plants Cultivated in Northern Chile, *Bol. Soc. Chil. Quim.* **2002**, *47 (3)*, 279–287.

[8] Q. Qiu, Y. T. Wang, Z. Y. Yang, J. L. Xin, J. G. Yuan, J. B. Wang, G. R. Xin, Responses of Different Chinese Flowering Cabbage (*Brassica parachinensis* L.) Cultivars to Cadmium and Lead Exposure: Screening for Cd^{2+} Pb^{2+} Pollution-Safe Cultivars, *Clean – Soil Air Water* **2011**, *39 (11)*, 925–932.

[9] M. Chiban, A. Soudani, F. Sinan, S. Tahrouch, M. Persin, Characterization and Application of Dried Plants to Remove Heavy Metals, Nitrate, and Phosphate Ions from Industrial Wastewaters, *Clean – Soil Air Water* **2011**, *39 (4)*, 376–383.

[10] M. R. Khan, M. M. Khan, Effect of Varying Concentration of Nickel and Cobalt on the Plant Growth and Yield of Chickpea, *Aust. J. Basic Appl. Sci.* **2010**, *4 (6)*, 1036–1046.

[11] Y. Lu, X. R. Li, M. Z. He, Z. N. Wang, H. J. Tan, Nickel Effects on Growth and Antioxidative Enzymes Activities in Desert Plant *Zygophyllum xanthoxylon* (Bunge) Maxim, *Sci. Cold Arid Regions* **2010**, *2 (5)*, 436–444.

[12] S. K. Yadav, Heavy Metals Toxicity in Plants: an Overview on the Role of Glutathione and Phytochelatins in Heavy Metal Stress Tolerance of Plants, *S. Afr. J. Bot.* **2010**, *76 (2)*, 167–179.

[13] H. Kumar, D. Sharma, V. Kumar, Nickel-Induced Oxidative Stress and Role of Antioxidant Defense in Barley Roots and Leaves, *Int. J. Environ. Biol.* **2012**, *2 (3)*, 121–128.

[14] V. Seregin, A. D. Kozhevnikova, Physiological Role of Nickel and Its Toxic Effects on Higher Plants, *Russ. J. Plant Physiol.* **2006**, *53 (2)*, 257–277.

[15] R. Brooks, in *Plants as Biomonitors. Indicators for Heavy Metals in the Terrestrial Environmental*[Q2] (Ed.: B. Markert) VCH Weinheim, **1993**, pp. 127–148.

[16] J. Proctor, A. J. M. Baker, The importance of nickel for plant growth in ultramafic (Serpentine) soils, in *Toxic Metals in Soil–Plant Systems* (Ed.: S. M. Ross), John Wiley & Sons, New York **1994**, pp. 417–432.

[17] R. D. Reeves, A. J. M. Baker, Metal-accumulating plants, in *Phytoremediation of Toxic Metals: Using Plants to Clean up the Environment* (Eds.: I. Raskin, B. D. Ensley), Wiley, New York **1999**, pp. 193–229.

[18] C. W. A. Nascimento, B. Xing, Phytoextraction: A Review on Enhanced Metal Availability and Plant Accumulation, *Sci. Agric.* **2006**, *63 (3)*, 299–311.

[19] J. F. Ma, S. J. Zheng, H. Matsumoto, Detoxifying Aluminum with Buckwheat, *Nature* **1997**, *390*, 569–570.

[20] H. Tamura, M. Honda, T. Sato, H. Kamachi, Pb Hyperaccumulation and Tolerance in Common Buckwheat (*Fagopyrum esculentum* Moench) *J. Plant Res.* **2005**, *118*, 355–359.

[21] R. Salim, M. M. Al-Subu, A. Atallah, Effects of Root Foliar Treatments with Lead, Cadmium, Copper on the Uptake Distribution Growth of Radish Plants, *Environ. Int.* **1993**, *19 (4)*, 393–404.

[22] M. N. V. Prasad, K. Strzalka, *Physiology and Biochemistry of Metal Toxicity and Tolerance in Plants*, Kluwer Academic Publishers, Dordrecht, The Netherlands **2002**, p. 432ff.

[23] R. L. Heath, L. Packer, Photoperoxidation in Isolated Chloroplasts. I. Kinetics and Stoichiometry of Fatty Acid Peroxidation, *Arch. Biochem. Biophys.* **1968**, *125*, 189–198.

[24] V. L. Singleton, J. A. Rossi, Colorimetry of Total Phenolics with Phosphomolybdic-Phosphotungstic Acid Reagents, *Am. J. Enol. Vitic.* **1965**, *16*, 144–158.

[25] Q. Hayata, S. Hayata, M. Irfana, A. Ahmad, Effect of Exogenous Salicylic Acid under Changing Environment: A Review, *Environ. Exp. Bot.* **2010**, *68 (1)*, 14–25.

[26] R. C. Cash, I. A. Leone, Effects of Foliar Applied Nickel on Tomato Plants, *J. Environ. Sci. Health, Part A* **1987**, *22 (1)*, 1093–4529.

[27] E. Gajewska, M. Skłodowska, Effect of Nickel on ROS Content and Antioxidative Enzyme Activities in Wheat Leaves, *BioMetals* **2007**, *20*, 27–36.

[28] E. Gajewska, M. Skłodowska, P. Bernat, J. Dłługoński, Effect of Nickel on Membrane Integrity, Lipid Peroxidation and Fatty Acid Composition in Wheat Seedlings, *J. Agro Crop Sci.* **2012**, *198*, 286–296.

[29] N. Pandey, C. P. Sharma, Effect of Heavy Metals Co^{2-}, Ni^{2-} and Cd^{2-} on Growth and Metabolism of Cabbage, *Plant Sci.* **2002**, *163*, 753–758.

[30] S. D. Ebbs, L. V. Kochian, Phytoextraction of Zinc by Oat (*Avena sativa*), Barley (*Hordeum vulgare*), and Indian mustard (*Brassica juncea*), *Environ. Sci. Technol.* **1998**, *32*, 802–806.

[31] R. Kaur, R. Bhardwaj, A. K. Thukral, Growth and Heavy Metal Uptake in *Brassica juncea* L. Seedlings as Affected by Binary Interactions between Nickel and Other Heavy Metals, *Can. J. Pure Appl. Sci.* **2010**, *4 (1)*, 1011–1019.

[32] Y. Guo, H. Marschner, Uptake, Distribution and Binding of Cadmium and Nickel in Different Plant Species, *J. Plant. Nutr.* **1995**, *18*, 2691–2706.

[33] F. Hao, X. Wang, J. Chen, Involvement of Plasma-Membrane NADPH Oxidase in Nickel-Induced Oxidative Stress in Roots of Wheat Seedlings, *Plant Sci.* **2006**, *170*, 151–158.

[34] N. Stanisavljević, J. Savić, Z?. Jovanović, J. Miljuš-Djukić, S. Radović, D. Vinterhalter, B. Vinterhalter, Antioxidative-Related Enzyme Activity in *Alyssum markgrafii* Shoot Cultures as Affected by Nickel Level, *Acta Physiol. Plant* **2012**, *34 (5)*, 1997–2006.

[35] M. B. Ali, P. Vajpayee, R. D. Tripathi, U. N. Rai, S. N. Singh, S. P. Singh, Phytoremediation of Lead, Nickel, and Copper by *Salix acmophylla* Boiss.: Role of Antioxidant Enzymes and Antioxidant Substances, *Bull. Environ. Contam. Toxicol.* **2003**, *70*, 462–469.

[36] D. Dubey, A. Pandey, Effect of Nickel (Ni) on Chlorophyll, Lipid Peroxidation and Antioxidant Enzymes Activities in Black Gram (*Vigna mungo*) Leaves, *Int. J. Sci. Nat.* **2011**, *2 (2)*, 395–401.

[37] Michalak Phenolic Compounds and, Their Antioxidant Activity in Plants Growing under Heavy Metal Stress, *Polish J. Environ. Stud.* **2006**, *15 (4)*, 523–530.

[38] C. Sgherri, E. Cosi, F. Navari-Izzo, Phenols and Antioxidative Status of *Raphanus sativus* Grown in Copper Excess, *Physiol. Plant* **2003**, *118*, 21–28.

[39] J. Díaz, A. Bernal, F. Pomar, F. Merino, Induction of Shikimate Dehydrogenase and Peroxidase in Pepper (*Capsicum annum* L.) Seedlings in Response to Copper Stress and Its Relation to Lignifications, *Plant Sci.* **2001**, *161*, 179–188.

[40] B. Winkel-Shirley, Biosynthesis of Flavonoids and Effects of Stress, *Curr. Opin. Plant Biol.* **2002**, *5 (3)*, 218–223.

[41] S. Uraguchi, I. Watanabe, A. Yoshitomi, M. Kiyono, K. Kuno, Characteristics of Cadmium Accumulation and Tolerance in Novel Cd-Accumulating Crops, *Avena strigosa* and *Crotalaria juncea*, *J. Exp. Bot.* **2006**, *57*, 2955–2965.

[42] J. Kováčik, B. Klejdus, Dynamics of Phenolic Acids and Lignin Accumulation in Metal-Treated *Matricaria chamomilla* Roots, *Plant Cell Rep.* **2008**, *27*, 605–615.

[43] E. Horváth, T. Janda, G. Szalai, E. Páldi, Differences between the Catalase Isozymes of Maize (*Zea mays* L.) in Respect of Inhibition by Various Phenolic Compounds, *Acta Biol. Szeged.* **2002**, *46 (3–4)*, 33–34.

[44] H. Yamasaki, R. Heshiki, N. Ikehara, Leaf-Goldening Induced by High Light in *Ficus microcarpa* L. f., a Tropical Fig, *J. Plant Res.* **1995**, *108*, 171–180.

[45] H. Yamasaki, S. Takahashi, R. Heshiki, The Tropical Fig *Ficus Microcarpa* L. f. Cv. Golden Leaves Lacks Heat-Stable Dehydroascorbate Reductase Activity, *Plant Cell Physiol.* **1999**, *40*, 640–646.

[46] K.-G. Lee, T. Shibamoto, G. R. Takeoka, S.-E. Lee, J.-H. Kim, B.-S. Park, Inhibitory Effects of Plant-Derived Flavonoids and Phenolic Acids on Malonaldehyde Formation from Ethyl Arachidonate, *Agric. Food Chem.* **2003**, *51 (24)*, 7203–7207.

[47] S. C. Grace, B. A. Logan, Energy Dissipation and Radical Scavenging by the Plant Phenylpropanoid Pathway, *Philos. Trans. R. Soc. Lond. Ser. B* **2000**, *355*, 1499–1510.

[48] R. Niggeweg, A. J. Michael, C. Martin, Engineering Plants with Increased Levels of Antioxidant Chlorogenic Acid, *Nat. Biotechnol.* **2004**, *22*, 746–754.

[49] U. Takahama, M. Hirotsu, T. Oniki, Age-Dependent Changes in Levels of Ascorbic Acid and Chlorogenic Acid, and Activities of Peroxidase and Superoxide Dismutase in the Apoplast of Tobacco Leaves: Mechanism of the Oxidation of Chlorogenic Acid in the Apoplast, *Plant Cell Physiol.* **1999**, *40*, 716–724.

[50] J. Kováčik, B. Klejdus, J. Hedbavny, M. Bačkor, Effect of Copper and Salicylic Acid on Phenolic Metabolites and Free Amino Acids in *Scenedesmus quadricauda* (Chlorophyceae), *Plant Sci.* **2010**, *178*, 307–311.

[51] Y. Sakihama, M. F. Cohen, S. C. Grace, H. Yamasaki, Plant Phenolic Antioxidant and Prooxidant Activities: Phenolics-Induced Oxidative Damage Mediated by Metals in Plants, *Toxicology* **2002**, *177*, 67–80.

[52] D. Białońska, A. M. Zobel, M. Kuraś, T. Tykarska, K. Sawicka-Kapusta, Phenolic Compounds and Cell Structure in Bilberry Leaves Affected by Emissions from a Zn–Pb Smelter, *Water Air Soil Pollut.* **2007**, *181*, 123–133.

[53] H. Sawada, I. S. Shim, K. Usui, Induction of Benzoic Acid 2-Hydroxylase and Salicylic Acid Biosynthesis-Modulation by Salt Stress in Rice Seedlings, *Plant Sci.* **2006**, *171 (2)*, 263–270.

[54] E. Horvath, M. Pal, G. Szalai, E. Páldi, T. Janda, Exogenous 4-Hydroxybenzoic Acid and Salicylic Acid Modulate the Effect of Short-Term Drought and Freezing Stress on Wheat Plants, *Biol. Planta* **2007**, *51 (3)*, 480–487.

[55] E. J. Choi, Antioxidative Effects of Hesperetin against 7,12-Dimethylbenz(α)anthracene-Induced Oxidative Stress in Mice, *Life Sci.* **2008**, *82 (21–22)*, 1059–1064.

[56] H. L. Yang, S. C. Chen, K. J. Kumar Senthil, K. N. Yu, P.-D. Lee Chao, S. Y. Tsai, Y. C. Hou, Y. C. Hseu, Antioxidant and Anti-Inflammatory Potential of Hesperetin Metabolites Obtained from Hesperetin-

Administered Rat Serum: An *Ex Vivo* Approach, *J. Agric. Food Chem.* **2012**, *60*, 522–532.

[57] B. Marquez-Garcia, M. A. Fernandez, F. Cordoba, Effects of Cadmium on Phenolic Composition and Antioxidant Activities of *Erica andevalensis*, *J. Bot.* **2012**, 1–6.

[58] R. P. Tolra, C. Poschenrieder, B. Luppi, J. Barcelor, Aluminium Induced Changes in the Profiles of Both Organic Acids and Phenolic Substances under Al Tolerance in *Rumex acetosela* L., *Environ. Exp. Bot.* **2005**, *54*, 231–238.

[59] A. R. de Ascensao, I. A. Dubery, Soluble and Wall-Bound Phenolic Polymers in *Musa acuminata* Roots Exposed to Elicitors from *Fusarium oxysporum* f. sp. Cubense, *Phytochemistry* **2003**, *63*, 679–686.

[60] L. Ederli, L. Reale, F. Ferranti, S. Pasqualini, Responses Induced by High Concentration of Cadmium in *Phragmites australis* Roots, *Physiol. Plant* **2004**, *121*, 66–74.

[61] T. M. Nieminen, L. Ukonmaanaho, N. Rausch, W. Shotyk, Biogeochemistry of Nickel and Its Release into the Environment, in *Metal Ions in Life Sciences*, Volume *2* (Eds.: A. Sigel, H. Sigel, R. K. O. Sigel), Wiley, Hoboken, NJ **2007**, pp. 1–30.

[62] M. T. Vasconcelos, M. Azenha, V. de Freitas, Role of Polyphenols in Copper Complexation in Red Wines, *J. Agric. Food Chem.* **1999**, *47*, 2791–2796.

[63] S. Hayat, S. A. Hasan, Q. Fariduddin, A. Ahmad, Growth of Tomato (*Lycopersicon esculentum*) in Response to Salicylic Acid under Water Stress, *J. Plant Int.* **2008**, *3 (4)*, 297–304.

[64] C. A. Rice-Evans, N. J. Miller, G. Paganga, Structure–Antioxidant Activity Relationships of Flavonoids and Phenolic Acids, *Free Radical Biol. Med.* **1996**, *20*, 933–956.

[65] Z. Sroka, W. Cisowski, Hydrogen Peroxide Scavenging, Antioxidant and Anti-Radical Activity of Some Phenolic Acids, *Food Chem. Toxicol.* **2003**, *41*, 753–758.

Q1: Author: Please spell out the first name (initials) of the author "M. N. V. Prasad."

Q2: Author: Please provide the chapter title and publisher location for Reference 15.

CLEAN
Soil Air Water

Reprint Order Form 2012
Please complete and return with your proofs

http://www.onlinelibrary.wiley.com

Dr. Prisca Henheik
Wiley-VCH Verlag GmbH & Co. KGaA
Boschstraße 12
69469 Weinheim, Germany

Tel.: +49 (0) 6201 – 606-520
Fax: +49 (0) 6201 – 606-525

E-mail: clean@wiley-vch.de

Editorial Office
CLEAN
Boschstraße 12
69469 Weinheim
Germany

Manuscript No.: _____

Author: _____

Date: _____

Reprints

You have the opportunity to order reprints, issues or a high resolution PDF (print quality) at the quoted rate. Please note that prices will be substantially higher after publication of the issue. All given prices are including postage and handling charges and excluding tax (VAT). If more than 500 copies are ordered, special prices are available upon request.

Please send me and bill me for

☐ no. of **reprints** via ☐ airmail (+ 25 Euro) ☐ surface mail

Please send me and bill me for

☐ no. of **copies of this issue** (1 copy: 20 Euro) via ☐ airmail (+ 25 Euro) ☐ surface mail

Please send me and bill me for

☐ **high-resolution PDF file** (330 Euro). (unlimited number of hardcopies)

My e-mail address:

Mail reprints / copies of the issue to:

_____

_____

_____

_____

_____

Send bill to:

_____

_____

_____

_____

_____

Please note: Authors are neither permitted to present a PDF file containing the printed version of the paper on the web nor to distribute the PDF file via e-mail to third parties.

For Institutions/Companies in the EU only:

VAT number:

VISA, MasterCard and AMERICAN EXPRESS.
Please use this link (Credit Card Token Generator) to create a secure Credit Card Token and include this number in the form instead of the credit card data.

https://www.wiley-vch.de/editorial_production/index.php

CREDIT CARD TOKEN NUMBER:

WILEY-VCH

Price List for Reprints (2013)

The prices listed below are valid only for orders received in the course of 2013 and before the proofs pass for press. Minimum order is 50 copies. Delivery time will be approximately 3 weeks after the date of publication.
If more than 500 copies are ordered, special prices are available upon request. **Single issues are available to authors at a reduced price**. The prices include mailing and handling charges (with the exception of the additional costs incurred for airmail delivery and courier services). The prices are exclusive of VAT. **Reprints, posters, and issues for overseas orders are shipped by airmail (25.00 Euro surcharge).** If you would like to receive them by surface mail please indicate this on the accompanying order form (postage for shipping posters within Europe: 15.00 Euro). If you would like to use a courier service please indicate this on the order form. The cost for the courier service is 75.00 Euro unless you provide your FedEx number, in which case you will be charged the appropriate amount based on your contract with FedEx.

Reprints	Price for orders (in Euro)					
Size (pages)	50 copies	100 copies	150 copies	200 copies	300 copies	500 copies
1 – 4	345.–	395.–	425.–	445.–	548.–	752.–
5 – 8	490.–	573.–	608.–	636.–	784.–	1077.–
9 – 12	640.–	739.–	786.–	824.–	1016.–	1396.–
13 – 16	780.–	900.–	958.–	1004.–	1237.–	1701.–
17 – 20	930.–	1070.–	1138.–	1196.–	1489.–	2022.–
for every additional 4 pages	147.–	169.–	175.–	188.–	231.–	315.–

Issues	1 copy: 20 Euro	**PDF (high resolution)**	330 Euro
Cover Posters	• DIN A2 (42 x 60 cm/ 17 x 24in): 29 Euro • DIN A1 (60 x 84 cm/ 24 x 33in): 39 Euro		

★Special Offer★
If you order 200 or more reprints you will get a **PDF (high resolution)** for half-price.

CLEAN
Soil Air Water

Annual Subscription rates 2013

Germany/Europe	EUR	1415
Switzerland	SFr.	2189
Outside Europe	US $	1741

Electronic only

All Wiley-VCH prices are exclusive of VAT. Prices are subject to change.

Chemosphere 89 (2012) 1056–1065

Contents lists available at SciVerse ScienceDirect

Chemosphere

journal homepage: www.elsevier.com/locate/chemosphere

Lead toxicity, defense strategies and associated indicative biomarkers in *Talinum triangulare* grown hydroponically

Abhay Kumar [a], M.N.V. Prasad [a,*], Oksana Sytar [a,b]

[a] Department of Plant Sciences, University of Hyderabad, Hyderabad 500 046, India
[b] Department of Plant Physiology and Ecology, Kyiv National University of Taras Shevchenko, Kyiv 01033, Volodymyrskya str. 64, Ukraine

HIGHLIGHTS

- *Talinum triangulare* in hydroponics was investigated for Lead (Pb) toxicity and tolerance biomarkers.
- Lead exposure resulted in oxidative stress in *T. triangulare*.
- Roots accumulated more Pb than stems, and below detectable level in leaves.
- Increased MDA and α-tocopherol, decreased GSH/GSSG ratio serve as biomarkers of Pb exposure.
- Lead toxicity reduced water transport and nutrient elements.

ARTICLE INFO

Article history:
Received 28 January 2012
Received in revised form 16 April 2012
Accepted 16 May 2012
Available online 20 June 2012

Keywords:
Ceylon spinach
Defense response
Energy-dispersive X-ray spectrometry
Non-enzymatic antioxidants
Oxidative stress
Toxicity biomarkers

ABSTRACT

Talinum species have been used to investigate a variety of environmental problems for e.g. determination of metal pollution index and total petroleum hydrocarbons in roadside soils, stabilization and reclamation of heavy metals (HMs) in dump sites, removal of HMs from storm water-runoff and green roof leachates. Species of *Talinum* are popular leaf vegetables having nutrient antinutrient properties. In this study, *Talinum triangulare* (Jacq.) Willd (Ceylon spinach) grown hydroponically were exposed to different concentrations of lead (Pb) (0, 0.25, 0.5, 0.75, 1.0 and 1.25 mM) to investigate the biomarkers of toxicity and tolerance mechanisms. Relative water content, cell death, photosynthetic pigments, sulphoquinovosyldiacylglycerol (SQDG), anthocyanins, α-tocopherol, malondialdehyde (MDA), reactive oxygen species (ROS) glutathione (GSH and GSSG) and elemental analysis have been investigated. The results showed that Pb in roots and shoots gradually increased as the function of Pb exposure; however Pb concentration in leaves was below detectable level. Chlorophylls and SQDG contents increased at 0.25 mM of Pb treatment in comparison to control at all treated durations, thereafter decreased. Levels of carotenoid, anthocyanins, α-tocopherol, and lipid peroxidation increased in Pb treated plants compared to control. Water content, cells death and elemental analysis suggested the damage of transport system interfering with nutrient transport causing cell death. The present study also explained that Pb imposed indirect oxidative stress in leaves is characterized by decreases in GSH/GSSG ratio with increased doses of Pb treatment. Lead-induced oxidative stress was alleviated by carotenoids, anthocyanins, α-tocopherol and glutathione suggesting that these defense responses as potential biomarkers for detecting Pb toxicity.

1. Introduction

Lead (Pb) ranks second among all the hazardous heavy metals (HMs). Majority of the emissions to the environment are from metallurgy (mining, smelting, metal finishing and combustion of coal), energy production (gasoline, battery and power plants), fertilizers, pesticides, lead-containing paints, explosives, microelectronics, sewage sludge and waste waters (Sharma and Dubey, 2005; Sengar et al., 2008; Bindu et al., 2010). Lead is a non-essential for plant metabolism and exhibit varied degrees of phytotoxicity including adverse effects to photosynthesis (Tang et al., 2009). Lead accumulation in different parts of plant is not only depends upon the exogenous concentration, but also on the phytochemistry and soil physico-chemical conditions (Reddy et al., 2005; Mishra et al., 2006).

Excess Pb in plant cells cause molecular damage either directly or indirectly through the formation of reactive oxygen species (ROS) such as hydrogen peroxide (H_2O_2), hydroxyl radical ($OH^{\cdot}$) and superoxide radicals ($O_2^{\cdot-}$) (Sharma and Dubey, 2005; Sengar et al., 2008; Wang et al., 2010; Pourraut et al., 2011). The ROS changes membrane structure and function by attacking on the

* Corresponding author. Tel.: +91 40 23011604; fax: +91 40 23010120/145.
E-mail address: mnvsl@uohyd.ernet.in (M.N.V. Prasad).

0045-6535/$ - see front matter © 2012 Elsevier Ltd. All rights reserved.
http://dx.doi.org/10.1016/j.chemosphere.2012.05.070

polyunsaturated fatty acid of membrane lipids, initiating lipid peroxidation and altered cell biochemical activities (Reddy et al., 2005; Sun et al., 2010; Maldonado-Magaña et al., 2011). As a non-redox active metal, Pb can replace essential metals or cofactors at enzyme active site causing imbalance in cellular redox status. Plants exposed to Pb showed changes in photosynthetic rate due to distortion of chloroplast ultrastructure, impairments of chlorophyll synthesis, imbalance in plastoquinone, reduced minerals uptake and obstructed electron transport (Sharma and Dubey, 2005; Sengar et al., 2008; Cenkci et al., 2010; Pourraut et al., 2011) Chlorophylls and total carotenoid are considered as simple and reliable indicators of Pb-induced phytotoxicity in higher plants (Krupa et al., 1996). ROS production in higher plants not only affects the chlorophylls but also changes the lipids such as sulphoquinovosyldiacylglycerol (SQDG) compositions. SQDG is the deacylation product of sulpholipid and comprises up to 24% of the four major chloroplast lipids. In higher plants approximately 40% of the thylakoid SQDG was tightly associated with LHC II (Harwood and Okanenko, 2003). SQDG is implicated in regulation of light energy distribution between the two photosystems via the phosphorylation of the mobile antennae (Larsson and Andersson, 1985).

Plant cells are protected against ROS by enzymatic and non-enzymatic antioxidative defense systems. Non-enzymatic antioxidative system, involves carotenoids, phenols, flavonoids and glutathione etc., are known to play an important role in scavenging ROS. Anthocyanins (in vacuole) and α-tocopherol (membrane associated) are major secondary metabolites found in the plants against oxidative stresses (Araceli et al., 2009; Hernández et al., 2009). Their antioxidant activities are due to by capturing free radical ions by donation of phenolic hydrogen atoms and protect the plant cells from adverse effects of abiotic stresses (Hernández et al., 2009). Another important property of anthocyanins is that they react with alkaloids, other flavonoids, organic acids, biomolecules and metals forming complexes and stabilizing the color in plants (Araceli et al., 2009). The most active form of vitamin E is α-tocopherol, which is capable of scavenging free oxygen radicals and lipid peroxides. It has been reported that abiotic stress factors might alter tocopherol levels in plant tissues (Collin et al., 2008; Yusuf et al., 2010). In addition to flavonoids, glutathione is widely distributed in living cells and the oxidized form of glutathione (GSSG) is readily converted in to reduced form (GSH) by the enzyme glutathione reductase (GR) (Wang et al., 2010; Maldonado-Magaña et al., 2011). The tripeptide GSH (γ-Glu–Cys–Gly) is playing a key role in scavenging ROS and protecting membrane to damage by these free radicals. In plant cells, metal detoxification mechanisms involve synthesis of the phytochelatins (PCs), and specific metal binding ligands (Gupta et al., 1995, 1999; Mishra et al., 2006; Anjum et al., 2012).

Talinum triangulare (Jacq.) Willd (Ceylon spinach, Talinaceae) is a terrestrial succulent herbaceous plant is widely used, as ornamental and green leafy vegetable, in India, Africa, America and Arabia (Nyffeler and Eggli, 2010). It can be propagated through stem cuttings in hydroponic media (Kumar and Prasad, 2010). The extensively produced adventitious roots of plants are having the potential to absorb toxic substances from aqueous media. Plants that accumulate metals from contaminated media are useful for risk assessment studies of toxic metals (Gupta et al., 1995, 1999; Reddy et al., 2005; Tang et al., 2009). *T. triangulare* are reported to accumulate HMs from dump sites including green leachates and storm water runoff from (Rajkumar et al., 2009; Uwah et al., 2009; Aitkenhead-Peterson et al., 2011). In hydroponic experiments it produces adventitious roots and shoots that are convenient to harvest and for further analysis. Hydroponics are advantageous over soil (in pot culture) since the roots directly exposed to water and the plant metal interactions are direct without any interference. Thus, in hydroponics, plant roots exhibit true responses of Pb toxicity.

Lead toxicity and tolerance on various biological parameters have been investigated in a number of experimental model systems (Table S1). We investigated Pb-induced toxicity and tolerance biomarkers in *T. triangulare* in terms of oxidative damage and associated ROS production and elemental analysis by energy-dispersive X-ray spectrometer to provide insight on Pb-toxicity defense strategies and associated indicative biomarkers.

2. Materials and methods

2.1. Plant description

T. triangulare is a succulent herb that grows in shallow soil in rocky outcrops. Plants required for these experiments were collected from field gene bank, University of Hyderabad, India. *T. triangulare* was propagated through stem cuttings (30–50 mm diameter and 16–20 cm height), which gives extensive adventitious roots, leaves and vegetative propagules in hydroponic media under laboratory conditions in about three weeks (Kumar and Prasad, 2010).

2.2. Pb treatment in hydroponic experiment

Excised stem cuttings of *T. triangulare* were placed in conical flask containing 100 mL of modified Hoagland's media in plant growth chamber at 16/8 h d/night and at 28 ± 2 °C, (Hoagland and Arnon, 1950). Phosphate and sulfate were replaced by chloride and nitrate and the pH of the modified solution was maintained at 4.8 to avoid the precipitation of nutrient media. The nutrient media was replaced every 3 d to provide a fresh dose of nutrient elements. After 3 weeks of acclimatization, uniform stem cuttings with adventitious roots and leaves were selected and treated separately with $Pb(NO_3)_2$ at different Pb concentrations of 0 (control), 0.25, 0.5, 0.75, 1.0 and 1.25 mM and maintained under above conditions. Roots, leaves and stems were separated from treated plants after 1, 3, 5 and 7 d were used for the study of various parameters. All the treatments were repeated at least three times.

2.3. Quantification of Pb accumulation in plant

Metal treated plants roots were washed thoroughly with 0.1 M HNO_3 to remove metals adsorbed to the surface. Roots, stems and leaves were separated and oven dried at 80 °C for 2 d. Dried plant materials were acid digested with 4 mL of $HNO_3/HClO_4$ (3:1 v/v) and the digested material was dissolved in the 10 mL of 0.1 N HNO_3. This solution was analyzed for Pb content using atomic absorption spectrophotometer (GBC 932 plus, Australia).

2.4. Detection of relative water content (RWC)

Plant leaves were freshly weight (FW) and were kept in water at 4 °C for 2 h to know turgid weight (TW). After that leaves were oven dried at 60 °C till completely dry followed by the estimation of dry weight (DW). The relative water content (RWC) was calculated using $RWC\ (\%) = [(FW - DW/TW - FW)] \times 100$ (Gao et al., 2010).

2.5. Detection of cell death

To determine changes in viability of cells after Pb treatment, 0.1 g of freshly harvested leaves were stained with 0.25% (w/v) aqueous solution of Evans blue for 15 min (Baker and Mock, 1994). After washing with miliQ water for 30 min, leaves were

excised and soaked with 3 mL of N,N-dimethylformamide for 1 h at room temperature. The absorbance of released Evans blue was measured at 600 and 652 nm and was expressed as A_{600} after correction for chlorophyll.

2.6. Photosynthetic pigments estimation

Extraction and estimation of chlorophyll and carotenoid contents were carried out by the method of Arnon (1949) and Duxbury and Yentsch (1956), respectively. *T. triangulare* leaves (0.1 g) were ground in 5 mL chilled 80% acetone in dark. After centrifugation at 5000*g* for 10 min at 4 °C, absorbance of supernatant was taken at 480, 645 and 663 nm.

2.7. Sulphoquinovosyl diacylglycerol estimation

Plant leaves (0.2 g) were homogenized with 0.5 g glass powder and 0.5 g $Na_2(SO_4)$. The homogenate was transferred to a glass column and 3 mL acetone was added for filtration. To the filtrate 1 mL hexane: benzene (4:1 v/v) and 2 mL H_2O was added and centrifuged at 5000 g for 5 min at room temperature (RT). After centrifugation 1 mL of the bottom layer was added to 1 mL of 0.01% azure (prepared in acetone) and 2 mL benzene, and again centrifuged at 5000*g* for 5 min at RT. The upper layer was collected and absorbance was measured at 610 nm. The calculation of SQDG was based on the standard curve of sodium dodecylsulfate according to Kean (1968).

2.8. Anthocyanins estimation

Anthocyanins were extracted from 0.5 g of leaves with 10 mL of mixture of *n*-propanol:HCl:H_2O (18:1:81, v/v/v). The samples were heated in boiling water bath for 30 min and then they were incubated for 24 h in the dark at 4 °C. Extracts were filtered and absorbance was taken at 535 and 650 nm. Anthocyanins contents were calculated according to Lange et al. (1971) and Bette and Kutschera (1996) and were expressed as A_{535} g^{-1} fresh weight after correction for chlorophyll: $A_{535} = A_{535} - 0.22 \times A_{650}$.

2.9. α-Tocopherol estimation

Concentration of α-tocopherol was measured in leaves as described by Szymańska and Kruk (2008) with some modifications. Fresh leaves (1 g) were homogenized in mortar with 20 mL of ice chilled methanol (HPLC grade). The extracts were centrifuged at 10000*g* for 15 min at 4 °C. The supernatant were collected and was filtered through 0.2 μm millipore filter and the filtrate was stored in ice in dark. The α-tocopherol content in filtrate was determined by using High Performance Liquid Chromatography (HPLC) with a C_{18} reverse-phase column (250 × 4.60 mm, 5 μm Phenomenax, UK) at a flow rate of 1 mL min^{-1}, using isocratic solvent system of methanol: ethyl acetate (1:4 v/v) as an eluant. Thirty microliters of the samples were injected by a microliter syringe and α-tocopherol content was quantified by UV–visible detector system at 295 nm (LC-10 AT VP Shimadzu, Japan). Peak identification of analyzed leaf extract was performed by comparing with the retention time of standard α-tocopherol. Chromatogram peak area of leaf sample was integrated and the concentration of α-tocopherol was calculated with regard to the area of the corresponding standard α-tocopherol.

2.10. Lipid peroxidation and ROS estimation

Lipid peroxidation in leaves was determined as a function of malondialdehyde (MDA) content following the method of Heath and Packer (1968) with slight modifications. Leaves (0.2 g) were homogenized in 3 mL 0.1 M tris buffer containing 0.3 M NaCl. After that 2 mL of 20% trichloroacetic acid (TCA) containing 0.5% 2-thiobarbituric acid (TBA) and 2 mL 20% TCA. Mixture was heated at 95 °C for 30 min and then homogenate was centrifuged at 10000*g* for 5 min. Absorbance of the supernatant was taken at 532 nm. MDA was calculated by using extinction coefficient of 155 mM^{-1} cm^{-1}. Level of ROS, hydrogen peroxide (H_2O_2), in leaves of *T. triangulare* treated with 0, 0.25 and 1.25 mM of Pb was determined by 5 μM 2′,7′-dichlorodihydrofluorescein diacetate (DCFDA) dye with using confocal microscope (Leica TCS SP2 AOBS Microscope, Germany) at 480 nm excitation and 520 nm emission wavelengths.

2.11. Glutathione estimation

Fresh leaf (0.5 g) was ground in 4 mL of 0.1 M sodium phosphate–EDTA buffer (pH 8.0) containing 25% H_3PO_3. The homogenate was centrifuged at 15000*g* for 20 min at 4 °C. In supernatant total glutathione (GSH and GSSG) content was determined fluorometrically after 15 min incubation with *o*-phthaldialdehyde (OPT) (Hissin and Hiff, 1976). Fluorescence intensity was measured at 420 nm after excitation at 350 nm on a FluoroMax 3 fluorescence spectrophotometer. Total GSH and GSSG in leaves were calculated from the standard curve.

2.12. Elemental analysis by energy dispersive spectroscopy (EDS)

Energy-dispersive X-ray spectroscopy (EDS) is an analytical technique used for the elemental/chemical analysis of specimen. A thin transverse section of leaves treated with 0, 0.25 and 1.25 mM of Pb were prepared. Sectioned tissues were dehydrated, mounted on aluminum stubs, coated with gold-palladium and elemental analyses were done with EDS (Oxford instruments) coupled with field emission scanning electron microscope (FESEM, Ultra 55-Carl Zeiss) and wavelength dispersive X-ray spectroscopy (WDS, Oxford instruments). The EDS analysis was carried out with INCA analyzer software at an operating voltage of 20 KV and working distance of 8.5 μm.

2.13. Statistical analysis

The experiment was repeated at least three times. The mean values ± standard errors (SE) are reported in the figures. Significant differences of these data were calculated using analysis of variance (ANOVA–Duncan's multiple test, SIGMASTAT 9.0). P values $\leqslant 0.05$ were considered significantly different and denoted by different letters.

3. Results

3.1. Lead accumulation in plant

T. triangulare was found to be sensitive to Pb exposure and the Pb accumulation was calculated in tissues on dry weights (dw) basis. When the *T. triangulare* cuttings were raised under increasing concentration of Pb, the Pb accumulation in plant parts increased significantly as compared to control (Table 1). Roots were the main accumulation site as they absorbed much higher quantities (19.9 mg g^{-1} dw) than stems (2.67 mg g^{-1} dw) while in leaves, Pb accumulation has been observed below detectable limit after 7 d of treatment.

Table 1
Lead accumulation in roots and stem of *T. triangulare* grown for 7 d in different doses of $Pb(NO_3)_2$.

Pb concentration (mM)	Concentration of Pb taken up by plant (mg g^{-1} dw)	
	Roots	Stem
0	ND	ND
0.25	3.14 ± 0.3^{a}	0.81 ± 0.04^{a}
0.50	7.85 ± 1.2^{b}	1.18 ± 0.28^{ab}
0.75	13.5 ± 1.4^{c}	1.70 ± 0.17^{b}
1.0	15.5 ± 1.6^{c}	1.88 ± 0.16^{c}
1.25	19.9 ± 0.9^{d}	2.67 ± 0.07^{d}

In a column, means followed by different letter(s) are significantly differ ($P \leqslant 0.05$) according to DMRT.
ND: not detectable.

3.2. Lead-induced changes in relative water content

Relative water content in the leaves of *T. triangulare*, after 7 d of Pb treatment, decreases gradually (Fig. 1). RWC significantly decreased by 6.33% at 0.25 mM to 19.6% at 1.25 mM of Pb, respectively in comparison to control. The water imbibition rates also decreased steadily with increasing Pb concentration.

3.3. Lead-induced cell death

Pb-induced oxidative damage in *T. triangulare* leaves were confirmed by the staining with Evans blue (Fig. 1). A dose-dependent response for cell death was also evident for treatments with different concentrations of Pb. There was no significant difference with control in 0.25 mM Pb treated plant leaf. Evans blue accumulation in leaf was significantly increased maximum by 137% at 1.25 mM Pb treatment in respect to control.

3.4. Lead-induced changes in photosynthetic pigments

The chlorophylls concentrations showed an inverted U-shaped curve with the increasing Pb concentrations after 1 d of treatment period. Chlorosis of leaves was observed after 5 d at higher Pb concentrations, which was further increased with subsequent treatment period. In leaves decreased chlorophylls and carotenoid concentrations were observed at higher concentrations (0.75, 1.0 and 1.25 mM) of Pb. The highest concentration of Chl *a*, *b* and total chlorophyll were found at 0.5 mM after 1 d and at 0.25 mM after 3, 5 and 7 d of Pb treatment. Contents of Chlorophyll *a*, *b* and total chlorophyll were significantly ($P \leqslant 0.05$) increase by 17%, 37% and 24% over control at 0.50 mM of Pb after 1 d, respectively. After 7 d at 1.25 mM of Pb concentration, there were ca. 19%, 8% and 14.8% decrease in Chlorophyll *a*, *b* and total chlorophyll in comparison to control, respectively (Fig. 2A). On the other hand, the carotenoid contents were significantly different (Duncan's multiple test, $P \leqslant 0.05$) at 0.25, 0.5 and 0.75 mM Pb among all treatment periods in comparison to control. After 1 and 3 d of treatment at 0.5 and 0.25 mM of Pb, carotenoid content was significantly increased up to 26% and 40% in comparison to control, respectively (Fig. 2B).

3.5. Lead-induced changes in SQDG concentration

The SQDG concentration significantly ($P \leqslant 0.05$) increased at 0.25, 0.5 and 0.75 mM and decreased at 1.0 and 1.25 mM of Pb treatment in comparison with control after 1 d (Fig. 3). The tendencies to decrease the SQDG concentrations were observed at 1.0 and 1.25 mM of Pb after all treatment periods. However, after 5 and 7 d the SQDG concentration showed dose-dependent reduction at higher concentration of Pb. After 1 d at 1.0 and 1.25 mM of Pb, SQDG concentrations were decreased and at control level, but in the subsequent period increase in SQDG concentrations have been observed. After 7 d SQDG concentrations at 0.75, 1.0 and 1.25 mM of Pb significantly ($P \leqslant 0.05$) decreased to ca. 119%, 226% and 212% in comparison to control, respectively, but with 0.5 mM of Pb concentration decreased to ca. 85%, 176% and 164%, respectively (Fig. 3).

3.6. Lead-induced changes in anthocyanins concentration

In our experiment, anthocyanins accumulation was higher at 0.25 mM of Pb compared with control after all treatment periods (Fig. 3). In comparison to control 1.7 fold reductions in anthocyanins have been observed at 1.25 mM of Pb treatment after 1 d. But interestingly after 7 d of Pb exposure, anthocyanins were increased and almost at the control level. Significant (at 0.25 mM of Pb) and insignificant (at 0.5–1.25 mM of Pb) increases in anthocyanins were observed after 3 d of treatment periods. The concentrations of anthocyanins were (significant, $P \leqslant 0.05$) increased at 0.5 and 0.75 mM of Pb treatment after 5 and 7 d of treatment period. Lead induced an intense anthocyanins accumulation, especially after the seventh day of treatment. The maximum concentrations of anthocyanins were observed at 0.5 and 0.75 μM of Pb and were 1.7 and 1.6 fold increased than control, respectively (Fig. 3).

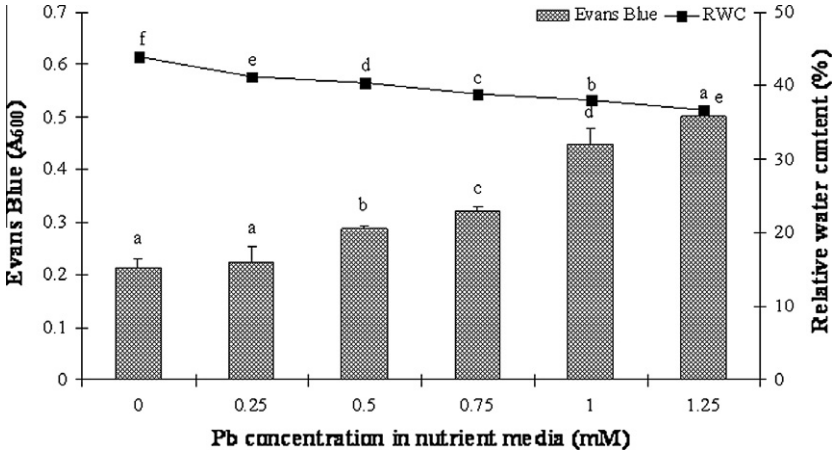

Fig. 1. Relative water content and cell death measurement in *T. triangulare* leaf after 7 d of lead treatment. All the values are mean of triplicates ± SE. ANNOVA significant at $P \leqslant 0.001$. Different letters indicate significantly different values ($P \leqslant 0.05$).

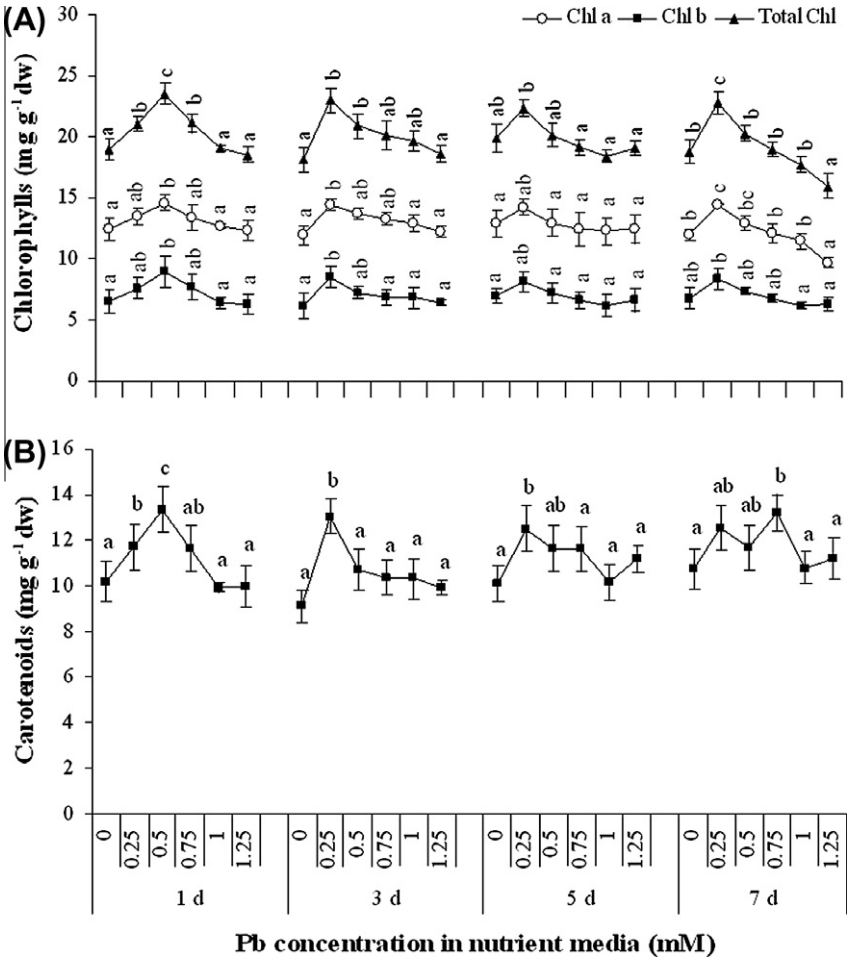

Fig. 2. Concentrations of chlorophyll *a*, chlorophyll *b* and total chlorophyll (A) and carotenoids (B) in *T. triangulare* after treated with lead. All the values are mean of triplicates ± SE. ANNOVA significant at $P \leqslant 0.001$. Different letters indicate significantly different values ($P \leqslant 0.05$).

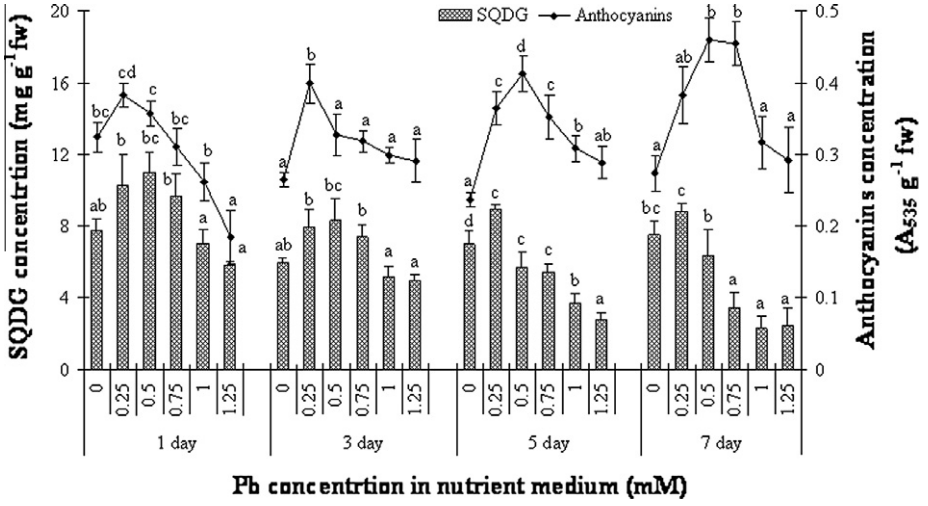

Fig. 3. Sulphoquinovosyl diacylglycerol (SQDG) concentration and accumulation of anthocyanins in leaves of *T. triangulare* treated with lead. All the values are mean of triplicates ± SE. ANNOVA significant at $P \leqslant 0.001$. Different letters indicate significantly different values ($P \leqslant 0.05$).

3.7. Lead-induced changes in α-tocopherol concentration

The HPLC analysis of leaf extracts were identified by comparison of retention time and UV absorption spectra with those obtained for corresponding standards. Peaks were observed at 3.42 ± 0.025 min for α-tocopherol (Fig. 4 inset). Results showed that the α-tocopherol content gradually increased in treated plants compared to control. But after 7 d significant ($P \leqslant 0.05$) increase in the α-tocopherol level has been observed at higher (0.75–1.25 mM) doses of Pb. The levels of increased α-tocopherol ranges between 1.2 and 2.2 fold at 0.25–1.25 mM of Pb in comparison to control (Fig. 4).

3.8. Lead-induced lipid peroxidation and ROS production

Experimental results of MDA estimation, an indicator of lipid peroxidation, showed that the MDA concentrations were significantly ($P \leqslant 0.05$) increased than control after Pb treatment and were directly related to the treatment concentrations. MDA concentration in leaves increased after 7 d due to Pb toxicity and the magnitude of elevation ranged from 1.4 to 2.1 folds at 0.25–1.25 mM of Pb compared to respective controls (Fig. 4). Seven days of Pb treatment prompted a greater increase in the level of MDA at 1.25 mM and was 1.5 fold increased compared to 0.25 mM of Pb exposure. Pb-induced production of ROS was quantified by DCFDA staining (Fig. S1). A dose-dependent response for ROS production was observed and the level of ROS was higher in plant treated with 1.25 mM of Pb than the plant treated with 0.25 mM of Pb.

3.9. Lead-induced changes in glutathione

The level of reduced (GSH) and oxidized (GSSG) glutathione directly point towards the induction of oxidative stress by Pb (Fig. 5). GSH content in plant leaves were found to increase at all Pb treatment except that 1.25 mM of Pb. The level of GSH was not significantly affected at 0.25 and 1.25 mM of Pb. GSH level showed a maximum value at 0.50 mM of Pb which was about 72% higher than control. GSH content depleted with maximum of ca. 12.5% in plant treated with 1.25 mM of Pb (Fig. 5). On the other hand, GSSG level was found to gradually increased at concentration in comparison to control. Maximum GSSG content was found at 1.25 mM which was ca. 172% higher than control. However, the ratio of GSH to GSSG significantly decline and was inversely related to the Pb treatments.

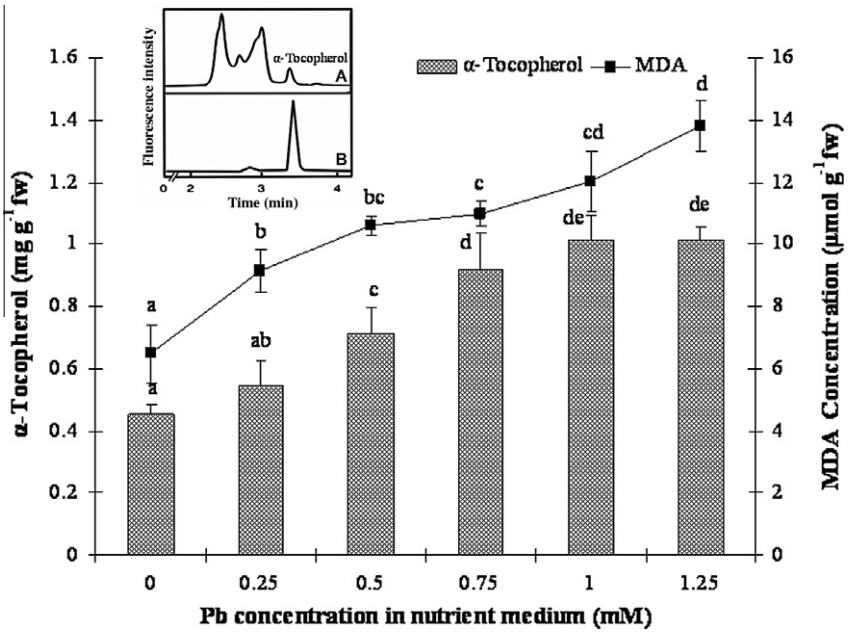

Fig. 4. α-Tocopherol and malondialdehyde (MDA), as a measure of lipid peroxidation, concentrations in leaves of *T. triangulare* treated with lead. All the values are mean of triplicates ± SE. ANNOVA significant at $P \leqslant 0.001$. Different letters indicate significantly different values ($P \leqslant 0.05$). In inset, chromatograms of α-tocopherol: (A) treated leaf extract (B) standard solution.

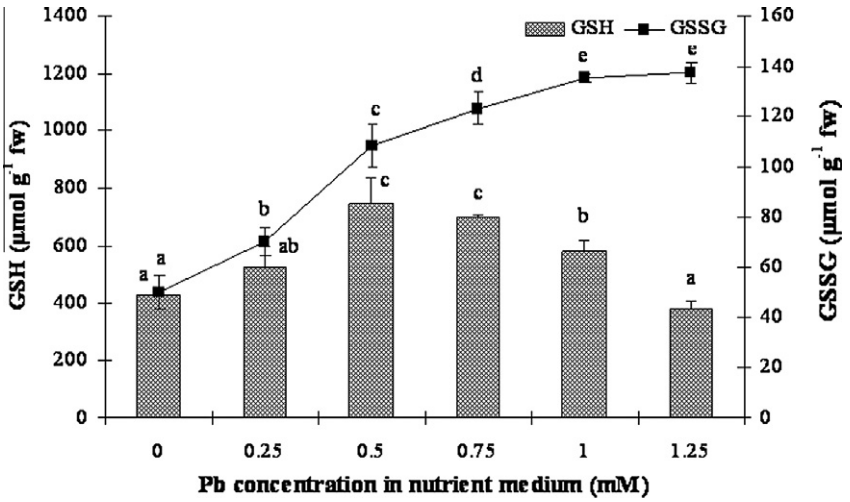

Fig. 5. Levels of reduced (GSH) and oxidized (GSSG) glutathione in the leaves of *T. triangulare* treated with lead. All the values are mean of triplicates ± SE. ANNOVA significant at $P \leqslant 0.001$. Different letters indicate significantly different values ($P \leqslant 0.05$).

3.10. Elemental analysis by EDS

Results of energy dispersion spectroscopy give the atomic or chemical characteristics of analyzed tissue. As a first barrier to metals toxicity, most plants accumulate metals and nutrients in the roots and restrict its transport to the shoots and leaves. Microanalysis of elements was performed at the same site in 0, 0.25 and 1.25 mM of Pb-treated plant samples. In all sample the Pb concentration was below the EDS detectable limit (Fig. 6). The other elements such as oxygen (O), potassium (K), magnesium (Mg), chlorine (Cl), sodium (Na), silicon (Si) and copper (Cu) were also detected in leaf tissues (Fig. 6). In analyzed sample, O and K were contributed as major elements. Trace elements include Mg, Cl, Na, Si, Cu and Ca. X-ray microanalysis of untreated samples showed high spectral peak for all elements, except for O, in comparison to treated (at both 0.25 and 1.25 mM of Pb) plant. Only calcium (Ca) was observed in leaf sample treated with 1.25 mM of Pb (Table S2). Qualitative percentage composition analysis revealed that the percentages of all elements were decreased in both treated plant leaves except O which was increased in Pb treated plant leaves.

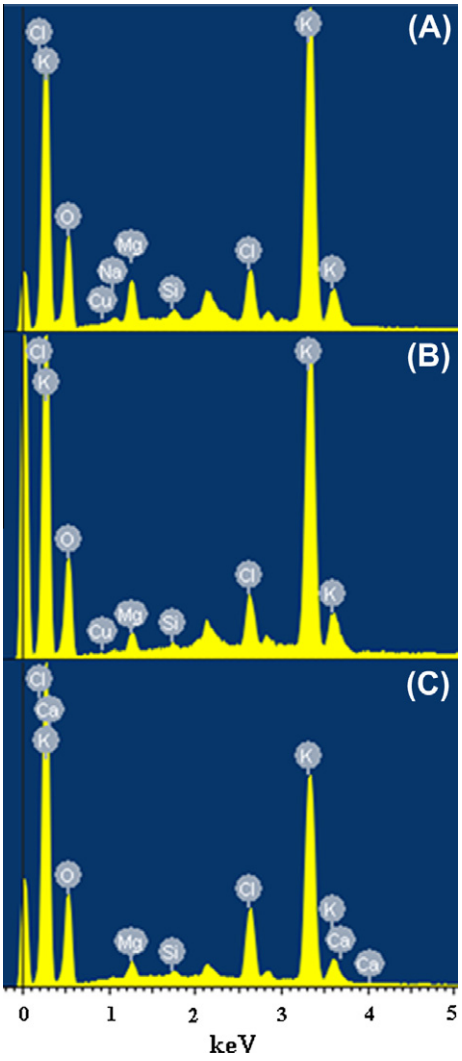

Fig. 6. Energy dispersive X-ray spectral line profile of a transverse section of *T. triangulare* leaf, control (A), 0.25 mM Pb (B) and 1.25 mM Pb (C). Percent weight elemental composition of the imaged area for the *Talinum* leaf sample using SEM/EDS.

4. Discussion

In the present study, the Pb accumulation in the tissues increased as the exogenous Pb concentration increased. The efficiency of metal uptake by plants depends on several processes for metal uptake by roots and its translocation from root to the shoot. Roots absorbed high amount of Pb than stem (Table 1). Probst et al. (2009) also reported that *Vicia faba* roots absorbed more metals than stems and leaves. The order of metal accumulation was root > leaf > stem for all HMs except for Pb and Cd where the order was root > stem > leaf for *Vicia faba* (Probst et al., 2009). This order in different species may vary. In our experimental system, no Pb was detected in the leaves of treated plants. Lower intensity of Pb in the stems (Table 1) and below detectable limit in leaves of Pb treated plants confirmed the decreased translocation of Pb within the plants. It is confirmed by Tian et al. (2011) that Pb is rather immobile within the plants, and accumulated mostly in the vascular bundles of the plant tissues and it could not re-translocated in the tissues even after treatment with a metal chelating agent i.e. EDTA (ethylenediaminetetraacetic acid). The immobilization of Pb^{+2} on *T. triangulare* leaves could represent a new and attractive characteristic for the development of phytoremediation strategies requiring that the large amount of the toxic substances remain tightly bound to plant tissues. In our experimental system Pb bioaccumulation in roots and stems through Hoagland's solution represents the Pb accumulation capacities of *T. triangulare* that are almost equivalent to those of efficient root accumulators of HMs like *Lathyrus sativus* (Brunet et al., 2008), and *Brassicae juncea* (Meyres et al., 2008) or less than *Sedum alfredii* (Tian et al., 2011). It is found that hydroponically cultivated adventitious roots of several terrestrial plants were used for rhizofiltration, a process used for absorbing or precipitating toxic metals effectively from a polluted site (Dushenkov et al., 1995). Adventitious roots of *Talinum* plants have the potential to absorb HMs and might be useful for a new rhizofiltration system.

Relative water content in HM stressed plants is an indicator of phytotoxicity. HMs generally causing a loss of leaf water potential than in non-treated plants (Prasad, 1997; Gao et al., 2010). The results showed that Pb caused phytotoxicity to the plants, which was evidenced by the significant decrease of water content in treated leaves. In the present experiment, RWC decreased with increasing Pb concentrations, and this could be due to decreased water uptake and transport from root to leaf. The damage of membrane integrity was detected by uptake of a non-permeable dye (Evans blue) into the leaf cells, which has been used as an indicator of cell death. Evans blue staining showed that Pb is able to cause death of plant leaf cells. This could be possible due to decline in water content and decrease in nutrient elements contents in leaf of treated plants in comparison to control.

Lead exerts adverse effects on the morphology, growth and photosynthetic processes of plants (Sharma and Dubey, 2005; Sengar et al., 2008; Cenkci et al., 2010; Pourraut et al., 2011). In our experiments we observed that the lower concentrations of Pb (0.25 and 0.5 mM) significantly increasing the chlorophylls content over the control at all duration (Fig. 2A). Exposure of low concentration of Pb has an opposite effects on high concentration exposure. In some cases, lower concentrations stimulate metabolic processes and enzymes involved i.e. photosynthesis and enzymatic activities and long term exposure reduced leaf growth, decreased photosynthetic pigments (Parys et al., 1998). Inhibition of the photosynthetic pigment biosynthesis is one of the primary events in plants during HMs stress and decreases in photosynthetic pigment content have also been reported in many plants under Pb stress (Shakya et al., 2008; Cenkci et al., 2010). It was suggested that HMs could interfere with chlorophylls biosynthesis either through the direct

inhibition of enzymatic steps or through the substitution of the central Mg ion (Sengar et al., 2008; Cenkci et al., 2010; Pourraut et al., 2011). Carotenoid serves as antioxidant against free radicals and photochemical damage (Sengar et al., 2008). Thus less effect on carotenoid might represent its supportive role against oxidative stress after 7 d (Fig. 2B). It is possible that at higher Pb concentrations affected the plant water status, causing water deficit, and finally reduced the chlorophylls content.

The SQDG defined the chlorophylls orientation in membrane and the changes in sulpholipid (SQDG) quantity under HMs stress as a marker of oxidative stress is known phenomenon and studies on stress responses have shown quantitative and qualitative changes in SQDG (Harwood and Okanenko, 2003). In our experiment, higher (0.75–1.25 mM) Pb concentration causes a decrease in SQDG concentration (Fig. 3). Similar results with decrease of SQDG concentrations were observed with influence of various concentrations of Pb on wheat seedling, leaves and roots which grew in hydroponic cultures (Okanenko et al., 2003). It has also been reported that Cd concentration induced a decrease in SQDG concentration in *Brassica napus* leaves (Youssef et al., 1998). The most HMs tested cause a decrease of SQDG concentration (Youssef et al., 1998; Pádua et al., 2003). It is possible that under stress conditions competitive use of sulfur for synthesis of sulfur containing *cys*-rich peptides. It is suppose that the influence of HMs can utilize sulfur preferentially for the synthesis of essential metabolites, such as glutathione and metal binding proteins (phytochelatins and metallothioneins), rather than for SQDG synthesis.

Results suggested that in plants, the synthesis of anthocyanins makes it an effective strategy against ROS generation due to Pb stress, but interestingly lower concentrations of Pb (0.25–0.75 mM) stimulated synthesis of anthocyanins more than higher concentrations (1.0 and 1.25 mM) of Pb (Fig. 3). This indicates that there is a strong correlation between the level of anthocyanins and the presence of HMs in the environment, which further corroborates the results obtained in *Zea mays* demonstrating that accumulation of anthocyanins increased under HMs stress (Krupa et al., 1996). Anthocyanins not only scavenge free radicals, but they also have the ability to bind HMs and are biosynthesized through the phenylpropanoid pathways, the first enzymatic step of the conversion of phenylalanine to trans-cinnamic acid that catalyzed by phenylalanine ammonium lyase (PAL) (Kitamura et al., 2002). It is suggested that PAL, a key enzyme in the flavonoids synthesis, to be the target of HMs inhibitory influence and finally inhibition of anthocyanins synthesis (Dube et al., 1993). However, it seems to be possible that 0.5 and 0.75 mM of Pb concentration stimulate PAL activity resulting in increased production of anthocyanins which may further bind with metals or metal inducing ions in vacuole and detoxify them from cell. Higher concentration of Pb i.e. 1.0 and 1.25 mM are is toxic and lethal to the plant cell, leading to an inhibition of PAL and thus decrease of the biosynthesis of anthocyanin. The initial increase followed by a decline of PAL activity was also observed under different concentration of Cd in *Azolla imbricate* (Dai et al., 2006).

HPLC data showed that Pb treatment to *T. triangulare* plant resulted in the enhancement of α-tocopherol level in leaves (Fig. 4). Probably, the gradual increase in α-tocopherol concentration can be associated with the increased oxidative stress, which supports it as a potential biomarker against oxidative stress. Results showed that tocopherol might be involved in the adaptation of plants against Pb stress. The important function of tocopherol is that to scavenging free radicals and protects polyunsaturated fatty acids (PUFAs) and inhibiting the lipid peroxides in membranes. Abiotic stress factors such as HMs have been found to initiate lipid peroxidation and start a chain reaction which further induces the tocopherols biosynthesis. Previous experimental results also showed that increase in tocopherol content in *Arabidopsis thaliana* exposed to Cd and Cu treatment (Collin et al., 2008) and *Brassica juncea* exposed to Cd (Yusuf et al., 2010), which confers with induced tolerance to plants against HMs stress. After 7 d at higher concentration of Pb, an increase in α-tocopherol concentrations was found in proportion with decrease in chlorophylls content. Previous report suggested that may be the partial degradation of chlorophyll induced the tocopherol content because chlorophyll derived phytol is acting as substrate for tocopherol biosynthesis (Rise et al., 1989).

In parallel with increase in α-tocopherol content, lipid peroxidation was also stimulated by Pb stress (Fig. 4). Lipid peroxidation is a biochemical marker of the Pb-induced free radical mediated oxidative damage in *Talinum* plants. Pb ions are known to induce lipid peroxidation, increasing unsaturated fatty acids and decreasing saturated fatty acids in plants (Mishra et al., 2006; Wang et al., 2010; Maldonado-Magaña et al., 2011; Pourraut et al., 2011). However, the percent increase in MDA content was relatively less (Fig. 4). Generally, free radical generation and membrane damage would be low in tolerant plants and thereby formation of lower levels of MDA content. Therefore, relatively lower degree of increase in MDA content in *Talinum* due to Pb stress may support its tolerant nature. Lead like other HMs induce oxidative stress conditions in plant cells, which is reflected by an increased production of ROS (Fig. S1). Results showed that in the leaves of *Talinum* exposed with Pb, there was an increased production of hydrogen peroxide (H_2O_2) has been observed after 7 d of treatment. It suggested that increased production of ROS is due to the disturbance of electron transport chain in membrane (Sharma and Dubey, 2005; Pourraut et al., 2011).

Glutathione (GSH) is usually the most abundant intracellular non-protein thiols. The result of GSH and GSSG estimation in Pb treated plants indicate an alteration in GSH content, and simultaneous increase in GSSG showed a true indication of oxidative stress. Glutathione is one of the major cellular safeguards, maintains the cellular redox status, which plays a protective role as a key antioxidant and a chelating bioligand responsible for detoxification of HMs (Gupta et al., 1995; Mishra et al., 2006; Maldonado-Magaña et al., 2011; Pourraut et al., 2011). In this study a significant increase in GSH content has been observed in leaves of *T. triangulare* followed by depletion at higher concentration (Fig. 5). At lower concentration induction of GSH accumulation and maintenance of high GSH/GSSG ratio might be attributed to Pb-induced GSH synthesis (Piechalak et al., 2002). Increase in GSSG and decline in GSH show correlation. Ratio of GSH/GSSG decline when Pb concentrations increased, this is evidently due to induction in GSH biosynthesis and rapid reduction of GSSG by the enzyme GR at lower concentration of Pb (Maldonado-Magaña et al., 2011). GSH, as a substrate, synthesize PC due to a reaction catalyzed by phytochelatin synthase (PCS) an enzyme activated by HMs ions including Pb. Decline in GSH at higher concentrations might be attributed to high consumption rate of GSH as antioxidant to combat oxidative stress or for the synthesis of PC. Pb-induced changes in GSH have been reported in *Acacia farnesiana* (Maldonado-Magaña et al., 2011), *Ceratophyllum demersum* L. (Mishra et al., 2006), *Vicia faba*, *Phaseolus vulgaris* (Piechalak et al., 2002), *Hydrilla verticillata* and *Vallisneria spiralis* L. (Gupta et al., 1995, 1999). During the depletion of GSH content, under high Pb stress, formation of Pb–GSH complexes and Pb-induced PC synthesis reduces free Pb concentration in cytoplasm and contributes to suppress the activation of the stress-related responses in plant metabolism (Mishra et al., 2006).

The X-ray microanalysis can qualitatively analyze and quantify the total amounts of elements present in tissues. Elemental microanalysis is becoming an important way to understand individual component within tissues deposits, which may be difficult to analyze by other methodology (Nagata, 2004; Shillito et al., 2009). Results of our EDS study showed the notable reduction of elements in

Pb treated plants in comparison to control (Table S2). From the results, it was shown that X-ray microanalysis using semi-thin sections observed by intermediate high voltage SEM at 20 KV was very useful resulting for quantifying some trace elements in biological specimens. The large decreases observed in Na and Mg concentrations suggest a barrier in transport through the stele or may be due to the damage of the transport system in the plant. Our result corroborate that the observed changes in other biological parameters are due to metal stress or due to decrease of nutrients.

5. Conclusions

It is concluded that *T. triangulare* plants grown hydroponically and exposed to Pb showed that the roots were the main accumulating site as they accumulated more Pb than stem and were below detectable level in leaves. This confirmed that Pb immobilization or decreased translocation within the plants, which represent an attractive aspect for the development of defense strategies. It can be suggest that Pb accumulation potential of *T. triangulare* were almost equivalent to efficient accumulators. The decrease in RWC, due to decreased water transport to leaf, elements atomic % and increased cell death showed that analyzed Pb concentrations have potential to cause oxidative damage in leaf through increase production of lipid peroxides. Photosynthetic pigments and SQDG contents have been increased at 0.25 and 0.5 mM Pb at early treatment period, which decreased at further concentration and treatment durations. Furthermore, increase level of anthocyanins, duration dependent, and α-tocopherol showed their involvement in the adaptation mechanisms in Pb treated plants. Alteration in glutathione levels showed that GSH maintained an important antioxidant system for the plant to accumulate higher concentration of toxic Pb and survive for longer period. These findings confirm the key role of the toxicity and tolerance strategy of *T. triangulare* and analyzed defense parameters suggesting that these might be the potential biomarkers for detecting Pb toxicity. Further research on the molecular mechanism(s) of Pb toxicity and its microlocalisation and detoxification mechanism is required to improve our understandings.

Acknowledgements

A.K. gratefully acknowledged to University of Hyderabad Research Scholarship through the University Grant Commission, New Delhi. O.S. gratefully acknowledges the 3 months research training scholarship in the laboratory of MNVP award by the Centre for International Co-operation in Science (CICS) (Formerly CCSTDS) Chennai, India. Thanks are due to Prof. V.S. Raju, (Emeritus), Kakatiya University, Warangal, India for helpful suggestions on nomenclature of this plant.

Appendix A. Supplementary material

Supplementary data associated with this article can be found, in the online version, at http://dx.doi.org/10.1016/j.chemosphere.2012.05.070.

References

Aitkenhead-Peterson, J.A., Dvorak, B.D., Volder, A., Stanley, N.C., 2011. Chemistry of growth medium and leachate from green roof system in South-central Texas. Urban Ecosyst. 14, 17–33.

Anjum, N.A., Ahmad, I., Mohmood, I., Pacheco, M., Duarte, A.C., Pereira, E., Umar, S., Ahmad, A., Khan, N.A., Iqbal, M., Prasad, M.N.V., 2012. Modulation of glutathione and its related enzymes in plants' responses to toxic metals and metalloids – a review. Environ. Exp. Bot. 75, 307–324.

Araceli, C.-O., Ma de Lourdes, P.-H., Ma Elena, P.-H., Rodríguez, J.A., Carlos Andrés, G.-V., 2009. Chemical studies of anthocyanins: review. Food Chem. 13, 859–871.

Arnon, D.I., 1949. Copper enzymes in isolated chloroplasts: polyphenoloxidases in *Beta vulgaris*. Plant Physiol. 24, 1–15.

Baker, C.J., Mock, N.M., 1994. An improved method for monitoring cell death in cell suspension and leaf disc assays using Evans blue. Plant Cell Tissue Org. Cult. 39, 7–12.

Bette, A., Kutschera, U., 1996. Pigment accumulation and photosynthesis in developing rye coleoptiles. Bot. Acta 109, 194–198.

Bindu, T., Sumi, M.M., Ramasamy, E.V., 2010. Decontamination of water polluted by heavy metals with Taro (*Colocasia esculenta*) cultured in a hydroponic NFT system. Environmentalist 30, 35–44.

Brunet, J., Repellin, A., Varrault, G., Terryn, N., Fodil, Y.Z., 2008. Lead accumulation in the roots of grass pea (*Lathyrus sativus* L.): a novel plant for phytoremediation systems? C.R. Biol. 331, 859–864.

Cenkci, S., Cigerci, I.H., Yildiz, M., Ozay, C., Bozdag, A., Terzi, H., 2010. Lead contamination reduces chlorophyll biosynthesis and genome template stability in *Brassica rapa* L.. Environ. Exp. Bot. 67, 467–473.

Collin, V.C., Eymery, F., Genty, B., Rey, P., Havaux, M., 2008. Vitamin E is essential for the tolerance of *Arabidopsis thaliana* to metal-induced oxidative stress. Plant Cell Environ. 31, 244–257.

Dai, L.-P., Xiong, Z.-T., Huang, Y., Li, M.-J., 2006. Cadmium-induced changes in pigments, total phenolics, and phenylalanine ammonia-lyase activity in fronds of *Azolla imbricate*. Environ. Toxicol. 21, 505–512.

Dube, A., Bharti, S., Laloraya, M.M., 1993. Inhibition of anthocyanin synthesis and phenylalanine ammonium lyase activity by Co^{2+} in the leaf disks of *Terminalia catappa*. Physiol. Plant. 88, 237–242.

Dushenkov, V., Kumar, P.B.A.N., Motto, H., Raskin, I., 1995. Rhizofiltration: the use of plants to remove heavy metals from aqueous streams. Environ. Sci. Technol. 29, 1239–1245.

Duxbury, A.C., Yentsch, C.S., 1956. Plankton pigment monograph. J. Mar. Res. 15, 93–101.

Gao, S., Ou-yang, C., Tang, L., Zhu, J., Xu, Y., Wang, S., Chen, F., 2010. Growth and antioxidant responses in *Jatropha curcas* seedling exposed to mercury toxicity. J. Hazard. Mater. 182, 591–597.

Gupta, M., Tripathi, R.D., Rai, U.N., Chandra, P., 1995. Lead induced changes in glutathione and phytochelatin in *Hydrilla verticillata*. Chemosphere 30, 2011–2020.

Gupta, M., Tripathi, R.D., Rai, U.N., Chandra, P., 1999. Lead induced synthesis of metal binding peptides (Phytochelatins) in submerged macrophyte *Vallisneria spiralis* L.. Physiol. Mol. Biol. Plants 5, 173–180.

Harwood, J.L., Okanenko, A.A., 2003. Sulphoquinovosyl Diacylglycerol (SQDG)—The sulpholipid of higher plants. Kluwer Acad. Publ., pp. 189–221.

Heath, R.L., Packer, L., 1968. Peroxidation in isolated chloroplasts 1. Kinetics and stoichiometry of fatty acid peroxidation. Arch. Biochem. Biophys. 125, 189–198.

Hernández, I., Alegre, L., Breusegem, F.V., Munné-Bosch, S., 2009. How relevant are flavonoids as antioxidants in plants? Trends Plant Sci. 14, 125–132.

Hissin, P.J., Hiff, R., 1976. A fluorometric method for determination of oxidized and reduced glutathione in tissues. Anal. Biochem. 74, 214–226.

Hoagland, D.R., Arnon, D.I., 1950. The water-culture for growing plants without soil. Calif. Agric. Exp. Stn. 337 Circ., p. 347.

Kean, E., 1968. A rapid sensitive spectrophotometric method for quantitative determination of sulfatides. J. Lipid Res. 9, 319–329.

Kitamura, Y., Ohta, M., Ikenaga, T., Watanabe, M., 2002. Responses of anthocyanin-producing and non-producing cells of *Glehnia littoralis* to radical generators. Phytochemistry 59, 63–68.

Krupa, Z., Baťanowska, M., Orzoł, D., 1996. Can anthocyanin be considered as a heavy metal stress indicator in higher plants? Acta Physiol. Plant. 18, 147–151.

Kumar, A., Prasad, M.N.V., 2010. Propagation of *Talinum cuneifolium* L. (Portulacaceae), an ornamental plant and leafy vegetable, by stem cuttings. Floricult. Ornament. Biotechnol. 4 (SI1), 68–71.

Lange, H., Shropshire, W., Mohr, H., 1971. An analysis of phytochrome-mediated anthocyanins synthesis. Plant Physiol. 47, 649–655.

Larsson, U.K., Andersson, B., 1985. Different degrees of phosphorylation and lateral mobility of two polypeptides belonging to the light-harvesting complex of photosystem II. Biochim. Biophys. Acta 809, 396–402.

Maldonado-Magaña, A., Favela-Torres, E., Rivera-Cabrera, F., Volke-Sepulveda, T.L., 2011. Lead bioaccumulation in *Acacia farnesiana* and its effect on lipid peroxidation and glutathione production. Plant Soil 339, 377–389.

Meyres, D.E.R., Aucherlonie, G.J., Webb, R.I., Wood, B., 2008. Uptake and localization of lead in the root system of *Brassica juncea*. Environ. Pollut. 153, 323–332.

Mishra, S., Srivastava, S., Tripathi, R.D., Kumar, R., Seth, C.S., Gupta, D.K., 2006. Lead detoxification by coontail (*Ceratophyllum demersum* L.) involves induction of phytochelatins and antioxidant system in response to its accumulation. Chemosphere 65, 1027–1039.

Nagata, T., 2004. X-ray microanalysis of biological specimens by high voltage electron microscopy. Prog. Histochem. Cytochem. 39, 185–319.

Nyffeler, R., Eggli, U., 2010. Disintegrating Portulacaceae: a new familial classification of the suborder Portulacineae (Caryophyllales) based on molecular and morphological data. Taxon 59, 227–240.

Okanenko, A., Taran, N., Kosyk, O., 2003. Sulphoquinovosyl diacylglycerol and adaptation syndrome. Adv. Res. Plant. Lipids Proc., 361–364.

Pádua, M., Aubert, S., Casimiro, A., Bligny, R., Maryse, A., 2003. Block Effects of a sub-lethal copper exposure on non-green *Acer pseudoplatanus* cell lipids. Plant Physiol. Biochem. 41, 471–477.

Parys, E., Romanowska, E., Siedlecka, M., Poskuta, J.W., 1998. The effect of lead on photosynthesis and respiration in detached leaves and in mesophyll protoplasts of *Pisum sativum*. Acta Physiol. Plant. 20, 313–322.

Piechalak, A., Tomaszewska, B., Baralkiewicz, D., Malecka, A., 2002. Accumulation and detoxification of lead ions in legumes. Phytochemistry 60, 153–162.

Pourraut, B., Shahid, M., Dumat, C., Winterton, P., Pinelli, E., 2011. Lead uptake, toxicity and detoxification in plants. Rev. Environ. Contam. Toxicol. 213, 113–136.

Prasad, M.N.V., 1997. Trace metals. In: Prasad, M.N.V. (Ed.), Plant Ecophysiology. John Wiley & Sons Inc., New York, pp. 207–249.

Probst, A., Liu, H., Fanjul, M., Liao, B., Hollande, E., 2009. Response of *Vicia faba* L. to metal toxicity on mine tailing substrate: geochemical and morphological changes in leaf and root. Environ. Exp. Bot. 66, 297–308.

Rajkumar, K., Sivakumar, S., Senthilkumar, P., Prabha, D., Subbhuraam, C.V., Song, Y.C., 2009. Effects of selected heavy metals (Pb, Cu, Ni and Cd) in the aquatic medium on the restoration potential and accumulation in the stem cuttings of the terrestrial plant, *Talinum triangulare* Linn.. Ecotoxicology 18, 952–960.

Reddy, A.M., Kumar, S.G., Jyothsnakumari, G., Thimmanaik, S., Sudhakar, C., 2005. Lead induced changes in antioxidant metabolism of horsegram (*Macrotyloma uniflorum* (Lam.) Verdc.) and bengal gram (*Cicer arietinum* L.). Chemosphere 60, 97–104.

Rise, M., Cojocaru, M., Gottlieb, H.E., Goldschmidt, E.E., 1989. Accumulation of α-tocopherol in senescing organs as related to chlorophyll degradation. Plant Physiol. 89, 1028–1030.

Sengar, R.K., Gautam, M., Sengar, R.K., Grag, S.K., Sengar, K., Chaudhary, R., 2008. Lead stress effects on physiobiochemical activities of higher plants. Rev. Environ. Contam. Toxicol. 196, 73–93.

Shakya, K., Chettri, M.K., Sawidis, T., 2008. Impact of heavy metals (copper, zinc and lead) on the chlorophyll content of some mosses. Arch. Environ. Contam. Toxicol. 54, 412–421.

Sharma, P., Dubey, R.S., 2005. Lead toxicity in plants. Braz. J. Plant Physiol. 17, 35–52.

Shillito, L.M., Almond, M.J., Nicholson, J., Pantos, M., Matthews, W., 2009. Rapid characterization of archaeological midden components using FT-IR spectroscopy, SEM–EDX and micro-XRD. Spectrochem. Acta Part A 73, 133–139.

Sun, S.-Q., He, M., Cao, T., Yusuyin, Y., Han, W., Li, J.-L., 2010. Antioxidative responses related to H_2O_2 depletion in *Hypnum plumaeforme* under the combined stress induced by Pb and Ni. Environ. Monit. Assess. 163, 303–312.

Szymańska, R., Kruk, J., 2008. Tocopherol content and isomers' composition in selected plant species. Plant Physiol. Biochem. 46, 29–33.

Tang, Y.T., Qiu, R.L., Zeng, X.W., Ying, R.R., Yu, F.M., Zhou, X.Y., 2009. Lead, zinc, cadmium hyperaccumulation and growth stimulation in *Arabis paniculata* Franch. Environ. Exp. Bot. 66, 126–134.

Tian, S.-k., Lu, L., Yang, X., Huang, H., Brown, P., Labavitch, J., Liao, H., He, Z., 2011. The impact of EDTA on lead distribution and speciation in the accumulator *Sedum alfredii* by synchrotron X-ray investigation. Environ. Pollut. 159, 782–788.

Uwah, E.I., Ndahi, N.P., Ogugbuaja, V.O., 2009. Study of the levels of some agricultural pollutants in soils and water leaf (*Talinum triangulare*) obtained in Maiduguri, Nigeria. J. Appl. Sci. Environ. Sanit. 4, 71–78.

Wang, C., Tian, Y., Wang, X., Geng, J., Jiang, J., Yu, H., Wang, C., 2010. Lead-contaminated soil induced oxidative stress, defense response and its indicative biomarkers in roots of *Vicia faba* seedlings. Ecotoxicology 19, 1130–1139.

Youssef, N.B., Zarrouk, M., Daoud, D., Lemal, F., Ouariti, O., Ghorbal, M.H., Cherif, A., 1998. Membrane lipid changes in *Brassica napus* induced by cadmium chloride. In: Sanchez, J., Cerda-Olmedo, E., Martinez-Force, E. (Eds.), Adv. Plant Lipid Res., pp. 534–537.

Yusuf, M.A., Kumar, D., Rajwanshi, R., Strasser, R.J., Tsimilli-Michael, M., Govindjee, Sarin, N.B., 2010. Overexpression of γ-tocopherol methyl transferase gene in transgenic *Brassica juncea* plants alleviates abiotic stress: physiological and chlorophyll a fluorescence measurements. Biochem. Biophy. Acta 1797, 1428–1438.